VASCULARITY OF MAMMALIAN RETINAE:

A COMPARATIVE ANATOMICAL STUDY OF MAMMALS WITH AND WITHOUT INTRARETINAL BLOOD VESSELS.

Robert Gordon Buttery M.B., B.S.(HONS), B.Med.Sc.

Anatomy Department

Submitted in fulfillment of the requirements for the degree of Doctor of Philosophy

University of Tasmania July 1990

ABSTRACT

The physical requirements necessary for the perception of light have produced peculiar adaptions to the way in which the eye is nourished. In many mammals there is a dual blood supply to the retina derived from both choroidal and intraretinal circulations. Interestingly, some species have only a choroidal blood supply. This study has addressed the coping strategies of those retinae which lack intraretinal blood vessels. Placental guinea pigs and diprotodont marsupial brushtail possums and sugar gliders, all of which lack retinal circulation (avascular retinae) have been compared with placental rats and polyprotodont marsupial quolls, Virginia opossums and Tasmanian devils, all of which possess intraretinal blood vessels (vascular retinae). Functional angiographic study has documented vascular patterns and demonstrated the close arteriovenous pairing within the polyprotodont marsupial retina. Avascular retinae are thinner than their vascular counterparts. The difference is not great (170μm versus 220μm). The limitation in thickness is borne by most retinal laminae but more so by those layers furthest from the choroidal supply. Morphological analysis suggests that spatial visual acuity is comparable in vascular and avascular species. Corrosion casting and microscopy of the ocular vasculature has shown that the choroid of the avascular species examined has no obvious morphological specialisations which might offset the lack of retinal vessels. However, the metabolic pathways within the inner layers of avascular retinae are markedly different, with limited oxidative metabolism as indicated by the activity of the mitochondrial enzyme, cytochrome oxidase. However, ATPase activity, as a measure of overall energy consumption, is known to be high within the inner layers of the avascular guinea pig retina (Ueno et al. 1981). This suggests that low cytochrome oxidase activity need not mean limited functional metabolic capacity. As a morphological accompaniment of oxidative activity, ultrastructural analysis would suggest that mitochondrial numbers may be reduced within the inner retinal layers of avascular retinae when compared with similar regions in vascular retinae. Central to these observations is the clinical question of whether the human retina can mimic the coping strategies of avascular retinae following pathological disruption of its intrinsic vasculature.

This thesis contains no material which has been accepted for the award of any other higher degree of graduate diploma in any tertiary institution and that, to the best of my knowledge and belief, the thesis contains no material previously published of written by another person, except where due reference is made in the text of the thesis.

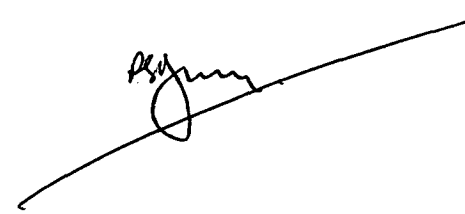

Robert Gordon Buttery

Dedicated to my kindred spirit

Narelle, Samuel, Rebecca, Hannah, and Esther

ACKNOWLEDGEMENTS

To paraphrase Edison, this project is the culmination of one percent inspiration and ninety-nine percent perspiration. To my supervisors, John Haight and Lee Weller, I am indebted for their role in providing inspiration and overseeing this thesis. They readily gave their time, energy, help and encouragment throughout all stages. As an undergraduate, Lee sowed the seeds of interest in functional morphology and John nurtured that interest and helped channel it into the neurological and visual sciences. They have been not only scientific seniors, whom I respect immensely, but also friends. John has taken on an added role as English teacher and proof reader, and with great tolerance and a big red pen, has pointed out, the all too frequent, split infinitives. Gordon Wise too has been inspirational as clinical mentor (from the Greek *Mentõr*, "wise man") and provided many hours of discussion and insight. His guiding hand along the road of clinical science has been warmly appreciated. Eric Colquhoun, Paula Wilson, Colin Hinrichsen, Ian Colrain, Janine Clarey, Lee Astheimer, Wilson Heriot, Nan Caroll, Ian Morgan, Sun Bin, James Vickers and Lyndsay McLeod have all added their encouragement along the way. Those who have provided perspirational help in the laboratory, have also provided inspirational guidance. Paul Laurie has given much practical support in equipment construction and animal preparation. Michael Stranger, the master of sardonic wit, works best in the dark, and has produced much of the photographic material. Similarly, Irene Jacobs has helped immensely with darkroom chores and electron microscopic processing. Kevin Bell of the Lions Eye Diagnostic Centre provided endless patience and time in execution of the angiographic study. David Jacobs, "The Creator of Animals" and his friendly staff maintained the animals in first class condition. Rob Tennent, the Departmental Social Director, taught me the useful lesson of less haste more speed, particularly applicable to bulls in china shops. Tony Van Galen, Bren Gannon, Weislaw Jablonski and others already mentioned were most helpful in teaching electron microscopic techniques. Ron Rainbow and Steve Weston of the Pathology Department, Royal Hobart Hospital and Ann Deal and Miriana Ristivojevic from the Anatomy Department, imparted secrets of histological processing. I am indebted to the National Heart Foundation of Australia for their generous financial support of this project. I am sure to have forgotten some crucial soul, but I must not forget, nor underestimate, the contribution that my wife and family have made to this project. To them, thank you. May it all be worthwhile.

TABLE OF CONTENTS

CHAPTER 1: VASCULARITY OF MAMMALIAN RETINAE

CHAPTER 2: FUNDOSCOPY AND ANGIOGRAPHY OF THE RETINA

REFERENCES

APPENDIX

LIST OF TABLES

CHAPTER 1:

CHAPTER 4:

CHAPTER 6:

ABBREVIATIONS

AV Arteriovenous

c/d cycles per degree of visual angle

cd/m^2 candelas per square meter.

CNS Central Nervous System

CO Cytochrome Oxidase

DAB Di-amino-benzidine

ERG Electroretinogram

GCL Ganglion Cell Layer

GMA Glycol Methacrylate

H&E Haematoxylin and Eosin

INL Inner Nuclear Layer

IPL Innner Plexiform Layer

LDH Lactate Dehydrogenase

LPCA Long Posterior Ciliary Artery

MDH Malate DeHydrogenase

NFL Nerve Fiber Layer

ONL Outer Nuclear Layer

OPL Outer Plexiform Layer

PAS Periodic Acid Schiff (stain)

RPE Retinal Pigment Epithelium. This is used interchangeably with the phrase retinal epithelium (RE). This latter term being more general and acknowledges that not all RPE need be pigmented.

SPCA Short Posterior Ciliary Artery

VER Visual Evoked Response

VEP Visual Evoked Potential

VV Vortex Vein

2-DG 2-Deoxyglucose

CHAPTER 1

INTRODUCTION:

VASCULARITY OF MAMMALIAN RETINAE.

1.1 Vision as a sense

"What tongue will it be that can unfold so great a wonder? Truly none!"
..... Leonardo Da Vinci speaking about vision.

Vision is one of the most emotive of the human senses. Threatened loss often produces dramatic reaction, many people claiming that they would rather die than lose their sense of sight.

In humans, sight is the richest sense, our major the link to the world and its wealth of imagery. The panorama of colour, light and visual perception provides so much of our daily experience. We perhaps take this sense for granted. Imagine life without visual images, surrounded by darkness, relying only on the remaining senses, smell, hearing, touch and taste for all information from the outside world.

The visual system presents an impressive array of functional components to provide these images. The human eye is able to resolve images separated by only half a minute of visual arc, to follow rapidly moving targets, to repeatedly erase and reform an impression of the outside world every 20 milliseconds, to capture images over a billion fold range of illumination, to detect colour differences of 2 nanometers in wavelength and to perceive the relativity of objects in space (Adler 1987).

In keeping with vision as one of the most important aspects of human sensory perception, the visual pathways within the brain constitute a major proportion of the neuronal allocation. It has been estimated that 40% of the cranial nerve afferents lie within the optic nerves (Last 1961).

1.2 Ocular anatomy

1.2.1 Marvel in minature: the retina

The retina transforms the optical images into nerve impulses, messages which are interpretable by the nervous system. The retina is a marvel of miniaturisation, order, and complexity (Masland, 1986). An infinite number of points in the three dimensional visual field must be sampled by the finite two dimensional photoreceptor grating and transduced into nervous format, coded for colour, intensity, contrast, movement and location in space. From

130 million photoreceptors the sampled image is pruned, and in a very sophisticated but economical way, coded and conducted from the eye in a conduit of only one million nerve fibres: the optic nerve. Yet despite this dramatic convergence of nervous pathways, the capacity for fine discrimination still remains. Resolution of the visual system in humans is no worse than that predicted by the photoreceptor grating found at the macula suggesting complex retinal processing (Westheimer 1987).

Notwithstanding the need for visual processing complexity, there are still limits to the physical size of the retina. In general, space is at a premium within the nervous system, but nowhere more so than in the retina. The photoreceptors must be packed together to enhance acuity but also the retina must be sufficiently thin not to impede the passage of light. Light has to pass through many layers before finally interacting with the visual pigments. An appreciation of the phylogeny of visual perception in part explains this anomalous inversion of the retina.

The vertebrate eye in its most primitive form is simply a surface placode of verted light sensitive cells. Light impinges on what was once a ciliated epithelium, without passing through the neural layers. With increasing sophistication of the nervous system, this palcode as part of the neural primordium becomes invaginated and pinched off to form a neural tube. The photoreceptors are now facing internally to the equivalent of the ventricular cavity; the ocular ventricle. This later becomes the subretinal space. The optic vesicle in turn invaginates but in so doing, the photoreceptor layer comes to lie buried deep within the layers of retinal neural tissue; an inverted retina (Duke-Elder 1958).

While this brings disadvantages it offers some benefit through apposition of the metabolically active photoreceptors with the equally rich vascular choroid (Bill 1983). Furthermore, it allows filters to be placed in the light path for selective absorption of part of the visual spectrum (Duke-Elder 1958) and for pigment granules, deep to the photoreceptors, to absorb stray light non selectively. The foveal zone is a further adaptation wherby the neural elements are swept to one side allowing incoming light more direct access to the photoreceptors.

Nonetheless, this inverted arrangement places constraints on the physical size of the retina and eye. Retinal neurons tend to be small (Masland 1986), have densely packed synaptic profiles and lack myelination. The globe itself is small given the large number of neural profiles it contains and the large angular three dimensional field of view which it represents.

Further evidence of the uniqueness of retinal organisation is seen in the regular arrangement of laminated cellular and synaptic regions, seldom matched elsewhere within the nervous system. This regularity together with the accessibility of the retina has lead to major advances

in the understanding of neural processing (Kaneko, 1979) and the correlation of structure with function. Sequential processing occurs from the photoreceptors to ganglion cells with lateral interaction occuring at each stage refining, enhancing and biologically weighting the visual information.

The retina is a remarkably conservative structure, showing little change in histological appearance from fish to man (Chase 1982). The retina may well be expected to operate with common functional threads between many different species.

1.2.2 Blood circulation

1.2.2.a An engineering marvel: Peculiar requirements

The retina is unique in its structure and function. It is not surprising that the vascular system nourishing the eye is also highly specialised.

(1) Visual axis

The perception of light places peculiar constraints on the vascularisation of the eye. No opacities, including blood vessels, should lie within the visual axis (Bill 1975). In part to satisfy this stipulation, the continual flow of a clear plasma filtrate, the aqueous humour, nourishes the lens and cornea whilst contributing to the soluble component of the vitreous (Davson 1980). Thus the cornea, lens and vitreous are devoid of vessels, presenting proportionately, the largest mass of avascular tissue within the body (Sears 1981).

In man, the fovea lies at the apex of the visual axis and is the most discriminating retinal region (Duke-Elder and Wybar 1961). With this area being devoid of retinal blood vessels, not one red cell need interfere with the passage of light.

(2) Dual vascularisation

Another adaptation seen is the dual vascularistaion of the retina. All vertebrate eyes are nourished by an external uveal vascular network, the choriocapillaris. However if this were the sole supply then restrictions upon retinal thickness and complexity would seem a logical corollary.

Many mammals have a dual vascular supply with the addition of true intraretinal vessels derived from the ophthalmic artery (Walls 1942). By definition, this type is referred to as being vascular whilst those retinae without intraretinal vessels are termed avascular. See section 1.2.3 for a discussion of the variation that is found among mammalian species.

Rather than intraretinal vessels, the birds have developed another strategy with a richly vascularised frond, the pecten, projecting into the vitreous cavity (Meyer 1977). Casey Albert Wood in 1917 published a comparative atlas of the fundus oculi of birds demonstrating the ophthalmoscopic appearance of the pecten of many different species. The most plausible role for this appendage is to provide nourishment for the inner layers of the avascular retina. Interestingly, up to thirty different theories have been proposed for its function (Duke-Elder 1958), but the high vascular permeability shown by Abelsdorff and Wessely (1909) indicates its primary nutritive role (See also Bellhorn et al. 1977 and Pettigrew et al. 1990). Optically the pecten offers no added hindrance to light as it occupies the optic disc, an area that normally is devoid of visual perception. It must be just as adequate as the diffuse intraretinal supply seen in many mammals (Duke-Elder 1958).

Indeed, the bird's eye is considered to be "supreme amongst all living creatures" (Duke-Elder 1958). Excellent visual acuity is clearly compatible with an avascular retina (Reymond 1985).

Yet other species have developed variations on this vitreal supply of the retina. Notably, the conus papillaris seen in some reptiles is an outgrowth of glial tissue, arising from the disc projecting into the vitreous (Johnson 1927). This too is richly vascular and nourishes the inner retinal layers of what is usually an otherwise avascular retina (Duke-Elder 1958 Chase 1982).

Rather than bring retinal blood vessels through the retina, the megachiroropteran bats have approached the problem by projecting vascular loops of choroid into the retina (Pedlar and Tilley 1969).

(3) Intraocular pressure

The need for a regular, distended, spherical and somewhat rigid globe too has dictated structural requirements with vascular implications. The globe is pressurised to 15mmHg, the intraocular pressure. Aqueous whilst contributing to nourishment serves also through its restricted outflow to distend and pressurise the eye. This adds to the perfusion pressure needed to supply blood to the eye (Bill 1975).

(4) Metabolically active tissue

Notwithstanding these vascular restrictions, the retina still needs to be nourished in accordance with its needs. If the retina may be considered an example of neural tissue, then, to a first approximation, it would have similar metabolic demands. The nervous system is known to be a metabolic dynamo, comprising only 2% of the body weight yet demanding 17% of the cardiac output and consuming nearly 20% of the body's oxygen (Barr and Kiernan 1983).

However, ocular blood flow is higher than that within the CNS, and may be in excess of blood flow required for purely metabolic needs (Alm and Bill 1973) Combined retinal and choroidal flow per 100gm of retina is about 10 times that of brain gray matter (Alm and Bill 1987). Either blood flow is subserving functions other than a simple nutritional role, or it is likely that the physical constraints of the eye are dictating extraordinary vascular strategies.

(5) Summary

A unique problem has produced a unique solution. Transduction of light (the retina) is metabolically demanding (very rich vascular supply of varying configurations), requires a clear optical axis (large mass of avascular tissue), which itself must be nourished (flow of aqueous) all of which occurs in a regular chamber (pressurised globe). Whilst an engineering marvel, retinal nourishment is perhaps a little precarious.

(6) A compromise

These vascular arrangements of the eye, which are necessary for the adequate detection of visual information, produce as a compromise heightened risk of degenerative problems. Many of the visual problems seen with age: cataract, glaucoma and macular degeneration, are likely the result of these potentially precarious vascular arrangements (Bill 1984).

1.2.3 Variations in vasculature

With that simple overview of vision and the retina, consider in more detail the observation that not all retinae are vascular. Clearly, whilst the problem of detection of light may be unique, the coping strategies for ocular nourishment, while having common themes, are by no means unique. Simply, how do some retinae function without retinal blood vessels when the

analogous situation in a vascular retina, the albeit pathologcal situation of retinal arterial occlusion, produces irreversible and complete loss of retinal function?

1.2.3.a Historical perspective

Early studies of vascular variation dates from the turn of the century when George Lindsay Johnson (1901) published his comparative survey of fundal appearance. Johnson was an ophthalmolgist whose broad interests also encompassed comparative anatomy, instrument design and photography. So keen was his thirst for comparative knowledge that he is reported as joining a whaling expedition to chart the ocular fundus of the whale. Prior to this he specifically designed a crane that would allow him to be lowered over the giant animal and view the interior of the eye (Duke-Elder 1958).

This original mammalian study was supplemented by a comparative study of amphibia and reptiles (Johnson 1927) and with a collection published many years after his death (Johnson 1968). The magnificent series of sketches have been quoted and redrawn in many subsequent sources (Duke-Elder 1958, Polyak 1957, François and Neetens 1974, Wise et al. 1971). Their accuracy and detail is of photographic quality and remain unsurpassed in their breadth of original comparative fundal observations. In all 232 mammalian species were examined.

These vertebrate studies have been complemented by numerous further studies, including histological information and more encompassing comparative discussion of the eye and its vasculature (For reviews see Duke-Elder 1958, François and Neetens 1974, Michaelson 1954, Prince 1956, Walls 1942, Wise et al. 1971).

1.2.3.b Classification of vasculature: general description

Distilled from the many observations has come a classification of the retinal vascular patterns found amongst the mammals but also applicable to many other vertebrates (Duke-Elder 1958, Leber 1903, François and Neetens 1974, Wise 1971). The classification of Leber (1903) is given below with that of Johnson in parentheses.

(a) holangiotic (euangiotic): the whole neuroretina is vascularised by an intraretinal circulation, eg humans.

(b) merangiotic (angiotic): only part of the retina is supplied with vessels.

(c) paurangiotic (pseudoangiotic): vessels lie only around the disc.

(d) anangiotic (anangiotic): no blood vessels within the retina.

Within each of these major groups differing vascular arrangements may be found producing secondary patterns. For example, the retinal vasculature of man (and many primates) shows asymmetry, with the retinal vessels delineating the macular region temporal to the optic disc. The rat and opossum by contrast have a radial and symmetrical radiation of vessels from the disc. Within the paurangiotic retinae variations in the number and arrangement of papillary vessels may be found.

Further combinations and permutations of fundal appearance exist with regard to pigmentation, ranging from the minor pigment differences found around the macula of the human fundus to the presence of highly reflecting and non-pigmented tapeta seen in many of the Carnivore fundi.

Before slotting various mammals into categories based on their retinal appearances a brief discussion of the taxonomy of this broad group of animals is necessary. From this classification, can any patterns be distilled which explain the diversity in retinal vascularisation?

1.2.3.c Taxonomy of mammals: placentals, monotremes and marsupials

Mammals present a diverse group of animals with structural, physiological and behavioural adaptations to a wide range of habitats (Vaughan 1986). The morphological characteristic after which the group is named is the mammary or milk producing gland: mammals lactate and care for their young. Associated features include complex circulatory, respiratory and neurological systems.

From the taxonomic viewpoint the mammalian class may be divided into the subclasses protheria (monotremes) and theria. This latter class is in turn divided into the infraclasses eutheria (placentals) and metatheria (marsupials) (Vaughan 1986).

The monotremes and marsupials are primitive in a number of respects, particularly in their means of reproduction. The monotremes are egg laying whilst the young of the marsupials are born immature and develop in a pouch or marsupium attached to the mother's lower abdomen.

The eutherian infraclass (placental mammals) represent a larger and more diverse group of animals with a broad range of habitats and lifestyles. The system of Simpson (1945) is often used in classsifiction. Placentals may be divided into the following orders:

Mostly "primitive" Unguiculata:

Insectivora - hedgehogs and shrews
Macroscelididea - elephant shrews
Scandentia - tree shrews
Dermoptera - flying lemurs
Chiroptera - bats
Primates - monkeys, apes and man

Mostly "advanced" Ferungulata:

Carnivora - wolves, foxes, cats, and bears
Hyracoidea - hyraxes
Proboscidea - elephants
Sirenia - manatees and dugongs
Perissodactayla -horses and rhinoceroses
Artiodactyla - swine, camels, hippopatami, sheep and goats
Edentata - armadillos, anteaters and sloths
Pholidota - scaly anteaters
Tubulidentata -aardvarks
Cetacea -whales and dolphins
Rodentia - beavers, squirrels, rats and guinea pigs
Lagomorophs - rabbits and hares

The metatherian mammals (marsupial) may be divided into the predominantly carnivorous polyprotodont and mainly herbivorous diprotodont orders (Strahan 1983). The latter line is thought to be the more advanced of the two whilst the omnivorous polyprotodont bandicoot suborder (Peramelomorphia) demonstrates taxonomic features intermediate between the two main orders (Strahan 1983). Simple classification is based on dentition with the polyprotodonta having "many front teeth" and the diprotodonta "two front teeth". This division is in accordance with the dietary habits of the two groups. Other features have been used in classification. These include the arrangement of the bones of the skull, structure of hindfoot, chromosomal arrangement and proteins of the blood (Strahan 1983, Kirsch 1977 a, b). Whilst these added features confirm the basic divisions they differ in interpretation of the relationships within the two groups (Strahan 1983).

The polyprotodonts are found in both the Americas and in Australasia (Kirsch 1977, Sanderson et al. 1984, Strahan 1983) whilst the diprotodonts are found only in Australia and neighbouring islands. The largest variety of marsupials is found in Australia with over 200 known species (Ride 1970). The American opossums, Didelphis spp. are thought to be representative of the primitive stem line of marsupials (Lee and Cockburn 1985).

The polyprotodonts commonly are divided into the following suborders (Kirsch 1977a):

Didelphimorphia - American marsupials
Dasyuromorphia - quolls, dunnarts, Tasmanian devil, numbat and thylacine
Peramelemorphia - bandicoots and bilbies
Notoryctemorphia - marsupial mole

The diprotodonts may be classified into the following superfamilies (Kirsch 1977a, Strahan 1983):

Vombatidae - wombats and koala
Phalangeroidea - gliders and possums
Tarsipedoiea - honey possum
Macropodoidea - potoroos, kangaroos and wallabies

The protherian subclass is divided into two families (Strahan 1983):

Ornithorhynchidae - platypus
Tachyglossidae - echidnas

1.2.3.d Who has vascular retinae?

(1) Placental mammals

If the eutherian group may be considered as the more advanced mammalian line then there appears to be no firm correlation between vascularity, with its presumptive advantages for increasing retinal thickness and complexity, and the increased sophistication of the eutherians as a whole. The complete range of vascularity may be found within the placentals. The rodents as an order demonstrate the largest variation within a particular group. This perhaps is hardly surprising since over 1750 species are found in this group (Vaughan 1986).

Based largely on the work of Johnson the following orders demonstrate vascularity of the whole retina: **holangiotic**.

> Insectivora, Primates, Carnivora, Artiodactyla, Cetacea and many but not all Rodentia.

The **merangiotic** retina is typified by the Lagomorphs, for example the rabbit. These animals possess vessels only along the horizontal meridian (Johnson 1901). This axis contains the medullated nerve fibres. Such an arrangement has been likened to a modified optic nerve projecting into the retina taking with it the intrinsic vascular supply of the nerve (Ashton 1968). The vessels in the main do not project into the substance of the retina (Wise et al. 1971).

Some overlap exists in the final two categories. Paurangiotic retinae to some include those retinae with a small papillary leash whilst to others this falls into the anangiotic class. For this discussion paurangiotic retina will be defined as those with any vasculature, no matter how small, within the confines of the disc or immmediate retina. Functionally, they behave like anangiotic retinae.

Paurangiotic retina include the following:

> Hyracoidea, Proboscidea, Sirenia, some Perissodactayla and many Rodentia.

Totally **anangiotic** retina include:

> Chiroptera, some Perissodactayla, Edentata, and some Rodentia

The hippopotamus (Artidactyla) is described by Johnson (1901) as being vascular but listed in Wise et al. (1971) as being anangiotic.

See Table 1.I for a more comprehensive description of the vascular patterns of placental mammals.

Relationship of phylogeny and lifestyle

As a generalisation, the more primitive families have avascular retinae. Within the Ungulates, the Perissodactyla (horses), more primitive than the Artidactyla (camels, sheep), are deficient in major retinal vascularisation (Vaughan 1986).

Amongst the rodents wide diversification is seen. The more primitive types Castoridae (beaver) Chinchillidae (chinchilla), Caviidae (guinea pig), Dasyproctidae (agoutis) and Sciuridae (squirrels) have avascular retinae. Interstingly, the related Geomyidae (fossorial pocket gophers), Muridae (rats and gerbils) and Dipodidae (jerboas) all have vascular retinae (Johnson 1901). These latter three families are thought to have arisen from a common ancestral stock (Vaughan 1968), indicating again the similarity in phylogeny and vascularity.

Lifestyle of the rodents is broad and seemingly not correlated with retinal vascularity. The semiaquatic beaver, the diurnal squirrel, the fossorial rock rats are all avascular. Within the huge vascular Muridae family examples of terrestial, fossorial, aquatic and arboreal species may be found (Walker et al. 1975). Whilst the rodents on the whole are herbivorous, the avascular examples seem almost exclusively so whilst some omnivorous vascular species may also be found (eg. common rats and jerboa).

Both vascular and avascular species may be found amongst the rodents in families confined to the Americas or Eurasia. This suggests that geographic isolation in the recent geological past can not account for one or other vascular form.

The Primates and Carnivores, as more advanced placental mammalian species, too demonstrate vascularisation of the retina.

Despite similarities in habitat the phylogenetic origin seem more important in dictating the vascular pattern. Amongst the placentals the derived trait appears to be retinal vascularisation. Retinal vascularisation in placentals is associated with increasing encephalisation of the brain, the need for greater eye hand coordination and the development of retinal regional specialisation for finer visual acuity.

(2) Marsupials and monotremes

The primitive monotremes are entirely anangiotic. Among marsupials, the less advanced polyprotodont group, including the stem didelphid family, are holangiotic. The more advanced diprotodont marsupials are on the whole paurangiotic, demonstrating only rudimentary vascularisation of the optic disc (see Fig. 2.9).

Relationship of phylogeny and lifestyle

If, as is commonly believed, the diprotodonts are the derived more advanced form of marsupial, then retinal avasacularity has arisen in conjunction with this progression. The

bandicoots too as a derived product of the didelphid line have lost retinal vascularistion. This would appear at variance with the pattern found in the placentals, where complexity of the nervous system, increasing specialisation of vision and retinal function, has brought with it vascularity of the retina.

Has lifestyle influenced the development of vascularity? The answer is probably not. As with the placentals, there is a diverse range of habitat in both the diprotodont and polyprotodont marsupials. Amongst the Dasyuridae, as examples of the polyprotodonts, there is a range in weight of 0.003 to 8 kg, locations within most terrestial habitats and dietary customs dependent on the local fare, being opportunistic feeders (Lee and Cockburn 1985). The diprotodonts are often herbivorous occupying arboreal (koala), terrestial (kangaroos), semifossorial (wombats) and scansorial (possums) habitats (Lee and Cockburn 1985, Ride 1970, Strahan 1983). Marsupials tend to be nocturnal with only the numbat being strictly diurnal (Lee and Cockburn 1985).

The sugar glider, an avascular diprotodont (despite the claim of Duke-Elder that this species is vascular), is known to occupy an arboreal habitat with the capacity for treetop gliding over distances of 55 metres (Walker et al. 1975). Functionally this animal could be expected to require superior vision. This suggests that avascularity is indeed compatible with adequate vision. By contrast, the Tasmanian devil, a vascular polyprotodont functions more by its sense of smell, being in the habit of continually nosing the ground in search for carion (Ride 1970). Functionally, this animal would appear less in need of acute vision yet has a vascularised retina.

The range of lifestyle is not as broad as with the placentals, but nonetheless, the lifestyle does not appear to correlate with the presence or absence of retinal vessels. Given that the diprotodonts are the more advanced line with more complex nervous system organisation perhaps vascularity does not need to go hand in hand with improved visual acuity.

Table 1.I: Known vascular patterns of placental mammalian retinae

Information for a number of families is not known. Available data regarding vascularity is based on Johnson's work. The information about lifestyle and taxonomy comes from Walker et al. (1975) and Vaughan (1986). In some cases it is difficult to be certain of the modern species. The species name is that given by Johnson except where the modern equivalent has been ascertained from Walker et al. (1975).

ORDER/FAMILY	SPECIES	COMMENTS	VASCULARITY
INSECTIVORA			
ERINACEIDAE	*E. europaeus*	hedgehog morphology primitive	merangiotic
TALIPIDAE	*T. europaea*	common mole fossorial eye 1mm diam	merangiotic
TENRECIDAE			
CHRYSOCHLORIDAE			
SOLENODONTIDAE			
SORICIDAE			
MACROSCELIDEA		elephant shrews	
SCANDENTIA		tree shrews	
DERMOPTERA		flying lemurs	
CHIROPTERA			
PTEROPODIDAE	*P. indicus*	megachiropta fruitbat nocturnal	anangiotic
VESPERTILIONIDAE	*V. nattereri*	commonbat	
PRIMATES			
LEMURIDAE	*L. macaco* *L. veriegatus*	lemur primitive, no macula	holangiotic
INDRIDIAE			
DAUBENTONIIDAE			
LORISIDAE	*L. tardigradus*	loris nocturnal, tapetum	holangiotic
GALAGIDAE			

Table 1.I continued: Known vascular patterns of placental mammalian retinae

ORDER/FAMILY	SPECIES	COMMENTS	VASCULARITY
TARSIIDAE			
CEBIDAE	*A. geoffroyi*	spider monkey platyrhinae, macula	holangiotic
CALLITHRICIDAE		marmosets macula	holangiotic
CEROPITHECIDAE	*M. rhesus*	old world monkey	holangiotic
PONGIDAE	*G. gorilla*	gorilla macula	holangiotic
HOMINIDAE	*H. sapiens*	macula	holangiotic
CARNIVORA			
CANIDAE	*C. familiaris*	dog tapetum	holangiotic
URSIDAE	*U. americanus*	bear tapetum	holangiotic
PROCYONIDAE		raccoon tapetum	
VIVERRIDAE	*P. typus*	civet tapetum	holangiotic
HYAENIDAE	*H. brunnea*	hyaena tapetum	holangiotic
FELIDAE	*F. leo*	lion tapetum	holangiotic
OTARIIDAE	*O. jubata*	sea lion tapetum	holangiotic
ODOBENIDAE		walrus	
PHOCIDAE		earless seals	
PROBOSCIDAE	*E. africanis*	elephant	paurangiotic
HYRACOIDEA	*H. capensis*	hyrax terrestrial	paurangiotic

Table 1.I continued: Known vascular patterns of placental mammalian retinae

ORDER/FAMILY	SPECIES	COMMENTS	VASCULARITY
SIRENIA		dugongs and manatee	
PERRISODACTYLA			
EQUIDAE	*E. caballus*	horse "tapetum"	paurangiotic
TAPIRIDAE	*T. americanus*	tapir	paurangiotic
RHINOCEROTIDAE	*R. unicornis*	rhinoceros	anangiotic
ARTIODACTYLA			
SUIDAE	*S. scrofa*	swine	
TAYASSUIDAE		javelinas	
HIPPOPOTOMIDAE	*H. amphibius*	hippopotamus	?holangiotic
CAMELIDAE	*C. bactrianus*	camel	holangiotic
TRAGULIDAE	*T. javanicus*	mouse deer	holangiotic
CERVIDAE	*C. porcinus*	deer	holangiotic
GIRAFFIDAE		giraffe	
BOVIDAE	*G. dorcas*	gazelle	holangiotic
EDENTATA			
MYRMECOPHAGIDAE	*M. jubata*	anteater	paurangiotic
BRADYOPIDAE	*B. tridactylus*	sloth	anangiotic
DASYPODIDAE	*D. villosus*	armadillo	anangiotic
PHOLIDOTA		scaly anteaters	
TUBULIDENTATA		aardvarks	
CETACEA			
BALAENIDAE		right whales	

Table 1.I continued: Known vascular patterns of placental mammalian retinae

ORDER/FAMILY	SPECIES	COMMENTS	VASCULARITY
CETACEA (CONTINUED)			
ESCHRICHTIIDAE		gray whale	
BALAENOPTERIDAE		rorquals	
PHYSETERIDAE	*P. catadon*	sperm whale	holangiotic
MONODONTIDAE		narwhals	
ZIPHIDIIDAE		beaked whales	
DELPHINIDAE		ocean dolphins	
PHOCOENIDAE		porpoise	
PLATANISTIDAE		river dolphins	
RODENTIA			
APLODONTIDAE		mountain beaver	
SCIURIDAE	*S. vulgaris*	squirrels herbivores, nocturnal	holangiotic
	P. alborufus	flying squirrel nocturnal tapetum	holangiotic
CASTORIDAE	*C. canadensis*	beaver	paurangiotic
GEOMYCIDAE	*G. americanus*	gopher fossorial	holangiotic
HETEROMYIDAE		pocket mice	
DIPODIDAE	*A. indica*	jerboa	holangiotic
MURIDAE	*M. rattus*	mice	holangiotic
ANOMALURIDAE		scaly tailed flying squirrel	
PEDETIDAE		spring hare	

Table 1.I continued: Known vascular patterns of placental mammalian retinae

ORDER/FAMILY	SPECIES	COMMENTS	VASCULARITY
RODENTIA (CONTINUED)			
CTENODACTYLIDAE		gundis	
GLIRIDAE	*M. dryus*	dormice	holangiotic
SELVINIIDAE		desert dormice	
BATHYERGIDAE		mole rats	
HYSTRICIDAE		old world porcupine	
PETROMURIDAE		rock rats	
THRYONOMYIDAE		cane rats	
ERETHIZONTIDAE	*S. villosus*	Brazillian porcupine	anangiotic
CHINCHILLIDAE	*C. lanigera*	chinchilla	paurangiotic
DINOMYIDAE		pacarana	
CAVIIDAE	*C. porcellus*	guinea pig	anangiotic
HYROCHOERIDAE		capybara	
DASYPROCTIDAE	*D. agouti*	agoutis	paurangiotic
AGOUTIDAE		pacas	
CTENOMYIDAE		tuco-tucos	
OCTODONTIDAE		rock rat	paurangiotic
ARBROCOMYIDAE		chinchilla rats	
LAGOMORPHS			
LEPORIDAE	*O. cuniculus*	rabbit	merangiotic

Table 1.II: Known vascular patterns of **polyprotodont** marsupial retinae

Scant detail only is available for this group. All kown species with the exception of the taxonomically problematic bandicoots and bilbies are vascular.

ORDER/FAMILY	SPECIES	COMMENTS	VASCULARITY
DIDELPHIDAE	*D. virginiana*	Virginia opossum Tapetum	holangiotic
DASYURIDAE	*S. harrisii*	Tas devil Tancred 1981	holangiotic
	D. viverrinus	Eastern quoll Walls 1942 O'Day 1938	holangiotic
THYLACINIDAE			
MYRMECOBIIDAE			
NOTORYCTOIDAE			
PERAMELOIDAE	*I. obesulus*	Brown bandicoot Tancred 1981	"avascular"
THYLACOMYIDAE	*M. lagotis*	Bilby Johnson 1901	anangiotic

Table 1.III: Known vascular patterns of **diprotodont** marsupial retinae

Information for a number of families is not known. Available data, with the notable exception of the flying phalanger, indicates that the retinae are essentially anangiotic or have only rudimentary vessels on the optic disc.

ORDER/FAMILY	SPECIES	COMMENTS	VASCULARITY
VOMBATIDAE	*L. latifrons*	hairy nosed wombat Tancred 1981	"avascular"
PETAURIDAE	*P. norfolcencis*	squirrel glider Johnson 1968	paurangiotic
	Petaurus	flying phalanger Duke-Elder 1958	vascular! See Fig. 2.10
PHALANGERIDAE	*T. vulpecula*	brush-tailed possum Freeman 1978	"avascular"
BURRAMYDIAE			
TARSIPEDIDAE			
POTOROIDAE			
MACROPODIDAE	*D. bennittianus*	Bennetts tree kangaroo Johnson 1901	paurangiotic
	M. rufus	red kangaroo Johnson 1901	paurangiotic
	M. eugenii	tammar wallaby Tancred 1981	"avascular"
	T. billiardieri	pademelon wallaby Tancred 1981	"avascular"
	P. penicillata	brush-tailed wallaby Johnson 1901	paurangiotic
	A. rufescens	Rufous rat-kangaroo Johnson 1901	paurangiotic

CHAPTER 2: FIGURES

1.3 Experimental plan

1.3.1 Aims and hypothesis

Clearly, there is great variety in the pattern of retinal vascularisation. Some animals cope without any intrinsic retinal vasculature altogether. However, pathological interruption of the intrinsic vasculature in the holangiotic human retina produces catastrophic loss of vision. What are the essential ingredients that make physiological avascularity so very different from the pathological variant? How do those retinae without intrinsic blood supply function, and may pathologically affected retinae be brought to use those same coping mechanisms to counter loss of retinal blood supply? This thesis addresses four separate, but related, aspects of retinal avascularity seeking to shed light upon these questions.

The approach taken has been to look broadly at both functional and morphological aspects of the ocular circulation and retina. What is the organisation of the ocular vasculature and how does it function if there are no intrinsic retinal blood vessels? What do avascular retinae look like and do they have metabolic modifications? Chapter 2 addresses the question of fundoscopic appearances and of blood flow within vascular and avascular eyes (functional ocular blood flow). Chapter 3 asks the question "Are there differences in the choroidal circulation (or other uveal vasculature) which might overcome the lack of intrinsic vasculature (morphology of ocular circulation)?". Chapter 4 looks at the thickness and the internal morphological structure of avascular retinae (morphology of the retina). In Chapter 5 the functional aspects of retinal energy production have been addressed through anatomical histochemical techniques (functional aspects of retinal metabolism). This story is integrated in Chapter 6 with some attempt to draw functional conclusions about how well an eye with an avascular retina is able to see.

Simply, the hypothesis under investigation is that avascular retinae will show modification in their blood flow and choroidal circulation and/or modification in their structure (thickness) and metabolism. It will be shown that in the species investigated, the major difference between vascular and avsacular retinae lies in their internal organisation (thickness and

lamination) and metabolism (oxidative energy consumption) rather than in their extra-retinal vascular supply.

1.3.2 Choice of animals

The broad aim in selection of animals has been to provide comparative information from different lineages in the both marsupial and placental mammals. This selection of animals serves a twofold purpose. Should differences in coping strategies be found amongst mammals, this might suggest alternative ways in which pathological avascularity could be converted to physiological avascularity. Secondly, if similarities are found, then this offers reassurance that such strategies are broadly applicable and that extrapolation of other results from one avascular species to another is valid and meaningful. This is particularly important when considering that results from *avascular* species may be erronously extrapolated to *vascular* species. It will be shown that this may not always be correct as there are significant differences, for example, in metabolism between the two groups.

The final choice of animals has in part been limited by availability of animals and also the desire to limit to a minimum the use of native animals. The earlier angiographic and subsequent histological processing results showed similarity in organisation within each marsupial group (for example between Tasmanian devil and quoll), therefore for the later experiments only one representative of each Australian marsupial lineage has been used, usually quoll and possum.

All experiments were approved by the University of Tasmania Ethics Committee adhering to the animal experimentation guidelines of the Australian National Health and Medical Research Council. Native mammals were collected under permit from the Tasmanian Department of Parks Wildlife and Heritage.

The ethical and logistic problems in using native marsupial animals were carefully weighed against the potential usefulness of this group in providing insight into retinal avascularity, both physiological and pathological. August Krogh once said "For many problems there is an animal on which it can be most conveniently studied" (Krebs 1975). Are species with avascular retinae ideal for the investigation of retinal vascular pathological conditions?

CHAPTER 2

FUNDOSCOPY AND ANGIOGRAPHY OF

MAMMALIAN RETINAE:

VASCULAR AND AVASCULAR MARSUPIAL RETINAE

VASCULAR PLACENTAL RETINAE.

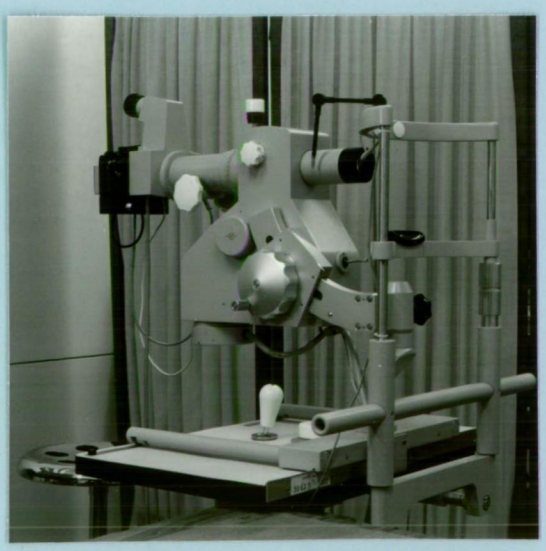

CHAPTER 2: FIGURES

2.1 INTRODUCTION

"Photography is a magic act - a little black box that can trap people and wild animals, strange places and well-loved ones, and bring them all back home."
..... The Camera. Time Life (1970).

All retinae are supplied indirectly by the underlying uveo-choroidal vascular network (Walls 1942). However, as already seen, intraretinal vasculature shows great diversity; reflecting the variety of evolutionary approaches taken to solve the common problem of providing adequate retinal nutrition without detracting unduly from the image forming capacity of the eye. This study, as the starting point for investigating vascularity and, more particularly, its lack, aims to define and document using modern photographic techniques some of the diverse vascular arrangements in selected marsupial and placental retinae.

An extension of the photographic technique, the widely used clinical technique of fluorescein angiography, has also been employed in both vascular and avascular marsupial retinae and compared with better known placental mammals. Not only is otherwise hidden morphological detail made apparent, but also dynamic, functional aspects of the circulation revealed.

A variant of the unusual end artery vascular architecture found throughout the marsupial CNS (Wislocki and Campbell 1937) is most likely present within vascular marsupial retinae. This architecture is probably responsible for the unusual features of the retinal angiogram.

2.2 MATERIALS AND METHODS

"You know my methods, Watson" ....
Memoirs of Sherlock Holmes, Sir Arthur Conan Doyle

Retinae from five marsupial species were examined, three with vascular retinae and two which were avascular. Material from three placental species was used both for comparative purposes and to test and verify the procedures.

2.2.1 Subjects

2.2.1.a Marsupials

The vascular species used were the native cat or quoll, *Dasyurus viverrinus*, Dasyuridae (N = 8; body weights, 750-1 000gm), the Tasmanian devil, *Sarcophilus harrisii*, Dasyuridae (N = 6; 5- 7kg) and the Virginia opossum, *Didelphis virginiana*, (N = 3; 2-4kg), all of which belong to the generalised order Polyprotodonta. The avascular species used were the sugar glider, *Petaurus breviceps*, Petauridae (N = 3; 180-200gm) and the brushtail possum, *Trichosurus vulpecula*, Phalangeridae (N = 5; 2-3kg), both diprotodonts. The Australian forms were captured in Tasmania; Virginia opossums were trapped in West Virginia in the U.S.A. All were adult and, except for the sugar gliders which were male, the sample included individuals of both sexes. Like virtually all marsupials, these five species are nocturnal but otherwise occupy a broad habitus range. The sugar glider is a highly arboreal species capable of gliding considerable distances through the tree tops (Strahan, 1983). The brushtail possum is not as acrobatic and would appear to be equally at home in trees or on the ground (Hughes 1981, Strahan 1983). Quolls are active, primarily terrestial predators with weasel-like habits while Tasmanian devils are strictly terrestial, sluggish carrion feeders (Ride 1970, Strahan 1983). The Virginia opossum is a semiarboreal omnivore (Walker et al. 1975). Visually, these marsupials would be expected to exhibit a wide range of visual capabilities. With the inclusion of the North American opossum, comparison of polyprotodonts with diverse evolutionary backgrounds may be made.

2.2.1.b Placentals

Six hooded Wistar rats (200-300gm) and 3 cats (2.3-5kg) were obtained from suppliers. Human material was selected from normal clinical records at the Lion's Eye Diagnostic Centre in Hobart.

2.2.2 Subject preparation

The animals were anaesthetised with chloral hydrate (rat), chloralose, sodium pentobarbital (brushtail possum, quoll, Tasmanian devil, Virginia opossum, cat) or ketamine-HCl (sugar gliders). See appendix 1 for further details of anaesthesia. In those destined for angiographic examination the femoral (Australian forms) or jugular (Virginia opossum) vein was exposed and cannulated. In humans anaesthesia is not required, and the dye is administered through

a wrist vein. In most cases pupillary dilatation was achieved with topical application of 1% tropicamide (Mydriacyl: Alcon Labs Pty Ltd, Brookville, NSW) and 10% phenylephrine (Neo-Synephrine: Winthrop, Ermington, NSW). Virginia opossums required topical atropine for best results. While anaesthetised, the animals' eyes were regularly irrigated with Balanced Salt Solution.

2.2.3 Fundus photography

In the United States a Topcon TRC-50VT fundus camera was employed; in Australia a Zeiss instrument was used, having been adapted for use with animal subjects. Wide angle angiography and fundus photography was also performed using a Nikon Retinapan 45 fundus camera (Australia).

In the highly dioptric eyes of smaller animals the wider angle of view afforded by the latter machine produced less overall magnification, but afforded considerable improvement in the depth of field. Retinal montages were then constructed from these wide angle views. To compensate for the marked reflecting properties of the tapetum in the quoll, neutral density filters (typically a ND 6.3 filter, optical density 1.222 or transmission of 6.3%) were required to diminish the flash intensity. In this way the exposure and detail seen in the tapetal portion could be equilibrated with that seen in the pigmented hemiretina.

Larger animals were placed in a holding box which held the head in a fixed position. Smaller animals were held in a stereotaxic frame which in turn was attached to a gimbaled table. In this way the subjects could be easily moved to obtain proper alignment of the camera along the animals' visual axes. At the end of the procedure a marker, indicating orientation in space, was photographed to permit later correlation of the fundoscopic picture with that of the visual field. Fundus photographs were taken with Kodak Ektachrome 64 slide film, Kodacolor Gold 100 print film or Konica SR-V 100 print film.

2.2.4 Angiography

The opossum angiography was performed by Dr John Haight during sabbatical leave in the United States of America, the remainder with the technical assistance of Mr Kevin Bell from the Lion's Eye Diagnostic Centre in Hobart. The approach was essentially that employed by Bell and Wise (1980) for routine clinical angiography with minor variations as required to cope with the animals' differing head morphologies. Proper optical alignment was essential,

especially with smaller eyes, as minor off axis variations produced extensive optical aberration and consequent fundal image degradation.

A bolus of 25% fluorescein, 0.05ml/kg (Australia) or 10%, 0.2ml/kg (United States), was administered through the venous cannula followed by a normal saline flush. Angiographic events were recorded on Kodak CFS or CFA (Australia) or Tri-X (United States) film at a maximum rate of two to three frames per second using a 485 nm excitation filter (band width 420-480 nm - cutoff 520 nm) and a Schott GG 14 barrier filter. The temporal sequence of the vascular events was recorded on the CFS photographic film using a "dataphot" camera back. The sensitivity of CFA film however, whilst being tuned more specifically to the emission peak of fluorescein, was insensitive to the red light emitting diodes of the databack. Nerertheless, it was more commonly used.

2.2.5 Carbon injection

Following angiography in one each of quoll, devil and rat the level of anaesthesia was deepened, thoracolaparotomy performed and the vascular system perfused with a flush of Hartmans solution then 5-10ml of Indian ink C11/1431a (Gunther Wagner, Pelikan Werke, Hanover, Germany). After immersion fixation of the eye in 4% formalin in normal saline, the retina was removed and flattened (Stone 1981). In order to calculate the scale factor the undehydrated vascular outline was projected onto the fundus photograph. In the avascular possum the retina was immersion fixed, removed and projected in similar manner but using the adherent pigment pattern as a landmark to determine the linear dimension.

2.3 RESULTS

"Data isn't information, information isn't knowledge and knowledge isn't wisdom" ..... Anon

2.3.1. Vascular marsupial retinae

2.3.1.a Pigmentation and tapetum lucidum

All three polyprotodont species exhibit heterogeneous retinal pigmentation, this being more marked in the quoll and opossum. The retina is divided horizontally into two zones, the line of division running just superior to the optic disc in the quoll and devil and inferior to it in the opossum (Fig. 2.1, 2.2, 2.3). Inferiorly, the retinal epithelium is dark brown; superiorly, in the quoll and opossum, but not in the Tasmanian devil, there is a reflective *tapetum lucidum*. When viewed in quolls through the transparent tapetum, the underlying choroid appears as a blotchy mosaic of pigmented clumps and scattered choroidal vessels. In the inferior retinae of all three species, the choroid is seen less perfectly through gaps in the pigment epithelium. Where visible, the streak-like choroidal vessels are not disimilar to those seen in the sugar glider (Fig. 2.10). In the Tasmanian devil's retina pigmentation is less intense superiorly, but as mentioned, there is no suggestion of a *tapetum lucidum* (Fig. 2.2). The underlying choroid is not clearly visible through the more densely pigmented retinal epithelium of the devil's retina. In both Australian marsupials, myelinated nerve fibres stand out in contrast against the pigmented background and can be seen converging upon the optic disc (Fig 2.2B).

2.3.1.b Retinal arteries

Freely dichotomising arteries radiate from the optic disc in all three retinae. Over most of the retina only arteries are visible; veins are seen clearly only near the optic disc (see below). In quolls and devils the vascular pattern is nearly identical. Three large arteries fan outward from the optic disc (Figs. 2.1, 2.2). One of these supplies the superior retina whilst the inferior retina is supplied by the remaining two large vessels plus two smaller arteries which extend horizontally toward the nasal and temporal peripheries.

Blood supply to the superior and inferior retina is separate. Fundoscopic and angiographic observations in both quolls and devils show a narrow, horizontally directed region, lacking large vasculature and lying immediately superior to the optic disc. In quolls this region lies

within the tapetum, just superior to the tapetal margin; in devils it remains near the border between the light and dark pigmentation zones. Terminal vessels from the superior and inferior vascular arcades converge upon but do not quite meet along this line (Fig. 2.7). Tancred (1981) has shown that in the Tasmanian devil this sparsely vascular region corresponds in position to the visual streak.

In both the quoll and the devil large calibre vessels project into the vitreous from the optic disk. In carbon injected fixed material these vessels measured up to 1mm in length. They resemble anomalous vessels which may be seen on rare occasion arising from the human papilla (Brown and Tasman 1983)

In the Virginia opossum seven to nine large vessels radiate from the optic disc, dividing the fundus into wedge-shaped sectors. Two somewhat larger vessels appear to supply most of the inferior (pigmented) hemiretina with the remainder supplying the equatorial and tapetal portions. Rather than a visual streak, the opossum has an area centralis (Kolb and Wang 1985, Rapaport et al. 1981). No obvious avascular region corresponding in position to the opossum's area centralis was visible.

2.3.1.c Retinal veins

As already noted, except near the optic disc, veins are not normally seen. This is because most veins are closely paired with a companion artery which generally overlies them (Fig. 2.4). Near the optic disc the vessels become too large to sustain this over-under arrangement, and they come to lie side by side. In some areas the arteriovenous pair may separate for a brief distance or, on occasion, a vein will even loop vitread over the artery (Fig. 2.2B). This close pairing of vessels is found throughout the CNS of marsupials (Wislocki and Campbell 1937) and, as will be seen, produces an unusual retinal angiogram (see below and Discussion).

2.3.1.d Angiography

Angiographic events in the quoll and Tasmanian devil commence with choroidal filling, followed after an interval by retinal arterial filling. Choroidal filling is particularly noticeable when the pigment epithelial cover is lacking, as in the superior (tapetal) retina of the quoll (Figs. 2.4, 2.5). The filling reflects known morphological patterns in other species, suggesting a common structural pattern. In placentals, the choroidal bed is known to consist of longitudinal feeding arterial vessels in the more superficial (sclerad) choroidal layers. These are derived from the short posterior ciliary vessels and radiate forward from the posterior pole.

These linearly arranged choroidal arteries intermittently branch, at almost 90 degrees, and send very short projecting vessels to supply the deeper (vitread) choriocapillaris network (Alm and Bill 1987, Hogan et al. 1971, Shimuzu et al. 1978). The venules draining the choriocapillaris alternate with the small abruptly ending feeding arterioles. The venous system then drains into the vortex veins located anteriorly at the four quadrants of the globe (Alm and Bill 1987).

This same pattern of choroidal filling is seen in the marsupial eye. The arteries fill first, being seen as either linear streaks of the long deep choroidal vessels (Fig. 2.5A, 2.6) or, in end on view, as speckled patchy choroidal fluorescence of the feeding arterioles as they dive toward the underlying choroidal meshwork (Fig. 2.4A, 2.6). Superimposition of the color fundus photos on these early frames showed that the speckled pigment clumps of the superior fundus corresponded to the similarly speckled early choroidal filling; the clumps must surround but not totally obscure these vessels. The dye appearing in this early arterial phase drains quickly into the more superficial choriocapillaris, imparting a gradually intensifying background flush. Against this choroidal fluorescence the as yet unfilled retinal vessels stand out in dark contrast. Larger scale, geographic variations, where whole choroidal regions are delayed in early filling, are seen in these and other angiograms (Fig. 2.8, 2.12, 2.11, 2.18); being readily ascribed to differing flow rates within vascular lobules (Hayreh 1975).

Simultaneously with the intensification of the choriocapillaris flush, the retinal arteries begin to fill with the dye progressing radially outward from the optic disc. Very shortly thereafter, ca. 250-300 msec., the large diameter venous segments near the optic disc are seen to fill. The dye in these larger veins at first takes on a 'lamellated' appearance. Two fluorescing streaks appear on either side of a non-fluorescing axial core (Fig. 2.4) as dye from tributary veins enters the main venous trunks but does not immediately mix with the blood which is already there. This feature is visible because, as noted above, only in this region do the arteries and veins appear as separate, side-by-side profiles; elsewhere in the retina arteries usually overlie and obscure the veins (Fig. 2.5). Later, dye and blood mix, and the veins fluoresce uniformly. In the peripheral retina venous flow is signaled by an apparent 'widening' of the larger vessels, as the larger diameter veins deep to the arteries fill with dye and begin to fluoresce. Hence, only near the disc are the details of the initial venous flow not obscured by the antecedent arterial circulation. Simultaneous with the first appearance of venous flow, the initial traces of the capillary flow gradually appear. Only after the intensification of venous flow does the capillary flush reach a maximum. Further filling of the capillary and venous components is followed by recirculation of dye and consequent uniform fluorescence of all elements. The retinal circulation remained patent throughout the angiogram with no fluorescence appearing outside vessel walls.

The angiographic pattern in the Virginia opossum differed from that of the quoll and Tasmanian devil in two particulars. First, choroidal and arterial filling occurred simultaneously. Second, in some opossums the capillary phase is not manifested by a uniform flush, but rather by a zonal filling whereupon some areas of the retina fill (and empty) at different times (Fig. 2.8). This is not dissimilar to what is seen with the patchy geographic choroidal filling in other marsupials, suggesting the possibility of multiple supplying vessels within the optic nerve, or staggered branching of the central retinal artery at the level of the optic papilla. Otherwise, angiographic events are similar in all three species. The time taken from first appearance of the dye to when it first begins to disappear from the arteries is 3 to 4 seconds.

2.3.2 Avascular marsupial retinae

2.3.2.a Fundus and choroidal vessels

In the brushtail possum and sugar glider only a papillary cluster of small vessels, protruding into the vitreous from the head of the optic disc, is seen (Fig. 2.9, 2.10); the two retinae are otherwise avascular.

In sugar gliders the entire retinal pigment epithelium presents as a coarse, irregular mosaic of heavily and lightly pigmented regions through the latter of which glimpses of the choroid and its deep vessels can be seen. These deep vessels are typically broad and straight.

As also noted by Freeman and Tancred (1978), the inferior half of the brushtail possum's retina is more heavily pigmented than the superior half (Fig. 2.9) with the boundary between the differentially pigmented hemiretinae passing superior to the optic disc. The deep, uniform pigmentation of the inferior retina prevents all but the faintest glimpse of the choroidal circulation. In the superior retina there are non-pigmented spots through which choroidal vessels are visible. These spots are smaller and more 'punctate' in appearance than the larger, irregularly shaped gaps seen in the glider, and they tend to form a more regular pattern. The pattern formed by these hypopigmented spots resembles that of the pigment clumps of the quoll's superior fundus: one appears as the negative image of the other. Associated with each gap in pigmentation in the possum is a vascular spot. These are seen clearly in normal fundus photographs (Fig. 2.9) and appear with special clarity in angiograms (Fig. 2.11), suggesting that they represent end on views of segmental choroidal arterioles having just branched and passing vitread to supply the choriocapillaris. The quoll pattern most likely represents the same vascular pattern with the vessel having acquired a cuff of pigment from the more sclerad choroid before its course through the tapetum to the

choriocapillaris. It is this perivascular pigmentation which stands out against the non pigmented and more vitread tapetal choroid. The typical long, straight and larger deep choroidal vessels are also visible in both animals.

Neither animal has a *tapetum lucidum* although the possum does show greater light reflection from the superior fundus.

2.3.2.b Angiography

In sugar gliders the papillary vessels and the choroid fluoresce simultaneously followed, upon recirculation, by a slower, more uniform choroidal intensification. In one glider zonal filling was seen with fluorescence first appearing in the papilla and peripapillary region, both of which then emptied and fluorescence then appeared in the peripheral retina (Fig. 2.12). The dye does not diffuse from the papillary vessels into the vitreous.

In brushtails, too, the dye fills the papillary vessels simultaneously with the initial choroidal flow. Fluorescence is visible only at the disc and in the superior, less pigmented dorsal hemiretina, appearing with particular strength through the pigment hiatuses (Fig. 2.11). Zonal variations in the choroidal filling pattern are occasionally seen akin to those in the quoll and sugar glider (Fig. 2.4, 2.6, 2.12). As with the sugar glider, there is no diffusion from the papillary vessels. The time taken for first appearance of dye to uniform fluorescence is 4 to 5 seconds.

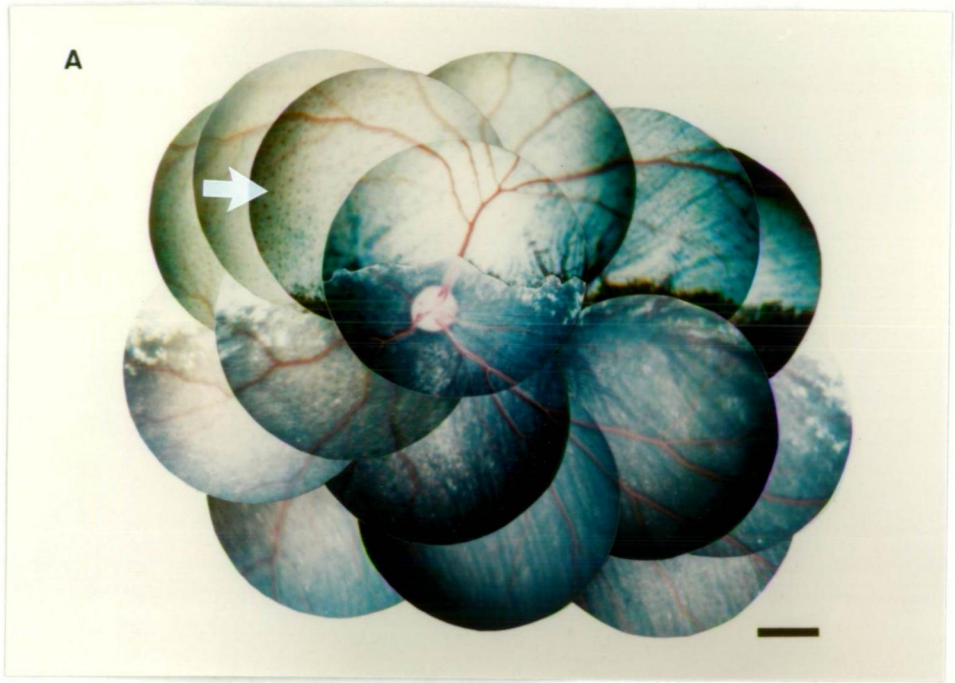

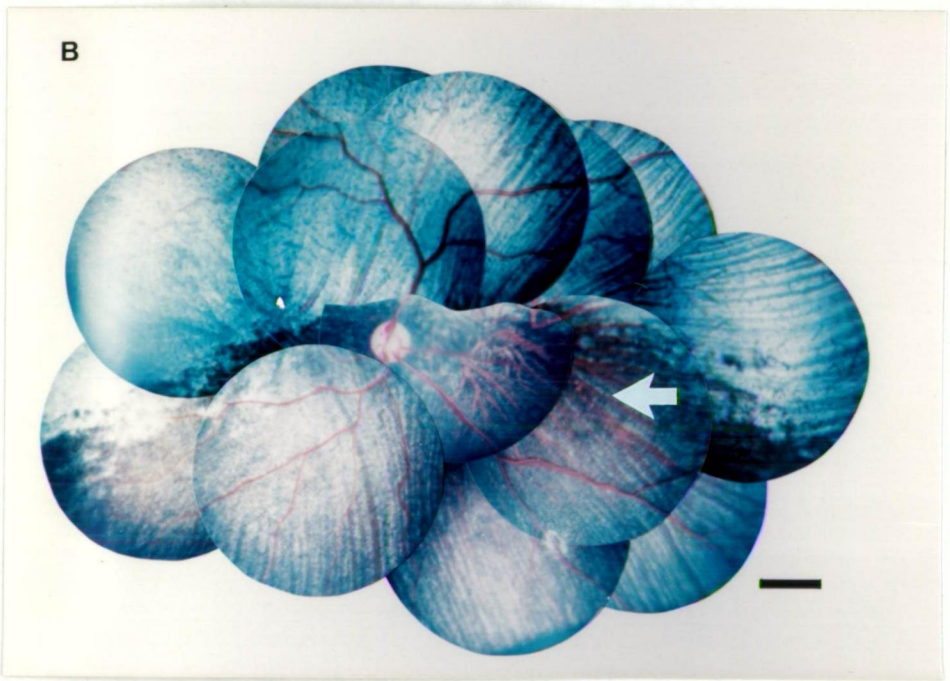

Figure 2.1: The quoll fundus

Wide angle montaged views of the fundus of the right eye. (A) Animal 88/20. Radiating from the optic disc, intraretinal blood vessels supply the superior and inferior retina leaving a horizontal vascular sparse zone above the tapetal border. The arteries overly the veins throughout most of the retina. A reflecting tapetum in the dorsal fundus allows the choroidal circulation to be seen. A mosaic of pigment clumps surround what may on the angiograms be seen as end on choroidal vessels (arrow).

(B) Animal 88/33 (Same eye as angiogram Fig. 2.5). Another animal demonstrating marked similarity in fundal appearance. Prominent linear choroidal vessels are apparent inferiorly, through less dense areas of pigmentation (arrow). These vessels are not unlike those seen in the glider (Fig. 2.10). Scale bar = 1mm.

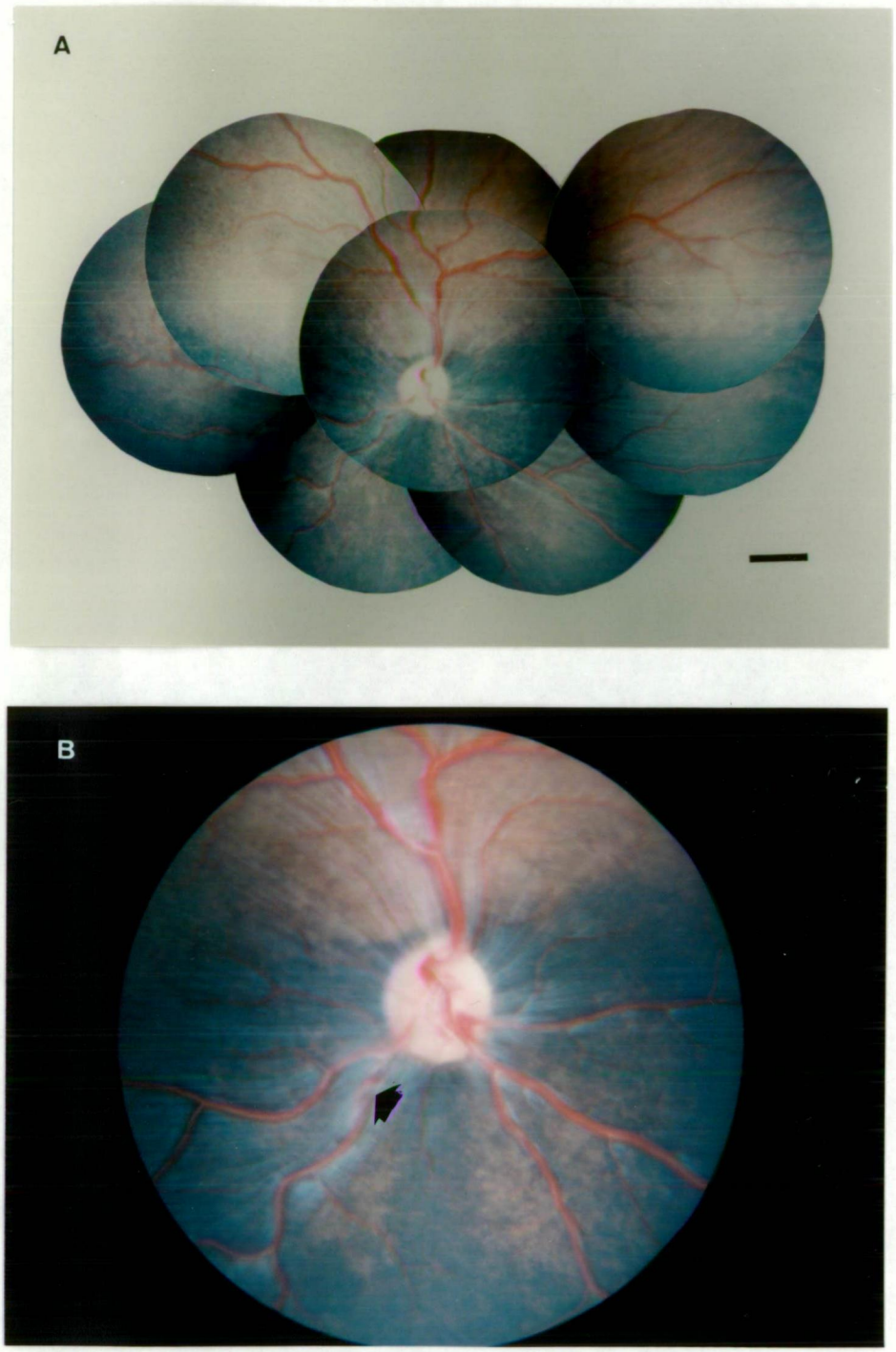

Figure 2.2: The Tasmanian devil fundus

(A) Wide angle montaged view of the right fundus. A true tapetum is not present, only differential pigmentation. The vascular pattern conforms to a similar arrangement as seen in the quoll (Fig. 2.1). One large trunk supplies the upper retina, two main branches to the inferior portion and smaller branches passing horizontally below the pigment border. A vascular sparse horizontal region lies above the optic disc corresponding to the visual streak. Scale bar = 1 mm.

(B) High powered view of the optic disc. Prominent white nerve fibres may be seen converging upon the optic disc. A small segment of vein is seen looping vitread over the companion artery (arrow); veins otherwise are hidden.

Figure 2.3: The opossum fundus

The opossum has a reflecting tapetum, but unlike the quoll, its lower margin passes below the optic disc. Inferiorly, gaps in the pigmentation allow glimpses of the choroidal circulation. Retinal vessels in distinction to the Australian cousins radiate in a more uniform pattern from the disc, dividing the retina into wedge shaped sectors. (Photograph taken by Dr John Haight during sabbatical leave in West Virginia and used with his kind permission).

Figure 2.4: Fluorescein angiogram in the quoll

(A) Choroidal filling and partial arterial filling. Note that in this animal choroidal filling is patchy. In the less intensely fluorescing part of the choroid, small spots of fluorescence can be seen indicating a choriocapillaris structure similar to that seen in the brushtail possum.

(B) Beginning of venous flow. Two laminar stripes of fluorescence can be seen within the large vein entering the optic disc (arrow). As yet there is no capillary flush.

(C) Lamination of fluorescence still visible in large vein (closed arrow); venous undershadowing of large inferior artery (open arrow) is visible. Capillary flush begins.

(D) Large vein is now filled and most of the arteries show 'broadening' effect due to filling of underlying veins. Capillary flush at a maximum. Note that choroidal filling has washed out retinal events in the tapetal part of the retina. The capillary vascular bed appears coarse.

Figure 2.4: Quoll angiogram

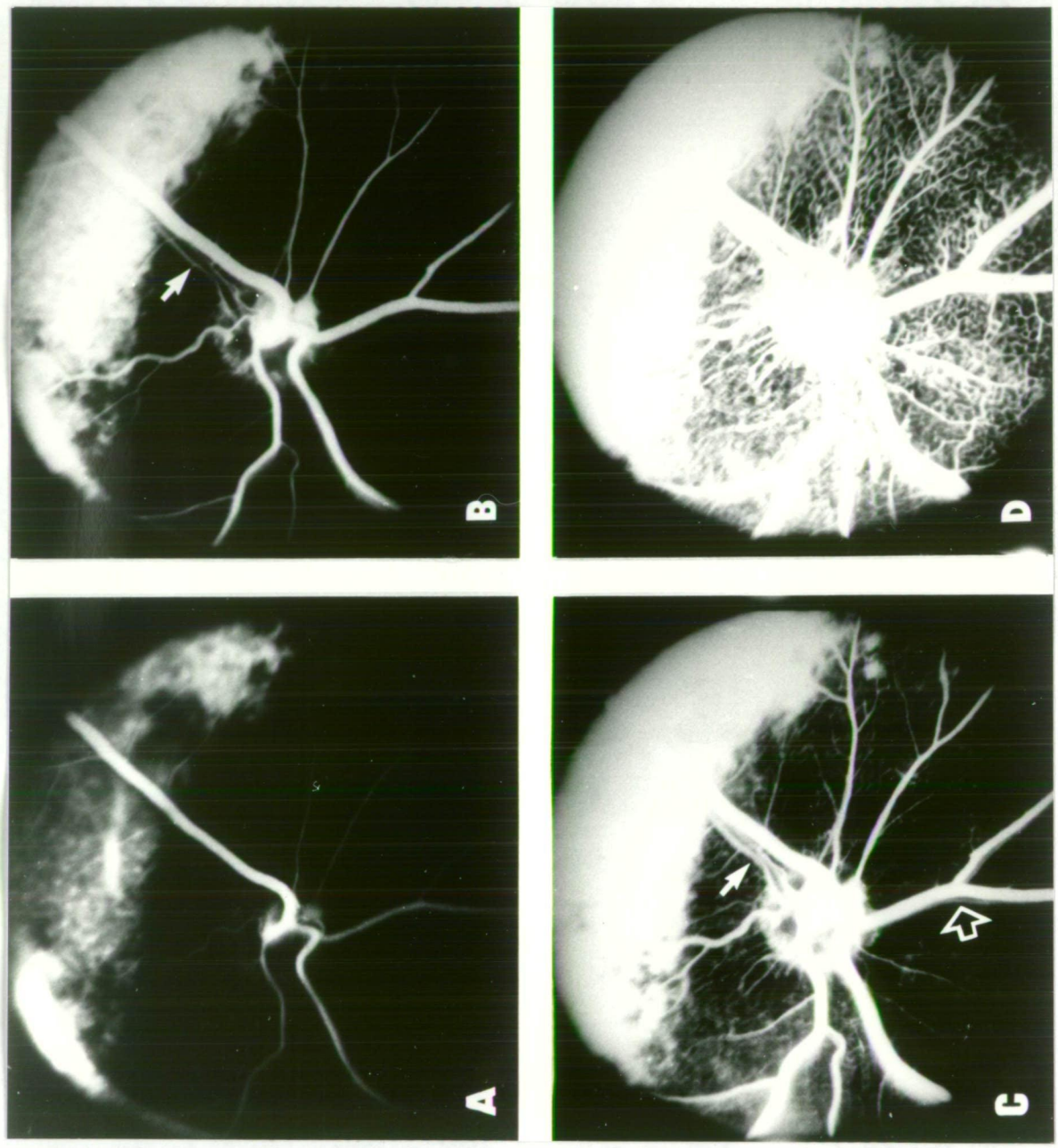

Figure 2.5: Wide angle angiogram in the quoll

(A-C) Patchy choroidal filling, which can only be seen through the tapetum in the superior retina, occurs first. Retinal vessels remain dark against the choroidal background (A, B). Next, the retinal arteries begin to fill. Slight fluorescence is seen near the optic disc in (B); filling is nearly complete in (C).

(D) The venous and capillary phases begin. A faint filling of the large vein paralleling the inferior most artery (arrow) can be seen. The V-shaped black space at the top of the figure represents an as yet unfilled vein which underlies the filled artery. A faint background flush of capillary filling is seen.

(E) Capillary flush and filling of proximal vein (arrow) intensifies. More peripheral vein at top of picture is still empty.

(F) The two large inferior arteries have 'broadened' as their underlying veins fill. Vacant Y at top of picture is also filled. Time taken for entire sequence, approximately 3-4 sec. Scale bar = 1mm.

Figure 2.5: Wide angle quoll angiogram

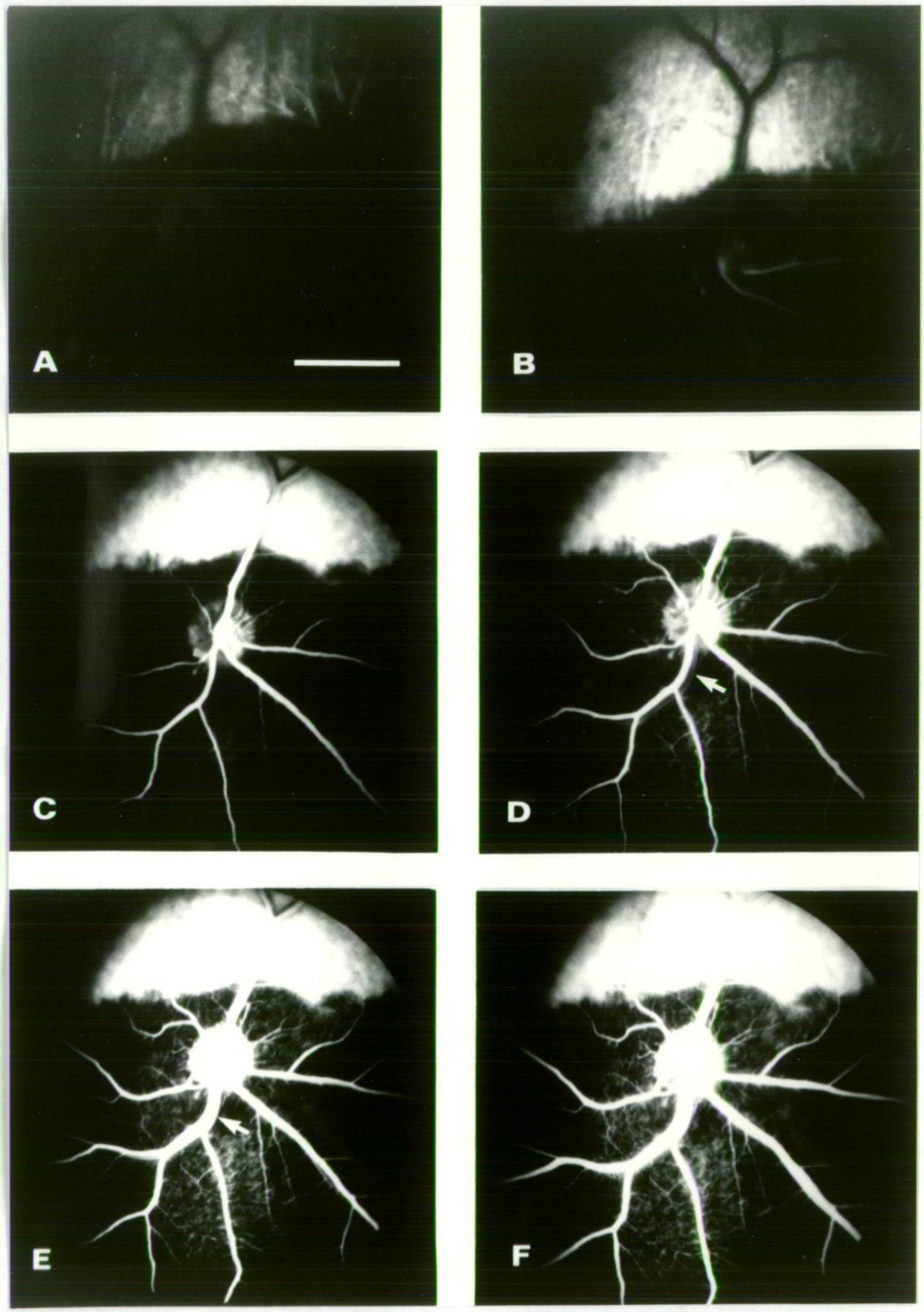

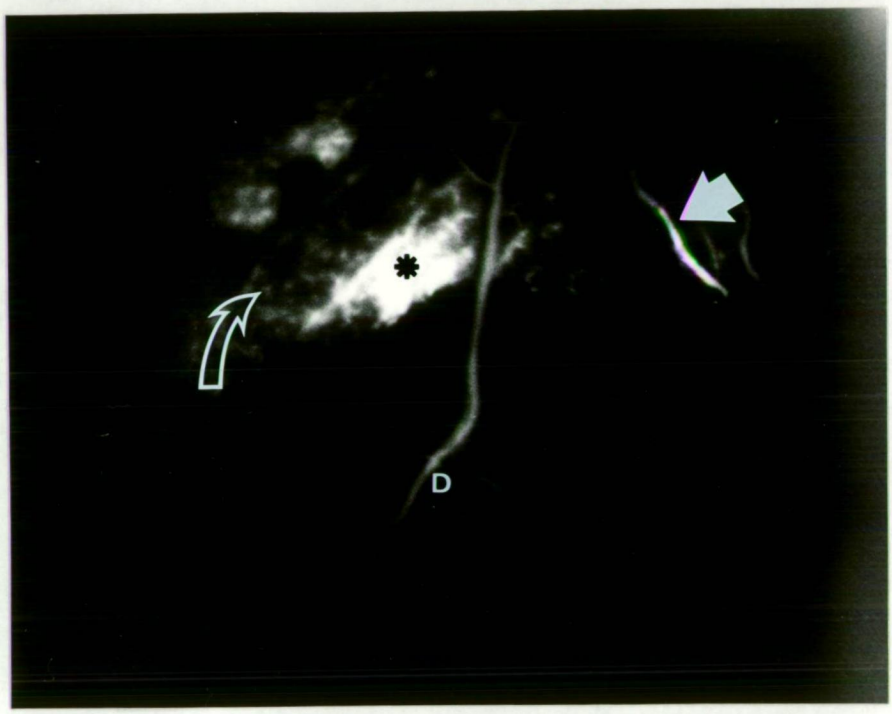

Figure 2.6: Early choroidal filling in the quoll

Magnified view of the optic disc region to demonstrate the stages of choroidal filling. The larger linear choroidal vessels (closed arrow) supply transverse feeding branches (open arrow) to the choriocapillaris (*) which fills in regional patches. Early retinal flow is also seen radiate from the optic disc (D).

Figure 2.7: Fluorescein angiogram in the Tasmanian devil

(A) Wide angle view of early arterial filling. Dense pigmentation blocks view of choroidal filling. Scale = 1mm.

(B) The non-fluorescing patch (white arrow) seen on the inferior artery is caused by a vein which is looping over the artery at that point. The white 'haze' appearing above the disc is choroidal fill, seen through a "thinning" of pigment density in the retinal epithelium.

(C) Arterial fill is complete and venous flush is apparent. Venous loop (white arrow) has now filled and the arteries are beginning to broaden as the underlying veins fill (curved arrows).

(D) Subsequent to early venous filling, the bulk of the capillary phase appears.

(E) Wide angle montage taken shortly after view seen in (D). Arrows mark the narrow band defined by the failure of large vessels from the superior and horizontal vascular arcades to meet. This region corresponds to the visual streak (see text).

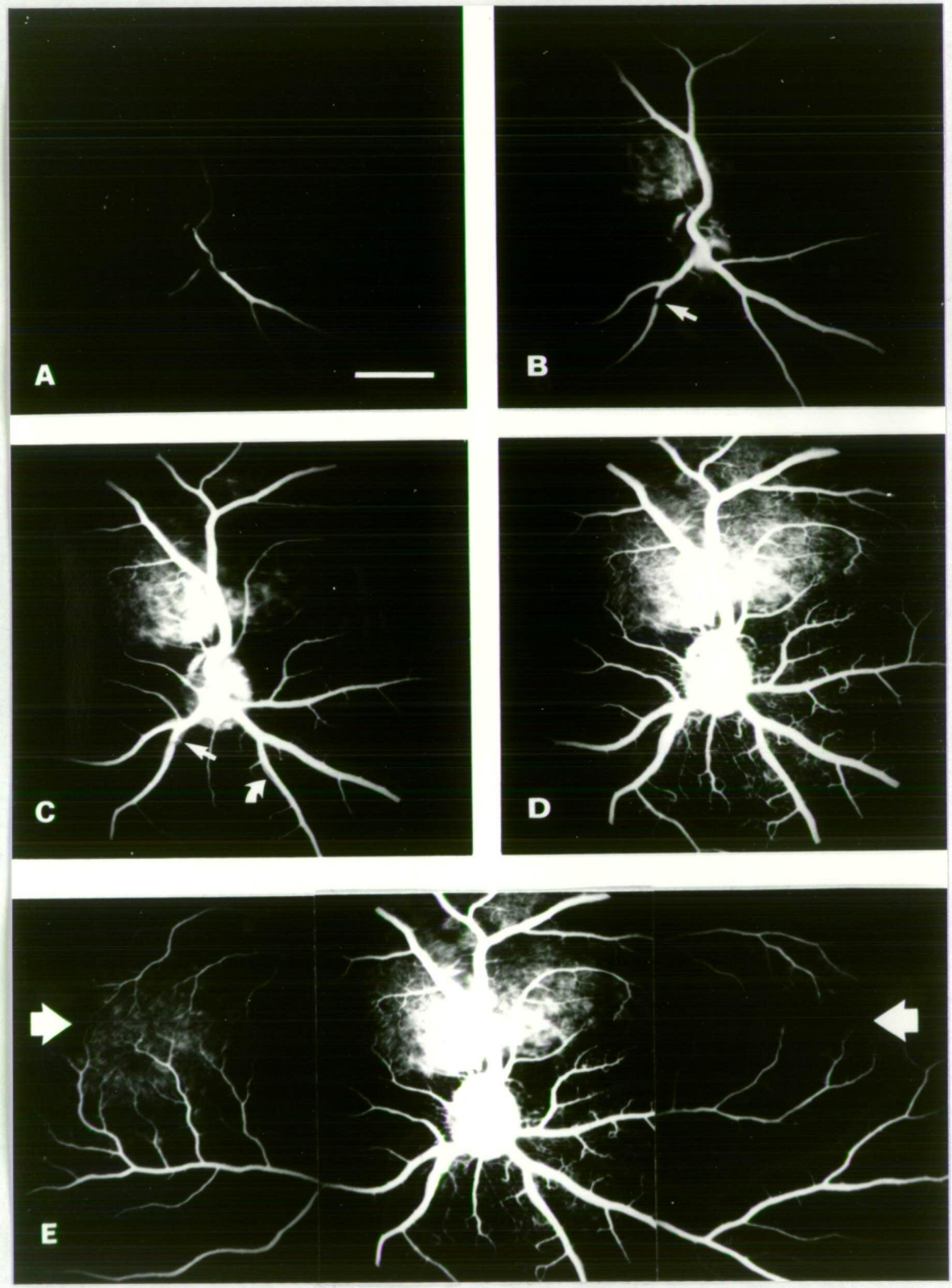
A
B
C
D
E

Figure 2.8: Fluorescein angiogram in the Virginia opossum

(A) Angiogram commences with simultaneous patchy filling of choroid, as viewed through the tapetum, and retinal arterial flow.

(C-F) Gradual intensification of capillary phase and characteristic broadening of the retinal arteries as the underlying veins fill with dye. In this angiogram the capillary filling can be seen to follow a pie shaped segmental sequence with various regions filling and emptying at differing times. In (E,F) an empty artery can be seen (arrow) outlined clearly by the strongly fluorescing vein deep to it. Arteries began to empty approximately 3 seconds after first appearance of fluorescence.

Underlying choroidal events only partially obscure retinal detail, suggesting a partial pigmentation barrier (tapetum) between the choriocapillaris and retina. Contrast this with the choroidal tapetum in the quoll (Figs. 2.4, 2.5) where no pigmentation or tapetum lies between retina and the choriocapillaris; intense choroidal events totally obscure retinal fluorescence.

(Angiogram performed by Dr John Haight during sabbatical leave in West Virginia and included with his kind permission.)

Figure 2.8: Virginia opossum angiogram

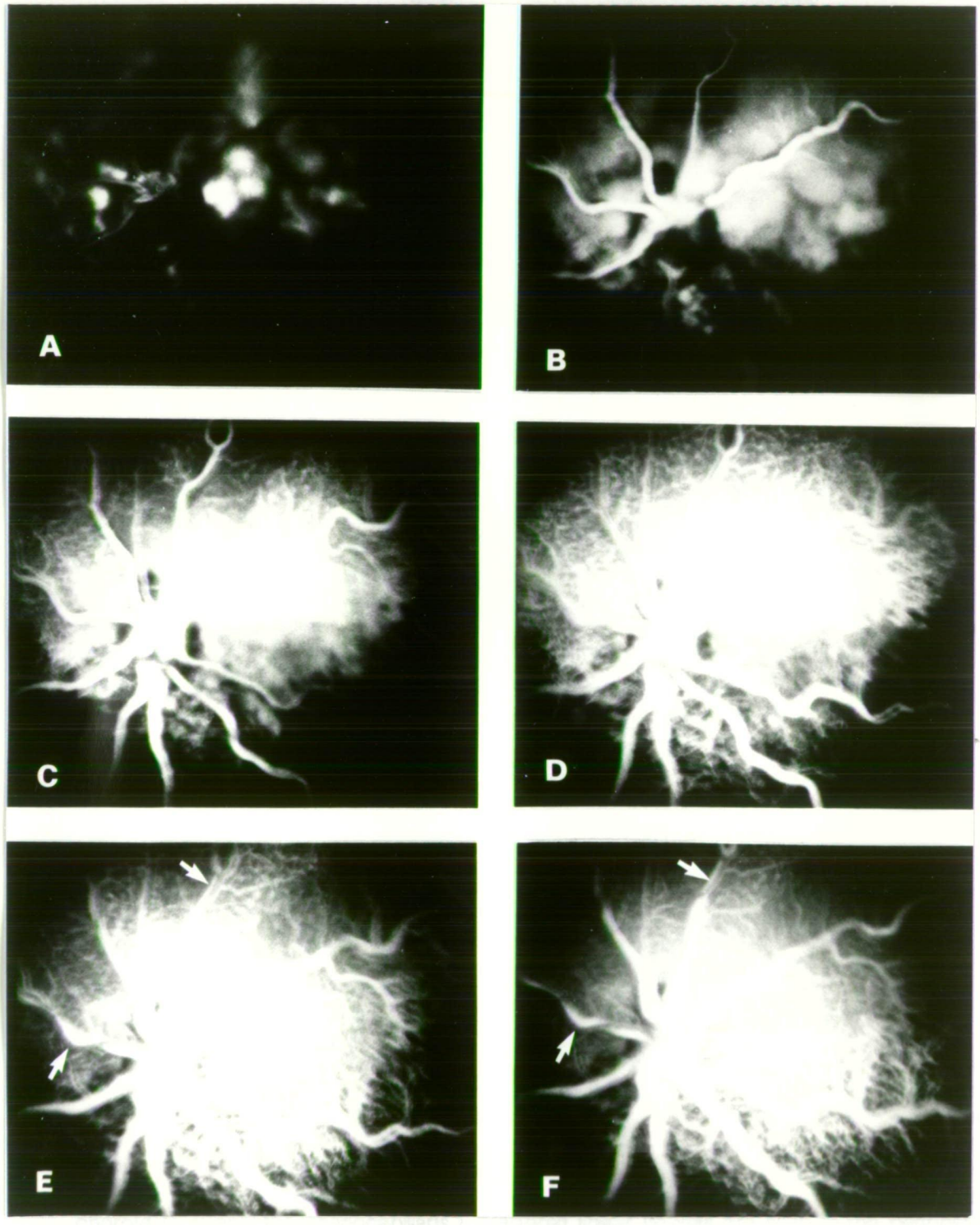

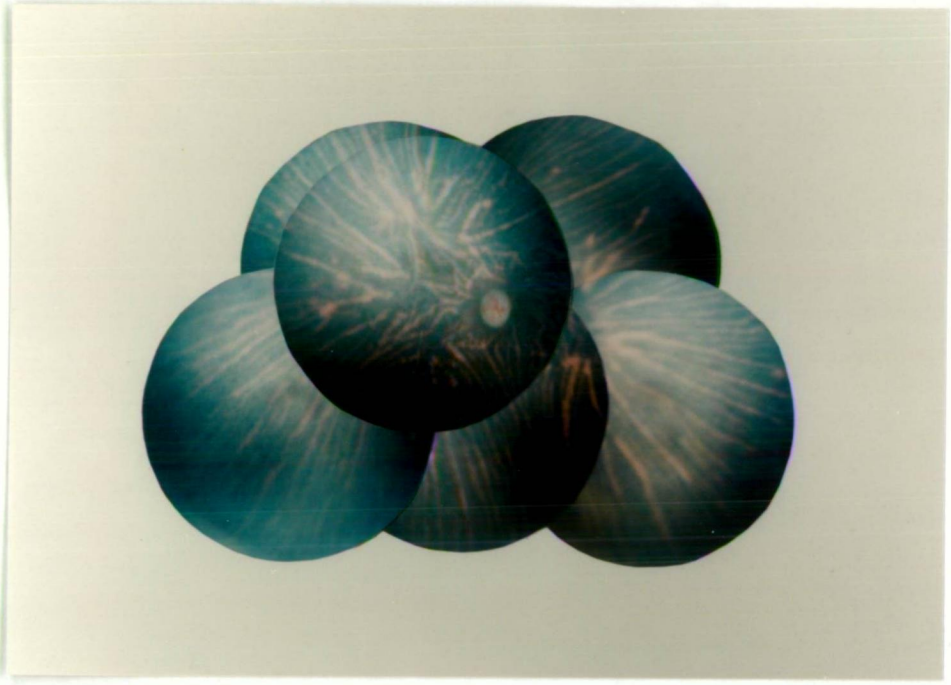

Figure 2.10: The sugar glider fundus

Wide angle view of the right eye. The retina is avascular, and like the possum, has a frond of vessels protruding from the disc. Streak-like choroidal vessels may be seen through gaps in the retinal pigment epithelium. Otherwise the fundus is uniformly pigmented.

Figure 2.11: Fluorescein angiogram in the brushtail possum

(A) Fluorescence appears simultaneously in the cluster of vessels in the optic disc and, in the superior retina only, in the choroid where a series of fluorescing white spots can be seen dimly in the background. The choroidal circulation, seen through the punctate pigment hiatuses in the superior retinal epithelium (see text).

(B,C) Intensification of choroidal fluorescence. Small vessels protruding from optic disc are clearly outlined.

(D) Further more uniform intensification. Scale bar = 100mμm; scale in (D) applies to (A-D)

(E) Higher power view of optic disc showing the large number of intertwining vessels protruding from the disc. Note the vessel walls are impermeable to fluorescein.

(F) Wide angle angiogram taken from the same possum showing zonal filling of choroid. The smaller scale, punctate appearance of choroidal filling resembles the early speckled choroidal arterial filling seen in the quoll superior retina (see Fig. 2.4A, 2.6). Note the larger scale geographic differential filling. Filling in the right side of the choroid is further advanced than on the left, with an irregular border dividing the two.

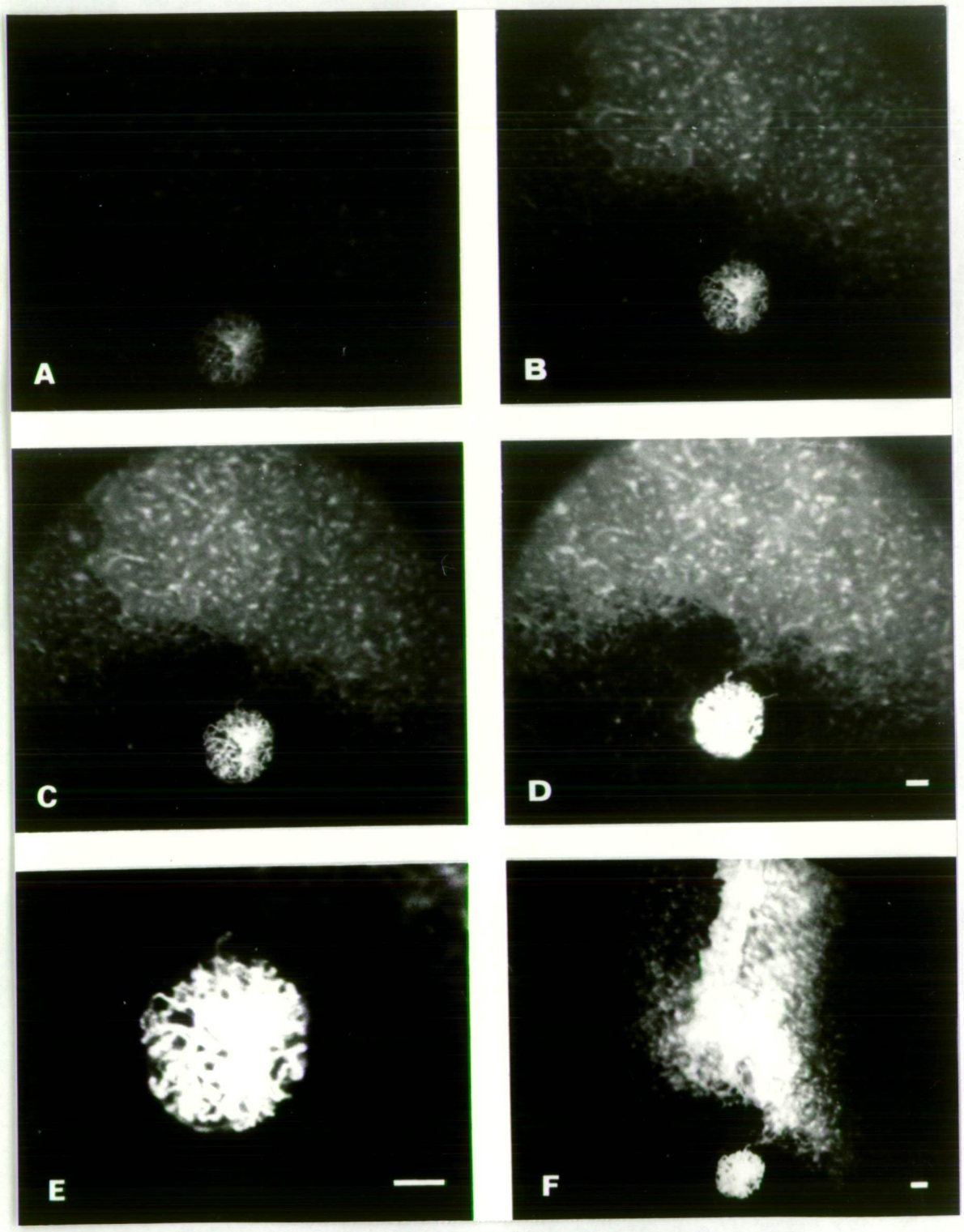
A
B
C
D
E
F

Figure 2.12: Fluorescein angiogram of the sugar glider

Unusual example of zonal choroidal filling. (A) Optic disc (centre) and choroid fluoresce simultaneously. Note choroidal area indicated by dots. (B) Disc retains fluorescence, but choroid dims. (C) Peripheral choroid begins to fill as optic disc vessels empty. Choroid in neighbourhood of disc remains relatively empty. Empty space corresponds in shape to that outlined in (A). (D) Upon recirculation, disc and choroid fluoresce with uniform intensity. The streak-like pigment defects seen in the fundus photograph of Fig. 2.10 are not visible here. They are seen only at greater distances from the optic disc than are afforded by this narrow angle of view.

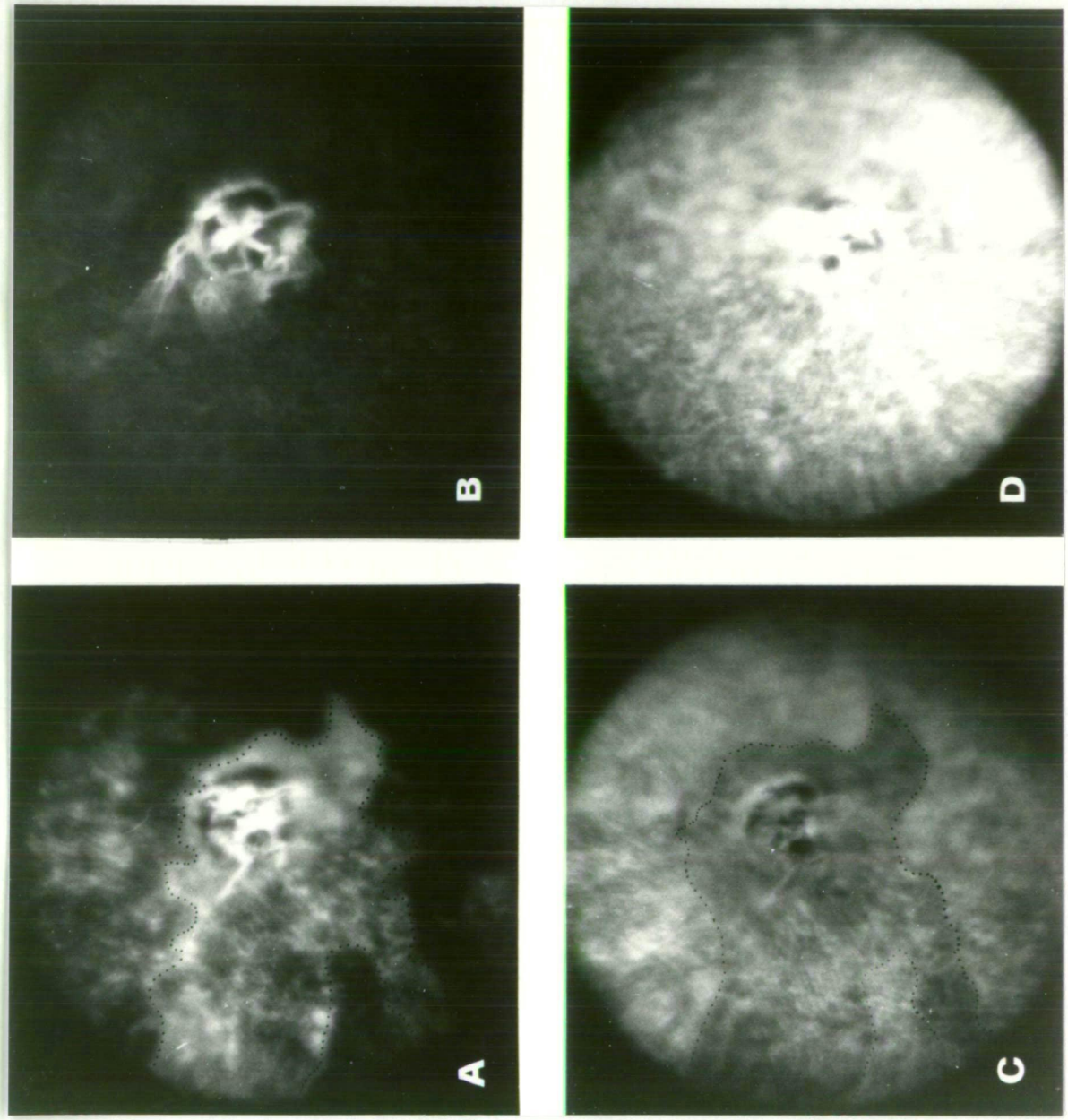
B
D
A
C

2.3.3 Placental comparisons

Retinal angiography of humans, cats and rats has been presented by other investigators (Bellhorn et al. 1977, Dobi et al. 1989, Flocks et al. 1959, Novotny and Alvis 1961). Angiographic results were gathered in these animals in order to facilitate marsupial-placental comparisons.

2.3.3.a Fundus

Normal rat and human fundi are pigmented in their entirety though some regional variation (See Howell et al. 1982) in pigment intensity is seen in rats (Fig. 2.13). The superior half of the cat's retina is backed by a reflective tapetum, whilst its lower half is conspicuous for its blue pigmentation (Fig. 2.13). In cats the region of maximum photoreceptor density, the area centralis, is backed by the tapetum (Hughes 1975). Fundoscopic observations suggest that in the quoll, too, the visual streak is backed by the *tapetum lucidum*. In cats, humans and many other primates a small circular sparsely vascular, or even truly avascular, region is seen temporal to the optic disc (Wong and Hughes 1987, Johnson 1901, 1968). This coincides with the position of the area centralis (cats) or macula (primates) and is analogous to similar regions of high ganglion cell density as seen in association with the visual streak in the Tasmanian devil's (Tancred 1981) and very probably the quoll's retinae (see discussion).

2.3.3.b Angiography

Retinal angiograms are similar in the placental species. Choroidal filling begins slightly before the beginning of the retinal phase. Radial filling of the retinal arteries is followed by filling of the retinal capillaries and, finally, by venous return (Figs. 2.15, 2.16, 2.17).

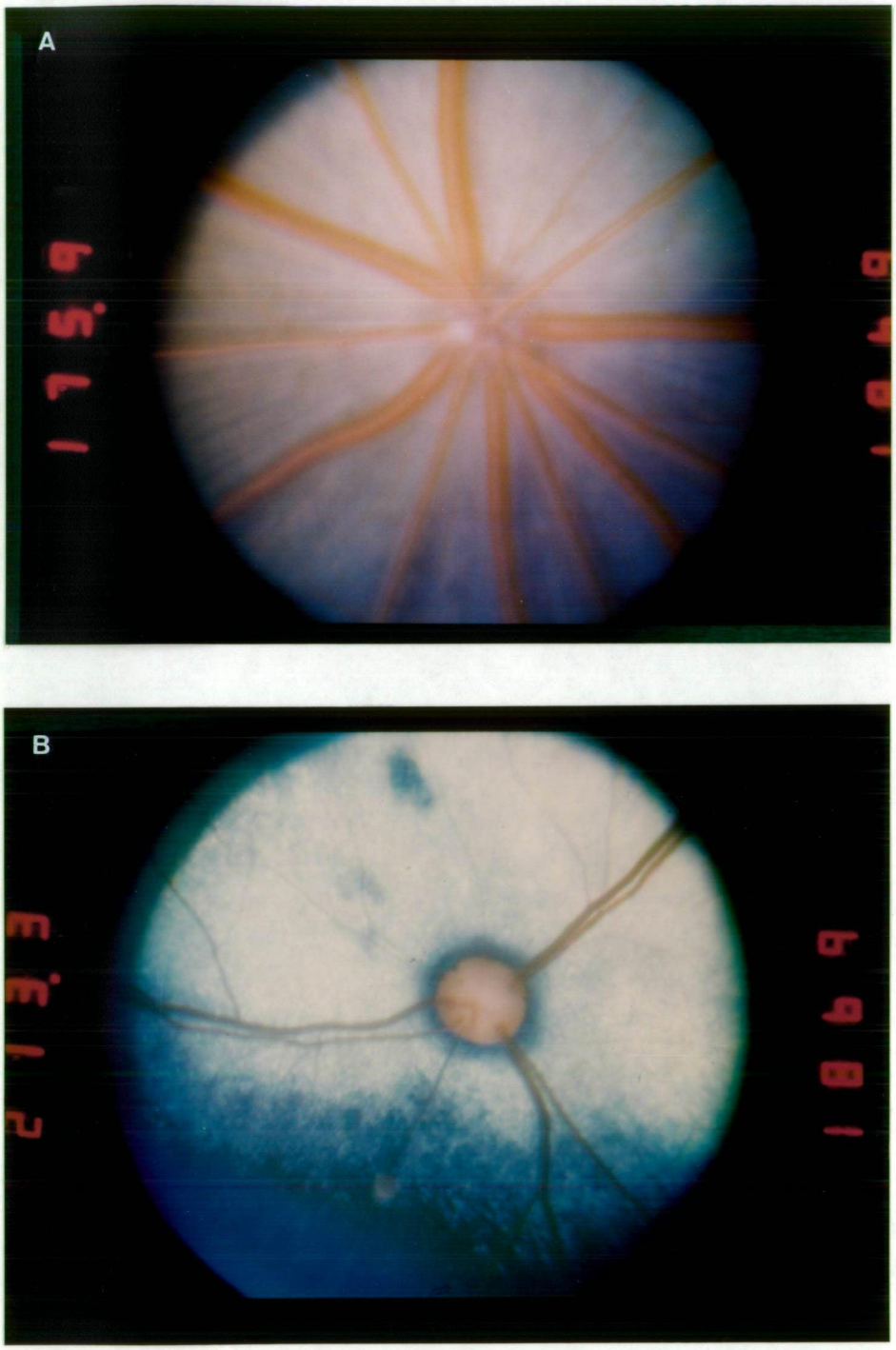

Figure 2.13: The fundus of the rat and cat

(A) Rat. Narrow angle views taken with the Zeiss fundus camera. Pigmentation is a little more prominent in the lower fundus. The vasculature radiates from the disc in a regular spoke-like pattern. The venous and arterial circulation is distinct and clearly discernible.

(B) Cat. A tapetum lucidum is present whose lower margin passes below the optic disc. Brilliant blue pigmentation is seen in the inferior hemiretina. Radiating vessels are visible emerging from the disc. Note that arterial and venous vasculature is separate.

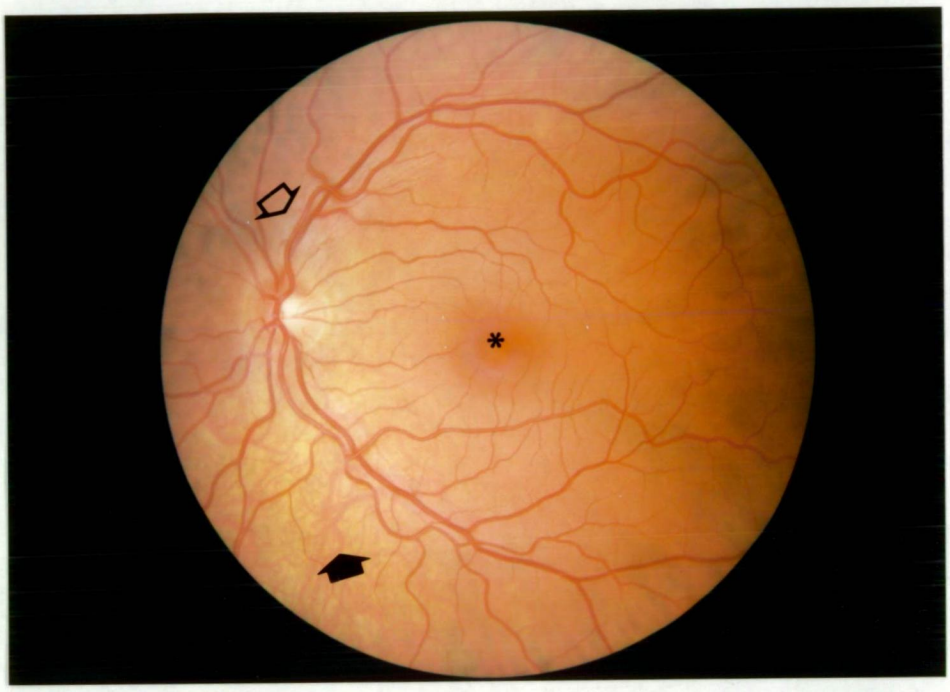

Figure 2.14: The human fundus

Single wide angle view of the left eye. The fundus is a uniform orange brown in colour. An asymmetric vascular pattern radiates from the optic disc, outlining the macula region temporal to the disc (*). Venous and arterial circulation is separate. White nerve fibres are visible superiorly (open arrow). Choroidal vasculature is visible inferiorly (closed arrow).

Figure 2.15: Fluorescein angiogram in the rat

(A) Retinal arterial filling commencing. Open arrow indicates artery whilst the closed arrow a vein poorly outlined aginst the initial capillary flow.

(B) The coarse capillary bed has filled and the typical lamination (arrow) of early venous filling is apparent. Note that the capillary phase has reached maximal intensity before venous filling, (C).

(D) With further venous flow, the arterial vasculature is beginning to empty, (open arrow).

Figure 2.15: Rat angiogram

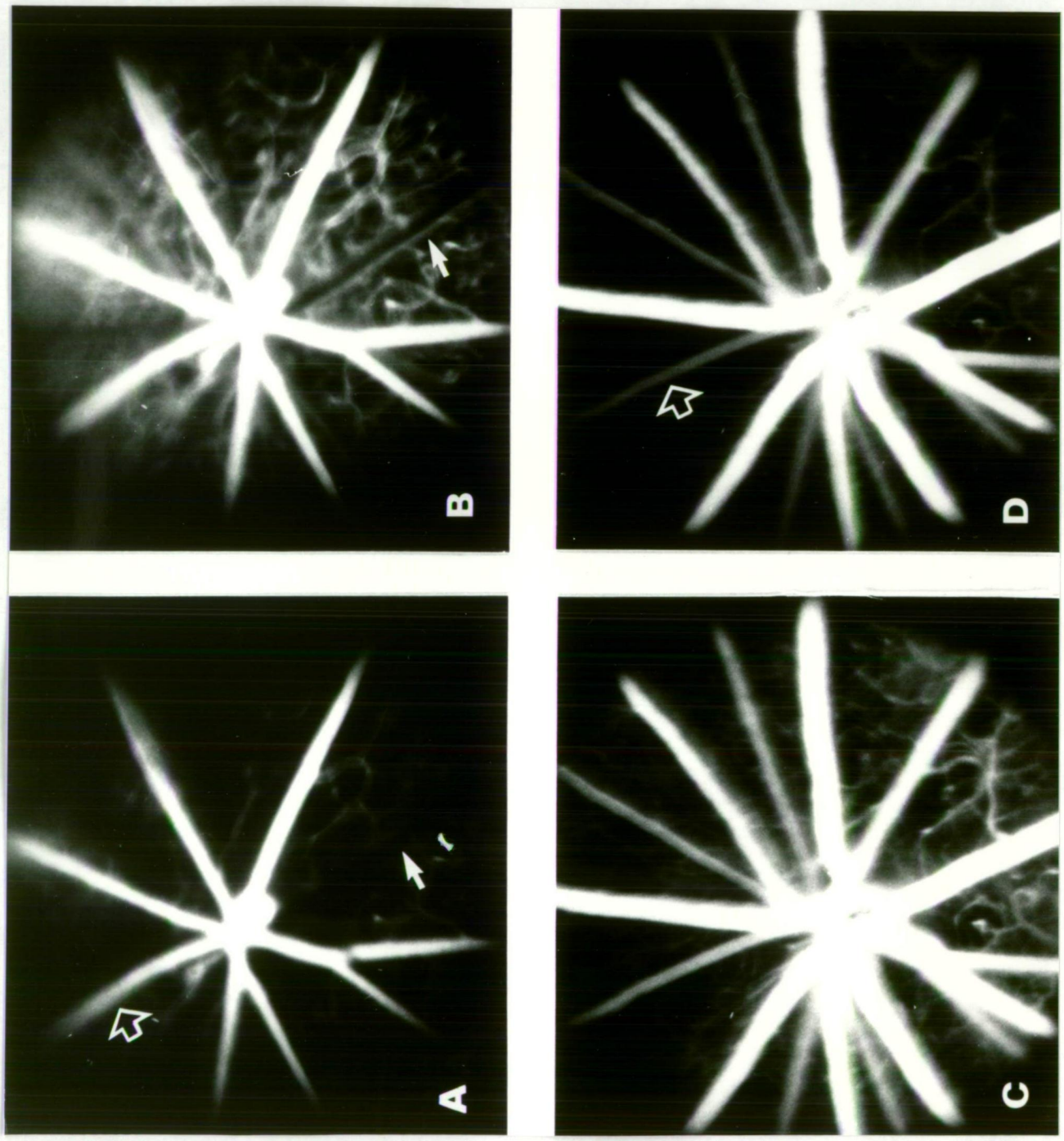

Figure 2.16: Fluorescein angiogram in the cat

(A) Intense choroidal filling evident through the tapetum above. Early retinal arterial filling.

(B) Commencement of venous phase with the typical lamination of early flow (arrow).

(C-D) Further venous filling. Capillary events muddied by the choroidal fluorescence.

Figure 2.16: Cat angiogram

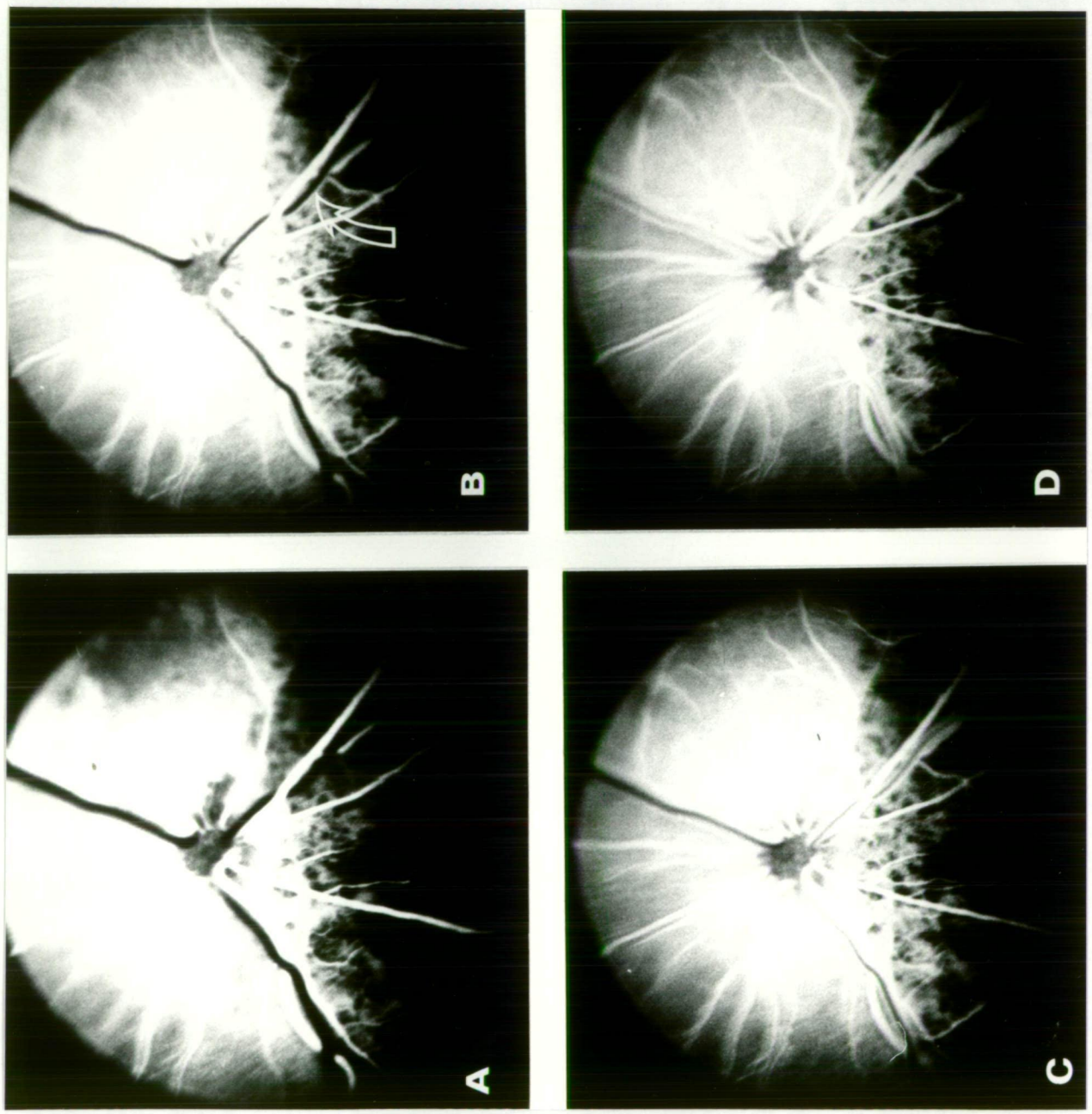

Figure 2.17: Human retinal angiogram

(A) Arterial phase with background choroidal flush. The veins are empty and outlined by underlying choroidal events.

(B) Retinal capillary flow and the typical lamination of early venous filling (arrow).

(C) Intensification of the venous phase.

(D) Further venous filling with arterial and capillary emptying. Compare the sequence with the quoll (Fig. 2.4, 2.5) and Tasmanian devil (Fig. 2.7) where venous filling parallels rather than follows capillary filling.

Figure 2.17: Human angiogram

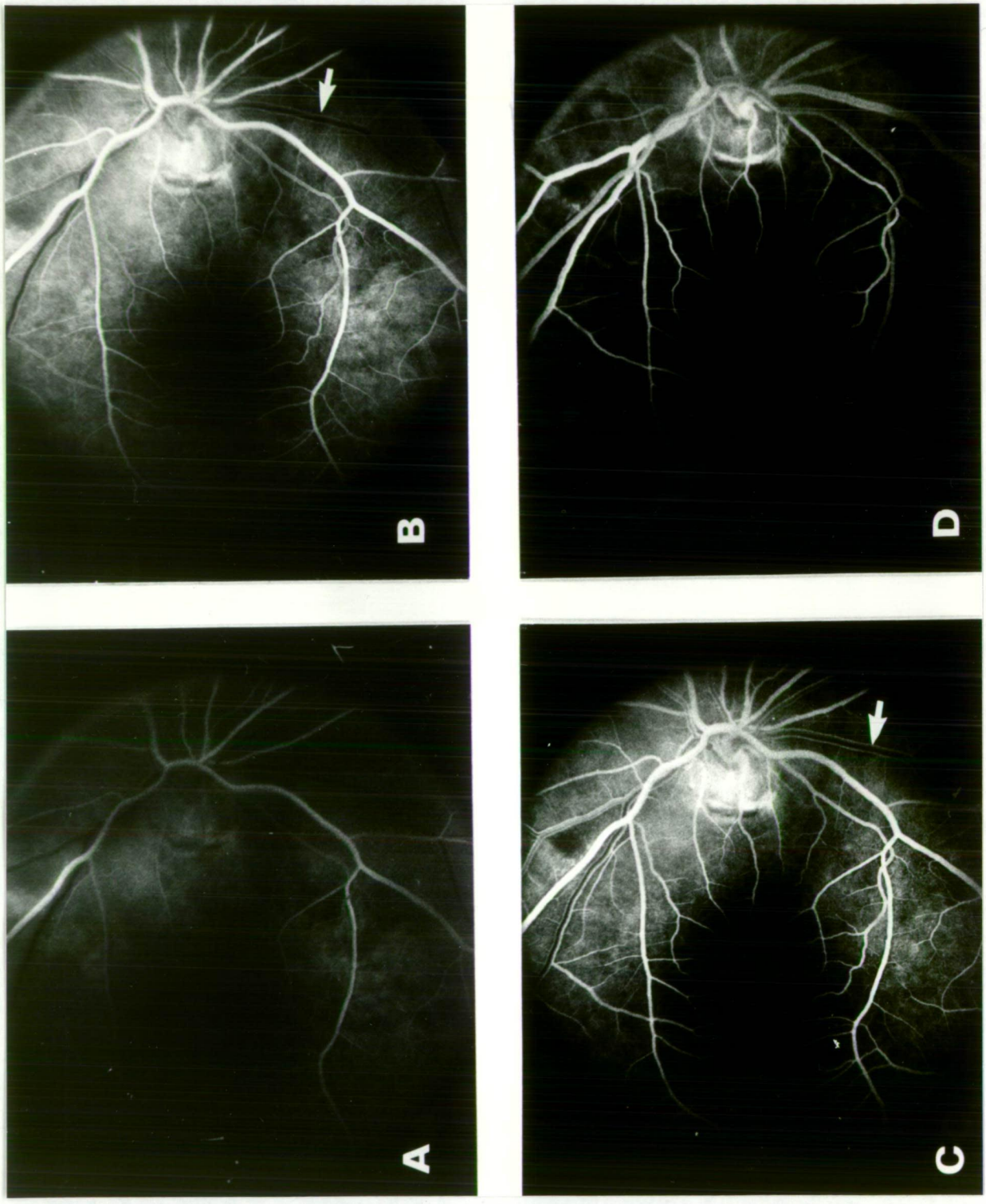

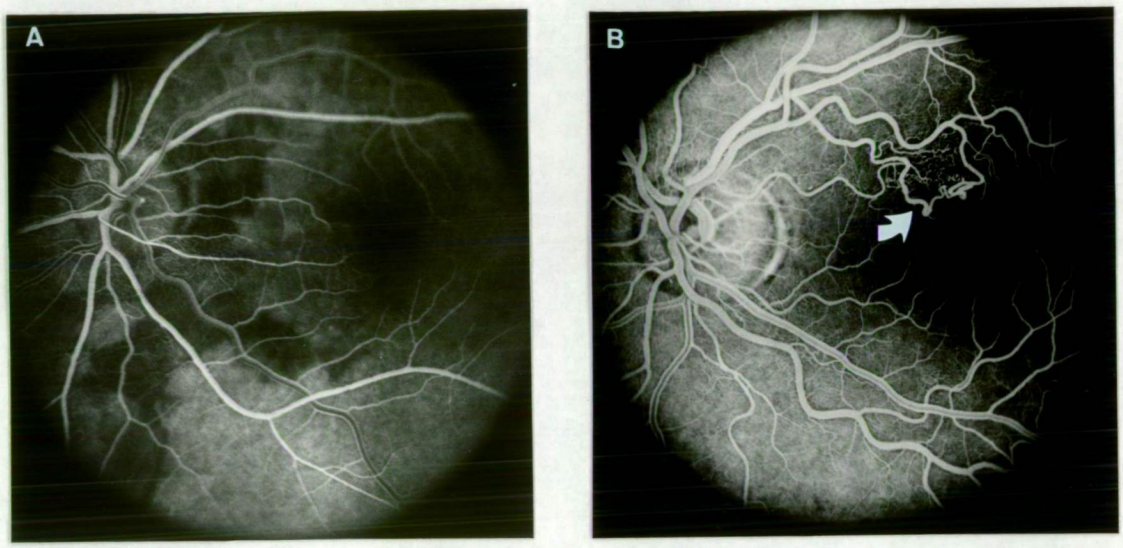

Figure 2.18: Features of the human angiogram

(A) The choroidal circulation is patchy in filling in the early phase. Compare Fig. 2.6, 2.11, 2.12).

(B) An arteriovenous anastomosis within the human retina, an unusual anatomical variant. Note that the superior venous circulation draining this anastomosis is further advanced than that draining the inferior, non-shunted retina.

2.4 DISCUSSION

"The time has come, the walrus said
to talk of many things" ..... Lewis Carroll.

Analysis of the findings needs to be predicated upon a consideration of the technique employed and its limitations. The descriptive aspects of retinal appearance are important in drawing conclusions about function and as a prelude to interpretation of the angiographic events.

2.4.1 Ophthalmoscopy and photography: history

The well known eyeshine seen in animals, particularly around twilight hours, is the simplest form of fundal viewing; the tapetum merely reflecting incoming light to the observer. This observatio no doubt to the ancients would have given many animals mystical properties with the eyes appearing to emit fire. A major optical advance, although not an ethical advance, was the observation by Jean Mery in 1704 that the cat fundus became visible when the animal was immersed in water (Wood, 1917). The magnificent appearance of the vasculature, tapetum and pigment was revealed but no doubt its significance was not fully understood. Visualisation of the fundus is however commonly attributed to Von Helmholtz, the celebrated physicist and father of fundoscopy who, in 1851, invented the ophthalmoscope (Westheimer 1983). A disciple at the time, Richard Liebreich popularised the instrument, developed a method for photography and published an Atlas of Ophthalmoscopy in 1863, being hailed as the "first iconographer of the fundus oculi" (Beherman, 1968).

The ophthalmoscope has subsequently gained immense clinical utility and has also been used widely to characterise many different mammalian, reptilian, amphibian and avian fundi (Bruns 1882, Johnson 1901, 1927, 1968, Prince 1956, Wood 1917).

In recent times improvements in the photographic capture of the fundoscopic appearance has come with the introduction of the task specific fundus camera, most famous of which is the Zeiss FF-4. The fundus camera relies on one of two means of visualising the retina. Either the camera acts as a telescope viewing the optically distant fundus, or alternatively, the refractive power of the eye is eliminated with a contact lens allowing the use of a

biomicroscope system to view posterior ocular structures (Leutwein and Littman 1985). The former approach is used in the fundus camera.

Improvements have come with wide angle attachments (Turner et al. 1981), stereoscopic viewing, bilateral synchronous angiography (Laux 1976) and video and digital angiography (Favilla et al. 1986). The fundus camera, like the ophthalmoscope, has established itself as an invaluable workhorse of both clinical and research practice.

2.4.2 Fundus photography: equipment and technique

The fundus cameras used were designed for the human eye and not for the smaller, highly dioptric eyes examined in this study. Hence the optical result is in some cases less than optimal. Attempts at adapting operating microscopes and conventional fluorescence microscopes produced inferior fundal imaging when compared with the fundus camera. Both of these alternative approaches required optical elimination of the refracting corneal surface. This was achieved with a contact lens which in its simplest form consisted of a cover slip applied to the eye with a layer of methylcellulose. Both approaches were lacking in one or more areas of illumination, camera attachment, sequential capture of angiographic events, depth of field, unwanted reflections or limited field of view. Thus, at the end of the day, despite the limitations of the fundus camera, better resolution was not afforded by any other instrument; the fundus camera, particularly the wide angle camera, being more than adequate for the needs of this study.

The magnification of the fundus camera is inversely proportional to the focal length of the eye (Leutwein and Littman 1985). Taking the axial length of the eye as a measure of focal length, greater overall magnification is afforded by small eyes (see Hughes 1977a, retinal magnification factor). Without a concomitant increase in the camera's depth of field, more of the image will be out of focus. However, the wide angle fundus camera, though providing less magnification by virtue of its design, does provide greater depth of field and, thus enhances image clarity (cf Figs. 2.4 and 2.5).

The optical results may be further affected by the intrinsic optical properties of the eye itself. If, as is accepted by some, the physical optics of an eye are matched to its neurological capabilities (Williams 1985), then one can assume that the low spatial acuity found in these predominantly nocturnal eyes would be accompanied by optics of lower quality than are seen in the diurnal and far more acute human eye. Thus, when using the optics of the eye in reverse, as is done during fundus photography and angiography, there would be an expected

degradation of image quality irrespective of the quality of the instruments used. A further consideration when viewing the fundus through a dilated pupil is the degradation of image quality that results from the optical aberrations of peripheral rays (Hughes 1979a). The examples of small animal (rat) photography seen in the study of Hughes (1977b) indicate the difficulty in obtaining good quality results in small eyes.

2.4.3 Angiography

2.4.3.a Fluorescein: the substance

Sodium fluorescein is weakly acidic dye of the xanthene series, having a molecular weight of 376 and a molecular size of 0.55nm (Jampol and Cunha-Vaz 1984). It has a number of favourable properties which lend itself to widespread use in ophthalmology; it is non toxic, water soluble, binds weakly to tissue and, importantly, possesses the attribute of fluorescence with a high quantum yield. In circulating blood the absorption peak is 465-490 nm and the emission peak 520 nm whilst the ocular absorption peak is 480 nm and the emission peak, as for blood, is 520 nm. Following systemic administration, fluorescein is conjugated in the liver to form fluorescein monoglucuronide, itself a fluorophore but with differing absorption properties (Grotte et al. 1985). This metabolite however is not important in the initial phases of fluorescein retinal angiography.

With increasing concentration of dye increasing fluorescence is seen until one or both of the following physical events occurs; covalent bonding produces dimerization and polymerization and/or quenching. This latter property is due to the nonradiative dissipation of absorbed energy (Jampol and Cunha-Vaz 1984); self absorption of emitted light reduces fluorescence and shifts the emission spectrum towards longer wavelengths explaining why concentrated solutions appear yellow-orange and dilute solutions appear greener. However the level at which quenching occurs, 2.5mg fluorescein/ml, is not normally achievable within blood given the 300 to 600 times dilution which occurs upon systemic venous administration (Flower and Hochheimer 1977).

In addition to the free salt of fluorescein, conjugation with large molocules such as albumin or dextran has been used as a means of determining relative permeability properties (Bellhorn et al. 1977, Sollom 1968). However, fluorescein itself still remains the mainstay of diagnostic use predominantly for retinal (and choroidal) angiography. Other dyes, for example indocyanine green, used separately for choroidal angiography (Bischoff and Flower 1985, Hochheimer

1979) or in conjunction with fluorescein (Flower and Hochheimer 1976) have failed to surpass fluorescein in its ability to supply functional information about ocular circulation.

2.4.3.b Fluorescein angiography

One of the earliest functional studies of retinal circulation dates to 1909 when Abelsdorff and Wessely described ophthalmoscopically the appearance of potassium fluorescein leaking into the vitreous from the avian pecten, suggesting the path whereby the vitreal surface of the avascular avian retina was nourished. Subsequent animal work by Kikai (1930) determined optimal dosage and optical filtration requirements and was followed in 1955 by human intravenous administration of flourescein with ophthalmoscopic viewing of retinal fluorescence (MacLean and Maumenee 1959). Photographic recording of the ocular passage of fluorescein followed in 1959 when Flocks et al. produced a cinephotographic study in the cat, soon followed by a report in humans prepared by two medical students, Novotny and Alvis (1961). This method has since proved to be of immense value in the diagnosis of human retinal pathologies (Aaberg 1980, Blacharski 1985, Hayreh 1974, Nielsen 1982, Schatz et al. 1978) and has provided useful functional information about blood flow in the vertebrate retina in general (Bellhorn and Bellhorn 1975, Bellhorn et al. 1977, Ben-Sira and Riva 1973, Hill and Young 1976, Laatikainen 1976, Newsom 1968 and Ringvöld and Olsen 1979).

By contrast, attempts to image blood flow within the choroid have proven less satisfactory. Firstly, the blocking effect of the retinal epitheium, whilst effectively absorbing stray light, also serves to block the prying light of any imaging device. Secondly, blood fills the entire choriod almost simultaneously, making temporal resolution difficult. Thirdly, the choroidal bed is a large, three dimensional network some parts of which obscure deeper vascular structures whilst other vascular segments are orientated perpendicular to the film plane. This makes capture on two dimensional film difficult. Finally, the permeabilty of the fenestrated choriocapillaris bed allows much of the poorly protein-bound fluorescein to leak into the extravascular space creating a background blur which further obscures vascular events. Thus, the emphasis upon retinal circulation events does not reflect a lack of importance of the choroidal circulation, but rather the difficulty in imaging this generally obscured vascular bed.

Not only has fluorescein angiography been applied to posterior structures but also to the anterior segment of the eye (Kottow 1980), providing functional information about blood flow and permeability of the vasculature within the iris, conjunctiva, sclera and episclera (Hayreh 1978, Meyer 1988). As a further measure of vascular function, fluorophotometry has been employed to determine permeability of the aqueous and blood retinal barriers. Permeability is

related to the build up of fluorescein within the chambers of the eye following systemic administration of the dye (Jampol and Cunha-Vaz 1984).

Retinal fluorescein angiography remains one of the most valuable clinical and experimental techniques for gauging morphological aspects of ocular vasculature and functional aspects of nourishment at the battlefront of visual transduction.

2.4.4 Vascular retinae

2.4.4.a Retinal pigmentation and the tapetum lucidum

Light absorbing pigments serve to reduce light scatter in the retina and within the globe, and thus contribute to greater visual acuity. A *tapetum lucidum*, on the other hand, enhances re-reflection of light through the photoreceptor layer, increasing sensitivity, but only at a cost to visual acuity. Tapeta lucida are typically found in animals that live in environments with low illumination levels. In many placental mammals the tapetum is confined to the upper half of the retina, thus serving that portion of the visual field which lies below the horizon. In cats the region of maximal visual acuity, as defined by the horizontally elongated area centralis, lies above the optic disc within the tapetal portion of the retina and corresponds to a peak ganglion cell density of up to 10 000 cells/mm^2 (Wong and Hughes 1987). Johnson's (1901, 1968) illustrations show that many placental mammals, among them the carnivorous raccoons, wolves, foxes and mongooses, as well as the herbivorous gazelles, deer, reindeer and cattle, all possess a tapetum in which the overlying retina displays a circular or horizontal area of low vascularity along the lower tapetal margin. This suggests that in all of these animals the region of maximum acuity is to be found within the tapetal area of the retina. Such an arrangement would presumably enhance an animal's ability to detect and fixate upon small movements, a valuable asset for both hunted and hunter. In these cases, the cost to visual acuity is most likely outweighed by the benefits of enhanced sensitivity.

Among marsupials, dorsal half tapeta are found in the American Virginia opossum, in the Australian quoll and in the now almost certainly extinct Tasmanian tiger, *Thylacinus cynocephalus* (Braekevelt 1976, Pirie 1966, Walls 1942). According to Walls (1942) and Pirie (1966) the tapetum in the Virginia opossum is of the primitive, retinal type such as found in fishes and reptiles, but not in mammals. Functionally, the opossum tapetum is reported to be 1-1.4 log units more reflective than the non-tapetal areas (Oswaldo-Cruz et al. 1979). Braekevelt (1976) demonstrated clearly that the Virginia opossum's tapetum is a part of the retinal (pigment) epithelium. In non-tapetal regions the epithelial cells contain typical

melanosomes; in the tapetal region these are replaced by reflective lipoidal spheres. This type of tapetum could significantly corrupt image clarity by enhancing random light scattering within the retinal epithelium. As these cells interdigitate with the outer segments of the photoreceptors, light scattering occurs right at the focal plane, optically the worst possible place for this to happen. The tapeta of Australian marsupials are of the reflective, choroidal type, as seen in most other mammals (Walls 1942). Such a tapetum mirrors rather than scatters light and, as long as the incident light is nearly perpendicular to the retinal surface, this tapetum may not affect acuity nearly as adversely as would the light scattering retinal type.

The Virginia opossum marches to a different drummer. This marsupial and its South American cousin, *Didelphis marsupialis*, have *areae centrales* rather than visual streaks (Hokoç and Oswaldo-Cruz 1979, Kolb and Wang 1985, Rapaport et al. 1981). The visual acuity of *D. marsupialis*, which most likely would be similar to its North American counterpart, has been estimated at around 1.25 cycles/degree (Silveira et al. 1982) This is less than the acuity of the quoll at 2.3 cycles/degree (Harman et al. 1986), the possum with an estimated acuity of 4.8 cycles/degree (Freeman and Tancred 1978) and considerably less than the 6-8 cycles/degree acuity of the cat (Blake 1988). The opossum's area centralis overlies a light scattering retinal tapetum. It is possible that this scatter has little effect upon the already limited acuity of this eye. It would seem that the opossum, with an already inbuilt and severe limitation on acuity, simply maximises sensitivity and retains a more primitive type of tapetum.

The angiographic results show that flow patterns in the quoll and opossum eye are consonant with their differing tapetal morphologies. In the quoll's angiogram the choroidal blush in the tapetal part of the retina eventually obscures the angiogram totally, indicating that the retinal epithelium in that portion of the retina is transparent (Fig. 2.4). By contrast, in the Virginia opossum the vascular events overlying the tapetum become muddied after choroidal filling, but are not totally obscured, demonstrating that a partial light barrier exists between the choroid and the neuroretina (Fig. 2.8).

Contrary to the report of Duke-Elder (1958), the Tasmanian devil would appear not to have a functional tapetum despite the claim that a *tapetum fibrosum* exists within the choroid.

2.4.4.b Vascular pattern

The Tasmanian devil and Virginia opossum findings confirm earlier ophthalmoscopic observations of Johnson (1901) and Tancred (1981) who reported vascular retinae in these marsupials. A nearly identical vascular pattern to that of the devil is seen in the closely related

quoll (Figs. 2.1, 2.2, 2.4, 2.7). In all marsupial retinae the vessels assume the parallel arteriovenous pairing long known to exist throughout the marsupial central nervous system and first described by Wislocki and Campbell (1937) in the Virginia opossum. See Figs. 3.26, 3.27. In this arrangement, the paired vessels remain together down to the hairpin-like terminal capillaries. This pattern has been confirmed in the brains of a number of marsupial species as well as in the retina of the Virginia opossum (Scharrer 1939, Wislocki 1940, Craigie 1938, Sunderland 1941). One result of this arrangement is that in vitread view most veins are not clearly seen; the more sclerad venous circulation is, in large measure, overlain by the retinal arteries (Walls 1942). Only near the optic disc, where the vessels are large, do they run side by side. Optical advantages may accrue from this overlap of vessels. The combined profile of this over-under vascular arrangement occupies less retinal area than does the side-by-side arrangement seen in many placental mammals. It will be shown in the Australian marsupials, however (Chapter 3), that the central nervous system end artery organisation of the capillary bed is not present throughout all of the retina.

2.4.4.c Angiography

(1) Marsupial "shunts"?

The results show that the pattern of blood flow in vascular marsupial retinae differs from that seen in vascular placental retinae. This is most likely a consequence of the unusual vascular arrangement within these retinae. In placentals the fluorescein flow follows the natural sequence: arteries - capillary bed - veins. In vascular marsupial retinae there is initial arterial filling followed almost immediately by filling of the larger veins. This is in turn followed by a simultaneous, slow filling of the 'capillaries' with venous intensification. This could be in part due to the presence of arteriovenous shunts, but, more likely, is simply a result of the unusual arteriovenous pairing. The wide time span for venous and capillary filling results from the fact that some AV pathways are necessarily much longer than others. In such a system the venous phase of the angiogram would be expected to commence immediately after the arterial phase and would gradually build up in intensity over time as the longer arteriovenous loops filled. For further discussion see Chapter 3.

The placental capillary bed could be expected to have more uniform distances from arterial to venous segments than is the case for marsupials. Hence, venous filling in marsupials would be initially apparent when only a few of the poorly visible shorter capillary loops had drained into the venous circulation. Given sufficient temporal and spatial resolution, it would not be unexpected to see similar early venous filling in placentals, particularly near to the disc where

shorter AV paths would necessarily exist, allowing venous filling before more peripheral segments of the capillary bed had filled.

(2) Could early venous filling be artefactual?

Another, less likely, possibility for the preeminent filling of the venous vascular bed is artefact due to the injection technique. Should the initial concentration of the dye bolus be markedly less than the main wave, then as the initial front passed through the arterial and vascular beds there might be sufficient bulk of dye to produce a detectable signal. However, within the capillary bed the further dilution of an already weak dye solution over a much larger area may lead to an undetectable signal. With subsequent, more concentrated waves of the bolus passing through the vascular bed, not only would the arterial and venous phases gain further prominence, but also the capillary bed would become apparent giving a false impression of late filling. This interpretation seems unlikely though as this difference was consistently seen only in the marsupials despite similarity of injection technique in all species.

(3) "Shunts" in health and disease

Given the unusual marsupial angiogram it is worth spending a few moments upon similar angiographic events which may be seen in placental retinae. True arteriovenous shunts have been reported in the human retina; however, such reports are rare and the underlying origin often pathological. Congenital AV communications range from isolated anomalies through more widespread vascular involvement to those associated with skin, central nervous system, and oropharyngeal arteriovenous anomalies (Mansour et al. 1987, 1989). Figure 2.18B demonstrates an asymptomatic arteriovenous communication, selected from the clinical records of the Lion's Eye Clinic in Hobart, no doubt the result of anomalous vascular development (Streeter 1918). In these cases the angiogram is characterised by filling of the venous communication immediately after the arterial phase (Mansour et al. 1987), not unlike the sequence seen in the polyprotodont angiogram.

By contrast, acquired AV communications are seen as pathological events. Takayasu's disease, an idiopathic inflammatory arterial condition, results in increased diameter of some capillary pathways leading to preferential channels. Also abnormal communications at the points of arteriovenous crossings leads to blood bypassing the capillary bed (Tanaka and Shimizu 1987). The end result is arteriovenous shunting. Similar shunts have been reported in diabetic retinopathy (Kuwabara and Cogan 1963) and Coat's disese (Henkind and Wise 1974).

Despite any similarity in angiographic sequence, the marsupial situation is most likely unrelated to the human pathological situation. The latter is associated with abnormal and often widespread disruption of the vascular bed, whereas the former is concerned with physiological variation of nourishment patterns. The true shunt results from increased flow through an abnormal arteriovenous communication whereby the capillary bed is bypassed, the marsupial angiographic pattern from the greater diversity of capillary pathway lengths linking venous and arterial vasculature.

(4) Capillary density

The marsupial vascular pattern (Fig. 2.4D) shows apparent coarseness when compared with the more uniform, poorly discernible terminal vascular bed of the placental cat or man (Figs. 2.16, 2.17). Between the finest order vessels in the polyprotodont marsupial retina, "fluorescein-free" space is seen, suggesting, at first glance, low capillary density. Do marsupials have physiological rarefaction of the vascular bed?

Arteriolar and capillary rarefaction is seen in hypertension; the vascular bed becoming attenuated in association with increased perfusion pressure (Harper et al. 1978). Simplistically, this may reflect closure of some vascular beds, the territory of which is adequately supplied by neighbouring beds at increased perfusion pressure (Green et al. 1964). Alternatively, hyperresponsiveness of arterioles to noradrenaline (Bohlein 1979) or after effects of arteriolar occlusion (Sokolova et al. 1985) have also been postulated as explanations.

However, the coarseness of the vascular bed in marsupials is more likely just a reflection of the enhanced magnification of the smaller marsupial eye when viewed through the fundus camera. Quantification of the density of the vascular bed would be necessary to test this hypothesis.

2.4.5 Avascular retinae

2.4.5.a Horizontal streak, retinal avascularity and ganglion cell density

Does retinal avascularity mean simpler organisation within the retina? If ganglion cell counts can be taken as a measure of retinal complexity, then intricacy is seen in both vascular and avascular species. Simpler organisation, and lower cellular density, together with the

functional implication of lower spatial acuity, are not necessarily an accompaniment of retinal avascularity, though temporal acuity may well be affected (Buttery et al. 1990b). Some indication of retinal organisation may be gained from the fundal appearance, particularly in polyprotodont and less so in diprotodont retinae, where vascular sparse zones or pigmentary changes indicate visually acute areas.

A brief discussion of ganglion cell counts in relation to fundal appearance is presented at this stage, with a more detailed discussion of visual function presented in Chapter 6.

Land bound mammals typically have a horizontal streak, a horizontal concentration of neural elements directed in a line across the retina rather than within a circular area centralis. It is claimed that this arrangement suits animals whose visual horizons are, quite literally, the horizon (Hughes 1977a). An *area centralis*, on the other hand, is seen in animals which need to examine their world from all directions. These include some of the hunters and those animals which occupy an arboreal, aerial or otherwise three dimensional world. Among marsupials both arrangements are seen. For example, isodensity maps of cells in the ganglion cell layer of the tree kangaroo's retina show a clear area centralis, while in other forest and dense scrub dwelling terrestial and semi-terrestial forms the area centralis is elongated nasally, giving these animals, in effect, both an area centralis and a visual streak (Beazley and Dunlop 1983, Freeman and Tancred 1978, Hughes 1975b, Tancred 1981, Wong et al. 1986). This arrangement is by no means uncommon in mammals. Stone and Johnson (1981) reported a similar arrangement in a variety of primates, including our own species. In the brushtail possum it would appear that the *area centralis*-visual streak lies entirely within the more lightly pigmented portion of the retina. In order to accommodate the expanded *area centralis* portion the border between heavily and lightly pigmented hemiretinae dips well below the optic disc on the temporal side (Fig. 2.9). The red kangaroo, which dwells in the open plains and low scrub of central Australia, has only a visual streak (Hughes 1975). Unfortunately, no information about the density of ganglion cells is available for any of the gliding possums, and, as these marsupials all have avascular retinae, no clues as to the existence of an area centralis or visual streak are forthcoming from examination of vascular patterns. One would, of course, predict an area centralis. Johnson's (1968) illustration of the retina of the glider, *Petaurus norfolcensis*, shows an intriguing, darkly pigmented choroidal spot into which the choroidal sinuses do not intrude. Whether this marks a marsupial attempt to minimise light scatter behind an area centralis remains a matter for speculation. Ophthalmoscopic examination of the closely related sugar glider did not reveal a similar spot.

Contrary to the report of Duke-Elder (1958) which cites *Petaurus* as having intraretinal vasculature, the retinae of this genus are avascular. The avascular fundi of the glider and

brushtail possum are similar to those otherwise reported in other diprotodont marsupials including: another gliding possum, *Petaurus norfolcensis*, Bennett's tree kangaroo, *Dendrolagus bennettianus*, Rufous rat kangaroo, *Aepyprymnus rufescens*, squirrel-like phalanger, '*Belideus sciureus*' and the common wombat, *Vombatus ursinus* (Johnson 1901, 1968).

2.4.5.b Angiography

(1) Choroidal papillae?

Could the possum's retina be nourished by physiological choroidal vascular loops? The punctate appearance of the superior fundus (Fig. 2.9) could suggest such a possibility. Choroidal loops are well known in other species. The megachiropteran bats (Chase 1982, Pedlar and Tilley 1969, Van Driel et al. 1985) have vascular loops projecting into the retina from the choroid. These loops however still follow the embryological borders between the two germ layers with the choroidal loops indenting the retina without truly penetrating Bruch's membrane (Pedlar and Tilley 1969). In pathological situations true vascular anastomoses may occur between choroid and retina (Doft 1983). These anastomoses are most often a response to some destructive process whereby Bruch's membrane and the retinal pigment epithelium are damaged.

The punctate appearance of the possum fundus represents end on views of the choroidal feeding vessels which supply the more vitread choriocapillaris. Detailed observation of these areas with the fundus camera did not suggest though that the blood vessel core intruded into the retina. Subsequent histological material showed that the retina is avascular and there are no intrusive choroidal loops (See chapter 3, Fig. 3.8).

(2) Avian pecten?

If the diprotodonts have not taken a leaf out of the megachiropteran book, perhaps they have taken one from the avian opus. The avian retina is characterised by a fluorescein permeable vascular frond, the pecten. Bellhorn et al. (1977), following on from the work of Abelsdorff and Wessely (1909), have demonstrated that in birds the pecten is permeable to fluorescein and therefore could serve to diffuse nutrients through the vitreous into the outer retina thereby complimenting the role of the deeper choroidal circulation. The frequent saccadic eye movements of birds may be important in aiding diffusion via this route (Pettigrew et al. 1990). The angiographic results in marsupials indicate that vitreal diffusion of nutrients into the outer retina from the papillary vessels is not a factor, as is the case with the larger and more

elaborate avian pecten. Observations in the two possums indicate that the papillary vessels do not play a similar role. They are totally impermeable to fluorescein, though this, of course, does not absolutely preclude permeability to other substances. These vessels are more likely either embryological remnants or, aids to local disc nourishment, thus allowing increased local thickness in this region (see later discussion on vascular anatomy, Chapter 3).

2.4.6 Comparison of fundi

2.4.6.a Marsupials

Despite the dramatic differences in retinal vascularisation, all Australian marsupials examined show similarities in choroidal organisation. The streak-like choroidal vessels seen in the quoll's fundus (Fig. 2.1) resemble those of the sugar glider (Fig. 2.10). The punctate vascular pattern of the tapetal retina of the quoll (Fig. 2.1) resembles that seen in the superior portion of the possum's fundus (Fig. 2.9). These glimpses of the choroid suggests similar arrangement of linear feeding vessels and penetrating arteries supplying the underlying choriocapillaris. This suggests that the basic choroidal pattern is established independently of the vascular or avascular condition of the overlying retina.

2.4.6.b Geographic choroidal filling

Particularly dramatic is the patchy choroidal early fluorescein filling seen in most marsupials examined (Figs. 2.4A, 2.5B, 2.6, 2.8A, 2.11F and 2.12A). The pigment deficiencies make the marsupials particularly suitable for this aspect of choroidal angiography and demonstrate unquestionably the differential filling of large choroidal regions. Hayreh (1975) has demonstrated clearly that the choroidal circulation is indeed segmental in nature. High speed angiographic investigation using intracarotid injections in monkeys has demonstrated that not only is the major supply through the ciliary vessels isolated to a particular area of the choroid, but also that each terminal choroidal artery supplies an independent segment of choriocapillaris. See Figure 2.18 for patchy early choroidal filling in the human angiogram.

The posterior ciliary vessels in the marsupials, too, conform to this regional distribution. The sugar glider showed not only variable filling but also variable emptying, with the peripapillary region clearing before the surrounding area began to fill (Fig. 2.12). This most likely was due to a particularly small bolus of dye in combination with variable flow lengths within the posterior ciliary vessels and a fortuitous sequence of angiogram shots.

The terminal arteriolar choroidal pattern most likely is also similar to that of placentals. Feeding vessels, seen in end on view, are apparent in both the quoll and possum. (Fig. 2.6, 2.11). However no conclusion can be drawn about anastomoses between lobules within the choriocapillaris as are known to exist in the placental choroid.

To conclude, it would seem that the choroid and its blood supply are probably similar in mammals. The intraretinal vasculature in marsupials, when present, has an angiographic pattern which differs from the placental norm. This is due to the unusual intraretinal arteriovenous pairing of the circulation in marsupials (See Chapter 3).

2.5 CONCLUSIONS

1. The diprotodont marsupials examined have avascular retinae. Only a small tuft of vessels is to be found projecting from the optic disc into the vitreous.

2. Polyprotodont retinae have intraretinal blood vessels, but these differ in morphology from those seen in placental retinae. The larger venous and arterial vessels are very closely approximated, consonant with the known organisation of the central nervous system circulation.

3. The mottled differentiation of retinal pigmentation in the possum allows end on and linear views of the choroidal feeding vessels in the dorsal fundus. Streak-like choroidal vessels are seen throughout the glider's fundus.

4. A choroidal tapetum is seen in the quoll, a retinal pigment epithelial tapetum in the opossum and differental pigmentation of the RPE in the devil, but no tapetum.

5. Angiographic events in the vascularised marsupial retinal species demonstrate arterial followed by early venous filling and subsequent capillary intensification. Rather than true arteriovenous shunts, this is most likely a consequence of the unusual, variable length organisation of the marsupial's vascular system.

6. Unlike the avian pecten, the diprotodont disc vessels are fluorescein impermeable.

CHAPTER 3

RETINAL VASCULAR MORPHOLOGY:

HISTOLOGY, SCANNING ELECTRON MICROSCOPY

AND CARBON INJECTED VASCULAR PATTERNS.

CHAPTER 3: FIGURES

CHAPTER 3: FIGURES, CONTINUED

3.1 INTRODUCTION

A common nexus within the biological world concerns the relationship between structure and function (Bock 1988). This theme recurs at all levels in biology, whether we are comparing functional anatomies of running versus loading limb bones or whether we are considering the way in which the shape of a macromolecule is related to its function. This is also exemplified within the vertebrate retina, where the unusually high metabolic activity and the need for clarity in the visual axis has produced unique structural arrangements of its vascular system. The further restriction in many retinae of the vasculature to the choroid alone raises the possibility of further unusual structural or functional specialisations in these species. These could lie within the vasculature itself, in distinctive retinal metabolic pathways or in novel neural function. This chapter addresses and compares the structural and, by implication, the functional properties of the ocular vasculature in mammals with vascular and avascular retinae.

3.1.1 Avascular retina

What are the perfusion arrangements within avascular retinae? Does the choroidal circulation appear in any way different from those retinae possessing both an intrinsic and choroidal supply? Are there supplemental mechanisms within the possum's eye, for example, choroidal indentations which could bring the "blood" closer to the neuroretina? This suggestion could not be totally discounted from the angiography findings (Chapter 2). Another possibility is that the choroidal supplies are morphologically similar in vascular and avascular retinae and other factors are responsible for adequate nourishment of the neuroretina in avascular species. Finally, do structural differences amongst taxonomically distant species suggest in any way that a variety of different mechanisms have evolved for coping with retinal avascularity?

3.1.2 Vascular retinae

As shown in Chapter 2, the ocular vasculature has distinct angiographic functional properties in certain polyprotodont marsupials. What are the structural correlates of the early venous filling? Are there anatomical shunts present and, in keeping with previous reports of the marsupial nervous system vasculature (Sunderland 1941, Wislocki and Campbell 1937,

Wislocki 1940), and are there loop-like capillary structures within Australian marsupial retinae? In this chapter I examine the choroidal and intraretinal vasculature of a number of marsupials and placentals in order to gain some morphological and functional insight into these questions.

3.2 MATERIALS AND METHODS

To portray the vascular system and its topographic relationships, the techniques of vascular corrosion casting and injection of the vessels with carbon particles have been employed. These have been supplemented with light and electron microscopic examination of vascular and surrounding tissue organisation.

3.2.1 Subjects

Adult mammals with avascular and vascular retinae from both placental and marsupial lineages have been compared.

3.2.1.a Corrosion casting

Species with avascular retinae were placental guinea pigs, *Cavia cobaya*, (4 females and 2 males, weight 850-1200gm) and marsupial brushtail possums, *Trichosurus vulpecula* (2 males and 3 females, weight 2300-3500gm). The vascular species were placental Wistar rats (4 males, weight 260-290gm) and marsupial quolls (Native cats), *Dasyurus viverrinus* (4 males, weight 700-900gm). The experimental approach was developed and verified using an additional group of rats.

3.2.1.b Carbon injection

The carbon injected material was gathered following the angiographic study of the ocular vasculature (See Chapter 2). In addition, a pouch possum (male, weight 24gm, crown rump length 124mm) was perfused in a similar manner to demonstrate the immature marsupial nervous system vasculature.

3.2.1.c Histology

Material from the thickness study was also used for the light microscopic study of the ocular vasculature (See Chapter 4). In addition perfused and immersion fixed material was used for ultrastructural examination. This included material from a further 3 brushtail possums (weight 2300-3000gm), 3 quolls (weight 650-900gm), 1 guinea pig (weight 920gm) and 3 rats (weight 260-300gm). For broader comparative purposes, 1 blackbird (weight 89gm) was perfusion fixed and its pecten examined ultrastructurally.

3.2.2 Corrosion casting

3.2.2.a Anaesthesia and surgery

Animals were deeply anaesthetised with intraperitoneal chloral hydrate (rats and guinea pigs) or inhalational halothane in the larger animals (marsupials). A thoracolaparotomy was performed using a midline abdominal incision and bilateral thoracic incisions. The anterior chest wall was then reflected rostrally allowing ready exposure of the heart and great vessels. The descending aorta was clamped so that only the upper half of the body was perfused. The left ventricular apex of the heart was incised and a canula (OD/ID, 2.0/3.0mm: Dural Plastics: Dural, NSW) inserted into the ascending aorta. This was secured into position with either a clamp or ligature. Subsequent incision of the right atrium allowed free egress of perfusing fluid. An anterior chamber paracentesis was performed in some eyes in order to enhance vascular perfusion pressure within the eye and to allow more complete filling of the vascular bed. This, however, did produce some distortion of ocular structure, as loss of the distending intraocular pressure partially collapsed the eye.

3.2.2.b Injection technique

The perfusion system consisted of a pressurised bottle, this being used for infusion of either wash solution or resin (Fig. 3.1; after Gannon 1978). Through a tube draining the sump of the bottle, the wash solution could be infused, or the pressurised air space above the fluid could be connected to a 50ml syringe for resin injection. At the end of the wash step, the cannula was swapped from the sump line to the resin syringe; three way taps being employed to control the patency of each line. An aneroid manometer was also connected to the air space in the upper portion of the bottle allowing measurement and control of injection pressure. Typically, the perfusion pressure was maintained between 120-140 mmHg for both wash and resin injection steps.

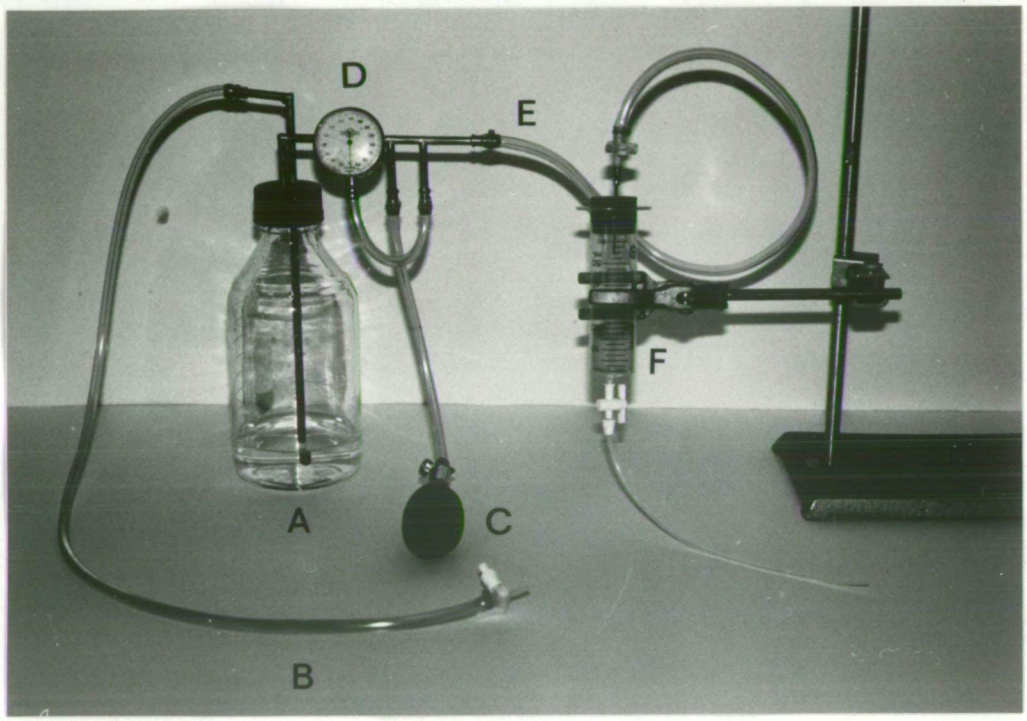

Figure 3.1: Perfusion apparatus

The sump of the perfusion bottle (A) was connected to the perfusing cannula (B). Pressure in the bottle was maintained by the sphygmomanometer bulb (C) connected to the air space of the upper portion of the bottle. Pressure could be measured using the aneroid gauge (D) connected to the air space line (E). Following the saline flush the resin was injected through the syringe (F) using the pressurised line (E). The patency of the flush and resin lines could be controlled using 3-way taps.

3.2.2.c Flush solution

Funk (1986) has suggested that no preliminary wash solution be employed in order to portray vascular relationships more accurately. However, most authors suggest the use of a clearing rinse prior to resin casting (Lametschwandtner et al. 1984). I chose to clear the vascular system with a short flush (100-200ml) of 0.9% saline or Hartmann's solution at room temperature (Travenol Laboratories: NSW, Australia). This should be filtered prior to use (Gannon 1978). More sophisticated wash solutions, for example those containing the vasodilator, sodium nitrite, polyvinylpyrrolidone (PVP), MW 40 000 (Sigma), and heparin, were abandoned following the failure of a number of casts to set completely. Trials of methacrylate mixture in the presence of each component of this wash solution, showed that the resin failed to cure when mixed with sodium nitrite. The aqueous component of this trial solution visibly changed in colour, suggesting chemical interaction with the acrylic mixture and its catalysts. Sodium nitrite can not be recommended as a vasodilator for corrosion casting.

Of all the species examined, guinea pig ocular vessels proved to be the most difficult to cast free of artefacts. Commonly the choroidal vasculature would show "blow out" of vessels with extravasation of resin in large sheets. To overcome this problem, an intermediary flush of 4% formalin in saline was used between the Hartmann's flush and resin injection. With this treatment the vessels remained intact during the curing process.

3.2.2.d Resin solution

The casting medium comprised partially polymerised methyl methacrylate plus its catalysts, initiators and plasticisers. Either a commercially available product, Batson's # 17 Plastic Replica and Corrosion Kit (Polyscience Inc: Warrington, USA), or resin prepared according to the approach of Gannon (1978, 1981, 1985) was used. This latter technique consisted of polymerising monomeric methacrylate to a viscosity of 2-5 centistoke using ultraviolet light and the catalyst 2,4-dichloro benzoylperoxide (Polyscience Inc: Warrington USA). To 20ml of this solution was added 0.4gm benzoyl peroxide (British Drug House Ltd.: Poole, England), 0.4ml n,n-dimethyl aniline (Ajax Chemicals Ltd: Sydney Australia) and 7.0ml hydroxypropyl methacrylate (Polaron Equipment Limited: Watford, England) to constitute the final injection solution.

When Polyscience Batson's mixture was used, the formulation employed was essentially that of Nopanitaya et al. (1979). To 25ml of base solution 7.5ml of catalyst, 0.5ml promotor and 12ml of monomeric methacrylate were added. Equivalent setting properties were found if 0.5gm of benzoyl peroxide (30 % water wetted, British Drug House Ltd: Poole, England) was

substituted for the catalyst, 0.5ml of n,n-dimethyl aniline for the promotor (Gannon 1981, 1985) and 7-8ml of di-n-butyl phthalate (Ajax Chemicals Ltd.: Sydney, Australia) was used as a plasticizer (Glauret 1975). Twelve ml of Polyscience monomeric methacrylate (inhibitor 25 ppm hydroquinone) was used to lower the viscosity.

3.2.2.e Resin injection

The components of the resin were mixed on ice in order to avoid premature polymerisation (Dollinger and Armstrong 1974). In the larger animals around 50ml and in the smaller animals (rats), 25ml of solution were infused. The venous outflow channel was then ligated and the perfusion pressure left at around 30 mmHg in order to maintain the vascular system under distension whilst the resin polymerised. Initially, the venae cavae were ligated in order to stop efflux. Marsupials, like rodents (Greene 1955), have bilateral vena cavae, and both need to be ligated. In later experiments, satisfactory stasis of the vascular system was achieved by simply clamping the previously incised right atrium. Any overt leakage from the edges of the thoracotomy was controlled with haemostats (methacrostats) and diathermy. Excess resin was used for maintaining distension of the vasculature as the resin set; there being variable slow loss of resin from unidentified vascular leaks and flow into the incompletely isolated lower body circulation.

Other resins were tried but proved technically more difficult to use than methacrylate. Araldite (Ciba-Geigy: Australia) required rigid control of temperature for stable setting and was slow to polymerise. Cyanoacrylate resin, or Super glue (Selleys Chemical Company: Victoria, Australia), was not available in bulk quantities, and electron microscopic embedding agents, for example, Spurrs or Epon proved too slow to polymerise and were too viscous.

3.2.2.f Post perfusion treatment and SEM

Following injection, the animal's head was covered in ice in order to counter the substantial (up to 70°C) rise in temperature which accompanies polymerisation of resin (Buijs and Dogterom 1983). Application of ice has also been found to enhance filling in other vascular beds (Potter and Groom 1983). The specimen was allowed to set and placed overnight in slowly running hot water, a procedure which enhanced tissue maceration and ensured final polymerisation of the acrylic.

The eyes were then either carefully removed using an operating microscope or left in the head for maceration with 10-20 % KOH solution. Some of the removed eyes were further dissected or sectioned into smaller pieces prior to corrosion. This was achieved either by

freezing the eye then hemisecting it with a knife blade or by gently dissecting the intact globe under an operating microscope. Cutting the frozen eye ought to maintain tissue relationships, produce less distortion and to be more simply performed. However there was little difference in using this technique over dissection of the eye, providing that the dissection was carefully done. When globes were removed prior to maceration considerably less digestion time was required and the casts often had less residual debris.

After 2 or 3 changes of KOH, alternating with gentle tap water washes, final clearing and pigment removal was achieved with common bleach, sodium hypochlorite (available chlorine 12.5 % W/V). Various approaches were tried in the corrosion stage to limit the amount of unnecessary and potentially destructive handling. The best method found was to place the eye in a 20ml bottle with a wide mouthed opening. This was covered with a layer of fine mesh which allowed the continual exchange of fluid but did not allow the digesting fragments to escape from the bottle. This bottle was then placed with an excess of fluid in a larger beaker which in turn could be gently agitated. When fluid changes were necessary, the smaller container holding the casts was simply removed, the fluid exchanged, then the smaller container was replaced. In this way handling was kept to a minimum and the specimen was always immersed in fluid.

Finally, the specimen was then trimmed to a suitable size, washed in detergent and rinsed many times in distilled water. At this stage some casts were osmicated in order to enhance the rigidity of the specimen prior to drying. Following air drying, the specimen was sputter coated with gold, further dissection, where necessary, was performed and then examined with a Philips 505 Scanning Electron Microscope using an accelerating voltage of 10-15kV.

3.2.3 Light microscopy

Samples of glycol methacrylate embedded retinal and choroidal specimens (Appendix 2) were used for light microscopic demonstration of the vascular/tissue relationships. Photographs were taken with a Leitz Orthoplan photomicroscope using a CB12 colour correction filter and tungsten light source. Kodacolor Gold 100 or black and white Panatomic X film was used (Kodak Australia Pty Ltd: Melbourne Australia).

3.2.4 Transmission electron microscopy

Specimens were fixed either by perfusion or immersion in mixed aldehydes and processed for ultrastructural analysis of the vasculature (See Appendix 3). Resin injection was not employed in these specimens. Sections were examined using a Philips 410 Transmission Electron Microscope.

3.2.5 Carbon injection

The material used for the carbon replication of the vasculature was that employed for the post angiographic measurement of retinal dimension (Chapter 2). In brief, the animals were deeply anaesthised, the vascular system perfused with percardiac wash solution followed by injection of 5-10ml of Indian ink C11/1431a (Gunther Wagner, Pelikan Werke, Hanover, Germany). This preparation is designed for biological application (Peterson et al. 1965). Carbon particle size is 200-500nm, suspended in 4.3% fish gelatine with 0.9% phenol added as preservative (Tennent 1974).

Following immersion fixation in 4% formalin in normal saline the retina was removed and prepared as a retinal wholemount (Stone 1981). Photography was performed as in section 3.2.3.

3.3 RESULTS

"Be sure of it; give me the ocular proof"

..... Othello, William Shakespeare

The information obtained from the light microscopy, plus transmission and scanning electron microscopy is combined in a description of the vascular components of each eye.

3.3.1 Marsupial ocular vasculature

3.3.1.a Brushtail possum

(1) General vascular pattern

As in other mammalian eyes, the vascular network is derived from the posterior pole and drains into anterior venous channels (Figs. 3.2, 3.3A). Long posterior ciliary arteries (LPCAs) extend anteriorly, pass through the sclera, and finally supply anterior structures. They do not give direct branches to the choroid. The posterior supply to the iris and ciliary body is complemented by venous communications with the anterior choroidal circulation.

(2) Retinal circulation

As indicated from my angiographic results and from other published reports (Freeman and Tancred 1978), the possum's eye lacks intrinsic retinal circulation. The only vestige is the leash of vessels arising from the optic disc (Fig. 3.3B, 3.4). A similar structure is seen in the quoll. The leash is capillary-like and rudimentary (Fig. 3.5) and bears little resemblance to either the avian pecten or to the conus of snakes and lizards (François and Neetens 1974). For comparison, Fig. 3.6 shows the ultrastructure of the blackbird's pecten. This is much larger and more elaborate, with microvillous processes projecting into the lumen of the smaller vessels.

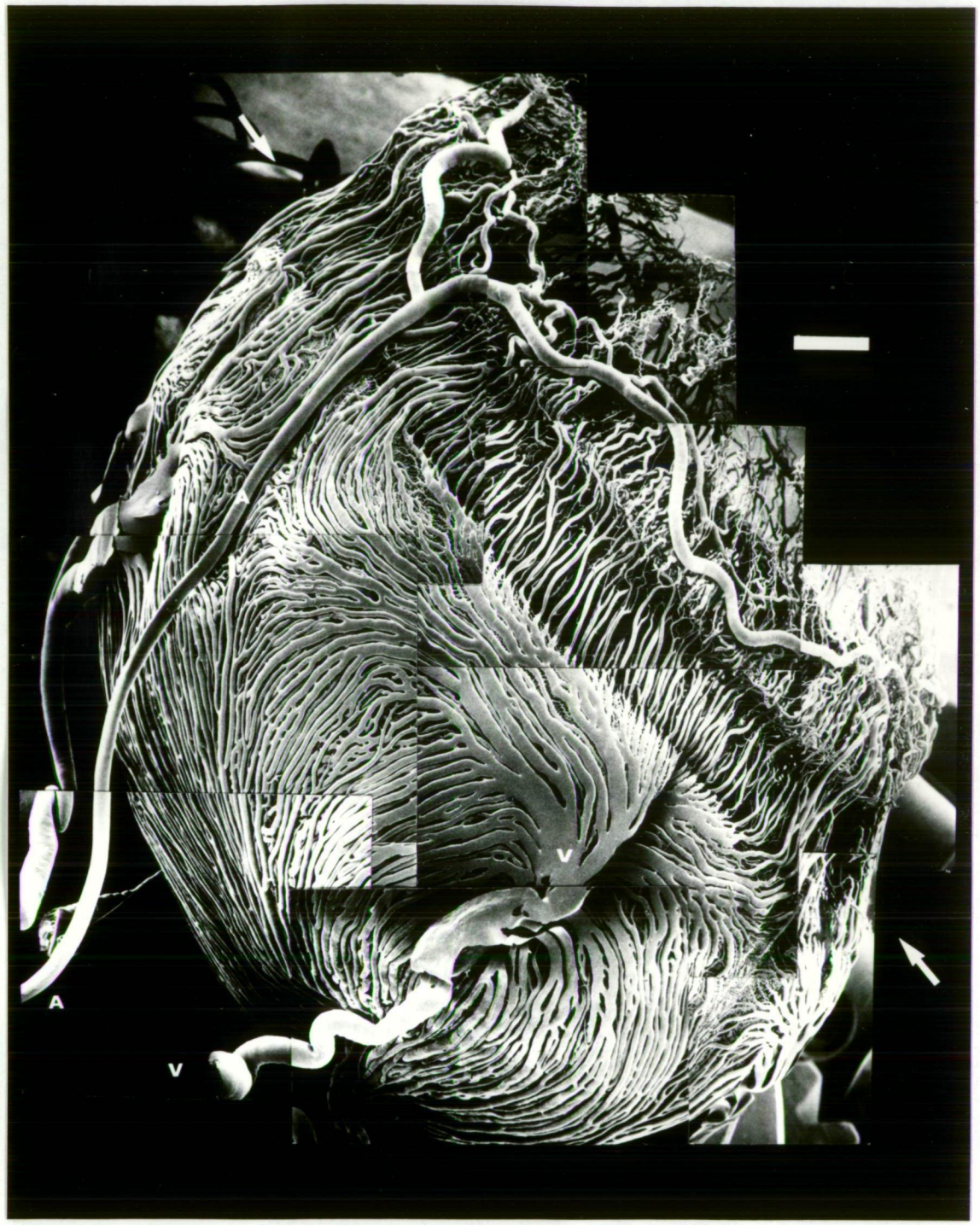

Figure 3.2: Vasculature of the possum's eye

Corrosion cast montage of the whole eye. A dense network of large choroidal vessels surrounds the eye. This is supplied by short posterior ciliary vessels at the posterior pole (not shown) and drains into vortex veins anteriorly (V). The long posterior ciliary arteries (A) supply the anterior uveal structures, ciliary body (Arrows) and the iris. The LPCAs do not give branches to the choroidal circulation. Scale bar = 1 mm.

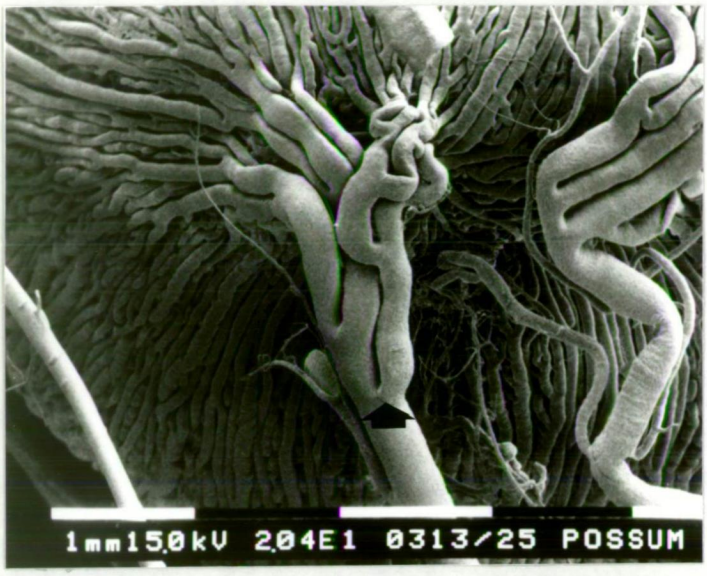

Figure 3.3A: Posterior pole of the possum's eye

Corrosion cast. External view of the SPCA's at the posterior pole (Arrow). Multiple vascular branches arise form each side of the optic nerve and pass anteriorly to supply the choroid. Scale bar is shown above the photographic caption (bar = 1mm) along with magnification (20.4x), microscope accelerating voltage (15 kV) and identifying legend.

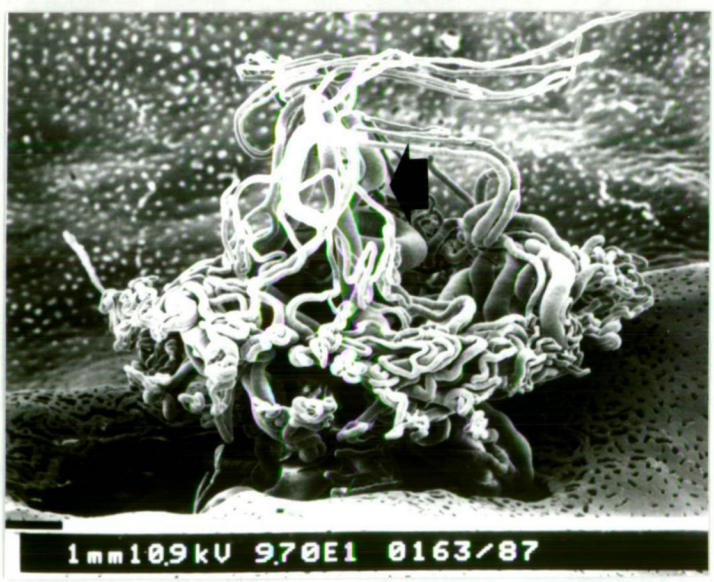

Figure 3.3B: Optic disc of the possum's eye

View of the optic disc vessels from inside the globe. This leash consists of multiple small and large calibre vessels (Arrow). The surrounding choroiocapillaris is thrown into a number of artefactual folds.

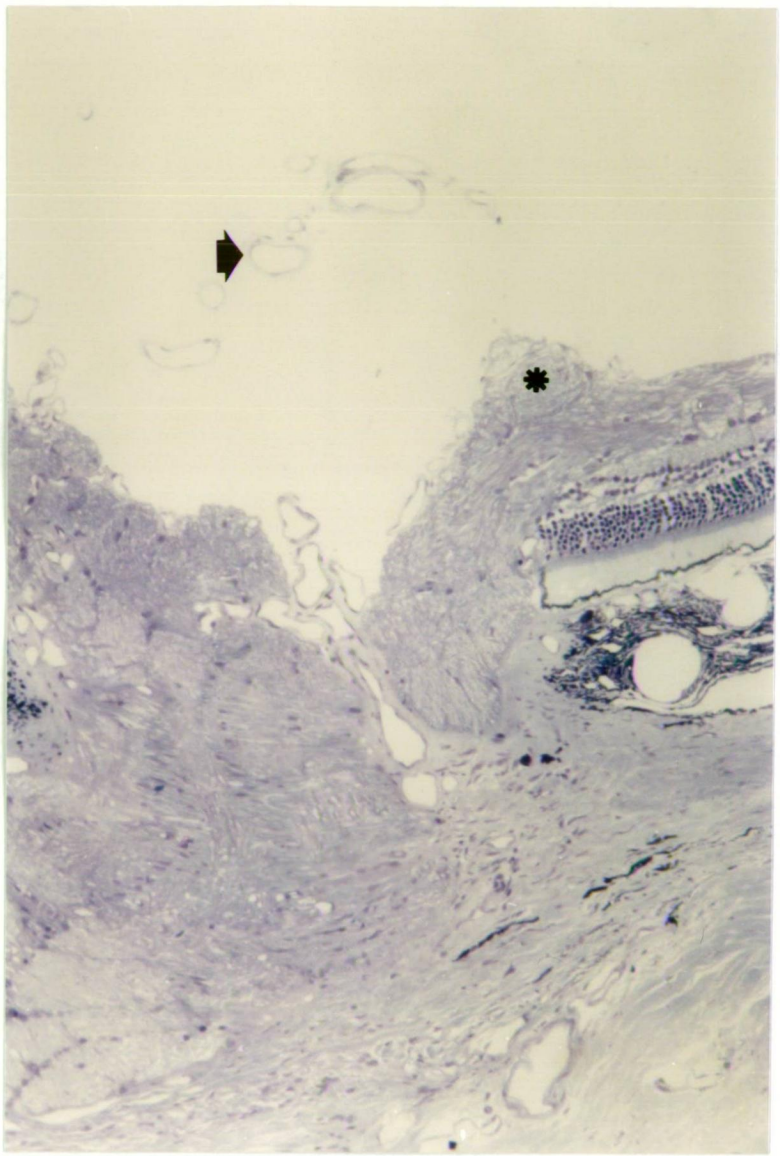

Figure 3.4: Histology of the possum's optic disc

Light micrograph of the optic disc. Plastic embedded toluidine blue stain. Vessels may be seen arising from the nerve head and projecting into the vitreous (Arrow). They are few in number and variable in calibre. Note the thickened nerve fibre layer in the adjacent retina (*). Scale bar = 100μm.

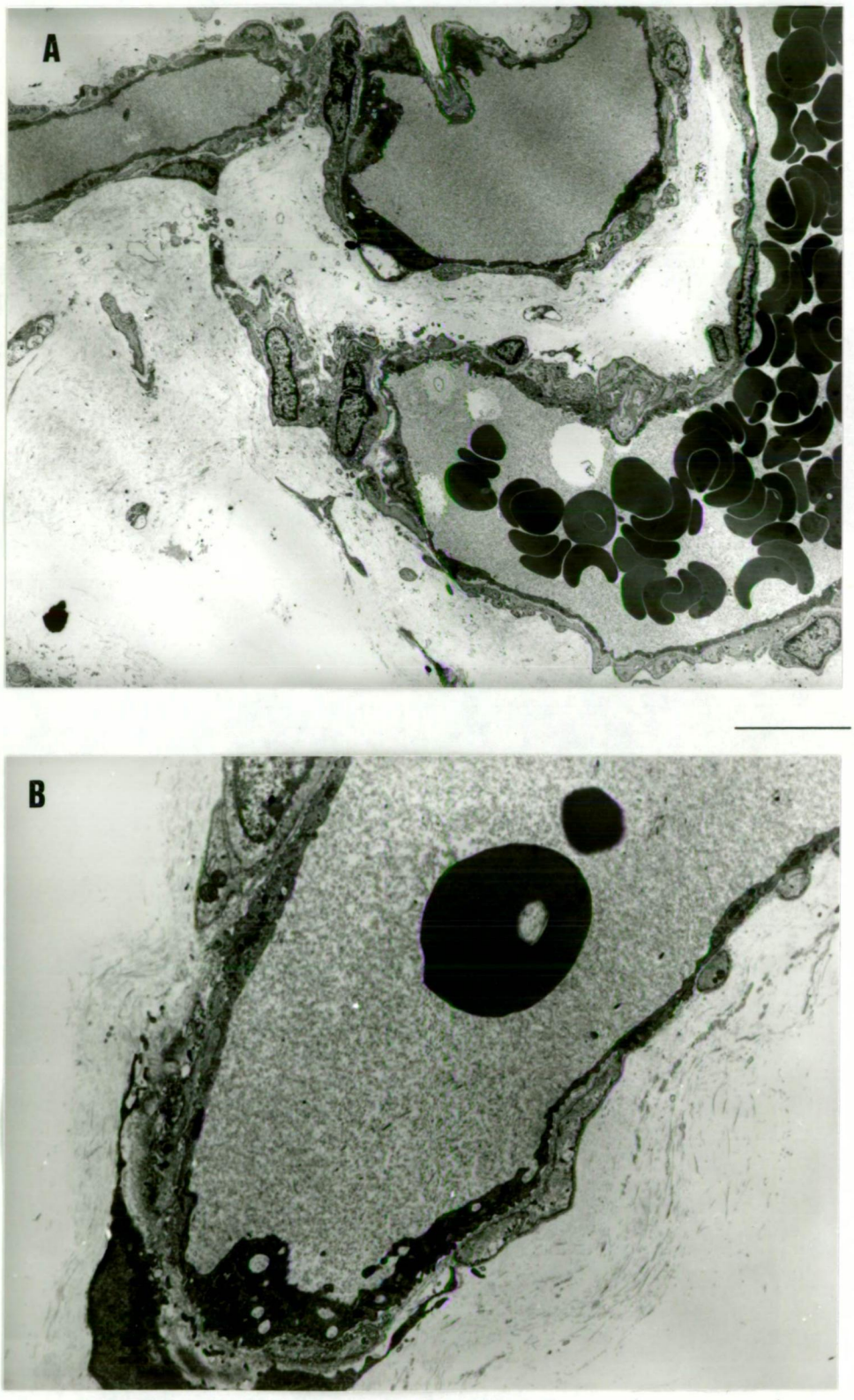

Figure 3.5: Ultrastructure of the possum's optic disc vessels

(A) The disc leash comprises simple endothelial lined vessels with little muscular or pericytic wall. This is embedded in a fibrous matrix (Arrow). Scale bar = 10μm. (B) At higher power, the endothelial lining is seen to consist of non-fenestrated cells. Scale bar = 3μm. Compare with Fig. 3.6.

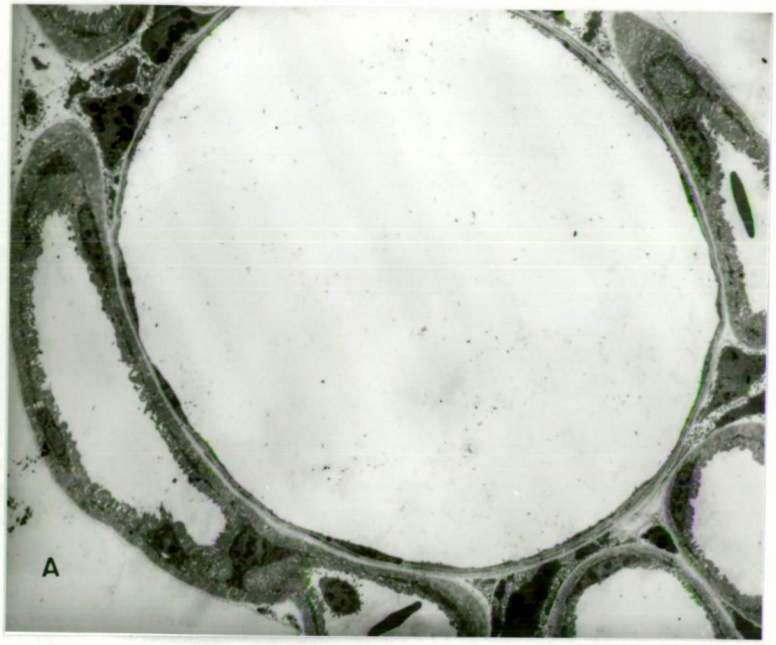

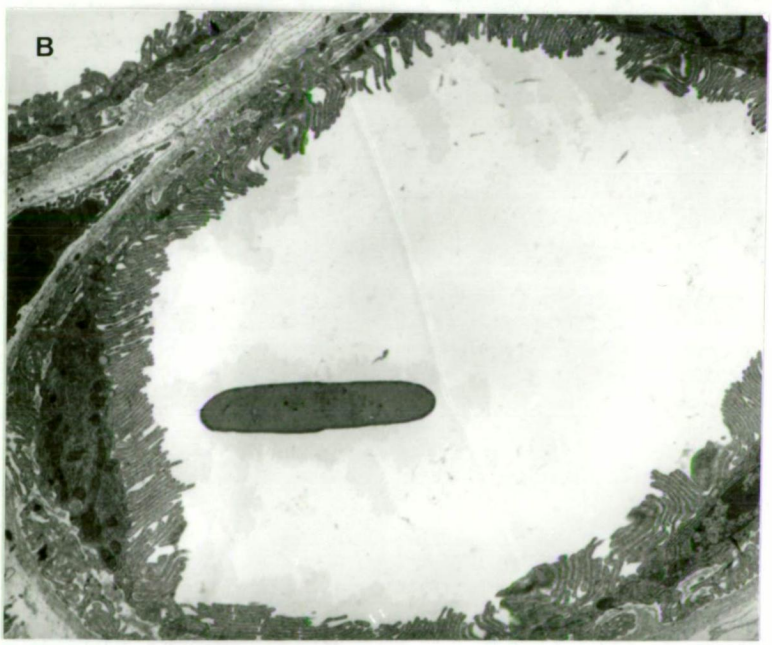

Figure 3.6: The avian pecten

(A) The pecten is very much larger and consists of both feeding and draining vessels and a modified capillary bed. Scale bar = 10μm. (B) At higher power, the endothelial lining is seen to consist of non-fenestrated cells which have extensive microvillous projections. Scale bar = 3μm. Compare with Fig. 3.5.

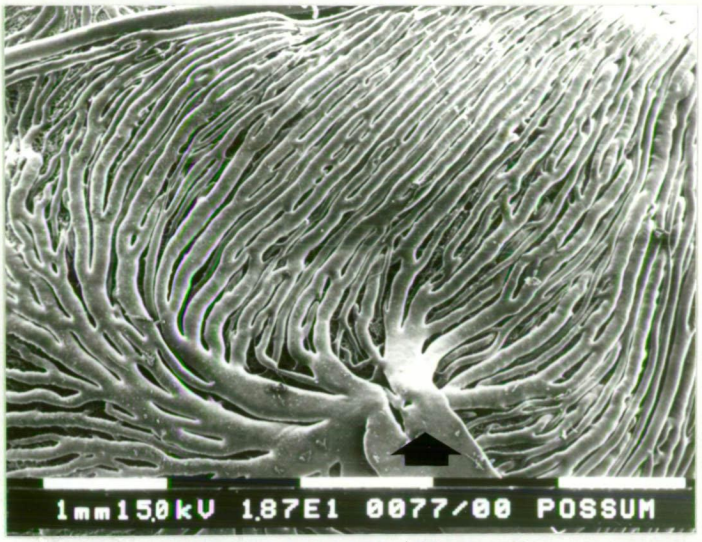

Figure 3.7A: Possum choroidal circulation

Corrosion cast of the choroid as viewed externally. A large vortex vein (Arrow) drains multiple venous channels which interdigitate with artrerial branches derived from the SPCAs.

Figure 3.7B: Possum choroidal circulation; high magnification

Tributaries of a vortex vein (Arrow) interdigitate with arterial choroidal vessels (a). Glimpses of the choroiocapillaris may be seen deep to this network (*). A LPCA may also be seen (A).

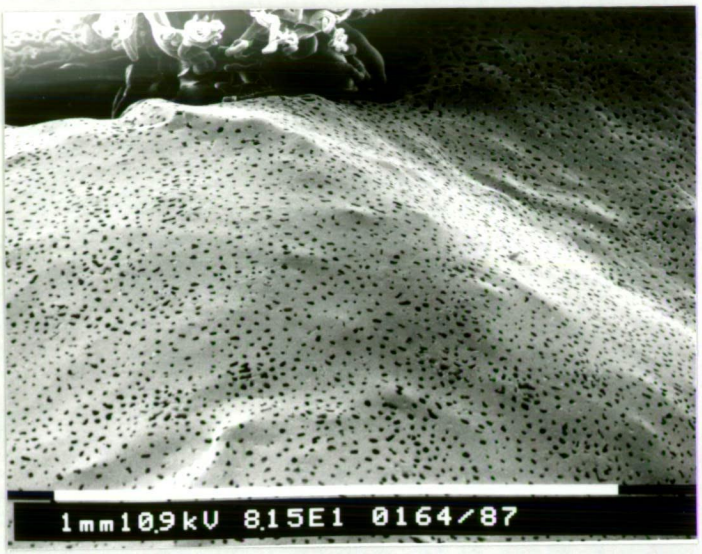

Figure 3.8A: Possum's choriocapillaris

Corrosion cast of the possum choroid viewed from the vitreal surface. Note the dense choroicapillaris network. There are no choroidal indentations to supplement retinal nourishment. The optic disc vasculature may be seen at the upper edge of the micrograph.

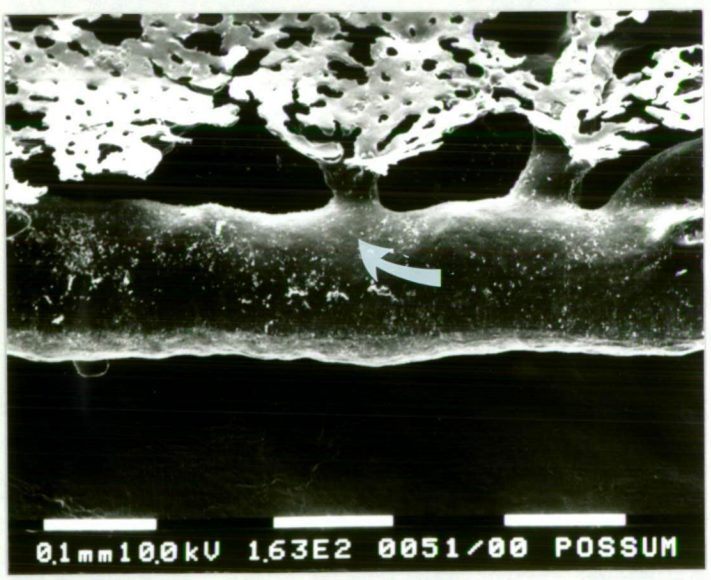

Figure 3.8B: Possum's choriocapillaris

Side on view of a micro-dissected corrosion cast specimen of the choroidal vasculature. A large choroidal vessel (Arrow) is seen to give multiple short branches which pass perpendicular to the stem vessel and supply the choriocapillaris.

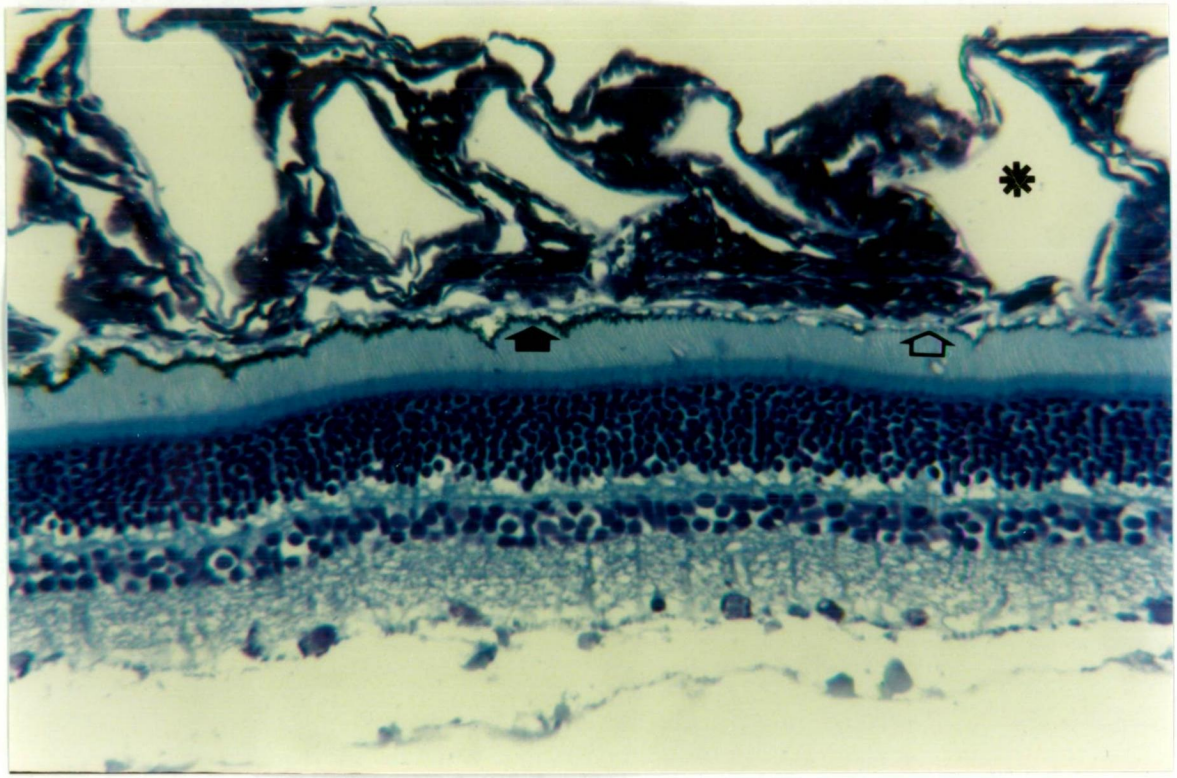

Figure 3.9: Possum's choroid, light microscopy

Light microscopic appearance of the possum retina, RE and choroid. Plastic embedded toluidine blue stained section. This section passes through the equator and shows heavily pigmented RPE on the left (closed arrow), and lightly pigmented RPE on the right (open arrow). The choroid changes little across this transition zone being heavily pigmented throughout. The external layer of large choroidal vessels is seen in cross section (*). Scale bar = 50μm.

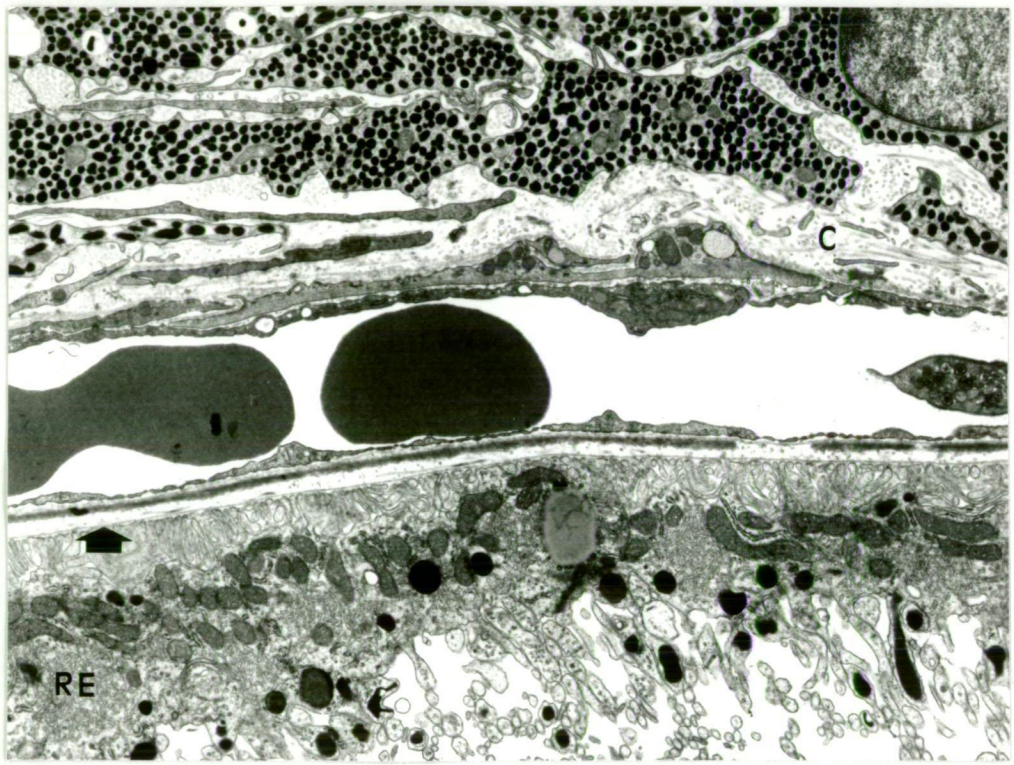

Figure 3.10: Possum's choroidal ultrastructure

Electron microscopic appearance of the RE (RE) and choroid (C). The RE is separated from the choriocapillaris by a multilayered Bruch's membrane (Arrow). The choroid incorporates melanosome containing pigment cells (P). Scale bar = 1μm.

Figure 3.11: Possum's choriocapillaris

Ultrastructure of the RE choriocapillaris junction. The basal surface of the RE is thrown into multiple microvillous folds (Arrow). Bruch's membrane separates the RE from the fenestrated choriocapillaris (C). Scale bar = 1μm.

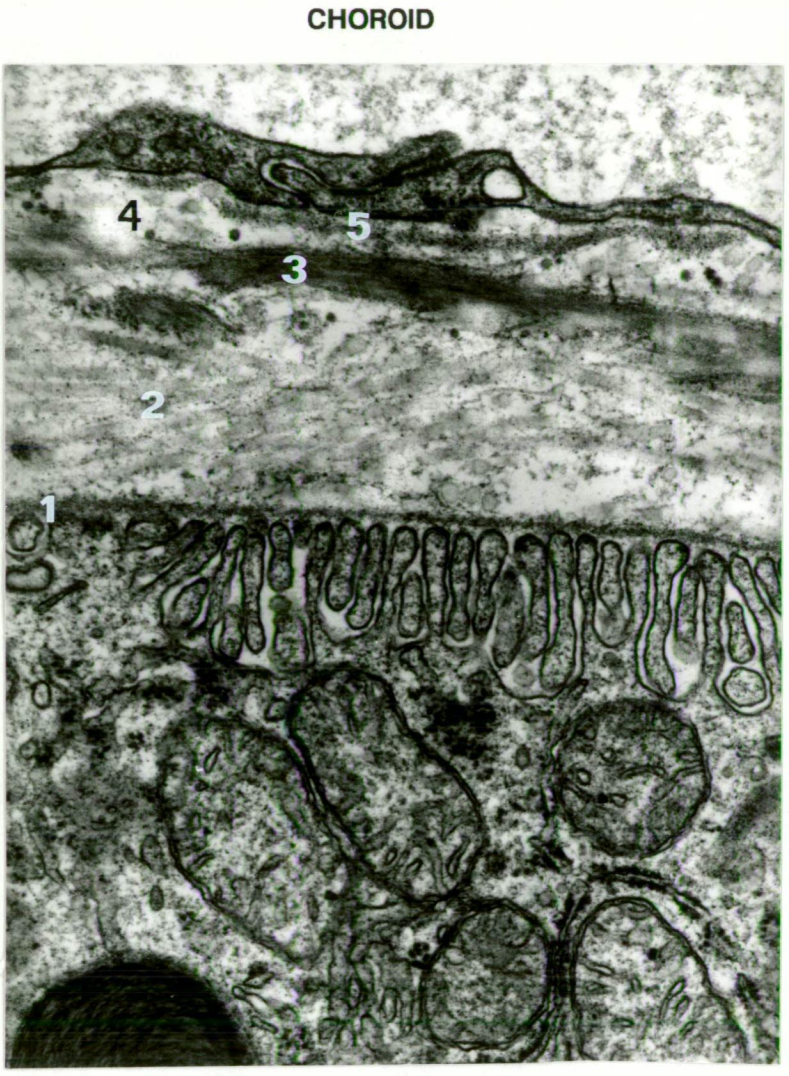

Figure 3.12: Possum Bruch's membrane

Ultrastructure of Bruch's membrane. The basal infoldings of the RE cells (Arrow) have their own basment membrane (1). This is continuous with the inner collagenous layer of Bruch's membrane (2). The electron dense elastic lamina (3) separates the inner from the outer collagenous layer (4). The choriocapillaris basal lamina forms the fifth layer of Bruch's membrane (5). Scale bar = 0.5μm.

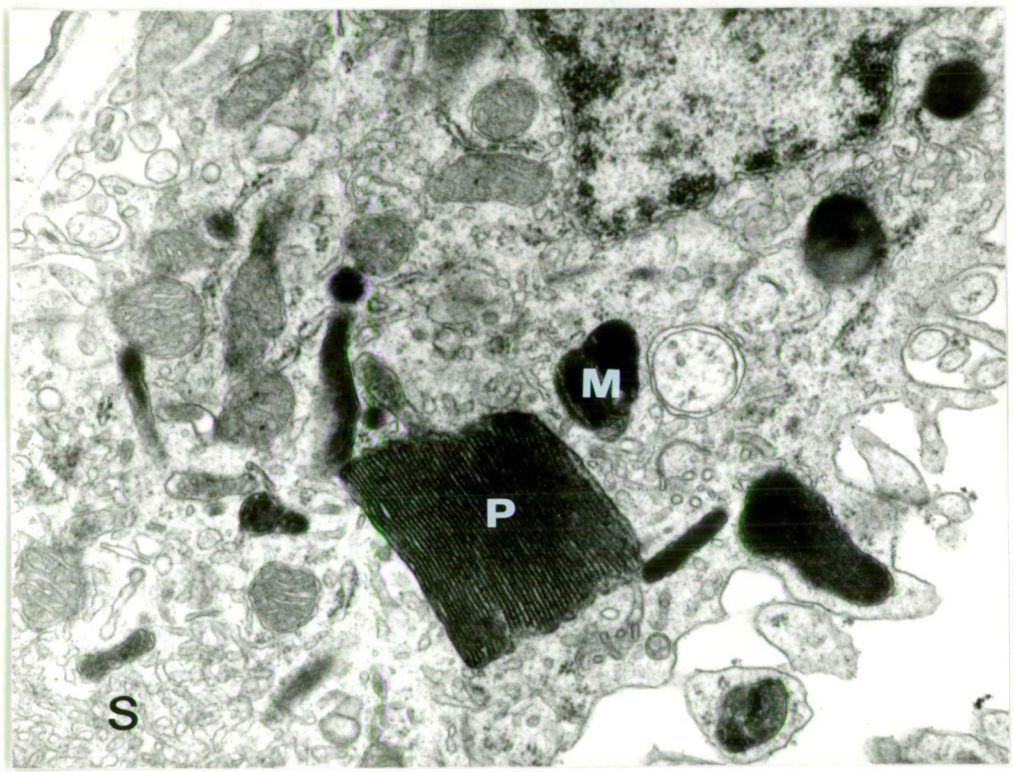

Figure 3.13: Possum's retinal epithelium

Ultrastructure of the RE. This interdigitates with the photoreceptor outer segments at its apical surface and with Bruch's membrane at its basal surface. Within the cytoplasm of the RE there are melansomes (M), mitochondria, smooth endoplasmic reticulum (S) and digested membranes of the photoreceptors (P). Scale bar = 0.5μm.

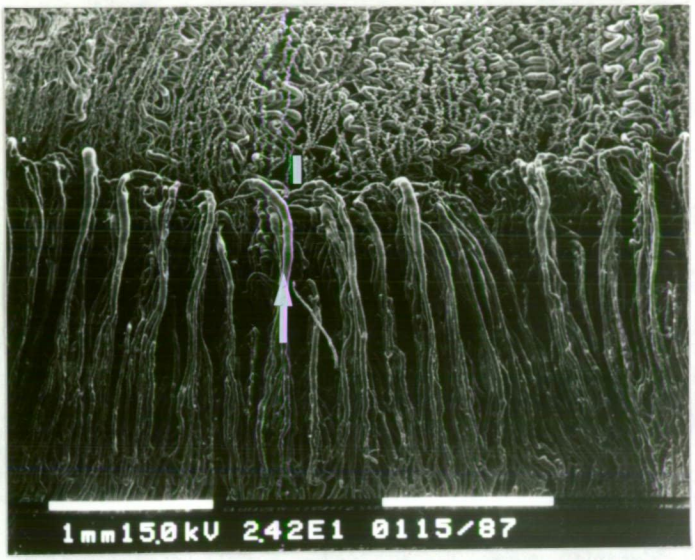

Figure 3.14A: Possum's ciliary body

Corrosion cast specimen of the anterior possum uvea as viewed from the vitreal surface. The ciliary body has a vascular core within each process (Arrow). This is adjacent to the iris circulation (I).

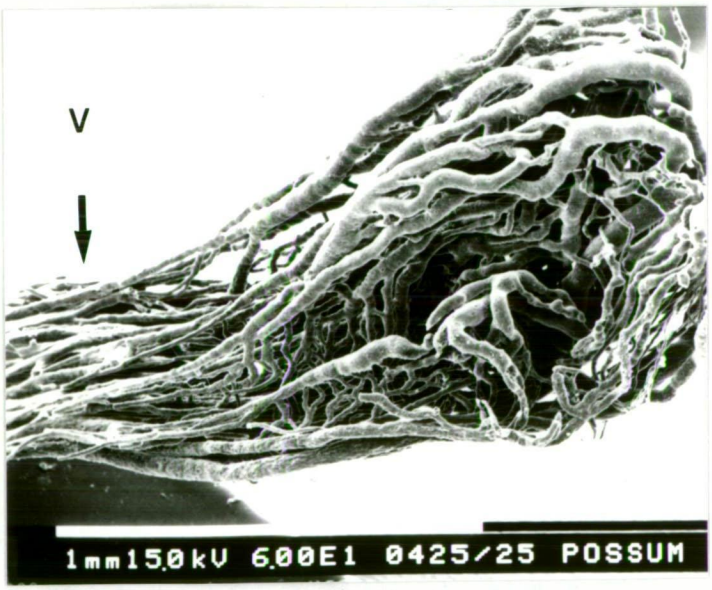

Figure 3.14B: Possum's ciliary process

Micro-dissected corrosion cast specimen of the ciliary body. Each ciliary process derives an arterial supply from the major circle of the iris and drains into the anterior choroid (Arrow). There are multiple vascular pathways in the substance of the process. Vitreous (V).

(3) Choroidal circulation

Overall choroidal organisation

The choroidal vessels, like those of other mammals, are very abundant forming an almost complete coat around the eye (Fig. 3.2). This layer is deficient anteriorly to allow the passage of light along the visual axis. Typically, the choroid is bilayered, with the dense capillary network of the vitread choriocapillaris and the sclerad, often longitudinally arranged, arterial elements intermingled with the venous drainage (Fig. 3.7). The arterial supply derives from a series of short posterior ciliary vessels entering the globe around the optic disc (Fig. 3.3). The long posterior ciliary arteries do not give any contribution to the choroid (Fig. 3.2). The choroidal veins coalesce into a swirling pattern of vortex vessels draining ultimately from the anterior four quadrants of the globe (Figs. 3.2, 3.7). Where the vortex vein pierces the sclera, an ampulla lies proximal to the scleral impression.

Choriocapillaris

The choriocapillaris forms a dense vascular network (Fig. 3.8) which occupies all areas of the globe except for the cornea, iris and ciliary body. The supplying vessels from the more superficial choroid are typically short and branch abruptly, being intertwined with the pigment cells of the choroid (Figs. 3.8, 3.9). The choriocapillaris, is a loose network of fenestrated sinusoids abutting onto the villous processes of the retinal pigment epithelium (Figs. 3.8, 3.10). There are no choroidal loops extending into the neuoretina as seen in the megachiropteran bats (Pedlar and Tilley 1969).

Ultrasructurally, the choriocapillaris constitutes a fenestrated sinusoidal lake, separated from the RE by a pentalaminate membrane, Bruch's membrane (Figs. 3.11, 3.12). This membrane consists of the respective basement membranes of the endothelial cells and the retinal epithelium encapsulating a central core of collagen and elastic fibrils (Nakaizumi 1964). These fibrils in turn are surrounded by an interstitial matrix producing a five layered conformation (Fig. 3.12).

Retinal epithelium (RE)

The basal surface of the RE is a convoluted microvillous layer, its apical surface interdigitating with the tips of the photoreceptor outer segments. Each cell is joined to its neighbour by an occluding tight junction, usually located more apically than basally. Within the cytoplasm, interspersed amongst the pigment granules, are numerous mitochondria, quite extensive

smooth endoplasmic reticulum, limited rough endoplasmic reticulum and scattered phagosomes containing partially digested photoreceptor outer segments (Fig. 3.13).

A choroidal *tapetum lucidum* is absent. The variegated fundal appearance (Figs. 2.9, 2.11) is accounted for by differential pigmentation of the retinal "pigment" epithelium (Fig. 3.9).

(4) Iris and ciliary body

The iris vasculature is linked to the peripheral choroidal supply by the ciliary body (Fig. 3.14). The ciliary body region is highly vascular and organised around the ciliary processes of the *pars plicata*. Arterial supply is from the major arterial circle of the iris and venous drainage is to the anterior choroid. An interdigitating array of capillary channels lies within the triangular confines of each ciliary process.

3.3.1.b Polyprotodont marsupials

(1) General vascular pattern

The gross organisation of the ocular vasculature in the quoll is similar to that of the possum with one major difference, the presence of intraretinal vessels.

(2) Retinal circulation

The arteriovenous pairing of the larger intraretinal vessels, as seen in the angiograms and fundus photographs (Figs. 2.1, 2.4, 2.5), is confirmed in the anatomical material. For most of its distribution, each arterial segment is accompanied by a similarly sized vein (Fig. 3.15). However, this relationship breaks down closer to the capillary network (Fig. 3.16). Here, various combinations of separate and paired branchings of the smaller vessels may then be seen. The capillary bed shows a mixed pattern. Whilst part of the retina shows the traditional end artery organisation reported in the CNS and retina of other marsupials (Fig. 3.17), the remainder of the retinal capillary bed only partially adheres to this configuration (FIgs. 3.18, 3.19, 3.21). The larger vessels avoid the visual streak region above the dividing line of the tapetum (See also angiography and fundus photography, Figs. 2.4, 2.5). In the central retina, anatomical communication does exist between adjacent capillary regions, and the bed is more akin to a reticular capillary anastomosis than to an end artery looped circulation (Fig. 3.15). Even the definite anatomical dividing line, as defined by the ganglion cell visual streak, shows anastomoses of the capillary beds derived from distant stem vessels, branches of the

superior and inferior arcades as well as by contributions from the superiorly directed major vessel arising from the optic disc (Fig. 3.15).

The peripheral capillary bed is more akin to that reported eleswhere in the marsupial CNS. The capillary bed demonstrates pairing of vessels down to the characteristic terminal capillary loops (Fig. 3.17). The retinal circulation does not extend to the ora serrata (Fig. 3.19). Finally, around the optic disc the circulation is atypical also with an added layer of looped retinal capillary vessels (Fig. 3.20).

In retinal cross section, the capillary bed is seen to be bilayered with a vitread network located within the nerve fibre layer and a more sclerad network within the outer plexiform layer (Figs. 3.21, 3.32, see also Buttery et al. 1990a). The region between the outer plexiform layer and the choriocapillaris lacks retinal vessels.

While the angiographic interpretation of retinal blood flow suggested the possibility of arteriovenous anastomoses, no preferential AV communications were seen in the corrosion cast material.

The optic disc, like the possum's, has a small vascular clump of vessels (Fig. 3.22). This arises from the disc from a large diameter vessel and consists mainly of 10μm diameter tortuous vessels (Fig. 3.23). The leash was however more compact than that of the possum's disc (Figs. 3.3, 3.4) and lies ensheathed in a capsule (Fig. 3.22).

Some arteriolar branches, especially if unpaired and arising abruptly from a large parent artery, often show an annular impression at the junction (Fig. 3.24). However most dichotomous branches of the arterial system show no such impressions.

The ultrastructural appearance of the retinal capillaries is that of a tight junctioned, non-fenestrated endothelium (Fig. 3.25).

(3) Comparison of retinal and central nervous system vasculature

To determine if the retinal capillary bed was representative of that seen elsewhere within the marsupial central nervous system, the vasculature of the brain was also investigated. The pattern seen was that of arteriovenous pairs down to, and including, the non anastomosing looped terminal capillary bed (Figs. 3.26, 3.27). Portions at least of the quoll's retinal vasculature display a pattern which is atypical for the marsupial CNS.

(4) Choroidal circulation

As in the possum's sye, the choroid is elaborate, complex and voluminous (Figs. 3.28, 3.29). Arising from the posterior pole, short posterior ciliary vessels give rise to multiple branches which intermingle with the anteriorly directed and draining vortex channels.

The paired long posterior ciliary arteries pass anteriorly on either side of the globe ending in the major arterial circle of the iris. As in the possum's circulation, they do not give branches to the choroid along their course (Fig. 3.28).

The choriocapillaris is again similar to, and comparable in coverage to, that of its avascular diprotodont counterpart (Fig. 3.30). Differences are found in the organisation of the supplying branches to and from the choriocapillaris. The substantial thickness of the intervening choroidal tapetum necessitates that these branches be longer (Fig. 3.31). The more sclerad organisation is the same as the possum's.

The tapetum consists of collagenous sheets lying within the choroidal stroma, a *tapetum fibrosum* (Figs. 3.32, 3.33, 3.34). The choriocapillaris and RE ultrastructure are similar to that of the possum (Fig. 3.35). The choriocapillaris consists of a fenestrated endothelium separated from the RE by a multilayered Bruch's membrane. The RE itself has a villous basal surface, numerous mitochondrial and endoplasmic reticulum profiles and, in the lower fundus, pigment granules within the cytoplasm. The apical surface interdigitates with the photoreceptors.

(5) Iris and ciliary body

Blood vessels in the iris and ciliary body conform to a pattern whereby choroidal and posterior ciliary vessels contribute to the vasculature of both structures. Within each ciliary process the vessels are abundant and tortous. The arterial supply derives predominantly from the iris vessels while the venous drainage is to the terminal end of the choroidal vortex vasculature (Fig. 3.36).

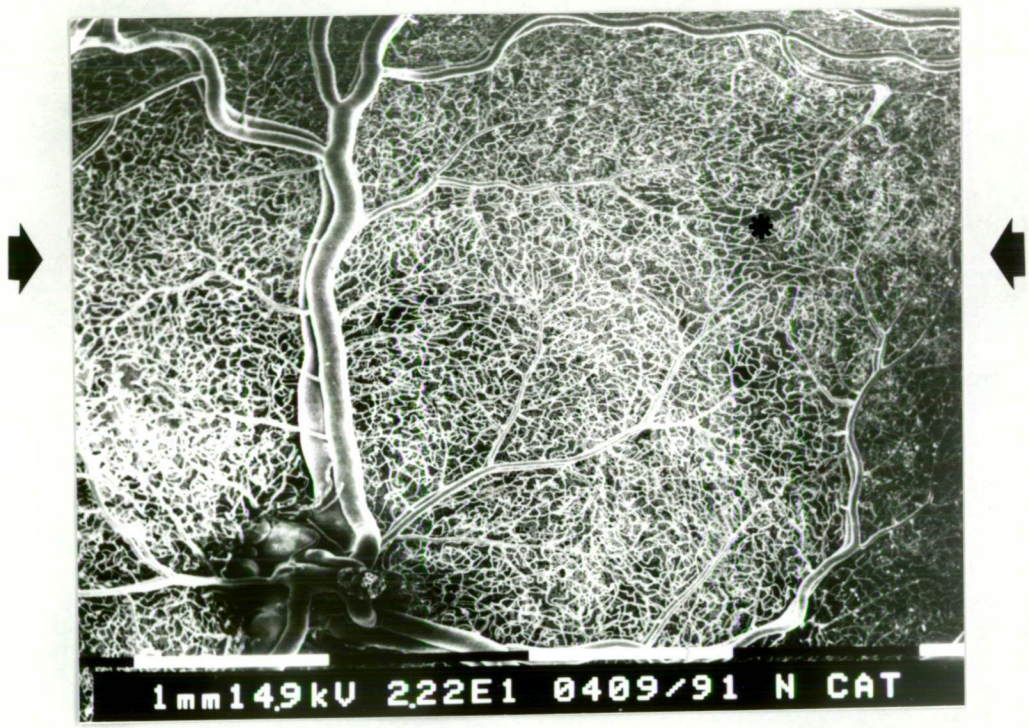

Figure 3.15: Quoll's retinal circulation

Corrosion cast appearance of the retinal circulation viewed from the vitreal surface. Emanating from the optic disc are paired arteries and veins. Above the optic disc, the larger vessels avoid the horizontal visual streak (Arrows). The area centralis (*) is supplied by an anastomosing capillary network which is derived from multiple feeder vessels.

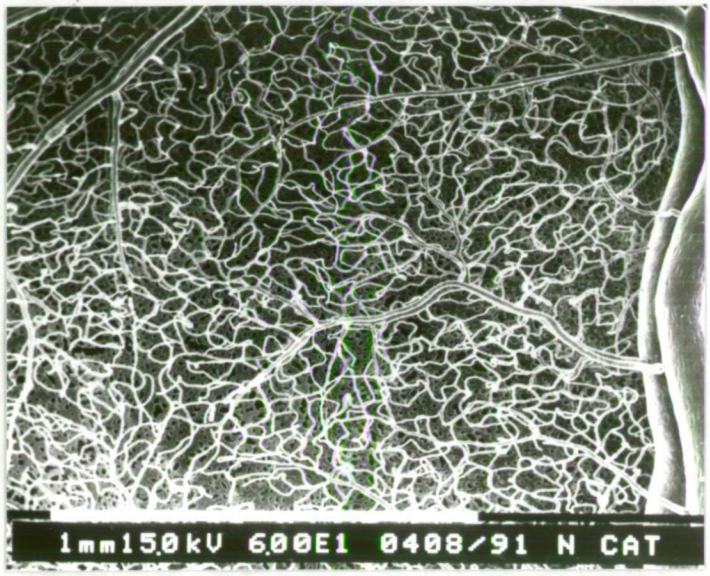

Figure 3.16A: Quoll's retinal capillary bed; low magnification view

Corrosion cast view of the capillary bed in the superior retina adjacent to the vertical midline. A paired artery and vein are seen in the extreme right of the micrograph. Longitudinal nuclear impressions, characteristic of arterial endothelial cells, are seen in the more vitread artery. The capillary network itself is not organised into the same paired configuration as the larger vessels.

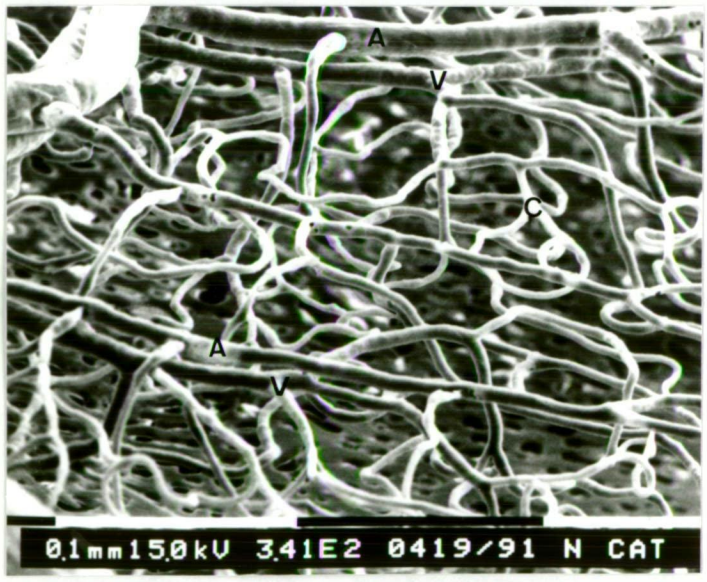

Figure 3.16B: Quoll's retinal capillary bed; oblique view

Corrosion cast view of the capillary bed. When viewed obliquely, the larger feeding (A) and draining vessels (V) are seen to remain paired down to the capillary bed (C). This bed is not looped. The choriocapillaris network (N) may be seen in the background.

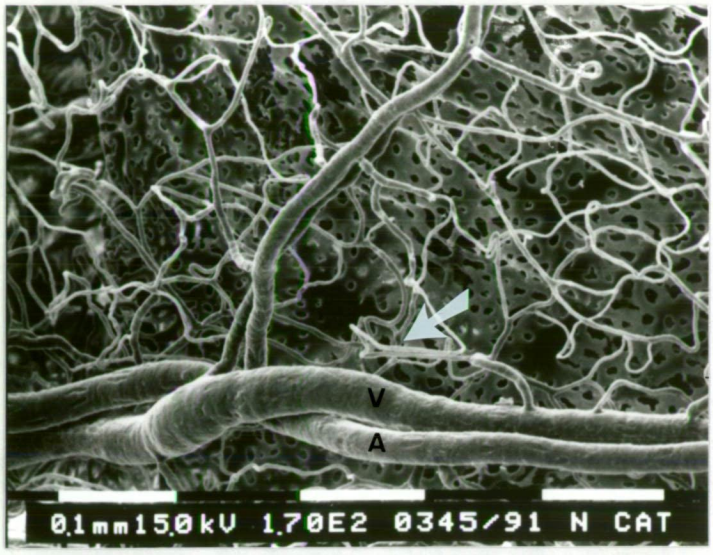

Figure 3.17A: Quoll's central retinal capillary bed

Corrosion cast of the quoll capillary bed as viewed from the vitreal surface. The capillary bed shows some loop like properties (Arrow) but on the whole is more like the general mammalian capillary pattern than that seen in the marsupial CNS. A paired artery and vein may be seen to loop around each other, a feature seen during fluorescein angiography. The choroidal bed is seen deep to the retinal circulation.

Figure 3.17B: Quoll's peripheral retinal capillary bed

Corrosion cast of the quoll peripheral capillary bed as viewed from the vitreal surface. The terminal bed shows capillary loops more akin to those seen within the marsupial CNS (Arrow). The capillary bed here forms one layer. The choriocapillaris circulation is seen deep to the retinal bed.

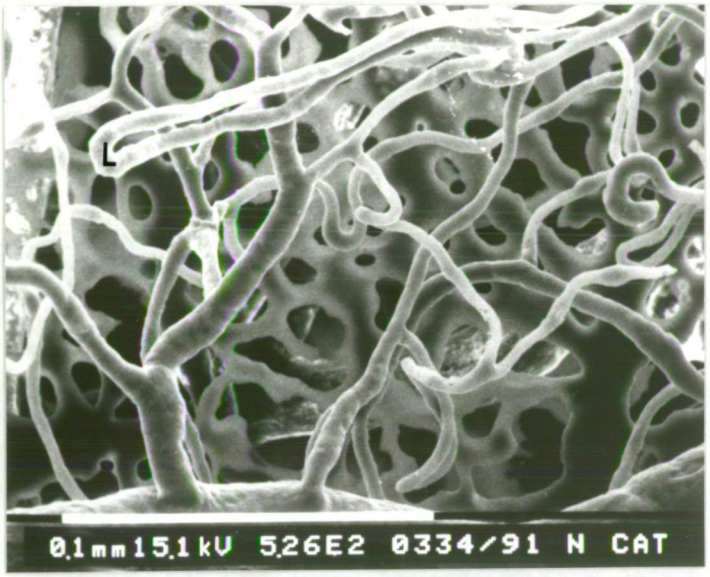

Figure 3.18A: Quoll's central retinal capillary bed

Higher magnification view of the quoll's retinal vasculature. Some of the capillary profiles show loop like configuration (L); others do not.

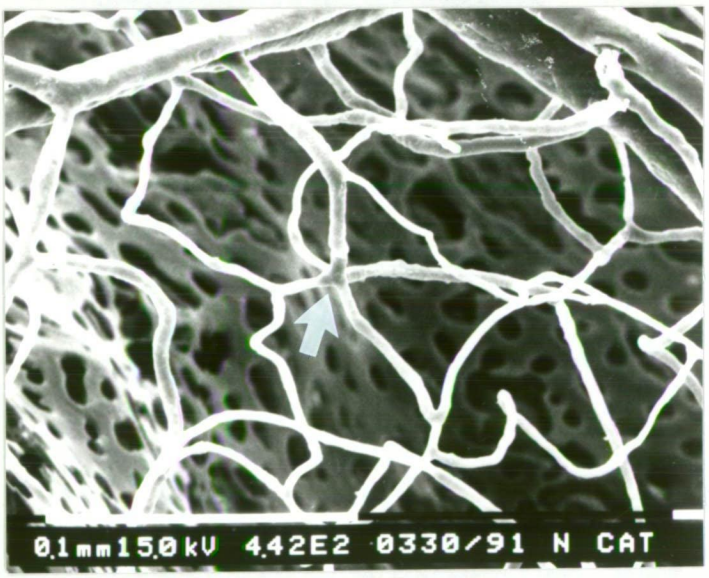

Figure 3.18B: Quoll's central retinal capillary bed

Corrosion cast of the retinal circulation. Most of the capillary bed in the Quoll is non-loop like. Stellate branching of capillaries around a central feeding (or draining) vessel is a common pattern (Arrow), distinctly non-loop like characteristics.

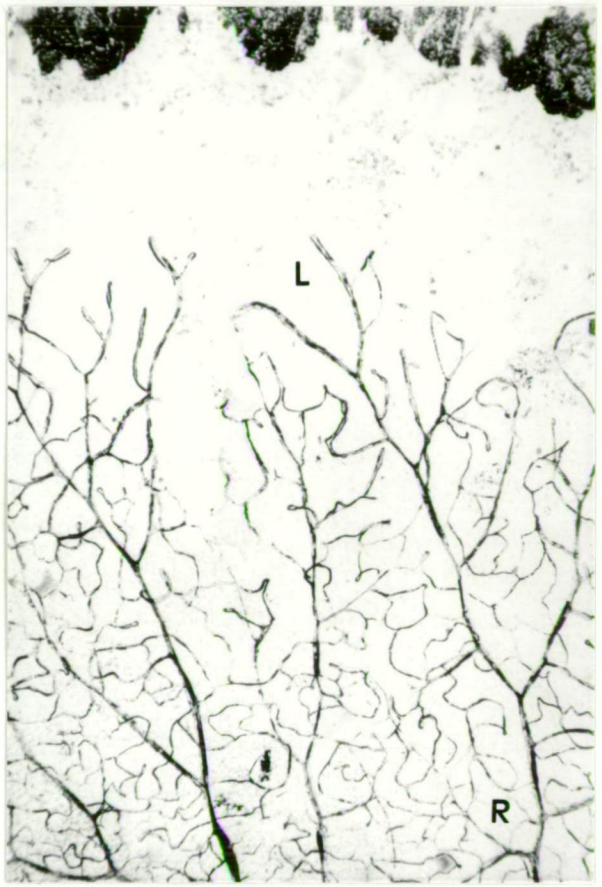

Figure 3.19: Quoll's peripheral retina

Carbon injected retina. Peripheral retina showing the loop-like apical capillary bed (L) and the more central reticular bed (R). The pigmented areas (Arrow) define the ora serrata showing that the peripheral retina is avascular. Scale bar = 50μm.

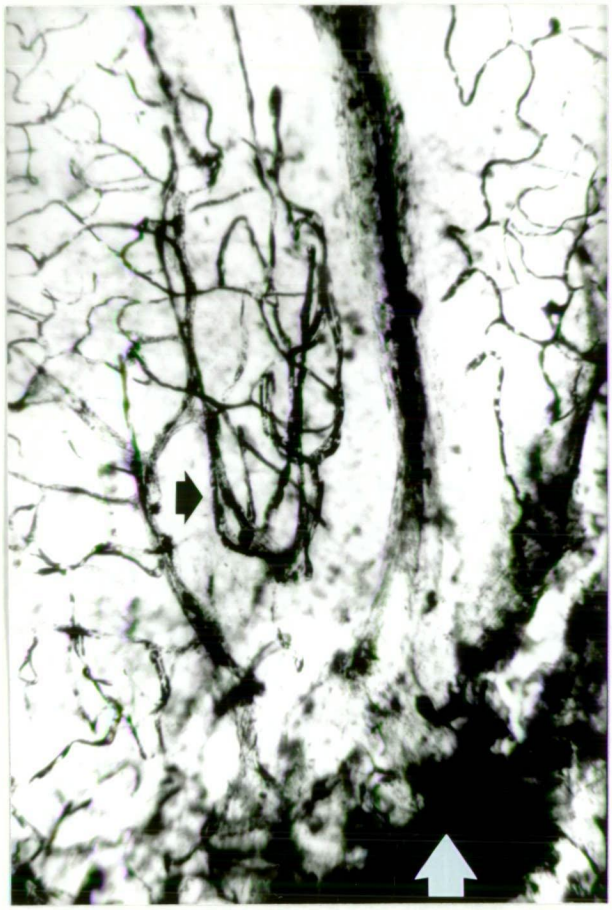

Figure 3.20: Tasmanian devil's peripapillary retinal vessels

Carbon injected retinal material in the devil. This example has been used for illustrative purposes (rather than the quoll) as it showed better the loop like extra layer of retinal vessels (Black Arrow) found in the region of the optic disc (White Arrow). Scale bar = 200μm.

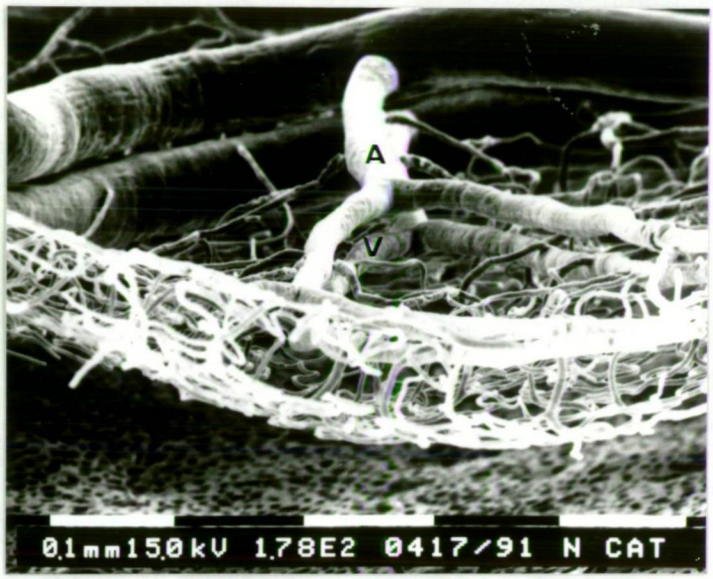

Figure 3.21A: Quoll's retinal capillary bed

Corrosion cast of retinal vasculature, side on view. The pairing of the larger arteries (A) and veins (V) may be seen down to, but not including, the terminal capillary bed. The capillary bed is bilayered (Arrow). Correlation with histological sections show that these capillary beds lie in the NFL/GCL and in the OPL.

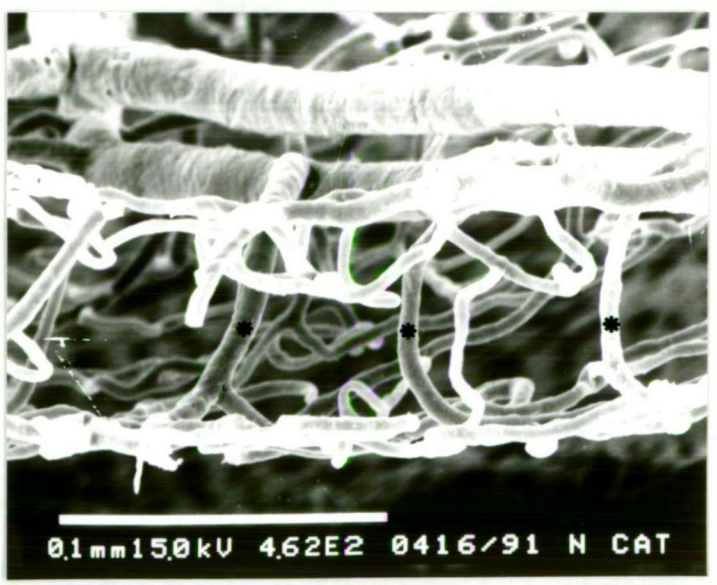

Figure 3.21B: Quoll's retinal capillary bed

Corrosion cast of the quoll retinal capillary bed, side on view at higher magnification. The bilayered bed is more clearly seen. Joining vessels pass between the two beds (*).

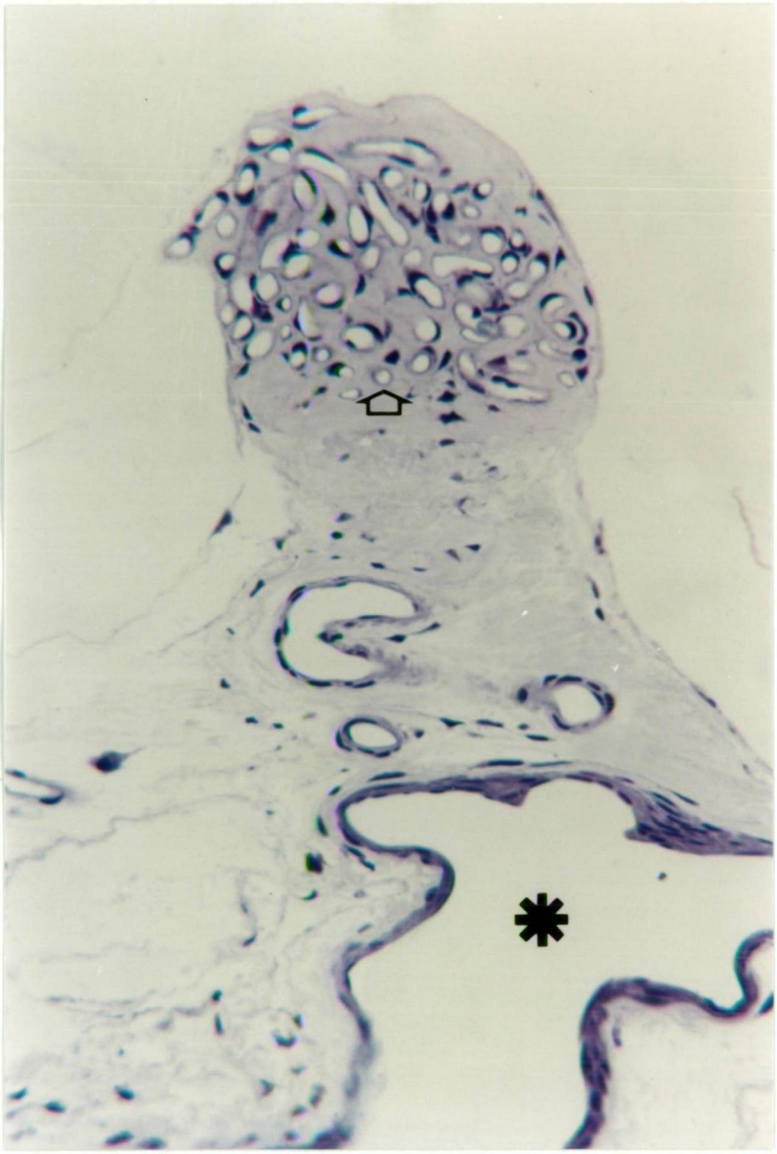

Figure 3.22: Histology of the quoll's optic disc vessels

Light microscopic appearance of the optic disc vascular leash. Plastic embedded 1μm thick toluidine blue stained section. The disc vessels consist of a tightly clumped array of small diameter capillary channels (Arrow). This is surrounded by a fibrous capsule. Large diameter feeding vessels may also be seen (*). Compare with the possum disc leash, Fig. 3.4. Scale bar = 50μm.

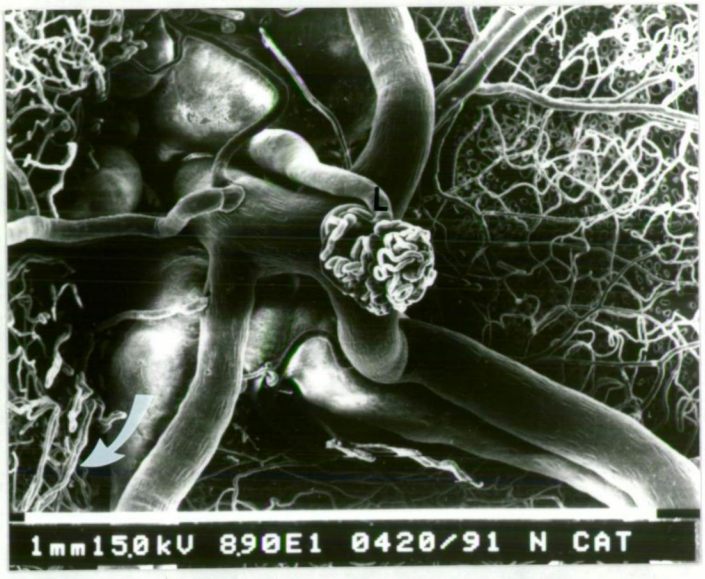

Figure 3.23A: Quoll's optic disc vessels

Corrosion cast of the quoll optic disc as viewed from the vitreal surface. The leash of capillary vessels (L) may be seen arising from the large vasculature of the optic disc. Note the occasional retinal capillary loop adjacent to the optic disc (Arrow).

Figure 3.23B: Quoll's optic disc vessels

Corrosion cast appearance of the optic disc, side on view. This complements Fig. 3.22, demonstrating the large feeding vessels arising from the retinal circulation and the dense network of capillary channels within the leash.

Figure 3.24A: Quoll's retinal vascular dichotomous branching

Corrosion cast of the retinal vessels. Branching of the vasculature is usually dichotomous and without sphincteric impressions. Both divisions are of similar diameter. The artery (A) and vein (V) are paired.

Figure 3.24B: Quoll's retinal vascular side arm branching

Corrosion cast of the retinal vasculature. Smaller side branches often have an annular sphincteric impression at the site of branching (Arrow). These branches are usually much smaller than the parent vessel.

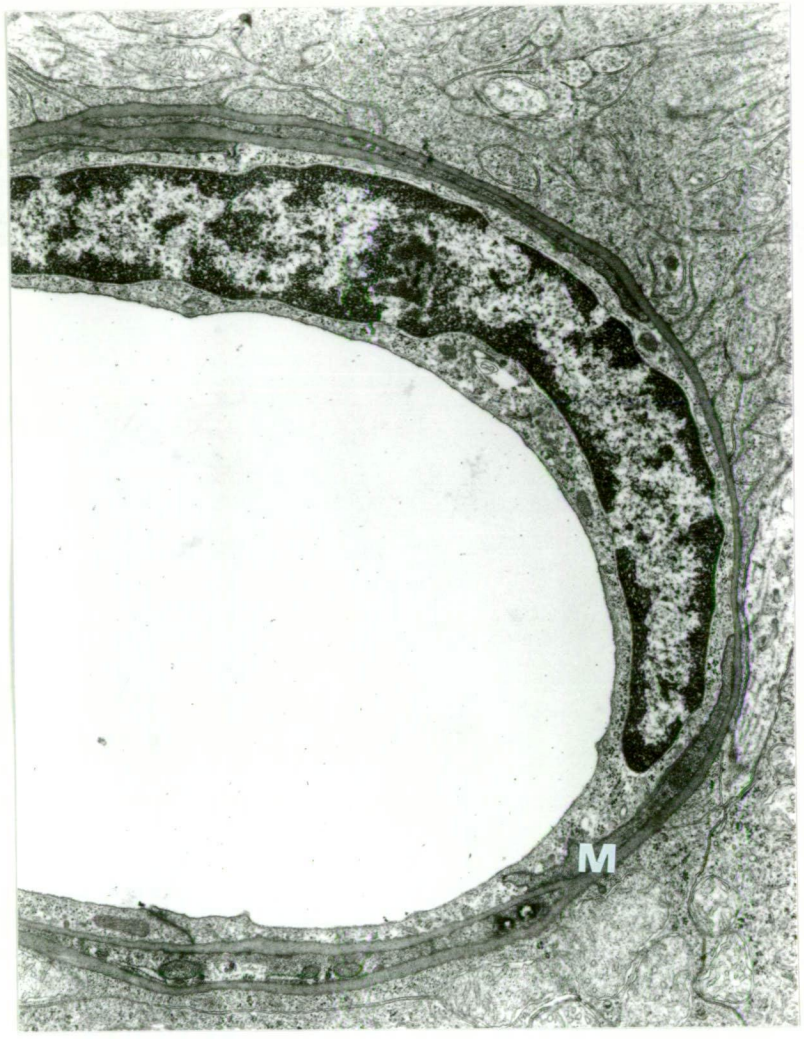

Figure 3.25: Quoll's retinal capillary ultrastructure

The capillary ultrastructure in the quoll retina is that of a non-fenestrated endothelium. A basement membrane (M) surrounds the endothelial layer.

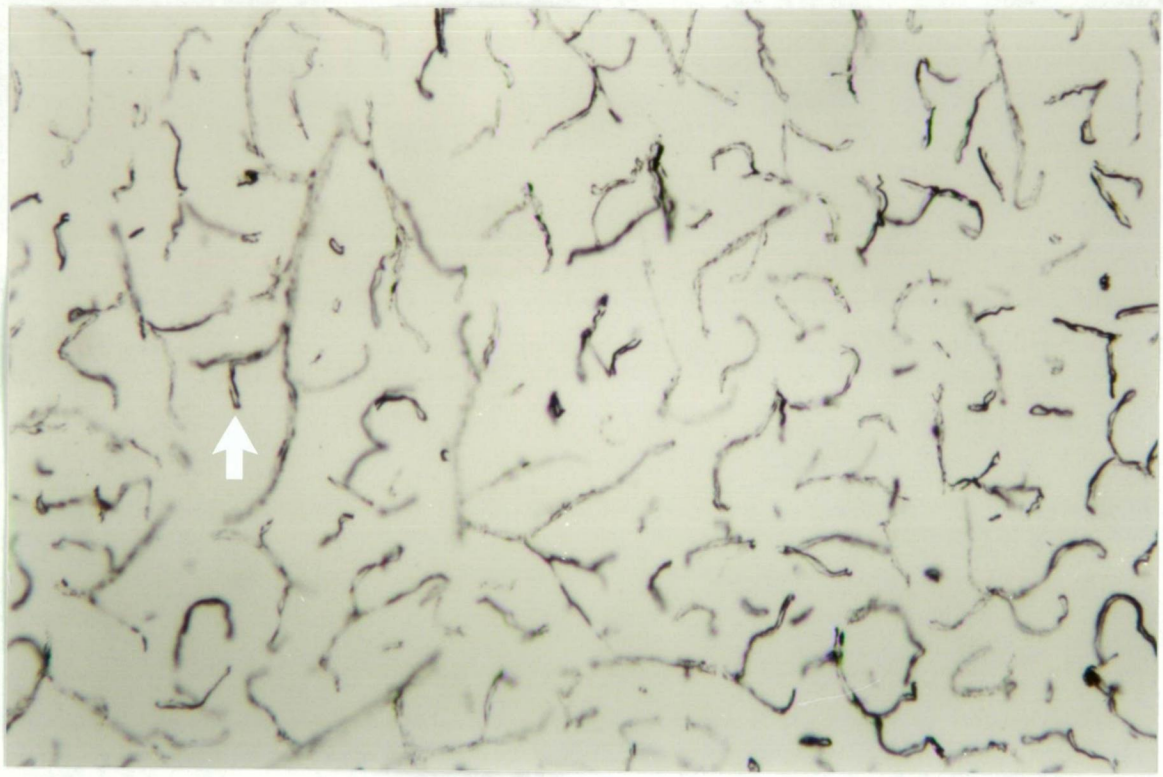

Figure 3.26: Quoll's CNS vasculature

Carbon injected vasculature of adult quoll CNS (gray matter). Unstained 100μm thick section showing capillary detail. All profiles are paired (Arrow), unlike the capillary bed within the retina. Scale bar = 100μm

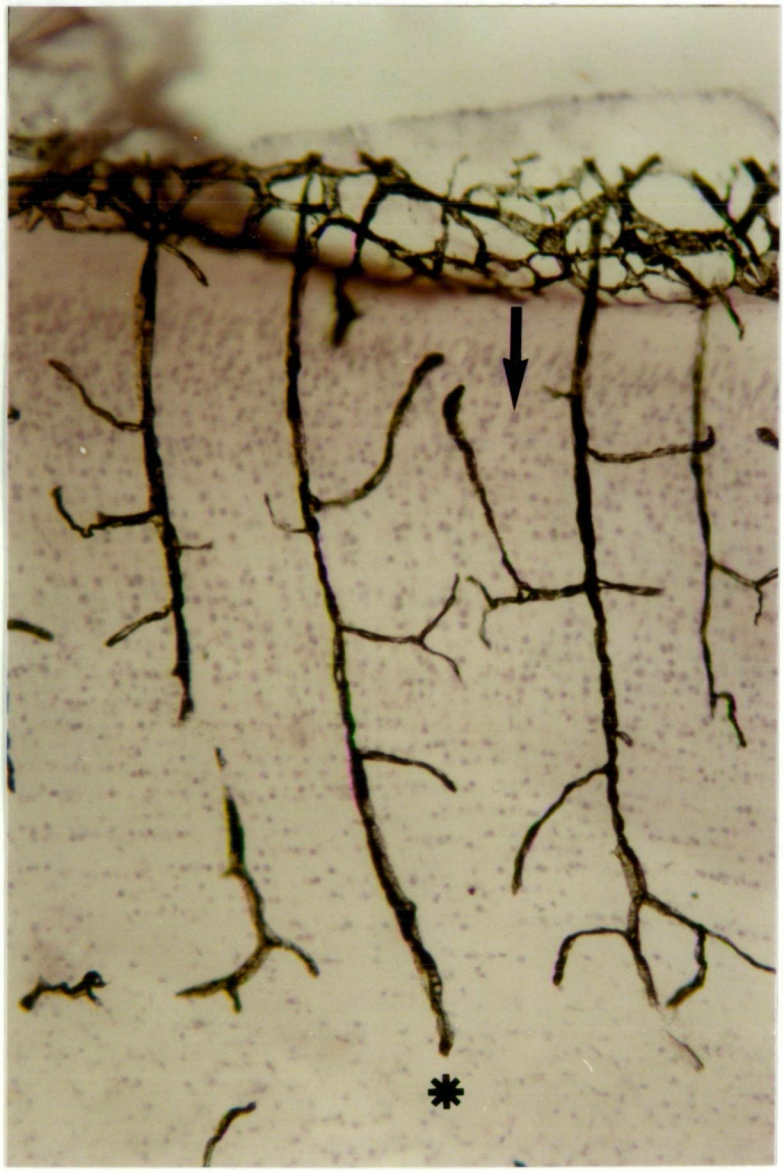

Figure 3.27: Possum's CNS vasculature

Carbon injected vasculture of neonatal possum CNS (cortex). Counterstained 100μm thick tangential section of cortex showing vascular bed. The vascular pairs arise form the pia and penetrate into the brain (Arrow). The terminal capillaries are looped and paired (*). There is no communication between adjacent capillary beds. Scale bar = 100μm.

Figure 3.28: Quoll's ocular vasculature

Corrosion cast of the quoll's eye, external view. The arterial supply to the choroid is derived from the posterior pole through a number of SPCAs (Arrow). These intermingle with the venous channels which drain into the vortex veins (See Fig. 3.29). The external layer of choroidal vessels forms an almost complete vascular coat. One of the two LPCAs (one nasal and the other temporal) may be seen as it passes anteriorly to supply the iris and ciliary body without giving branches to the choroid along its course (*).

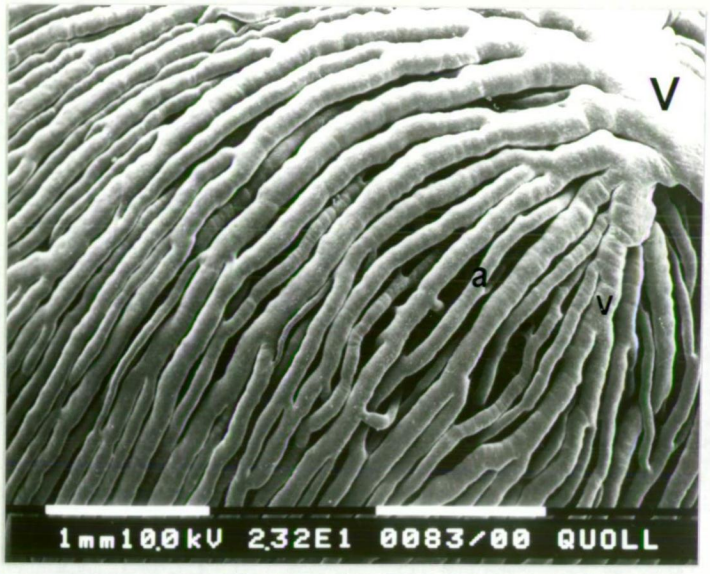

Figure 3.29A: Quoll's choroidal vasculature

Corrosion cast of a choroidal vortex vein (V) viewed externally. The draining veins (v) intermingle with the terminal branches of the SPCAs (a).

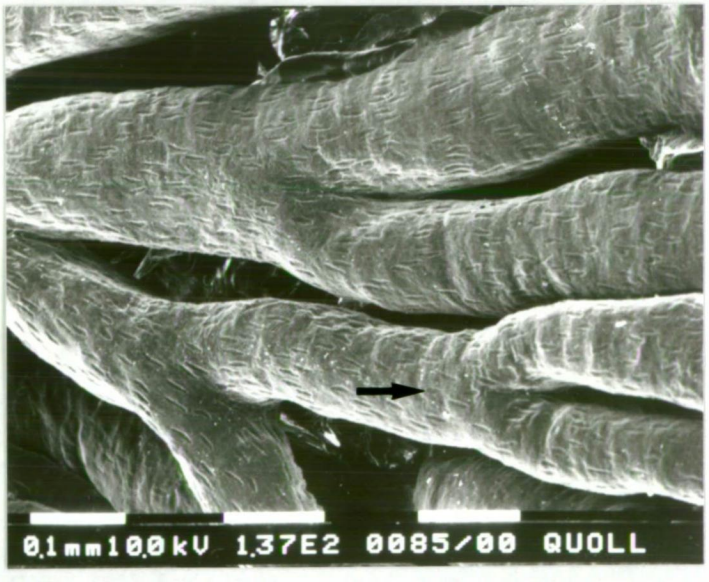

Figure 3.29B: Quoll, choroidal arteries

Corrosion cast of the choroidal arteries viewed externally. Branches of the SPCAs supply the choroid. The longitudinal endothelial nuclear impressions are clearly seen (Arrow).

VITREOUS

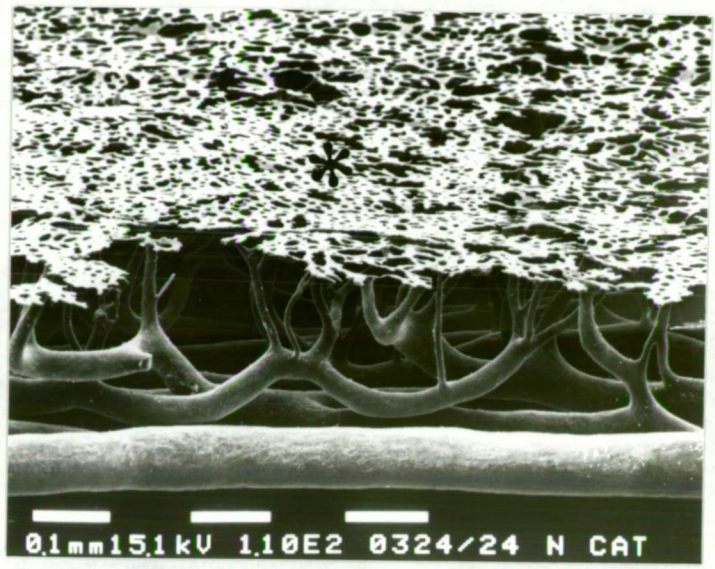

CHOROID

Figure 3.30A: Quoll, choroidal vasculature

Corroision cast of the choroid. Side on view of a micro-dissected specimen. The choriocapillaris is an almost complete sheet of vessels (*). It is supplied by long branches from the external layer of choroidal vessels.

VITREOUS

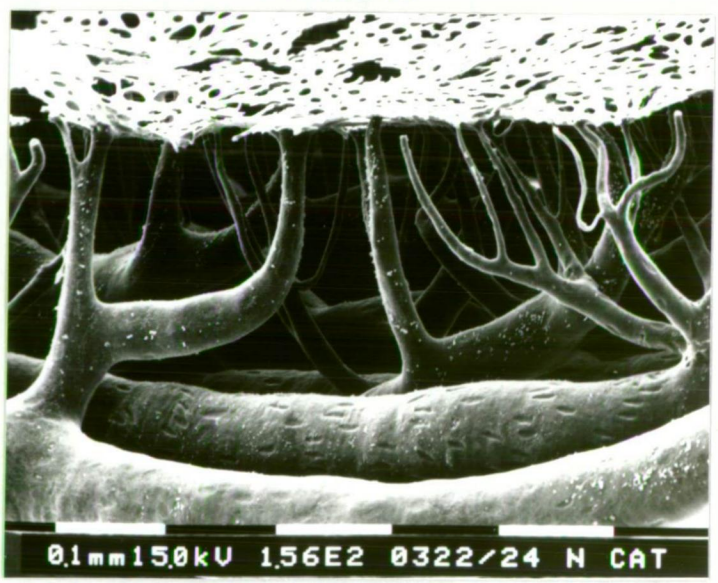

CHOROID

Figure 3.30B: Quoll, choroidal vasculature

Corroision cast of the choroid at higher magnification. Side on view of a micro-dissected specimen. Note the long branches supplying the choriocapillaris. The tapetum intermingles with these long branches. Arterial nuclear impressions may be seen.

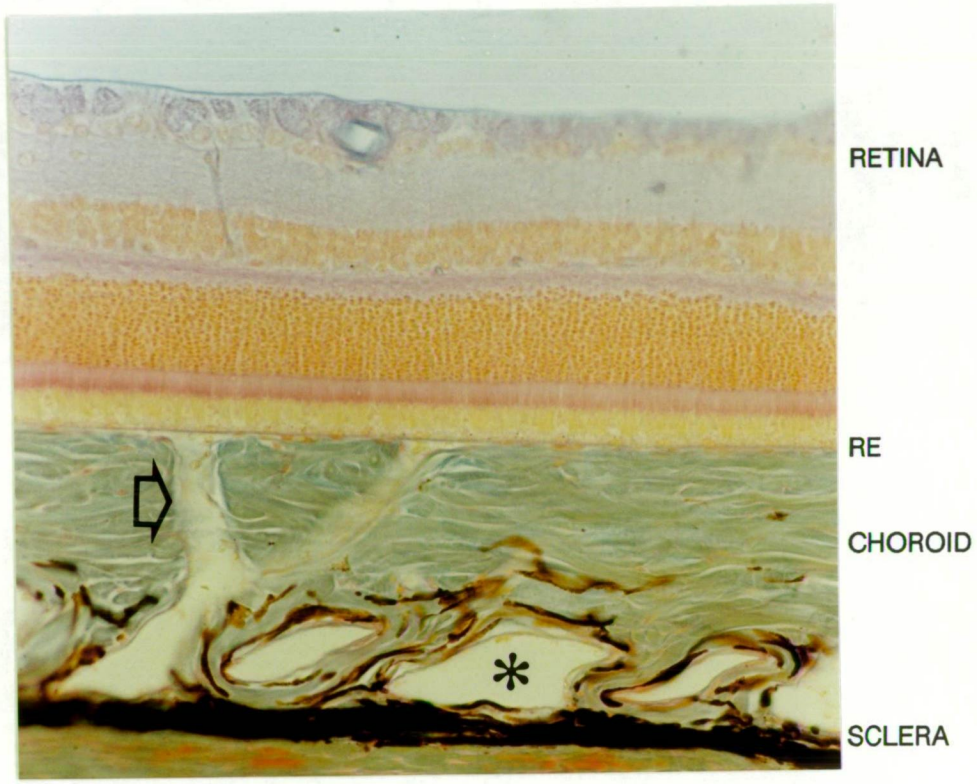

Figure 3.31: Histology of the choroid

Histological section of an unspecified Dasyurus species taken from the Kevin O'Day Collection. The branching choroidal vessels may be seen passing through the choroidal tapetum (Arrow). They are derived from the external layer of larger vessels (*). There is no pigmentation within the RE cells at the junction of the choroid and retina, indicating that the specimen was from the superior retina. There is however, pigmentation between the choroid and sclera. Specimen used with the kind permission of Dr Edward Ryan, Curator of the O'Day Collection, Royal Victorian Eye and Ear Hospital Melbourne. Scale bar = 50μm.

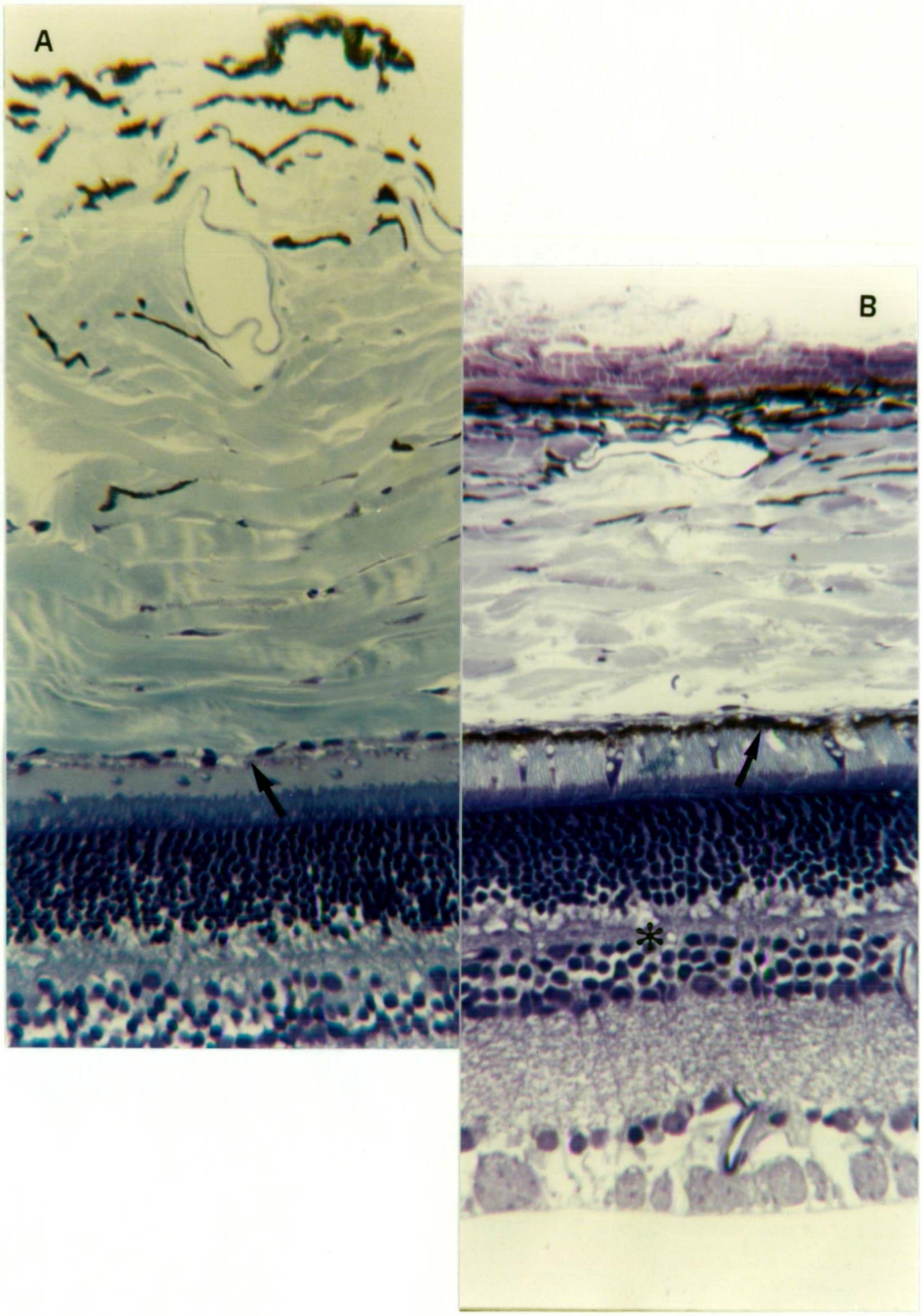

Figure 3.32: Quoll's tapetal pigment variation

Histological section of the choroid and retina. Plastic embedded, 1μm thick toluidine blue counterstained sections. (A) In the superior retina pigmentation is absent from the RE (Arrow). The choroidal tapetum (T) here is thicker than inferiorly. (B) In the inferior retina the RE contains pigment (Arrow) which blocks the effect of the choroidal tapetum (T). Note the capillary profiles within the OPL (*). Scale bar = 50μm.

Figure 3.33: Quoll's tapetal ultrastructure

The quoll's choroidal tapetum consists of collagen fibers (*) lying between the RE (not shown) and the external pigment layer (Arrow). Note the myelinated axons lying within the choroid (N). Scale bar = 1μm.

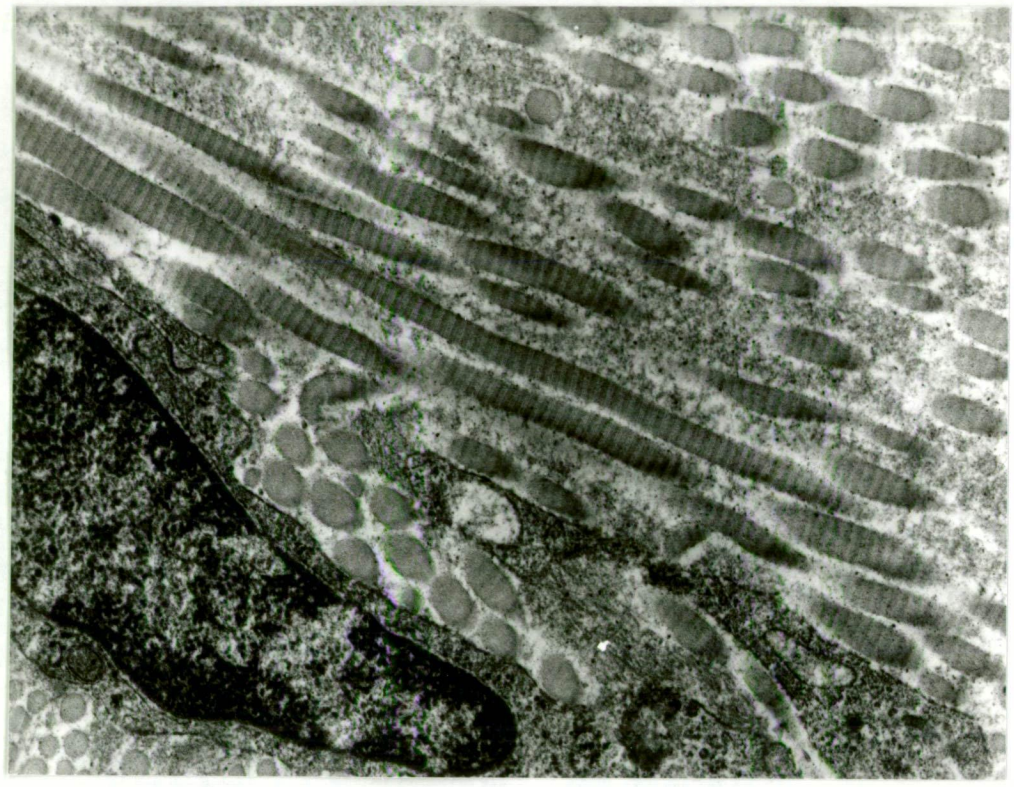

Figure 3.34: Quoll's tapetal ultrastructure

The tapetum at higher magnification is seen to consist of collagen bundles. Scale bar = 0.5μm.

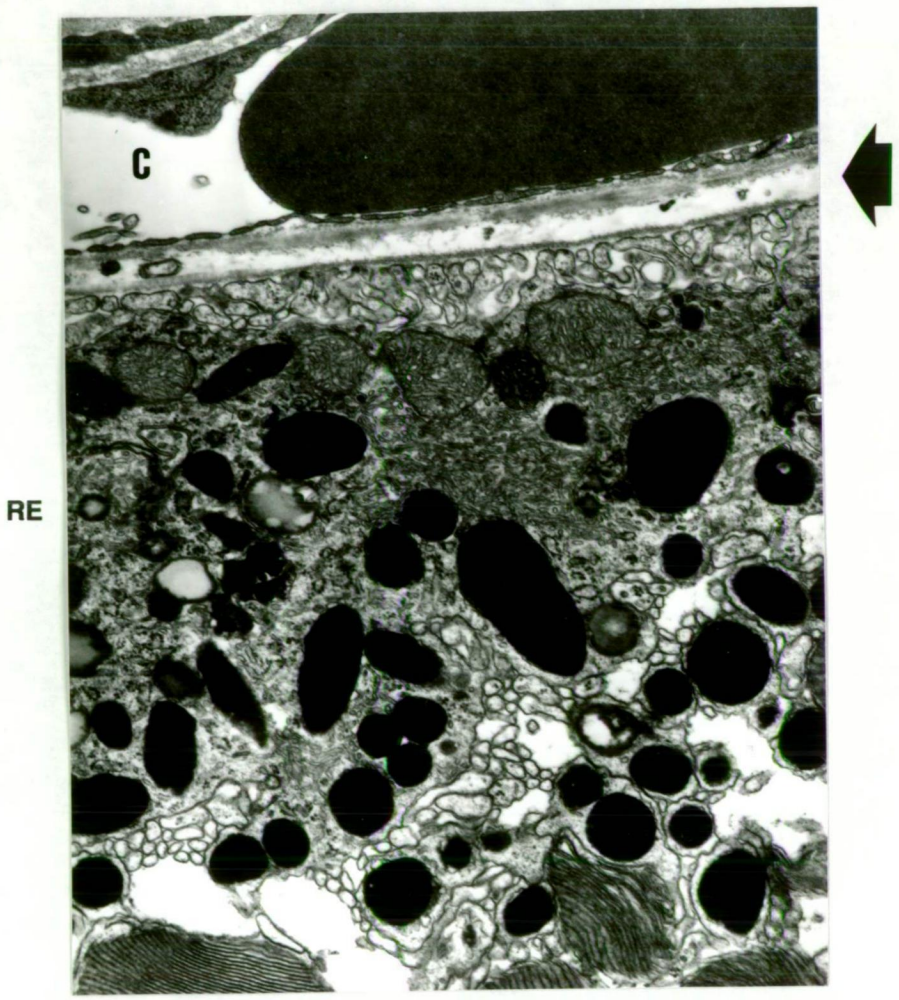

Figure 3.35: Quoll's retinal epithelium and choriocapillaris

Ultrastructure of the choroidal-retinal junction. The RE has a villous basal surface adjacent to the multilayered Bruch's membrane (Arrow). The choriocapillaris consists of a fenestrated capillary bed (C). The RE cells have mitochondria, smooth endoplasmic reticulum and, in this specimen, scattered pigment granules. Scale bar = 0.5μm.

Figure 3.36A: Quoll's ciliary body

Corrosion cast of of the ciliary body viewed obliquely from the vitreal surface. Each process has a dense network of capillaries. These drain into the anterior choroidal circulation (Arrow).

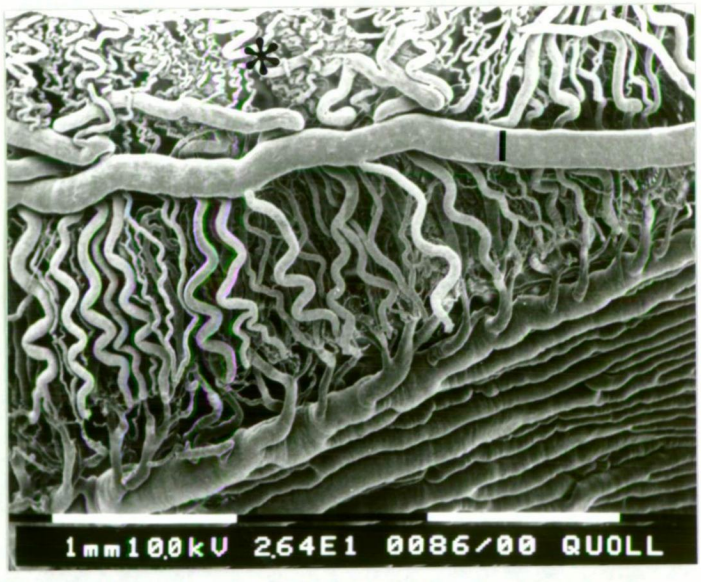

Figure 3.36B: Quoll's ciliary body

Corrosion cast of the ciliary body viewed externally. The ciliary body circulation is derived from the major arterial circle of the iris (I), a branch of the LPCA. This also supplies the iris circulation anteriorly (*).

3.3.2 Placental ocular vasculature

3.3.2.a Guinea pig

(1) Overall appearance

The general vascular pattern conforms to that seen in other mammals. The choroid is richly endowed with a network of ciliary branches and vortex draining channels. The long posterior ciliary arteries run anteriorly giving multiple branches to the choroid itself before suppling the iris and ciliary body.

(2) Retinal circulation

The retina is avascular. There is no leash of vessels arising from the optic disc as seen in the marsupials, merely the terminal branches of the optic nerve vasculature (Fig. 3.37).

(3) Choroidal circulation

Multiple ciliary vessels supply the choriocapillaris network which in turn drains into the vortex system (Fig. 3.38). The LPCAs give direct branches to the choroid along their course (Fig. 3.39). The choroid is bilayered with an external layer of large feeding and draining vessels. This supplies short branches to the choriocapillaris (Fig. 3.40). Anteriorly, the external layer is incomplete and the arterial and venous arrangement of the choroid is more easily discerned (Fig. 3.41). The choriocapillaris network is of similar extent to that of the other species examined, except anteriorly where the coverage is less complete. The threads of the mesh are around 10μm in diameter.

3.3.2.b Rat

(1) Overall appearance

Though small, the rat's eye has a choroidal pattern similar to that seen in the other species (Fig. 3.43). Externally, the choroidal vasculature forms an almost complete sheet. Arising from the posterior pole, branches from both the short and long posterior ciliary vessels fan out to supply the choriocapillaris. These branches intermingle with the venous system which

coalesces at the four anterior quadrants to form the draining vortex veins. The retina is vascular.

(2) Retinal circulation

The retinal vessels radiate from the otic disc in a segmental and symmetrical pattern (Fig. 3.44) Between five and seven retinal arteries alternate with a similar number of retinal veins. The capillary bed arises from dichotomous branching (Fig. 3.45) of the larger retinal vessels and freely anastomoses with neighbouring beds. The capillary bed is mostly bilayered with one plexus in the vitread retinal layers and a second in the outer plexiform layer (Fig. 3.46). Between the pigment epithelium and the OPL the retina contains no blood vessels.

Characteristic identifying features of arterial and venous casts are seen in Fig. 3.45. The arterial nuclear impressions are typically longitudinal and flame-shaped whilst those of the venous segments are round and are less easily discerned. Perivascular sphincter regions surrounding the branches of some arterioles may be seen in Fig. 3.45. These typically are seen at side arm branches rather than at sites of dichotomous branching.

(3) Choroidal circulation

Both long and short ciliary vessels supply the choroid. The long posterior arteries are paired, anteriorly directed and terminate in the major arterial circle of the iris. Like the guinea pig, but unlike the marsupials, multiple LPCA's branches add to the SPCA supply (Fig. 3.43, 3.47).

The choriocapillaris is hidden externally by this network of vessels. The feeding and draining arterioles and venules linking this network to the choriocapillaris are typically short and branch at 90° to the parent vessel (Fig. 3.48). The choriocapillaris, like all the other species examined in this study, is a dense mesh lying immediately sclerad to the retinal epithelium.

Figure 3.37: Guinea pig's optic disc

Corrosion cast of the guinea pig ocular vasculature viewed from the vitreal surface in the vicinity of the optic disc. Micro-dissected specimen. The choroid is shown in cross section at the upper edge of the micrograph. The choriocapillaris circulation is thrown into a number of artefactual folds. There are no retinal vessels, only the terminal vessels of the optic nerve (Arrow).

CAUDAL **ROSTRAL**

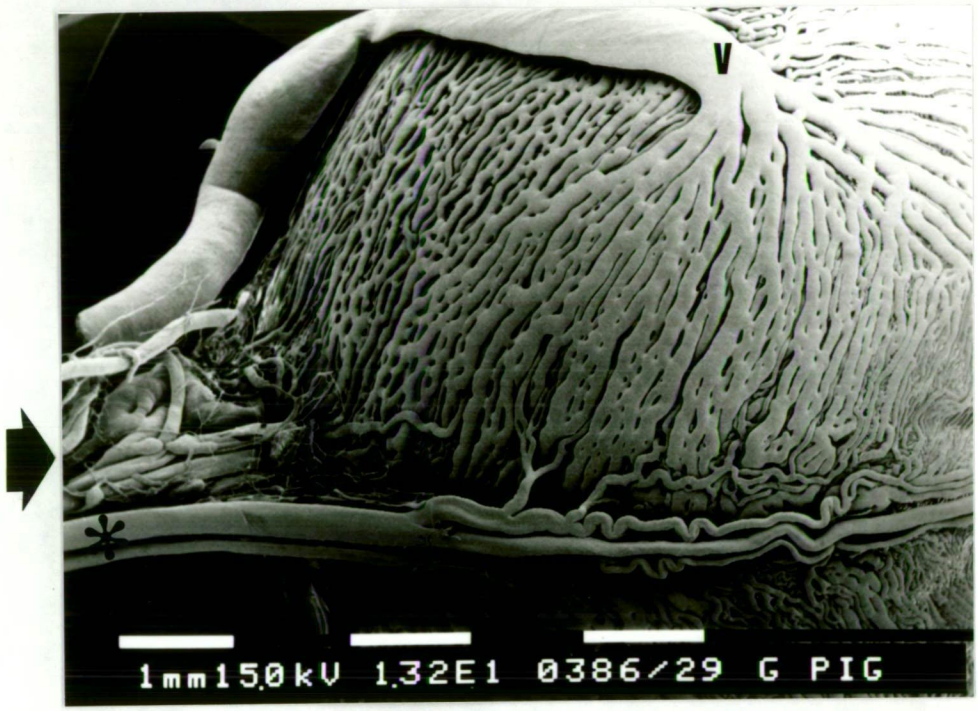

Figure 3.38: Guinea pig's choroidal vasculature

Corrosion cast of the ocular vasculature viewed externally. The choroid is supplied by branches of the SPCAs (Arrow) and LPCAs (*). Vortex veins drain the anterior quadrants of the choroid (V).

Figure 3.39A: Guinea pig's choroidal vasculature

Corrosion cast of a choroidal LPCA viewed externally. The artery (*) gives direct branches to the choroid.

Figure 3.39B: Guinea pig's choroidal vasculature

Corrosion cast of the choroidal circulation in the equatorial region viewed externally. The arterial branches (A) intermingle with the draining branches of the vortex veins (V).

Figure 3.40A: Guinea pig, organisation of the choroidal vasculature

Corrosion cast of the choroidal vasculature viewed obliquely in a micro-dissected specimen. The choroid is bilayered with an external layer of large vessels below and the internal choriocapillaris (CC) above.

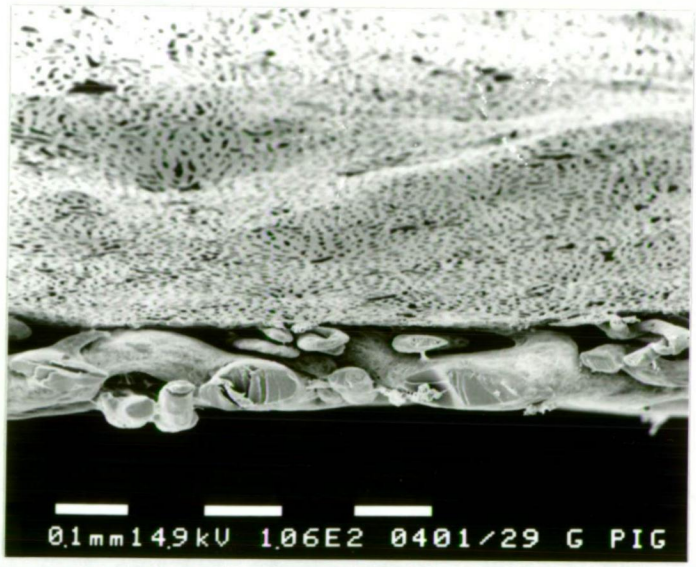

Figure 3.40B: Guinea pig, organisation of the choroidal vasculature

Corrosion cast of the choroidal vasculature. Same area as shown in (A) rotated to show a transverse section of the choroid. The choroid is again seen to be bilayered with short communicating branches between the two layers. CC = choriocapillaris

Figure 3.41A: Guinea pig, anterior choroidal vasculature

Corrosion cast of the choroid viewed externally. Here the external vasculature is less complete, allowing a view of the underlying choroiocapillaris.

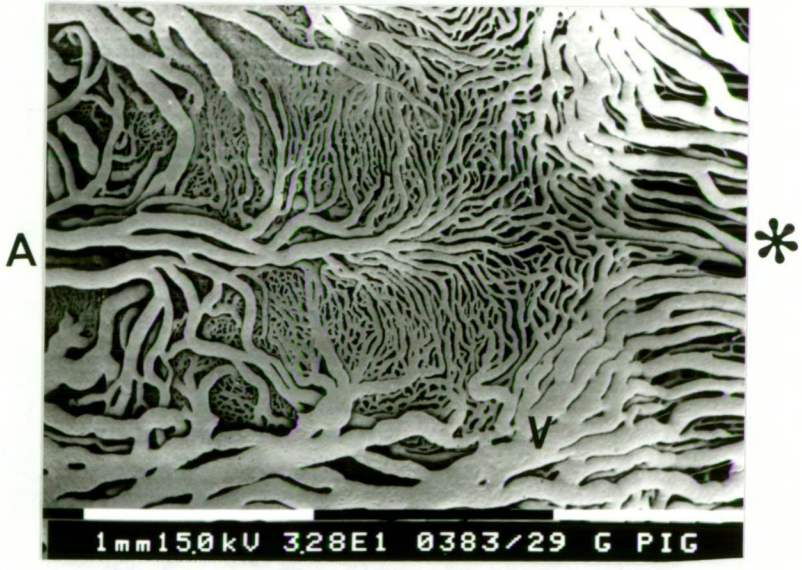

Figure 3.41B: Guinea pig, anterior choroidal vasculature

Corrosion cast of the choroid viewed externally. Higher magnification of (A). The arterial supply (A) intermingles with the venous drainage (V). Anteriorly there is communication with the ciliary body (*).

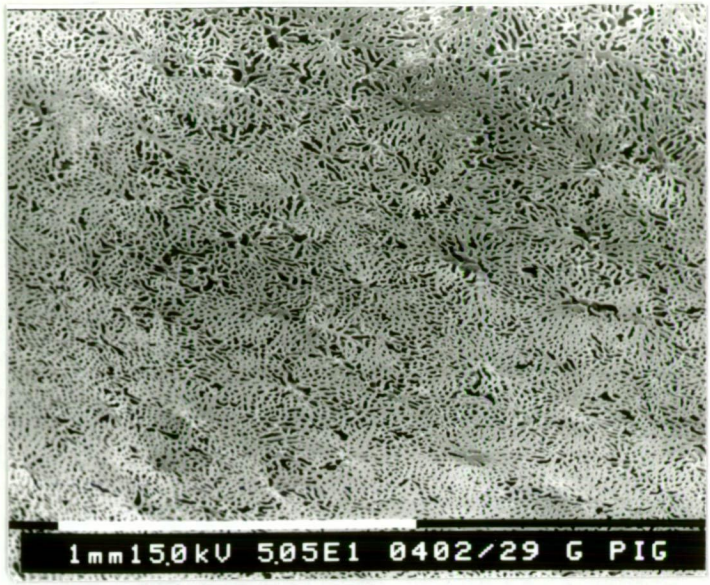

Figure 3.42A: Guinea pig's choriocapillaris

Corrosion cast of the choriocapillaris viewed from the vitreal surface. Note the regular choriocapillaris mosaic. There are no choroidal indentations.

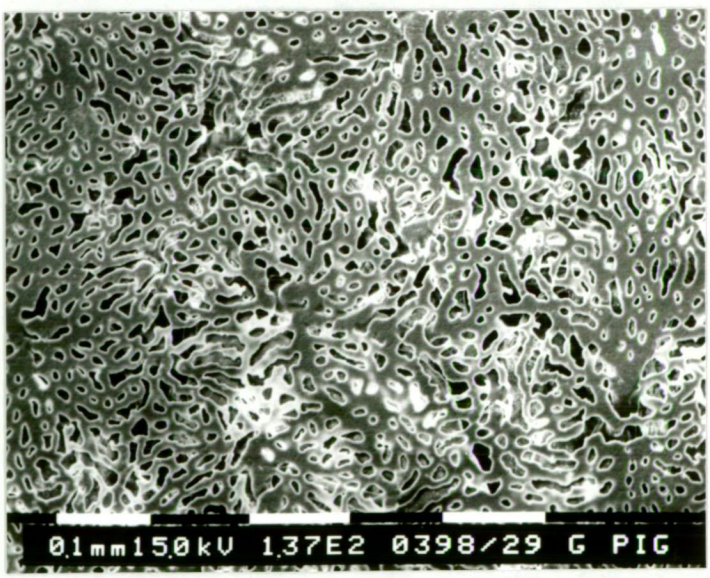

Figure 3.42B: Guinea pig's choriocapillaris

Higher magnification view of (A). The network of capillary channels is clearly seen.

ROSTRAL

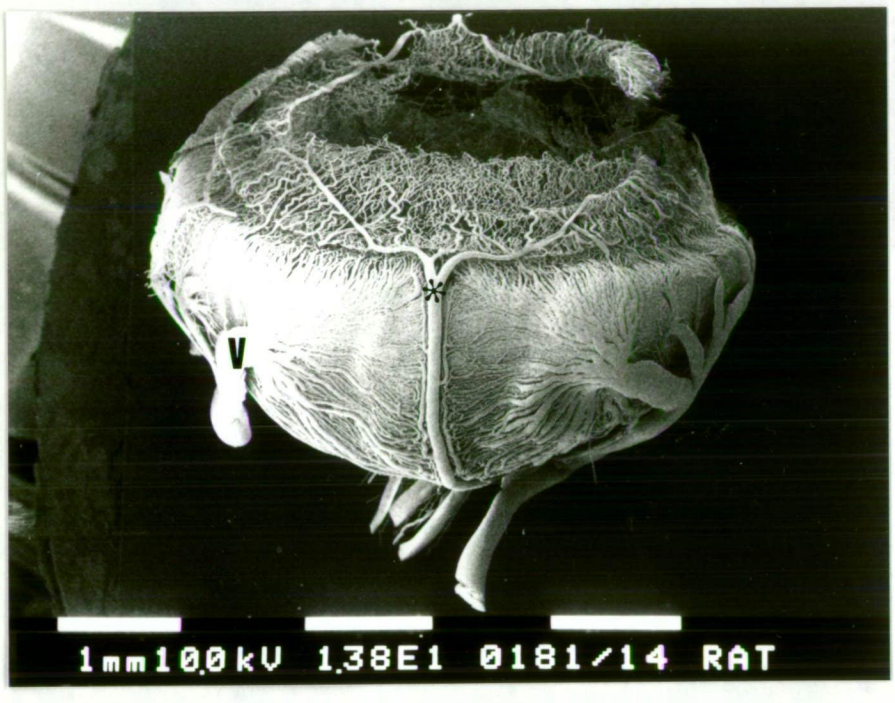

CAUDAL

Figure 3.43: Rat's ocular vasculature

Corrosion cast of the rat's ocular vasculature viewed externally. The choroidal circulation is formed by a dense layer of alternating arteries and veins. The arterial supply is from both the LPCAs (*) and SPCAs. Venous drainage is through the anteriorly located vortex veins (V). The LPCAs also supply the iris and ciliary body circulation.

Figure 3.44A: Rat, optic disc vessels

Corrosion cast of the optic disc viewed from the vitreal surface. The retinal circulation is derived from a radiating and symmetrical arterial branches (A) which alternate with the venous drainage (V).

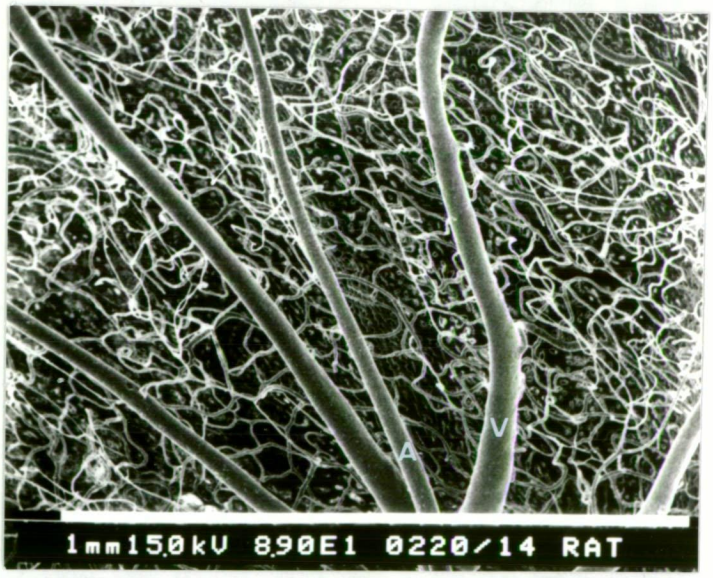

Figure 3.44B: Rat, para disc vasculature

Corrosion cast of the retinal vasculature adjacent to the optic disc viewed from the vitreal surface. Large arteries (A) and veins (V) are separate. The intervening capillary bed is reticular, like much of the quoll's retinal bed.

Figure 3.45A: Rat, retinal capillary bed

Corrosion cast of the retinal circulation viewed from the vitreal surface. The capillary bed demonstrates dichotomous branching. Note the longitudinal endothelial impressions on the artery (A) and the rounder impressions seen on the veins (V).

Figure 3.45B: Rat, retinal vascular side-arm branching

Corrosion cast of the retinal circulation. At the sites of side-arm branching there is often an annular shincteric impression (Arrow).

Figure 3.46: Rat, retinal capillary bed in cross section

Carbon injected rat retina, 100μm thick cross section. The bilayered capillary bed may be seen. Counterstained section located these beds within the GCL/NFL and the OPL. Note that the region between the pigmented RE and the outer layer of the capillary bed is avascular. Around half of a "vascular retina" is avascular. Scale bar = 100μm.

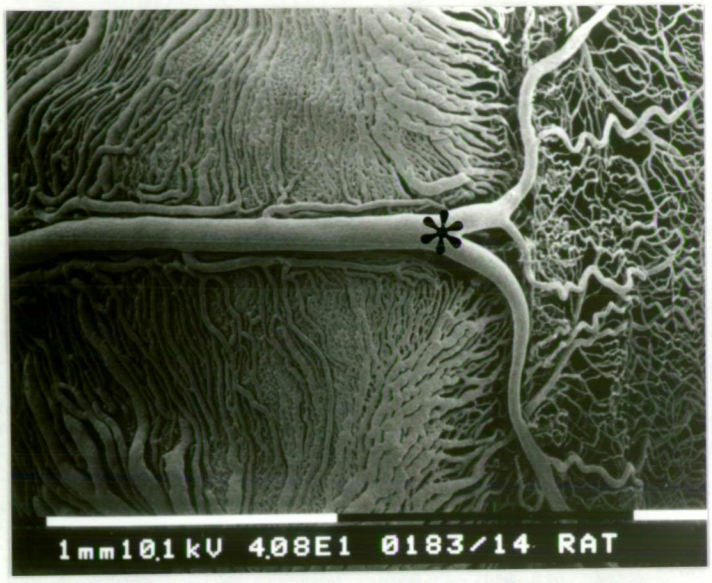

Figure 3.47A: Rat's choroidal circulation in the equatorial region

Corrosion cast of the rat's ocular vasculature viewed externally in the region of the horizontal equator. The LPCA (*) gives direct branches to the choroid before supplying the iris and ciliary body.

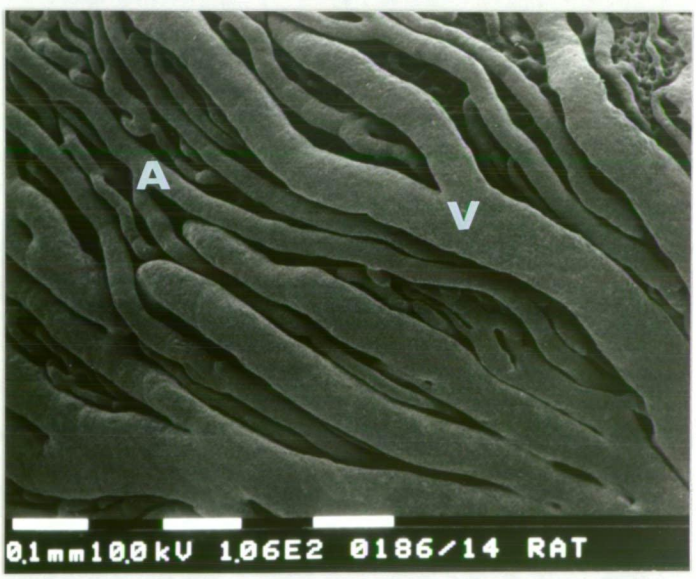

Figure 3.47B: Rat's choroidal vessels

Corrosion cast of large choroidal vessels viewed externally. This outer layer of choroid has intermingling arteries (A) and veins (V).

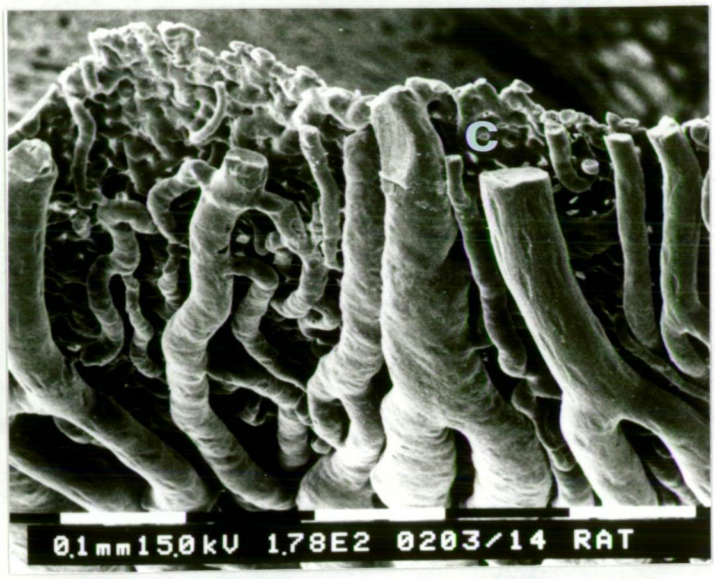

Figure 3.48A: Rat's choroidal vasculature; oblique view

Corrosion cast of a micro-dissected specimen, viewed obliquely. The bilayered choroidal vasculature is clearly seen. The outer layer of larger vessels provide short branches to the choriocapillaris (C).

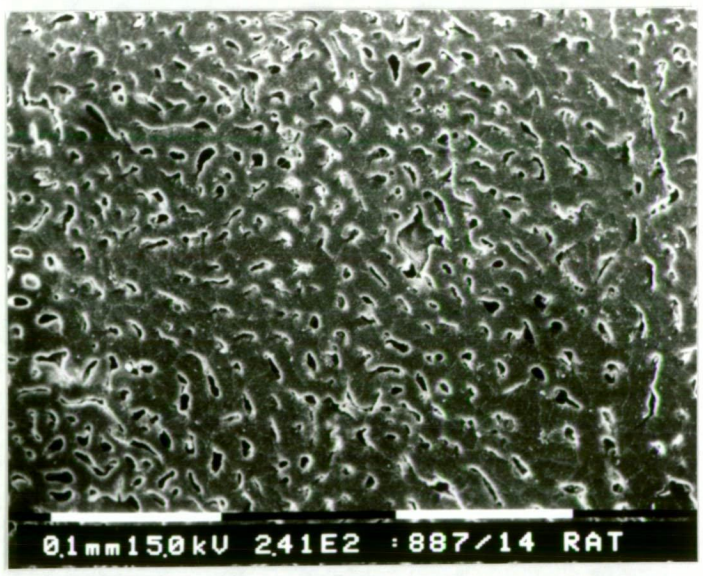

Figure 3.48B: Rat's choriocapillaris

Corrosion cast of the rat's choroid viewed from the vitreal surface. This shows the dense network of capillary channels which constitutes the choriocapillaris.

3.4 DISCUSSION

3.4.1 Demonstration of the vasculature: historical

Since the seminal work of the 17th-century Englishman, William Harvey, the mechanics of the vascular system as a continuous system of conduits has supplanted the ebb and flow theory pronounced by the Greek luminary, Galen (Nourse 1972). The fluid connnective tissue, blood, is recycled through a seemingly endless system of pipes replenishing tissue nutrients and removing wastes. The arrangement, morphology and functional relationships of the vascular system therefore are not new concepts. Similarly, the demonstration of the three dimensional organisation of anatomical tissue spaces is a time honoured technique which predates the work of Harvey. Leonardo Da Vinci (1452-1519) used melted wax to obtain casts of the cerebral ventricular system and of the chambers of the heart (Hodde and Nowell 1980). Indeed injection media such as air and mercury were used by Harvey himself to delineate the vascular system.

3.4.2 Corrosion casting

Since these earlier efforts, the injection technique has had periods of vogue (Cole 1921, Kus 1969, Narat 1935 and Tompsett 1970) with the application of a wide variety of injection media: milk, mercury, gelatine, alloys, plaster of paris, latex rubber, plastics and resins (Gannon 1985) When these methods are coupled with the removal by digestion of surrounding tissue, the vascular system is further isolated and the technique referred to as corrosion casting.

3.4.2.a Background

The preferred name is corrosion casting, but the technique is also variously known as injection method, microcorrosion casting, injection replica, and vascular cast; all terms having the same meaning (Lametschwandtner et al. 1984).

Casts are produced by filling the vessels with a fluid medium which sets *in situ*. With the corrosion of the surrounding tissue the remaining replica represents the topographical organisation of the vascular tree. In recent years the approach has been further refined by the preparation of microcasts of minute tissue spaces and the viewing of these casts using

scanning electron microscopy, complementing imaging techniques using light microscopy and X-rays. Murakami (1971) is attributed with the popularisation of this significant advance (Lametschwandtner et al. 1984). He took Batson's (1955) observation that acrylate monomers autopolymerise with little shrinkage, and therefore are ideally suited to delineate a vascular space, and applied SEM techniques to these casts.

The SEM approach offers particular advantages through its exquisite replication of detail and the three dimensional representation of vascular configuration. The portrayal of anatomical detail is so accurate that both arteries and veins can be identified based on the differing impressions left in the casts by the endothelial cell nuclei (Hodde and Nowell 1980).

3.4.2.b Technical factors

Parallelling the upsurge of interest in corrosion casting, a considerable, but still evolving, literature about physical properties and preparation techniques has also appeared. For adequate injection of the micro-vasculature the following conditions must be met. The resin employed ought to be of sufficiently low viscosity so as to fill vessels of 5μm calibre, must polymerise uniformly without shrinkage or distortion, must not alter the vascular system under scrutiny, must withstand the quite considerable chemical agitation of the digestion process and remain stable and visible, after suitable preparation, in the beam of the electron microscope (Hodde and Nowell 1980).

The most commonly used agents, satisfying many of these criteria, have been methylmethacrylate based acrylic resins (Hodde and Nowell 1980, Lametschwandtner et al. 1984, Murakami et al. 1983, Weiger et al. 1986). Methacrylate resins may be prepared using the original mixture of Murakami (1971) or with the modifications of Gannon (1978, 1981, 1985). Commercially prepared resins are available such as Batson's # 17 (Polyscience Inc: Warrington PA) or Mercox (Japan Vilence Co. Ltd: Tokyo, Japan). The Batsons mixture is commonly used with the viscosity lowering modification of Nopanitaya et al. (1979), which simply involves the addition of monomeric methacrylate to the commercial kit.

3.4.2.c Literature review of corrosion casts

Many hundreds of papers have addressed vascular questions in a wide range of tissues in many different species using corrosion casting: for a recent review see Lametschwandtner et al. (1984). Ocular tissue has not escaped microvascular corrosion casting scrutiny. Shimizu et al. (1978) have produced a monograph on the ocular vasculature of the monkey eye supported by work by Risco et al. (1981). Studies of normal human eyes have been

performed by Fryczkowski et al. (1984), Olver and McCartney (1989), Olver et al. (1990), Ujiie and Hanyuda (1977), Woodlief (1980), Woodlief and Eifrig (1980), Yoneya et al. (1983) and Yoneya and Tso (1987). These have been supplemented by pathological studies of photocoagulated diabetic retinae (Wilson and Green 1987), diabetes (Fryczkowski 1987, Fryczkowski et al. 1989), retinopathy of prematurity (Fryczkowski et al. 1985) and other vascular anomalies (Fryczkowski et al. 1985). In the non-human eye, the cat (Risco and Nopanitaya 1980), rat choroid (Murata et al. 1980, rat iris vessels - one of the few studies using a non-methacrylate casting medium, araldite - (Funk 1986), avian eye (Hossler and Olson 1984), aqueous drainage pathways in the horse (Smith et al. 1988), and comparative ciliary vasculature (Morrison and Van Buskirk 1984, Morrison et al. 1987a, 1987b) have all been investigated with casts. Similarly, casts have been used for experimental studies of subretinal neovascularisation (Dobi et al. 1989, Ohkuma and Ryan 1983), retinal neovascularisation (Tano et al. 1981), phototoxicity (Shiraki et al. 1983) and oxygen induced retinopathy (Gole et al. 1982). For a more comprehensive review of corrosion casting in ophthalmic research see Burger et al. (1987).

These studies have all complemented scanning electron microscopic approaches to retinal structure (Borwein 1985) and the investigation of ocular vasculature, perhaps one of the most intensively investigated and accessible vascular systems (Shimizu et al. 1978).

3.4.2.d Limitations of corrosion casting

While the technique of casting is a powerful and widely applicable approach, the results need to be interpreted with caution. The many processing steps are sources of potential distortion and may lead to misrepresentation of the *in vivo* arrangements. All of the surrounding tissue relationships are lost. The filling may be incomplete or resin can extravasate to produce false portrayal of the vasculature. Even the resin or rinsing steps themselves may alter vascular properties (Wieslander et al. 1986). Seldom do authors acknowledge, or offer explanation for, their relatively high failure rate in complete and reliable replication the vascular system. Of those who have, Hossler et al. (1986), reported that only 50% of their myocardial preparations yielded complete casts. It is important therefore to analyze the corrosion results in light of known structure and function as determined with other techniques. Confidence may be increased when observations using other approaches correlate (Burger 1987).

3.4.3 Alternative techniques for demonstrating vasculature

While corrosion casting does give greater overall perspective it suffers from the problem of interpretation of tissue relationships, distortion during processing and an unknown extent of vascular filling which is usually presumed to be complete. Apart from corrosion casting technique, other approaches have been used to delineate the organisation of the vascular bed. Most of these rely on the demonstration of the vasculature within the framework of surrounding tissue, unlike the corrosion casting technique where the non-vascular mantle is removed. These additional techniques of vascular demonstration may be divided into a number of categories. Many of these, besides supplying information about topographic vascular arrangements, also answer questions regarding vascular permeability, histology and physiology.

3.4.3.a In vivo approach

Physiological observation of the living circulation is desirable to complement the static anatomical approach. For example the insertion of an observation chamber into a tissue bed may be used for vascular surveillance in the alert or anesthetised animal (Smith et al. 1985). Retinal angiography is an example of *in vivo* observation looking through the natural window created by the optically clear visual axis. But, it is the macrocirculation which is more readily observed by this approach. *In vivo* observation of the finer retinal circulation has been performed trans-sclerally (Friedman et al. 1964) whilst the ciliary body vasculature has been investigated through microendoscopy (Funk and Rohen 1987). These methods provide information more about the local functional properties and less about the geometrical arrangement of the vasculture.

3.4.3.b Perfusion demonstrated angioarchitecture

Where the thickness of tissue is less than 250μm (Smith et al. 1985), or where it may be sectioned into layers of this size, conventional light microscopic techniques may be used to examine the vascular bed and its surroundings. The retina, usually being less than this thickness, is ideally suited to wholemount preparation and the portrayal of its entire vasculature. For identification, some means of outlining the lumen is necessary. Stains such as PAS, used to good effect by Friedenwald (1949), stain the vessel wall basal lamina but also stain the outer segments of the photoreceptors obscuring the fine detail of the vasculature.

Vascular geometry has also been elucidated by the intravascular injection of an opaque marker. Indian ink (del Cerro et al. 1985), formulated for biological application without

waterproofing shellac (Peterson et al. 1965), various dyes, for example monastral blue (Joris et al. 1982), fluorescent ink (Coyle 1978), silicone rubber or Microfil (Cutright and Bhaskar 1967), silver nitrate (Hausler et al. 1956) and precipitated lead chromate (Lockard et al. 1959, Williams 1948) are just a few of the vascular markers which have been used. A further variation is the use of radioapaque markers as injection media. With the use of soft X-rays a two dimensional reconstruction of the vascular arrangements may be then seen (Ducournau 1982, Dueker 1974).

Following injection of the these markers, the tissue may be thick sectioned or mounted whole and then cleared to outline the vascular bed alone. Combination with a counterstain may also be used to further delineate tissue-vascular relationships. These approaches suffer from the disadvantage that not all vascular pathways are necessarily filled and that often far greater than physiological pressure is required to perfuse the vascular system producing vascular rupture artefact.

3.4.3.c Chemical delineation

Where a component has unique biochemical or other markers, not found elsewhere within that tissue, then this may be exploited to visualise that particular element. So, basement membrane (Williamson et al. 1980), microvascular alkaline phosphatase (Bell and Scarrow 1984, Scharrer 1950) or the endogenous peroxidase activity of red blood cells (Broadwell et al. 1987) may be exploited as specific markers to demonstrate the vascular system within tissue.

3.4.3.d Combined perfusion and chemical development

By combining the above two approaches, an exogenous marker may be introduced into the animal and then developed to reveal the vascular system. A commonly used method has been the vital or postmortem perfusion of the enzyme, horseradish peroxidase (HRP) which results in the widespread distribution of this enzyme throughout the vascular system (Olavarria et al. 1986). This is followed by subsequent deposition of an enzyme dependent chromogen. When viewed in whole mounts, or thick sections, the vascular system is contrasted with the surrounding unstained tisssue. Gregory et al. (1985) have also demonstrated the vasculature within the central nervous system following the intracisternal administration of HRP. The peroxidase reaction product here is localised to the abluminal surface of the vessel having tracked from the ventricular space, along the paravascular pathways, to localise around the vessels.

Similarly, intravascular administration of HRP labelled lectins have been used, having the added benefit of binding specifically to the vascular endothelium, so called "lectin angiography" (Minamikawa et al. 1987).

Finally, photographic emulsions have been administered systemically and literally developed within the vasculature to leave a dense silver deposit outlining vessels (Olson and Skuse 1969, Van Reempts et al. 1983).

3.4.3.e Trypsin digestion

The serendipitous observation of Kuwabara and Cogan (1960a) that trypsin digests of retina left the vascular scaffold with its cellular components (Cogan and Kuwabara 1984), led to a useful technique for the delineation of the retinal angioarchitecture. Retina itself is sensitive to digestion whilst its vasculature, with a significant mucoproteinaceous wall, is more resistant. Counterstaining the residue with H&E or PAS reveals not only geometric relationships but also the endothelial and pericyte structure of the vessels. Modifications to this approach have been described: the alternative use of pepsin for digestion (Ashton 1963); improved ways of maintaining vascular relationships during processing (Walker et al. 1978); application to brain tissue (Cogan and Kuwabara 1984); embedding in plastic (Toussiant at al. 1961) and the combination of digestion with injection of the vasculature (Knight 1966). These digestive methods continue to be useful for observation of perivascular tissue relationships.

In this study reliance has been placed mainly upon the corrosion casting-SEM approach to depict vascular organisation. It has been supplemented with carbon injected material and light and transmission electron microscopy of vascular-tissue relationships.

3.4.4 Ocular (and CNS) vascular anatomy

As the retina is an outpouching of the brain, its circulation is similar in many respects to that of the CNS. Indeed, the eye has been described as the little brain (Davson 1979). Therefore the circulations of both the eye and brain will be considered.

The details of the placental vascular bed are presented for comparative purposes, in order to relate the experimental techniques and findings to known patterns, and as a means of direct comparison of the placental with the marsupial arrangement. The emphasis in the discussion which follows is based predominantly upon the less well documented marsupial retinae and CNS.

3.4.4.a Marsupial central nervous system

The gross organisation of the cerebral vasculature of Australian marsupials and protherian monotremes has been described by Sunderland (1941) and of the American Virginia opossum by Voris in 1928. This has been supplemented by the work of Gillilan (1972) and Dom et al. (1970) and, more recently, reviewed by Johnson (1977). The presence of an *arteria tortuosa*, a structure somewhat similar to a carotid *rete mirable*, has been reported in the Tasmanian devil's brain (Shah et al. 1986, Shah and Nicol 1989). The vasculature of the macropodid marsupials has been reviewed by Gannon et al. (1989) while the corrosion cast appearance of intracranial capillary loops of the marsupial northern quoll has been described by Snyder et al. (1989).

However, Wislocki and Campbell (1937) were the first to describe the unusual end-loop microcirculation of the marsupial brain, a pattern observed in some fish, lizards and tailed amphibians (Craigie 1938b, Schobl 1878, 1882, Sterzi 1904). These observations were soon extended to the retinal circulation of the opossum (Garcia and Essinger 1985, Wislocki 1940) and to both polyprotodont and diprotodont Australian marsupials, suggesting that the pattern is common to the nervous system of all marsupials (Craigie 1938a, Scharrer 1940a, Sunderland 1941).

These reports are consistent in their description of the CNS vessels as paired arteries and veins down to and including the regular and evenly spaced array of terminal capillaries (Wislocki and Campbell 1937). The capillary network has been described as non-anastomosing, and loop-like, with a typical intercapillary spacing of around 50μm (Wislocki 1940). Whilst some interdigitation of the terminal vasculature is acknowledged (Wislocki and Campbell 1937), functionally, the vessels behave like end arteries. Scharrer (1939) embolised cerebral vessels and was able to produce distinct areas of infarction in the area supplied by a single arteriole. Together with the supplying and draining vascular pairs, such a system forms a structurally complete and independent unit (Wislocki and Campbell 1937). However, this pattern has not been confirmed within the nervous system of another mammalian group, the monotremes (Sunderland 1941).

The close association of arterial and venous segments has been likened to the angioarchitecture of the placenta where the fetal and maternal vessels run in parallel but opposite directions (Mossman 1926, Scharrer 1939).

The more general vascular pattern, within the nervous system of placental mammals is that of a freely anastomosing network with a true terminal capillary meshwork and the capacity for overlap and communication between nearby units. It would appear that the placental

mammal reticular pattern and the marsupial looped system are mutually exclusive. It is thought that the two systems are derived from different developmental mechanisms. It has been hypothesised that the placental reticular pattern is a result of primitive vascular network channels coalescing within the brain to form the definitive vascular pathways (Wislocki 1939). By contrast, in marsupials paired vascular cords grow into the developing nervous tissue from the pial plexus, unite at the tips and produce the terminal capillary bed of the looped system (Fig. 3.27). Elsewhere in the developing opossum embryo the vascular system is that of the more usual network pattern (Wislocki 1939).

Interestingly, if nervous tissue from another mammal with the network pattern of vasculature is grafted into the opossum brain the pattern of ingrowing vasculature remains that of the *host* brain (Scharrer 1940b), suggesting that within the marsupial CNS the intrinsic properties of the host tissue determine the pattern of growth and not the environment into which they grow.

A re-analysis of these early studies would be timely considering the experimental and clinical interest in new vessel growth and transplantation of neural tissue. Contrary to these early studies, it now generally thought that local tissue factors within the graft *do* govern the vascular properties (Stewart and Wiley 1981). Similarly, with pathological new vessel growth, the working hypothesis has been that the properties of the immediate tissue environment govern the morphological properties of the ingrowing vascular system (Bellhorn 1980).

However, these concepts have recently been brought into question by the finding that transplantation of placental nervous tissue into renal capsule induces blood vessel ingrowth from the host vascular system with host permeability and structural properties (Naradzay and Rosenstein 1989). The characteristic nature of the marsupial central nervous system vessels, which makes them readily identifiable, may well provide a useful model for investigating such vessel graft relationships.

3.4.4.b Marsupial ocular vasculature

Johnson's (1901, 1968) seminal work describing the fundal patterns of many mammalian species is the starting point for an appreciation of the vasculature of the marsupial, and indeed the mammalian eye. Since that time little has been written to complement these early morphological observations of marsupial ocular vasculature. Only occasional references, often as an aside to other aspects of retinal structure, have detailed ocular vasculature for the Australian marsupials (Duke-Elder 1958, Freeman and Tancred 1978, Tancred 1981).

(1) Retinal vessels

The arrangements of retinal capillaries in the quoll and the closely related Tasmanian devil differs from the rigidly adhered to end artery configuration found in the marsupial central nervous system and to that previously reported within the retina of the American opossum. The retinal vessels display the basic "marsupial" configuration of paired arterial and venous loops down to, but not always including, the terminal capillary level. An end-looped capillary bed is not always present. Furthermore, the capillaries freely anastomose with nearby vessels from the same arterial sector and communicate with branches from nearby arteries (Fig. 3.15). This difference is suggested in the angiographic findings, where in the American opossum retinal flow within nearby fan shaped sectors was seen to be temporally distinct, suggesting anatomical isolation of each retinal arterial and venous pair (Fig. 2.8). This sectorial separation was not seen in either the quoll or Tasmanian devil angiograms (Figs. 2.4, 2.5, 2.7).

In the retinal periphery, and to a lesser degree near to the optic disc, the retinal circulation of the quoll does conform to the more characteristic looped marsupial arrangement, thereby demonstrating a mixed pattern of both network and looped patterns at different locations within the same retina. By contrast, Wislocki's (1939) description of opossum retinal vessels leaves no doubt that the entire retinal circulation throughout is based on end artery looped organisation. Unfortunately, his illustration of the opossum's capillary bed depicts only peripheral retina which, in the vascular Australian marsupials examined, also shows a similar organisation of the capillary bed. More central regions, which in the Australian marsupials show anastomosis of neighbouring terminal beds with pairing of the larger arteries and veins, are not illustrated in Wislocki's work. Even though the quoll's peripheral capillary bed is similar to that of the American opossum's, it also bears some similarity to that seen in the placental retina. For example, the human peripheral retinal vessels are loop-like, but unpaired, with communication between the apical venous and arterial segments (Spitznas and Bornfeld 1977).

Interestingly, more central regions of the the human retinal capillary bed may become loop-like under certain pathological situations. Looped vasculature has been described in diabetic retinopathy (Ashton 1963). Following capillary closure the surrounding channels may become dilated and looped.

Despite these retinal findings, the CNS of the Australian marsupials, as previously reported in Bennett's wallaby, "*Macropus Bennetti*" (probably *Macropus rufogriseus*), the Eastern grey kangaroo (*Macropus giganteus*), the quoll, ringtail possum and the brushtail possum (Craigie 1938a, Sunderland 1941), does show the unusual end artery looping well seen for example in

the pouch possum (Fig. 3.27) or adult quoll (Fig. 3.26). Why the retinal circulation should differ is enigmatic.

Capillary bed

The quoll's retinal capillary bed otherwise shows features similar to the known placental patterns (Michaelson and Campbell 1940). The bed is bilayered with one layer in the vitread retina and a second in the outer plexiform layer. The two are connected by unpaired vascular channels. Towards the retinal periphery, the capillary network becomes unilaminar (Risco and Nopanitaya 1980, Shimizu et al. 1978). The peripapillary region of placentals is known to be three layered with the addition of radial peripapillary capillaries (Shimizu et al. 1978). Such trilamination in the quoll is not readily apparent although loop like supplemental capillary structures were seen within the retina in the vicinity of the optic disc.

Capillary density

As yet unanswered are quantitative questions about the density of the capillary bed. Within the CNS the looped terminal vascular bed produces a concentration of capillaries into closely related pairs (Ganon et al. 1989). The overall number of capillary profiles may be similar to the more general mammalian pattern. However, as the capillaries are closely paired, the average diffusion distances, as measured by intercapillary loop distances, may be somewhat higher (See Fig. 3.26). For the CNS of marsupials intercapillary diffusion distance has been calculated at around 22μm while for the rat, which has a similar overall capillary profile density, the diffusion distance is 15μm (Gannon et al. 1989). The retinal situation in the Australian polyprotodont marsupials may differ as the terminal vascular bed is more uniformly arranged with more even distribution of capillary profiles than in the CNS.

Retinal arteriolar branching

The vascular morphology at the site of branching of isolated arteriolar vessels is similar in marsupials to that seen in some placentals. An annular impression may be seen which probably represents a sphincteric indentation (Henkind and De Oliveira 1968, Risco and Nopanitaya 1980). This correlates with the *arteriolar annuli* of Kuwabara and Cogan's (1960a) PAS stained trypsin digest material of rats and cats. Typically, this is seen at the points of side arm branching and not at the points of dichotomous branching. Possibly this represents a control mechanism for regulation of flow and or pressure through these branches.

Counter current properties?

Any advantage that the parallel arrangement of arteries and veins may have is speculative. Counter curent flow is seen elsewhere in the body. For example flow of urine occurs through adjacent afferent and efferent limbs of medullary nephrons allowing for differential concentration of electrolytes and osmolality within the renal interstitium (Valtin 1983). However any advantage for such a system in the CNS of marsupials remains obscure. Perhaps the adjacent location of arteries and veins establishes a microenvironment which enhances the passage of certain substances in and out of the vascular system. Though well beyond the scope of this work, it would be interesting to look at the finer comparative details of the blood-CSF and blood-retinal barriers in marsupials. Alternatively, the arrangement may be merely an anatomical variant in the multiple mechanisms which are compatible with providing adequate retinal nourishment.

Arteriovenous shunts?

Fluorescein angiography suggests that preferential arteriovenous channels may have be present within the retina of polyprotodont marsupials (Figs. 2.4, 2.5, 2.7). However, this was not been supported by the anatomical vascular patterns portrayed in the casts. More likely the early venous filling of the angiograms is explained by differential distances through some capillary pathways. Shorter channels would allowed for venous appearance of some dye before the bulk of the capillary bed had filled.

Vascular ultrastructure

The arrangement of vascular pairs within the CNS and retina of the marsupials allows an unambiguous identification of arteries and veins. Like the previous report of the Virginia opossum, the larger vascular pairs are enclosed in a common connective tissue and glial sheath often with an intervening cellular process at the site of contact (Bubis and Luse 1964). The smaller capillary vessels are non-fenestrated and enclosed by a surrounding basal lamina. It is likely that the endothelial junctions of the capillary bed are tight, an observation that would need to be confirmed by more extensive sectioning and permeability marker studies. However, the immediate functional conclusion based upon ultrastructural grounds is the that vascular system of the polyprotodont retina, like its placental counterparts, constitutes a tight boundary and contributes to the blood-retinal barrier. Preliminary reports suggest that elsewhere within the CNS the marsupial vasculature constitutes a functional blood brain barrier (Carati et al. 1989).

(2) Choroidal circulation

The corrosion casts of the brushtail possum's eye confirms that it lacks intraretinal circulation. The choroidal supply most likely therefore supplies all of the retinal nourishment. The remaining circulation of the ciliary body and iris appears not to differ from the other species examined and is unlikely to offer any supplemental pathway for retinal nourishment.

The choroidal circulation of the possum however shows no obvious morphological specialisation which might complement retinal avascularity. The choriocapillaris is sheet like and expansive, the feeding choroidal vessels are numerous with arteries and veins interlacing externally. This bed of vessels is lobular in arrangement with alternating feeding and draining channels (Hayreh 1983). The connecting vessels are short and branch abrubtly, again characteristic features of the choroidal vasculature (Alm and Bill 1987). Ultrastructural analysis of the choriocapillaris shows it to be a fenestrated vascular network no different structurally from the other species examined in this study.

Functional properties of the choriocapillaris

However, ultrastructural homology need not mean functional equivalence. The luminal front of the endothelial surface comprises a complex array of surface macromolecules (Simionescu and Simionescu 1986). The proteoglycans, sialoglycoconjugates, glycoproteins, lectins, receptors and enzymes of this surface produce a domain of far greater complexity than that revealed through simple morphological examination (Simionescu 1983). The ultrastructural-biochemical makeup of both the luminal and abluminal surface of a number of vascular beds, including those of the eye, have been investigated using chemical and enzymatic markers (Ghinea and Simionescu 1985, Peress and Tompkins 1982, Raviola and Butler 1984, 1985, Schmidley 1987, Simionescu 1979, Simionescu et al. 1982a, 1982b).

The particular makeup of this biochemical microdomain determines its functional capability. This may vary amongst vascular beds, and in different regions of the same bed, producing differential permeability properties (Haraldsson et al. 1983, Simionescu et al. 1981, Studer and Potchen 1971). The proportion of cationic and anionic surface sites, as one aspect of the surface coat, will determine which charged molecules are able to bind to the surface and hence be transported across the endothelium (Charonis and Wissig 1983). The type and distribution of surface receptors and enzymes and the actual physical barrier created by the surface layer will further influence endothelial function.

Nonetheless, where comparative investigations of the overall vascular bed permeability have been performed, for example, in mice, guinea pigs, rabbits and for both adult and neonatal

rats, the permeability to intravenously injected ferritin is similar (Essner and Gordon 1983, Pino and Essner 1980, 1981, Pino et al. 1982). These studies suggests that the choriocapillaris presents a significant permeability barrier irrespective of the type of retinal vascularisation. This is surprising given that other fensetrated capillary beds are far more permeable (Pino and Essner 1980, 1981).

Despite this finding there is some discrepancy within the literature regarding the overall premeablity of the choriocapillaris. Physiological studies have indicated that permeability is high to macromolecules (Bill et al. 1980, 1983). On this basis albumin concentration in the choroidal tissue fluid should be 60-70% of that in plasma (Bill 1968). However, immunohistochemical localistion of endogenous proteins would suggest that albumin and gammaglobulin are not localised outside the vascular lumen of the choriocapillaris (Pino 1985). This is more consistent with the vascular bed of the choriocapillaris being an somewhat impermeable fenestrated endothelium.

This highlights the need for closer biochemical inspection of the endothelial cell surface and the need to be cautious in claiming functional capabilities on simple ultrastructural grounds. At the moment there appears to be no evidence one way or the other suggesting differential permeability of the choriocapillaris due to properties of the vascular microdomain.

Unusual choroidal structures

Gross choroidal structure is not similar in all species. The choroidal vessels of some fish are known to show unusual morphological features and to have equally unusual functional properties. Most teleost fish posses a choroidal *rete mirabile*, a structure which is able, through a counter current mechanism, to concentrate oxygen far in excess of that found in arterial blood (Wittenberg and Wittenberg 1962). This conditioned blood then supplies the choroicapillaris and hyaloid vessels at much elevated oxygen tension. This is functionally similar to the swim bladder rete and both depend upon carbonic anhydrase enzymatic activity for the secretion of oxygen (Desrochers 1985, Fairbanks et al. 1969, 1974, Steen 1963, Ubels and Hoffert 1981, Ubels et al. 1984). The morphological correlate is, not unexpectedly, complex. Interposed between the choriocapillaris and the incoming blood externally is the choroidal body while a smaller vascular lentiform body lies between the choriocapillaris and the hyaloid vascular system inside the eye (Copeland 1974, 1976, Copeland and Brown 1976).

The retinae of these fish are, according to the definition, avascular (Rodieck 1973), although they may have a vitreal hyaloid system of vessels. However, the possum, also with an

avascular retina, has no such morphological entity to suggest a similar functional specialisation of its choroid.

(3) Tapetum

A *tapetum lucidum* in general is a structure which lies external to or which surrounds the outer photoreceptors and by reflecting light gives this layer a second chance at capturing photons (Rodieck 1973, Walls 1942). This enhancement is ideal for animals which function in low light levels, for example, a nocturnal habitus or in deep and murky waters (Duke-Elder 1958). However, by enhancing light detection, spatial acuity is compromised.

In mammals, the structure may lie, and in most mammals usually does, within the choroid as either a cellular specialisation, a *tapetum cellulosum*, or as extracellular sheets of collagen, a *tapetum fibrosum*. Alternatively, a tapetum may consist of reflecting granules located within the retinal epithelium. Whilst being diverse in structure, in land animals they commonly are only located in a semicircular region of the superior fundus, representing the functionally important visual area below the horizon. In marine animals the three dimensional habitat makes for a more extensive tapetum throughout much of the fundus (Walls 1942). If there is a tapetum, then the pigmentation of the overlying retinal epithelium is deficient. Further sophistication of the retinal tapetum is seen in some fishes, with the capacity to occlude the tapetum in bright light. Migrating fuscin granules, by altering their position within the epithelium, can either allow light to strike the reflecting granules of the tapetum or can block impinging light (Walls 1942).

Retinal tapeta are seen in some teleosts and in the marsupial Virginia opossum (Braekevelt 1976, Hazlett 1976, Herman and Steinberg 1982a, 1982b, Pirie 1961, Rodieck 1973). The choroidal *tapetum cellulosum* constitutes layers of specialised cells laying external to the choriocapillaris. The cat tapetum is one of the best studied such tapeta (Rodieck 1973), but this type is also seen in many other species, particularly the carnivores including the seals (Braekevelt 1982, 1986, Walls 1942). A fibrous tapetum more commonly is seen in ungulates (Rodieck 1973).

The choroid of the quoll is similar to that of the possum with the added feature that it also accomodates a thick *tapetum fibrosum* between the choriocapillaris and the external vascular supply. Consequently, the alternating feeding and draining channels are longer and intermingle with the collagenous sheets of the tapetum. Chase (1982) in reviewing retinal vascularity has argued that choroidal diffusion would be limited by a tapetum and that as a consequence it should not be found in avascular retinae. The possum's eye, plus those of

other maraupials with avascular retinae, all appear to lack tapeta, confirming Chase's arguments. However, in an attempt to gain some enhancement of light detection, there is differential pigmentation of the retinal epithelium producing a "weak tapetum" superiorly (Freeman and Tancred 1978) or, to be more accurate, producing increased light absorption inferiorly. However, there is no choroidal structure *per se* which acts as a specialised reflector of light or, more importantly, a structure which might limit vascular perfusion pressure or nutritional diffusion gradients.

Collagen may optically be reflecting as seen in the tapetum, transparent as seen in the cornea (Waltman and Hart 1987) or opaque as seen in the sclera and other supporting structures. By judicious alteration of fibrous and background matrix components, light may thus be refracted, reflected or absorbed.

(4) Retinal epithelium (RE)

Lying between the choriocapillaris and retina is the embryological remnant of the outer layer of the optic cup, the retinal pigment epithelium, or to be more general and acknowledge that it need not be pigmented, the retinal epithelium. This layer forms a functional component of the blood retinal barrier, is important in metabolism of the contiguous photoreceptors and contributes to the adhesion of the retina to the choroid (Cohen 1987, Saari 1987). Furthermore, differential arrangement of pigment granules within this layer allows the absorption of stray light or the passage and return of reflected light. As a barrier, and hence guardian of what can and can not pass into and out of an avascular retina, does it differ amongst the avascular and vascular species? On simple morphological criteria, it would appear not.

The possum's RE forms a single layer of low cuboidal cells which are tightly bound through lateral junctional complexes to form a structural barrier. Metabolic machinery, mitochondria, endoplasmic reticulum and phagosomes, are typical of the other species examined. The layer is firmly adherent to the underlying photoreceptors, consistent with its supportive and nutritional role. Variable pigmentation is found in keeping with a dual role in either spatial (dark) and quantal (transparent) enhancement of acuity. RE morphologies suggest nothing unusual in terms of functional properties. The RE of the quoll conforms to the same pattern. Only the RE of the Australian marsupial, the diprotodont quokka (*Sertonix brachyurus*), has been described previously (Braekevelt 1973). In morphological appearance it resembles that seen in the Australian marsupials of this study.

(5) Disc protrusion

Arising from the optic disc is a small protrusion, or leash, of vessels in both the quoll and possum. These are small and the component vessels are capillary like. Rarely, similar prepapillary loops are seen in man (Brown and Tasman 1983). Disc specialisations in other animals are thought to provide supplemental nourishment such as the conus of reptiles or the pecten of birds (Deiterich 1976, Meyer 1977). Perhaps this is a vestigial conus as suggested by Walls (1942). However the conus and pecten are larger and more elaborate and show complex ultrastructural features consistent with an active transport and nutrional role. The marsupial leash hardly falls into this morphological category, yet its presence in both species examined could indicate some special functional role. The retina in this region of the possum is marginally thicker than the surrounding retina, and perhaps the leash serves a local supplemental nourishment role where the metabolism of the thickened nerve fibre layer can not be sustained alone by the choroidal circulation. It probably does not represent an embryological remnant of the regressed hyaloid system (François and Neetens 1974). Goldstein and Wexler (1929) have demonstrated that the rare and analogous prepapillary loops in humans are derived from the central retinal artery. The loops may grow into the glial tissue anterior to the optic nerve, known as Bergmeister's papilla, but are independent of the hyaloid vascular system.

Minor differences suggest that role of the tuft may vary between the two species. The capillary channels within the possum "conus" are more loosely organised whilst those of the quoll are tightly packed and supplied by large diameter vessels.

(6) Ciliary body and iris

The ciliary body circulation is an underrated, poorly understood yet very important vascular bed. If mere bulk is an indicator, then it ought to have significance in excess of its apportioned role in production of aqueous humor, supplying ciliary smooth muscle, and to a lesser extent contributing to what is thought of as stable and metabolically inactive vitreous (Caprioli 1987). The bed is very large in volume and the vascular density very concentrated.

This basic structure of the iris and ciliary body circulation is similar across species. The supply is from the major arterial circle of the iris anteriorly which originates solely from the LPCA. Venous drainage is posterior, into the vortex system. The capillary bed in between is often convoluted

Where the ciliary body vasculature has however been investigated in more detail, for example through microdissection of corrosion casts, interspecies variations have been identified. For

example, two morphological regions may be seen in the rabbit and primate ciliary body (Morrison et al. 1987a). Each has a dual arteriolar supply with the anterior iridial vessels serving the area important for the production of aqueous (Morrison et al. 1987b). However, amongst some ungulates, rodents and carnivores there is little difference in arterial supply (Morrison et al. 1987b).

Subtle differences exist though in the fine structure of the ciliary body. The ciliary processes of the guinea pig and rat, when viewed in gross specimens, are known to have anterior webs connecting adjacent leaves of the ciliary body (Morrison et al. 1987b). The ciliary processes of the ungulates are broad and flat and are supplied by multiple arteriolar branches (Morrison et al. 1987b). Between the arterial and venous supply, the intervening capillary bed of rodents is irregular, convoluted and directed posteriorly throughout the length of the process. This is similar to the pattern seen in primates (Morrison et al. 1987b). Capillary connections join adjacent ciliary processes. The capillary bed of ungulates and carnivores in contrast is more locally organised and each arteriolar unit does not extend throughout the length of the process (See Fig. 13 of Morrison et al. 1987b).

As an alternative coping strategy, the species with avascular retinae might be expected to have a large intravitreal turnover of nutrients which might complement choroidal blood supply. However, the morphological appearances disclosed by this study do not suggest any such special function for the ciliary body.

3.4.4.c Mammalian ocular vasculature

In summary, with the exception of intraretinal blood vessels, ocular vascular structure differs little between vascular and avascular species or between placentals and marsupials. A choroidal circulation is common to all species examined, and shows only minor variations across species.

Retinal vasculature differs between the placentals and marsupials with vascular branching patterns in placentals being dichotomous. The arterial and venous vasculature is separated spatially. The marsupial pattern in contrast is one of closely paired arterial and venous segments down to, but not always including, the terminal capillary bed.

3.5 CONCLUSIONS

1. The retina of the Australian marsupial brushtail possum is avascular.

2. Despite retinal avascularity, the choroidal circulation of the possum is conventionally organised with an external coat of supplying and draining vessels which are connected through short abrupt branches to the extensive network of the choriocapillaris. There is no specialisation of the choriocapillaris such as choroidal loops indenting the retina.

3. The retinal epithelium of the possum shows no morphological specialisation which would infer any advantage in nourishment of its avascular retina.

4. Anterior uveal circulation in the avascular species shows no unusual structural features which would account for enhanced transvitreal retinal nourishment.

5. The marsupial quoll's eye has both retinal and choroidal circulations. The choroidal circulation is similar to the possum's except that it accomodates interweaving sheets of a *tapetum fibrosum* amongst the supplying arterioles and draining venules.

6. While the central nervous system of the marsupials has been described as having a looped end artery capillary bed organisation, the retinal circulation of the quoll has a mixture of looped capillary bed peripherally and a more typical placental-type anastomosing and unpaired capillary bed centrally. However, the arteries and veins are, on the whole, paired and retain this affiliation throughout most of the retina down to, but not including, the capillary bed.

7. Arising from the disc in both the possum and quoll is a leash of small capillaries. Its role, if any, remains enigmatic. Perhaps it constitutes a rudimentary vitreal radiator or perhaps it is merely an embryological remnant.

8. The marsupial pattern of ocular vasculature has been compared with that of the placental guinea pig and rat. Like the possum, the retina of the guinea pig is avascular; its choroid is morphologically similar, suggesting common functional patterns in these mammals.

9. Whatever the coping strategies are in avascular retinae, there appears not to be any major structural modification of the external uvea and its circulation which might allow enhanced retinal nourishment via this route.

10. Whether supplying a vascular or avascular retina, the choroid is fundamentally similar in all four mammals studied. This offers hope that a vascular retina, which has had its intrinsic circulation interrupted, could survive, in part, upon the existing choroidal supply if the avascular coping strategies were known and could be applied in this pathological situation.

If the nourishment strategy of avascular retinae is not achieved through obvious modifications to the extraretinal vasculature, what then are the coping mechanisms? One possibility may lie in the maximum thickness attainable in an avascular retina. This is addressed in Chapter 4. Alternatively, the metabolic pathways may be different between vascular and avascular retinae. This is addressed in Chapter 5.

CHAPTER 4

MENSURATION AND ORGANISATION OF MAMMALIAN RETINAE:

HOW THICK IS AN AVASCULAR RETINA?

CHAPTER 4: FIGURES

4.1 INTRODUCTION

"I've measured it from side to side:
Tis three feet long and two feet wide"
..... William Wordsworth

4.1.1 Why measure thickness?

Seldom does measurement of absolute distance figure prominently within the histological realm. More often, dehydrated, processed and sectioned material forms an adequate basis for relative quantitative measurements. This approach is inherently inaccurate due to the well known shrinkage artifacts involved with tissue processing (Humason 1972). However, where relative quantitative data are sufficient, the accuracy of such techniques is often adequate to answer the question under scrutiny; commonly comparisons are made between similarly processed material. However, there are occasions when not only relative information is important but also quantification relative to some absolute standard becomes essential. One of these is the question of retinal thickness.

A need for absolute measurements arises when considering comparative aspects of retinal nourishment strategies. Not only must the relative thickness of one retina to another be considered, but also the absolute thickness of retinae must be examined relative to the true distance over which nutrients and waste metabolites must pass. The movement of these substances and their exchange within tissues are governed by general physiological principles, involving diffusion limited concentration gradients (Keele et al. 1984).

An exact measure of these distances is necessary. Only when absolute dimensions are known can proper comparison be made with known absolute physical limits. Overall thickness in avascular retinae has been presumed to be limited by the availability of oxygen (Chase, 1982). Nonetheless, restriction in the supply of other nutrients and the removal of waste products may be contributory factors. In the absence of information about these, only oxygen transfer will be considered. Retinal oxygen diffusion has been considered by Dollery et al. (1969), who, using theoretical arguments, demonstrated how choroidal oxygen supply might be enhanced during pure oxygen breathing. Their calculations using a static non-haemodynamically perfused model, indicated that oxygen could diffuse up to 143μm through the retina when *pure oxygen* was breathed at one atmosphere, hardly a normal

physiological circumstance. With air breathing, at normal pressure, their model predicts an oxygen diffusion distance of only 60μm.

Chase (1982) in reviewing retinal vascularity compared retinal thickness in a number of mammalian species and indicated that none of the retinae in avascular species exceeded 143μm in thickness. However, it must be added that, by necessity in this review article, little detail of actual measurement techniques is provided. Unfortunately, in interpreting Dollery et al's. (1969) figures, she has taken 143μm to be the maximum limit for retinal oxygen diffusion *during air breathing*, and postulated that this value provides a theoretical maximum thickness for any avascular retina. Thus, it is probably only coincidence that this limit is observed in a number of different retinae and that it appears to apply in certain pathological situations. For example, when local regions of the intraretinal vasculature are destroyed by laser photocoagulation, the affected portions of the retina thin to less than 140μm, a figure which requires the caveat that it has been derived from histologically prepared material (Brown, Watanabe and Murakami, 1965; Stone, 1969). The finding of Brown et al. (1965) that the avascular foveal region of the cynomologous monkey (derived from histological material) is at least 160μm thick, show that avascular retinae or avascular regions within vascular retinae may exceed 143μm.

The arguments of Dollery et al. (1969), whilst providing a useful framework for oxygen transport, have not met with universal acceptance. For example, Popel, Pittman and Ellsworth (1989) recently presented an oxygen model based upon haemodynamically perfused tissue rather than upon the static, non-perfused models used previously. This model suggests that the actual oxygen permeability through tissue might be as much as an order of magnitude higher than that obtained using the static model. Limitations to oxygen transport may reside mainly in the capillary wall and blood and not be uniformly distributed throughout all tissue layers. If so, this would cast doubt upon the figures derived form Dollery's model.

4.1.2 Aims and questions

As seen, avascular retinae in mammals appear to rely wholly upon choroidal circulation, which should therefore impose certain limits on retinal dimensions. In this study, retinal thickness and consequent structural correlates have been investigated. Does avascularity imply reduced thickness, simpler organisation and therefore inferior function? Specifically, the following have been addressed.

4.1.2.a Absolute thickness of the retina

The major aim is to measure in near absolute terms retinal thickness thus gauging maximal intraretinal diffusion distances of metabolites. As Chase (1982) has postulated, based on somewhat uncertain grounds, are avascular retinae always thinner than 143μm?

4.1.2.b Regional variations in thickness

Limitations in retinal thickness could also impose constraints upon retinal taper, the known centroperipheral variation in organisation and thickness, characteristic of vascular retinae. An avascular retina may be more likely to have more uniform thickness, approaching the maximal distance throughout, in an attempt to maximise nutritive efficiency. What, if any, is the regional variation in retinal thickness?

4.1.2.c Comparative retinal thickness

What are the comparative retinal thicknesses of vascular and avascular species and among related species? Do all avascular retinae need be the same thickness? Placental and marsupial species with and without intraretinal vessels have therefore been chosen for study.

4.1.2.d Intraretinal organisation

Any metabolic limitations which may be placed upon the retina can not be divorced from function. The well known cytoarchitectural organisation within the retina lends itself to quantitative analysis of sublamination and should afford some functional insight into how an animal with an avascular retina will see. Should avascularity impose organisational restraints, where within the retina do these limitations lie? For example, an avascular retina with proportionately less neuropil has different implications for vision than would low numbers of intermediary processing cells or differing sizes of photoreceptors.

4.1.2.e Eye size

A final hypothesis under consideration in this section relates to eye size. One possibility is that an avascular retina could counteract any diffusional constraints placed upon it by having the same volume of neural tissue devoted to vision but of diminished thickness and spread out over a larger area; a bigger eye. A proper answer to this question would require an allometric analysis of many species. Tentatively, I suggest that a useful indicator might involve an estimation of retinal area derived from measurements of globe diameter.

4.2 MATERIALS AND METHODS

"Though this be madness, yet there is method in't"

..... Hamlet, William Shakespeare

Retinae from the laboratory rat, a murid rodent, and the quoll, a dasyurid marsupial, were compared with those of the guinea pig, a caviid rodent, and the brushtail possum, a phalangerid marsupial. As information about the cat is available in the literature, material from this animal was also used, both for comparative purposes, and for verification of measurement techniques.

4.2.1 Subjects

In all, 5 male Wistar rats (weight 260 gm, age 13 weeks), 5 female guinea pigs (weight range 920-1 190gm, age 8 months), 1 male and 2 female cats (weight range 2 700-3 400gm), 3 male and 2 female brushtail possums (weight range 2 400-3 800gm) and 4 male quolls (weight range 700-1 300gm) have been examined in this study. The approach was verified and developed using a further number of rats.

The rats and guinea pigs were obtained from breeding colonies maintained at the University of Tasmania and had been reared under 12:12 light dark cycles whilst the remaining animals were taken from wild populations.

4.2.2 Animal perfusion

The smaller animals were anaesthetised with intraperitoneal chloral hydrate (rats and guinea pigs) or with a combination of halothane and nembutal in the larger animals (marsupials and cats); see Appendix 1. Once deeply anaesthetised, thoracolaparotomy was performed and trans cardiac perfusion of the vascular system followed. A short flush of Hartmanns solution (Travenol Labs: Toongabbie NSW, Aust), typically 50 ml, was followed by 250 to 500 mls, depending on animal size, of 4% formalin in 0.9% NaCl solution. The external surface of the eye was marked at 12 o'clock, the eye removed and stored in the same fixative.

4.2.3 Retinal thickness

4.2.3.a Eye preparation

Following a total fixation time of 30 to 45 minutes the eye was hemisected through the ora serrata region, an orientation cut made at 12 o'clock and the retina removed (Stone 1981). Shorter fixation times made flattening considerably easier yet produced no difference in measured dimension when compared with samples fixed for longer periods. Particular care was taken to minimise retinal damage, to include the optic disc region and, where possible, to separate the retina with some adherent pigment epithelium, thus ensuring that the retina had not been cleaved leaving photoreceptors behind. The retina was then laid flat on a glass slide with one or two small radial relieving incisions or, in the larger eyes, with horizontal incisions 2-3mm above and below the disc. The pattern of flattening may be seen in figures 4.2 to 4.6.

Following this incomplete flattening, the surface of the retina was covered with 1% protamine sulphate solution in sodium chloride (CP Pharmaceuticals: Wrexham, UK) for 5 minutes. Prior to this step, as much vitreous as possible was removed using scissors in order to limit the contracture that resulted, particularly around the edges of the wholemount, once protamine solution was applied. Protamine produced obvious collapse of the vitreous with precipitation of the fibrous component. This fibrous layer was then readily peeled off the surface allowing the retina to be laid completely flat and free of adherent vitreous. The mounted retina was then washed in the fixing solution for a further 5 minutes.

The retina was then placed onto a finely machined, flat brass measuring block with the vitreous surface uppermost. A thin layer of 4% gelatine solution in normal saline was used to facilitate adherence. Final flattening was achieved by gently patting the retina flat with surgical spears (Edward Weck and Co. Inc: U.S.A.). The whole procedure was performed under a high powered operating microscope, using an oblique viewing angle. This gave visual assurance that the retina was free of undulations. To overcome the rapid dehydration which occured in the uncovered retina, a layer of inert, nonconducting paraffin (F.H. Faulding and Co.: Australia) was poured over the retina. If left uncovered, the retina was reduced to one third of its original thickness within fifteen minutes. However, once covered with paraffin oil, the preparation remained dimensionally stable for many hours.

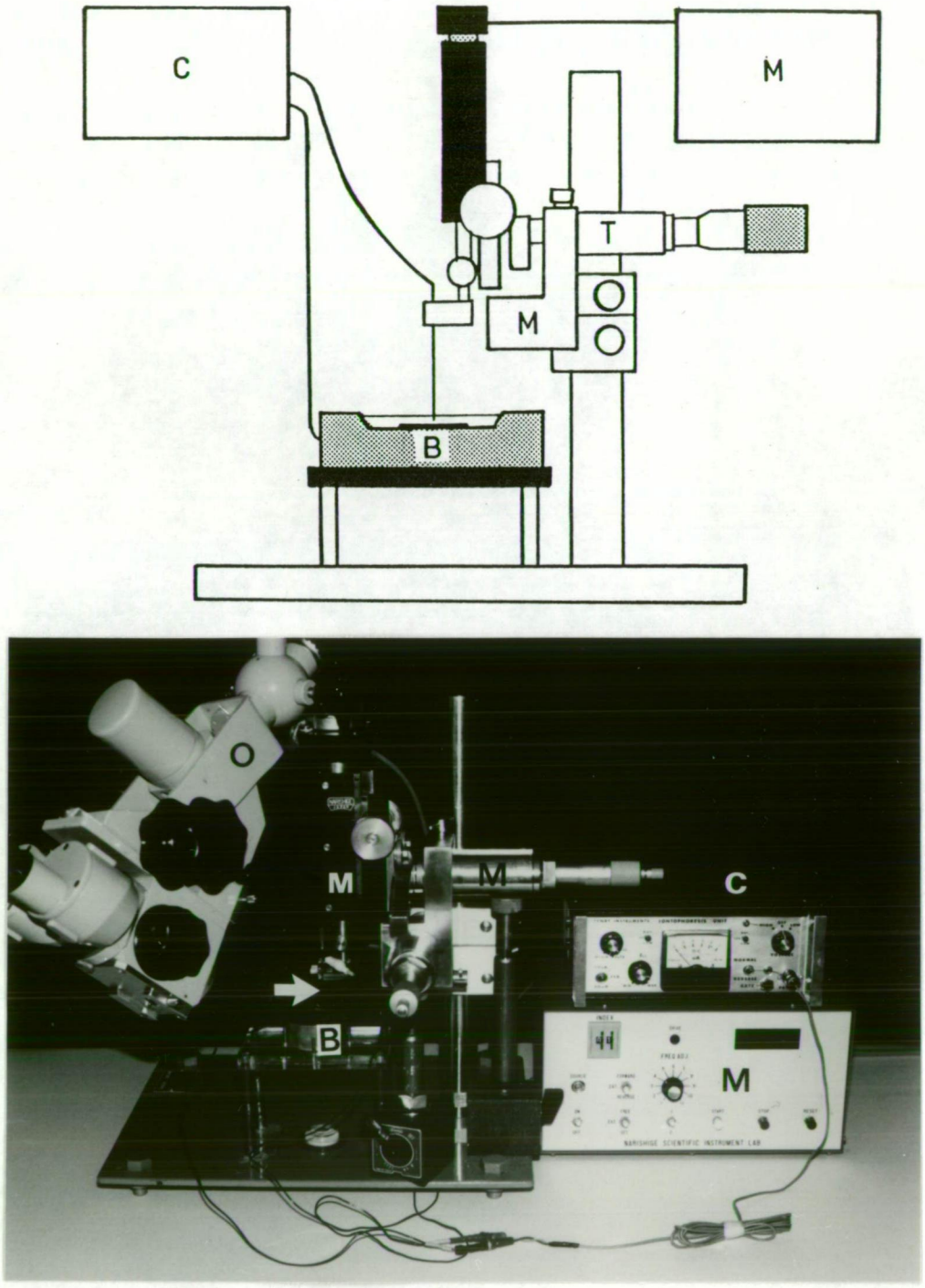

Figure 4.1: Micromanipulator measuring device

To determine retinal thickness the retinal wholemount was placed on the brass measuring plate (B) under a layer of inert non-conducting oil. A micromanipulator (M) was used to determine retinal thickness by moving along the Z axis a fine electrode and contacting the retina, thus completing an electrical curcuit through a constant current generator (C). The manipulator could be moved in the same X-Y plane as the retina through the tracking arm (T). The thickness was calculated by subtracting this Z axis reading at the point of electrical contact with the retina from the value of the baseplate (B). The point of contact could be checked visually with the operating microscope (O). Special thanks to Colin Hinrichsen for the use of this diagram.

4.2.3.b Thickness measurement

Retinal thickness was measured with a micromanipulator (Narishige Scientific Instrument Lab: Tokyo Japan), Fig. 4.1. This device could be tracked in the same X-Y plane as the brass block and lowered vertically along the Z-axis onto the retina. Considerable effort was employed to ensure that the X-Y track of the manipulator was parallel to the brass block to within a tolerance of 1-2μm over a tracking distance of 10mm. Knowing the vertical coordinates of the brass block, the thickness of the retina could then be calculated from the point of contact of the manipulator electrode with the surface of the flattened retina. This point was found by determining the point in the Z-axis at which the circuit was completed through a constant current generator, the electrode, the retina and the brass block. The point of contact was also confirmed visually with high magnification optics of the operating microscope.

Measurements were taken at 0.5 (small retinae) to 1mm (large retinae) steps over a maximal distance of 20mm in X and Y axes. Representative examples of these values on a scaled outiline drawing provide a *thickness map* of retinal wholemounts (Figs. 4.2A-6B). Pooled and averaged data from comparable anatomical regions in different retinae were also used to construct a *horizontal profile* of retinal thickness in each species at of near the level of the optic disc. For each retina a series of thickness values were obtained along three horizontal transects: through the level of the optic disc and 1mm above and 1mm below it (0.5mm in the rat). Corresponding points at the same horizontal distance from the disc were averaged to calculate a mean value for each 1mm interval (0.5mm in the rat). These averaged values for each point were then combined from at least three animals to determine a composite score and construct the horizontal profiles Figs. 4.2B-6B).

4.2.3.c Controls and safeguards

As with any measurement technique, validation of the approach taken is necessary. To minimise systematic errors, the following controls were undertaken.

(1) Effects of fixation

In principle, samples of retinal tissue ought to be measured before and after fixation to determine dimensional changes imposed by the fixating and washing solutions. However removal of suitable unfixed, undistorted retinal tissue without adherent vitreous, proved almost impossible. Hence cerebral cortex was used to compare measurements pre and post fixation. Samples were harvested fresh and cut with a razor blade into slices approximately

400μm in thickness. Following baseline measurement, the samples were immersion fixed and further measurements performed. Two different samples measured over 6 hours were found to vary by less than 3% and 5% respectively from the mean value during this time. Due to technical difficulty, the theoretically desirable comparison of pre and post perfusion fixation was not performed. One could possibly estimate the effect of perfusion itself upon dimensions of the central nervous system, by securing an animal in a stable stereotactic apparatus, removing the skull and then performing measurements before and after perfusion.

(2) Processing the eye

Considerable manipulation is necessary in order to take a three dimensional, curved, deformable biological tissue and smooth it out into a stable flattened preparation. Where possible, samples were measured before and after many of the intervening steps to ensure that there was minimal change in dimension.

Protamine, as a positively charged protein, electrostatically neutralises hyaluronic acid (Gloor 1987). While treatment with this substance collapsed vitreous, it had no measurable effect upon neural tissue proteins. Samples of fixed central nervous system were measured before and after a 5 minute wash of protamine and found not to alter in dimensions.

The gelatine layer was necessary to ensure adherence of the whole retina. Small pieces of retina were measured without gelatine adhesion and found not to vary from companion samples in which it was used.

Measurements before and after the paraffin oil coating were found to have a variance of less than 2-3μm indicating minimal effect from the oil.

(3) A true measurement? Comparison with other techniques

Liver, a more robust biological tissue, and hence a little easier to cut at known and consistent thickness, was fixed in the same way and sectioned at 100 and 500μm using the Oxford vibratome. A small tangential sample was removed with razor blade and, using a calibrated microscope, thickness was confirmed to be within 5% of the stated value. The sections were then treated in the same way as the retina; measurements were performed before and after protamine, with and without the gelatine adhering layer and sequentially over a 8 hour period. These observations confirmed that the apparatus gave consistent, comparable and stable readings when applied to biological tissue of known thickness. For example, a 500μm

vibratome section measured 525μm under the microscope and 530μm using the manipulator. Over a 22 hour period this sample varied in thickness by less than 3%.

Assuming the microscope reading to be more accurate than the vibratome calibration, the micromanipulator technique was over estimating thickness by a maximum of 5μm, well within the absolute error of the manipulator. This overestimation was possibly caused by the effect of residual surface water producing premature electrical contact.

With these controls reassurance was gained that the process of laying the tissue out flat produced little change in the dimensions.

(4) Manipulator reproducibility and accuracy

Repeated measurements in the one spot produced the same reading indicating that the electrode did not deform the surface and that the mechanical property of the apparatus was stable in the vertical plane. Return to a previously measured point produced variation of up to 10μm. This is partly explained by the possibility that the electrode was not always measuring exactly the same spot, perhaps by some flow of the retina with time, by ongoing shrinkage effects of the fixative, and by some error in the X-Y tracking capabilities of the manipulator arms. Even so, this is remarkably constant, given that the variation observed was less than the dimension of a single cell.

The manipulator itself was calibrated with precisely machined engineering gauge blocks and found to be accurate to within 1% of measured distance.

(5) Histological appearance post measurement

After measurement, some retinae were processed and blocked into glycol methacrylate for histological viewing (see below). These sections showed no difference from those processed for normal histology, indicating that the structural relationships had remained intact and that no unwanted component was removed in processing. The plane of cleavage that was obtained in removing the retina from the choroid was found to be through the RPE-photoreceptor region. The measurements were not therefore artifactually high, due to adherent choroid, nor too low, due to partially removed photoreceptors.

4.2.4 Retinal histology and intraretinal laminae

To determine the microscopic structural makeup of the retina, horizontal sections including optic disc of the unmeasured eyes were processed through ascending alcohols and embedded in glycol methacrylate resin (Polaron Equipment: Watford, England) as outlined in Appendix 4. One μm sections were cut on a Sorvall JB-4 microtome and stained with 1% toluidine blue in 1% borax. Representative regions from central retina, midway between the ora serrata and the optic disc were sampled. Thickness of the retina was measured and sublaminar proportions were calculated as a percentage of overall thickness. This was performed on a captured video image of the histological section and measured using the calibrated measuring facility of an image analysis system (Image Action, Imaging Technology: Massachusetts, U.S.A.) attached to a conventional microscope. At least three readings per retina from at least three different eyes were measured using a x 100 oil immersion objective. See Table 4.I.

4.2.5 Eye length

The anteroposterior length of the marsupial's, guinea pig's and cat's eyes was determined simply using vernier calipers and fixed enucleated eyes, measuring from the corneal vertex anteriorly to the exit of the optic nerve posteriorly. Results from at least four animals in each group have been used in determining averages.

4.3 RESULTS

"History teaches that the commencement of every branch of science is nothing more than a series of observations and experiments which had no obvious connection with one another" ... Justus von Liebig (1846).

4.3.1 Retinal thickness

4.3.1.a Horizontal profiles, regional variation

Results are presented from two viewpoints: (1) pooled data from a temporo-nasal cross section passing through the optic disc, *horizontal profiles*, and (2) representative *thickness maps* overlying an outline of retinal wholemounts. Difficulty resulted when trying to pool data

from areas outside the horizontal meridian as non comparable anatomical regions were being pooled into the same X-Y categories, depending on the location and orientation of the relieving incisions. Hence representative raw data is presented from one animal in each group to depict the regional variations in the thickness maps.

(1) Vascular placental cat

The horizontal profile of the cat's retina (Fig. 4.2) demonstrates a thickness profile between 200-250μm. Due to the limited tracking distance of the manipulator, this profile does not extend to the ora serrata. The temporal retina is, on average, thicker than the nasal side. The thickness map shows marginal increase in thickness temporally and superiorly, which corresponds to the position of the area centralis (Wong and Hughes 1987).

(2) Vascular placental rat

Retinal thickness in the rat is similar to the cat, with peripheral regions being up to 20μm less, and the central regions 20μm more, than 200μm (Fig. 4.3). The thickness map is more symmetrical with little suggestion of regional enhancement.

(3) Vascular marsupial quoll

The quoll's retina, like the cat's, is greater than 200μm in thickness (Fig. 4.4). The regional pattern shows temporo-superior increase in thickness in keeping with a presumed area centralis in this region. There is horizontal band 200μm or more thick immediately superior to the optic disc.

(4) Avascular placental guinea pig

This avascular species also shows little centro-peripheral taper in retinal thickness (Fig. 4.5). Thickness varies between 130 and 140μm throughout most of the retina, including the optic disc region. As in the possum, there is little regional enhancement.

(5) Avascular marsupial possum

The horizontal profile of the possum is less countoured than the vascular species (Fig. 4.6). In the region of the optic disc there is some increase in thickness to 170μm (Fig. 4.6B). On the whole, the thickness map is symmmetrical though with some superior increase in thickness.

4.3.1.b Comparative retinal thickness

In Fig. 4.7 horizontal profiles of the various retinae are compared according to whether they are avascular or vascular (Fig. 4.7A-B) or derive from the marsupial or placental linage (Fig. 4.7C-D). The three vascular retinae (Fig. 4.7B) have peak thickness values between 225-250μm, well in excess of the 140-170μm maxima observed in the two avascular retinae (Fig. 4.7A). There is little if any overlap in the range of thickness measurements between the vascular and avascular retinae, except in the extreme periphery where the (150-170μm) thickness of the possum's retina is comparable to that reported in some vascular species (Table 4.III).

4.3.2.c Histology of the retina

Illustrations of 1.0μm thick Nissl stained cross sections of rat, quoll, possum and guinea pig retinae are seen in Fig. 4.8. All sections are to the same scale and were taken from the mid-temporal region, near the horizontal equator. The four retinae display the typical laminated pattern of the vertebrate retinae, differing primarily in overall thickness and in the presence or absence of intraretinal vessels. In the outer segment layer of the quoll's retina a number of cones with oil droplet inclusions can be seen. Similar cones are found in the possum's retina though none are seen in this section. Higher magnification views of the photoreceptor layer from the same four retinae are shown in Fig. 4.9.

The averaged intraretinal measurements are presented in Table 4.I. Figure 4.10 depicts the absolute thickness, *internal profiles,* whilst Figure 4.11 outlines the comparative aspects of percentage thickness of each layer, *normalised internal profiles.* In Figure 4.10 each retina is aligned along the border between the outer nuclear and outer plexiform layers. This mode of presentation emphasises the differences in contribution to total retinal thickness made by the various retinal layers. Internal profile data are not presented for the domestic cat's retina as these measures are readily available in the literature (Brown and Tasaki, 1961).

The difference in overall dimensions between the representative micromanipulator retinal thickness and the value obtained from the glycol methacrylate embedded material was typically around 25%, indicating significant shrinkage during processing. This correction factor was applied in determining the absolute retinal proportions, assuming similar, linear shrinkage in all layers.

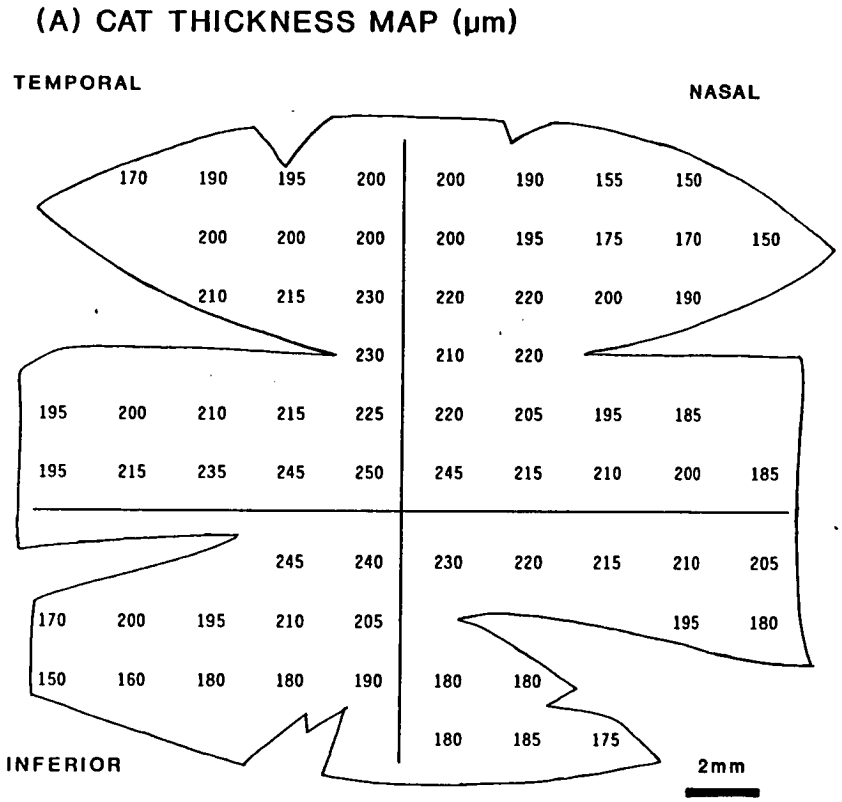

Figure 4.2: Thickness of the cat retina

(A) Wholemount map of the cat's retina centered on the optic disc. The profile of the retina demonstrates thickness values in a single representative animal. Over most of the retina thickness ranges from 200 to 250μm . Thickness is greatest in the superotemporal retina in keeping with known functional complexity in this area (Area centralis). (B) The horizontal profile is a composite of date taken near the level of the optic disc as described in the text. Note the centroperipheral taper in thickness. The sample does not extend all the way to the ora serrata due to the limited travel of the manipulator arm. Error bars depict ± 1 sd.

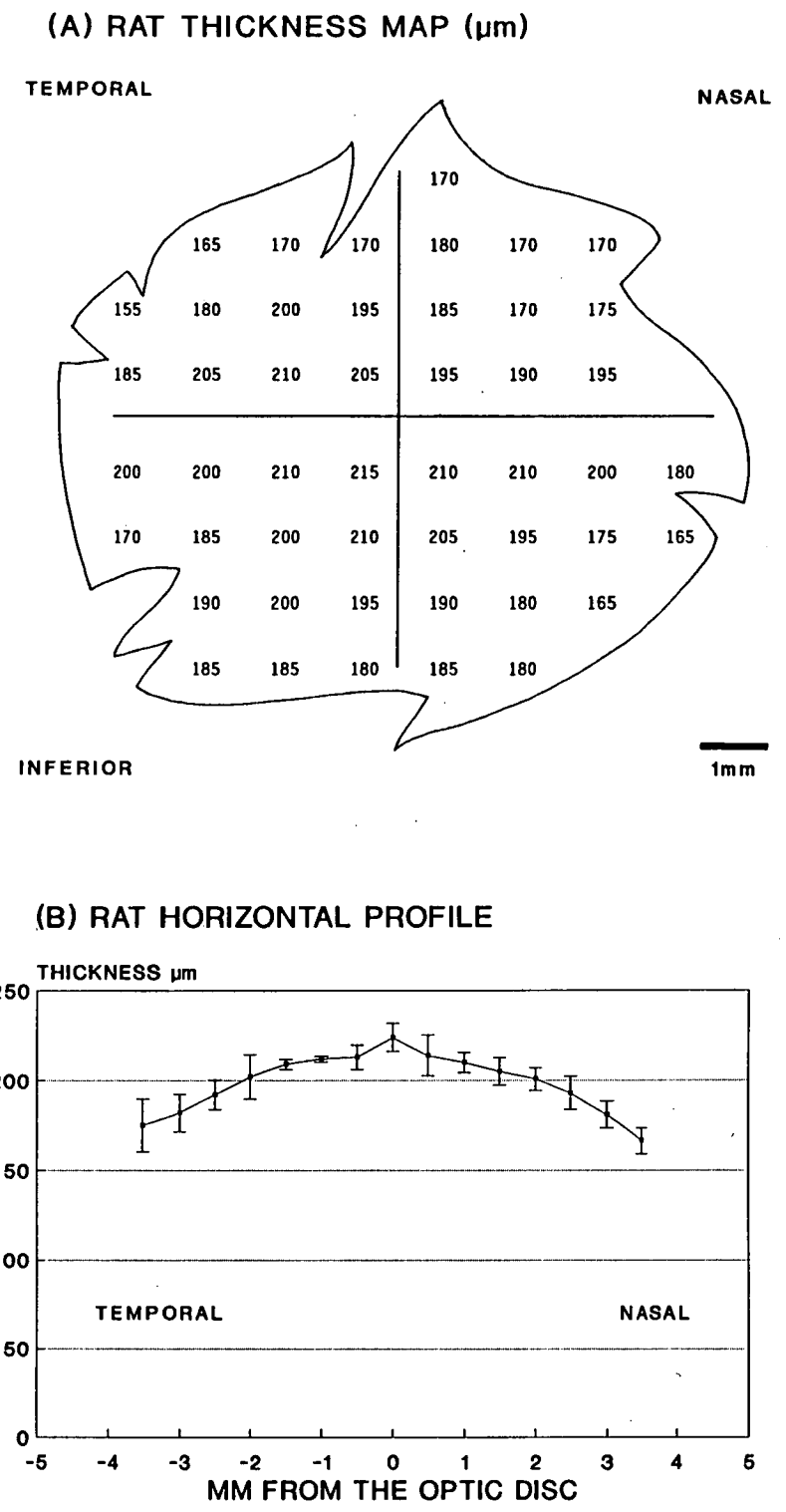

Figure 4.3: Thickness of the rat retina

Thickness profile of the rat retina. (A) Wholemount map: Note the essentially symmetrical distibution of thickness centered upon the optic disc. (B) Horizontal profile: This shows centroperipheral taper with maximal thickness around the optic disc. Error bars depict ± 1 sd.

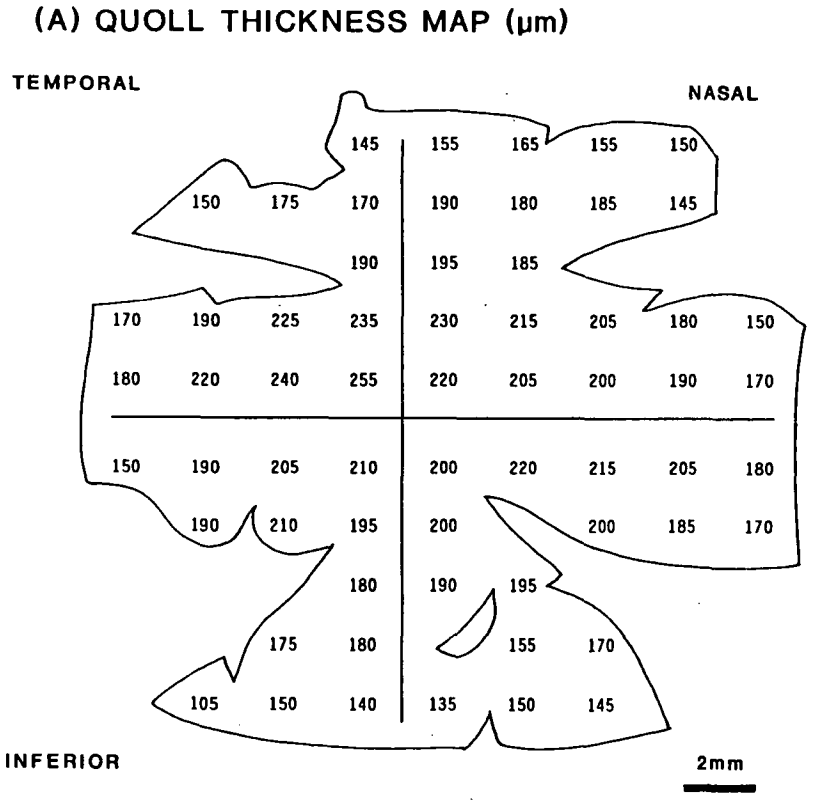

Figure 4.4: Thickness of the quoll retina

(A) The wholemount map of the quoll's retina, like the cat's retina, shows a small temporo-superior increase in thickness in keeping with an enlargement of the horizontal streak in this region. (B) The cross sectional analysis demonstrates centroperipheral taper and again temporal enlargement in thickness. Error bars ± 1 sd.

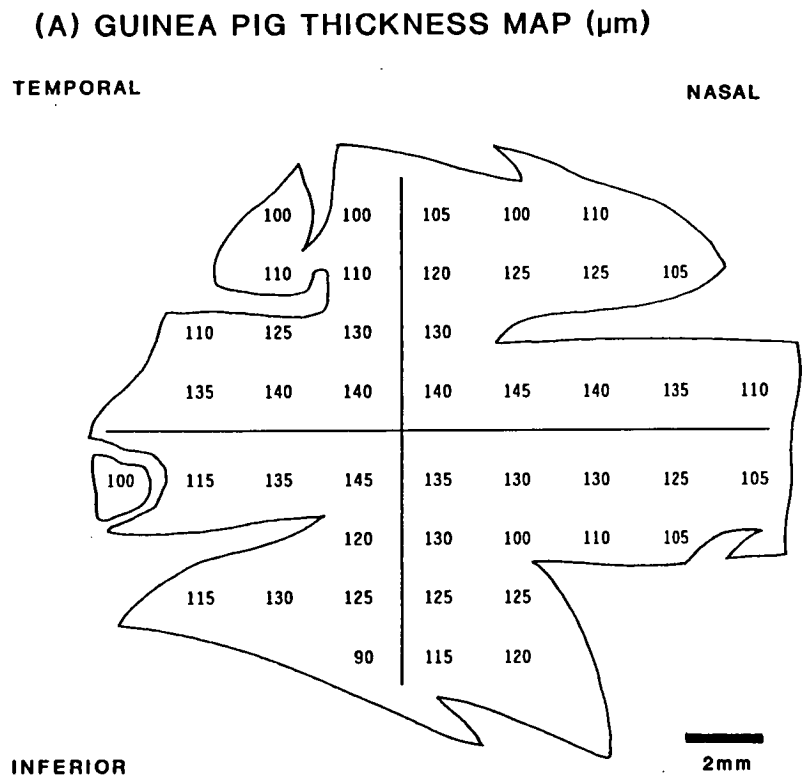

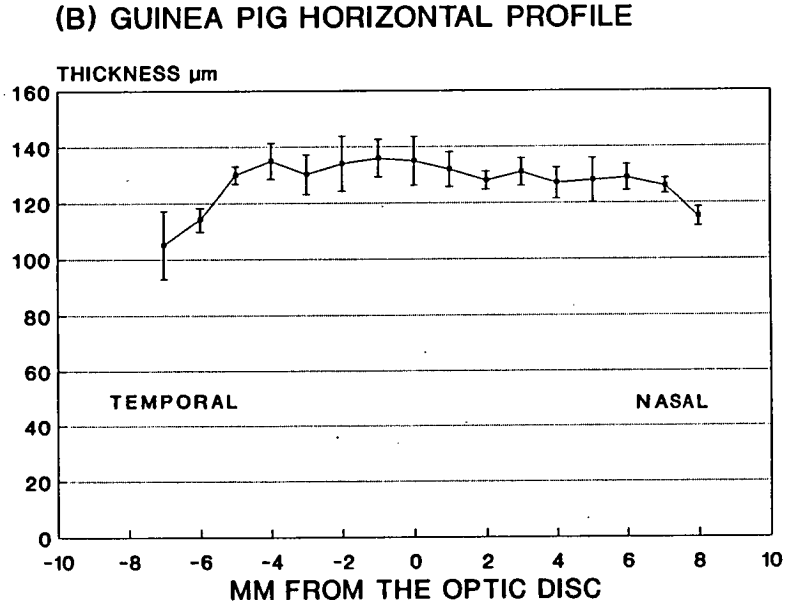

Figure 4.5: Thickness of the guinea pig retina

Profile of the guinea pig retina. (A) The wholemount map of retinal thickness shows a relatively flat retinal profile. In this example, maximum thickness values are at most 145μm. (B) In horizontal section the profile shows little taper until near the retinal periphery. Mean values are less than 140μm. Error bars ± 1 sd.

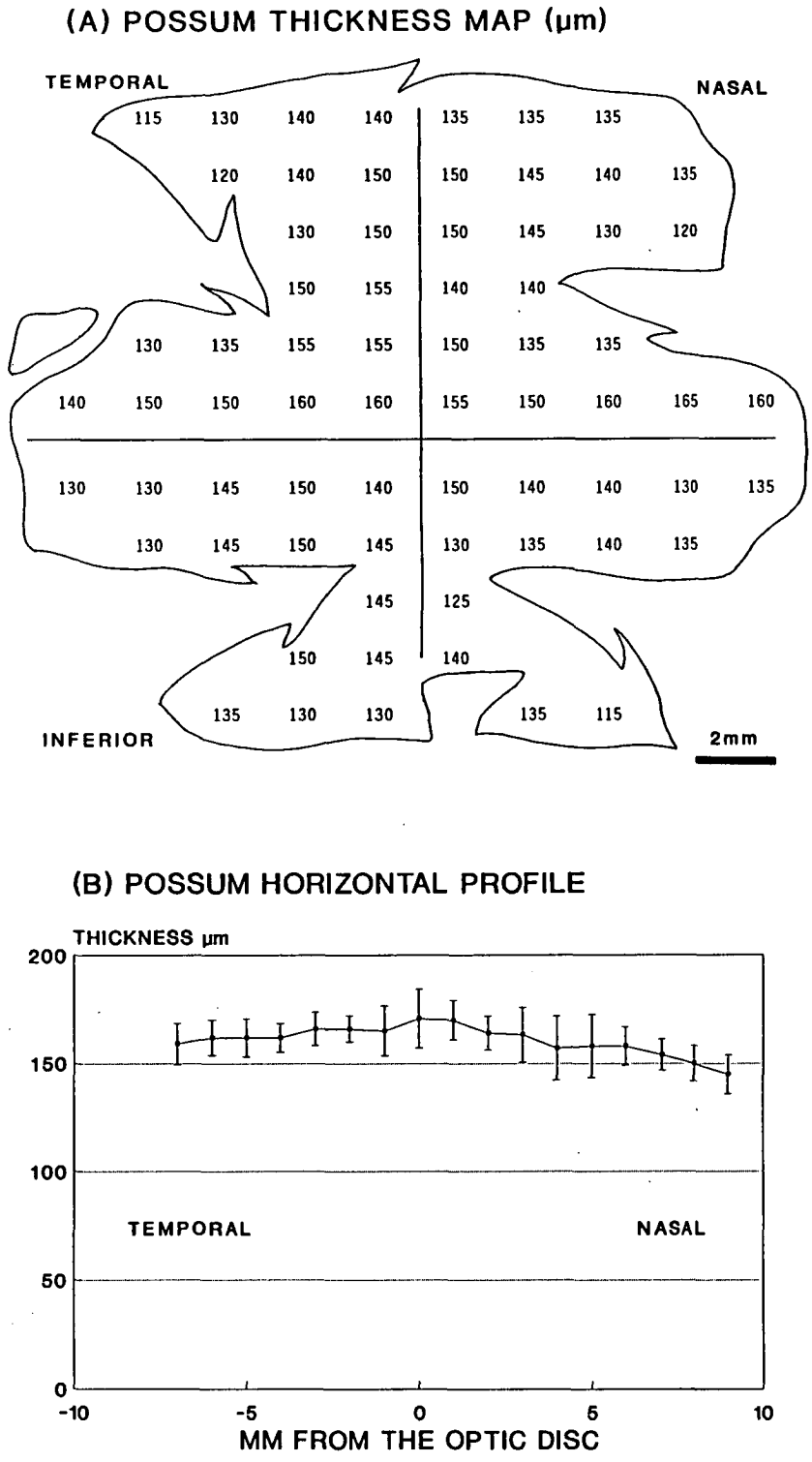

Figure 4.6: Thickness of the possum retina

Thickness profile of the possum retina (A) This particular example shows a symmmetrically organised map with a maximum thickness of 160μm in the region of the optic disc. (B) Using the pooled data which make up the horizontal profile, the average maximum value is around 170μm centrally tapering to 130μm peripherally. Throughout most of its extent, the retina shows constant thickness rather than centroperipheral taper seen in the vascular species. A slight increase in thickness is seen in the immmediate vicinity of the disc posssibly a consequence of the added localised nutritional supply of the disc vessels. Error bars ± 1 sd.

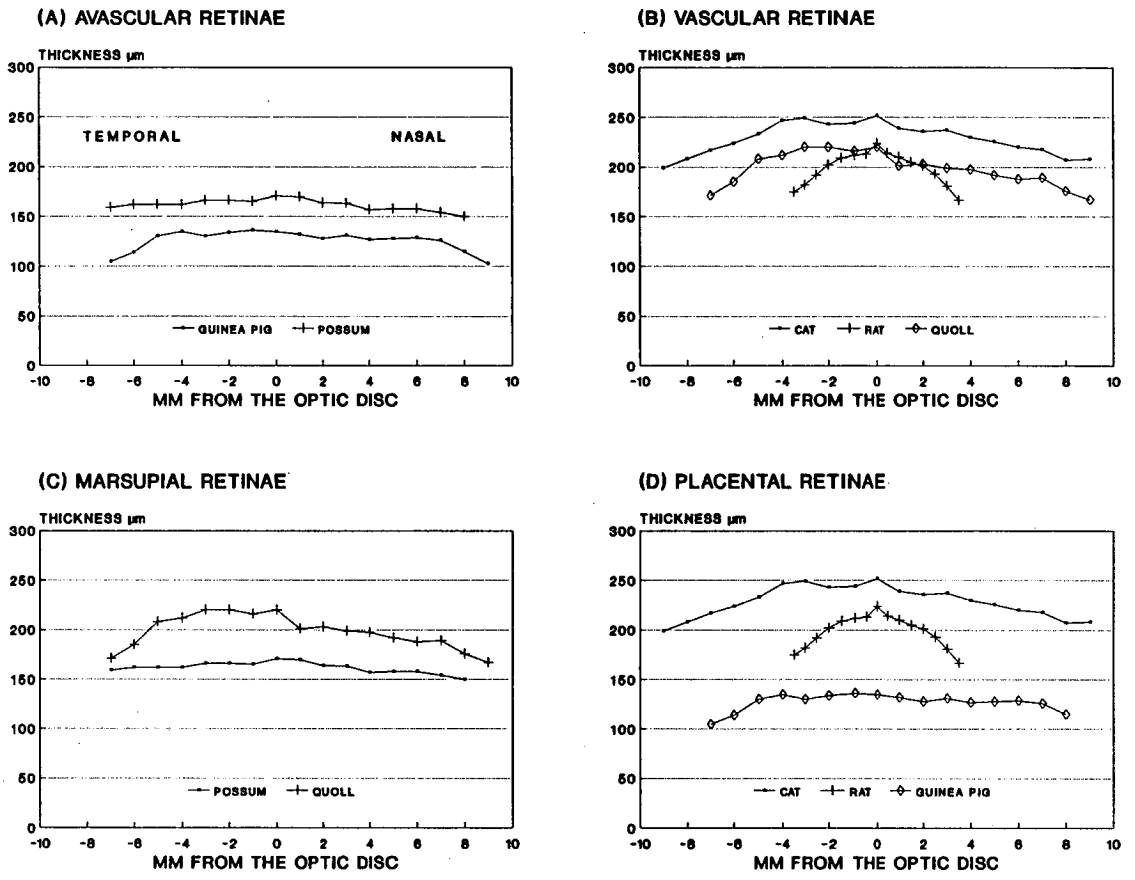

Figure 4.7: Horizontal profile comparison

The previously presented horizontal profiles have been grouped so that direct comparison may be made. (A) Avascular species: The possum's retina is 20-30μm thicker throughout most of its extent than the guinea pig's. The lack of centroperipheral taper is evident in both species. (B) Vascular species: They display greater similarity in organisation with centroperipheral taper. (C) Marsupial retinae: These display similar proportions in the periphery, but in the vascular quoll the retina is much thicker centrally. (D) Placental species: A twofold variation in thickness is seen.

(1) Common features

All retinae display the same internal organisation, comprising clearly defined outer and inner nuclear layers (ONL, INL), outer and inner plexiform layers (OPL, IPL), plus photoreceptor segment layer (RSL), ganglion cell (GCL) and optic nerve fibre layers (NFL). In the internal profiles layers NFL and GCL have been combined. In all species OPL is absolutely and proportionately the thinnest layer at 7-8% of the total retinal thickness (Figs. 4.10, 4.11). The INL occupies 10-12% of the total, the combined GCL-NFL from 15 to 17% and the total photoreceptor length (ONL-RSL) between 40-47%.

(2) Differences between vascular and avascular retinae

In absolute terms the retina and each of its component sublaminae are thinner in avascular than in vascular retinae (Table 4.I and Fig. 4.10). The differences are generally in close allometric proportion with the following exceptions. The IPL is disproportionately thicker in the rat's retina (28% of total thickness) than in the avascular retinae of possums and guinea pigs (19%) and the vascular retina of the quoll (22%), and total receptor cell length (RSL-ONL) in the possum's retina is 47% of total thickness, a value which exceeds slightly the 40-42% figures obtained from the other three retinae. All other percentage measures agree within two percentage points.

(3) Marsupial and placental differences

In the two marsupials, the ONL, which comprises the inner segments of the photoreceptors, is proportionately thicker (40-48μm or 22-26%) than in placentals (20-35μm or 16-17%). Conversely, the marsupials have somewhat shorter photoreceptor segments (20-21%) than do the placentals (23-28%). It should be noted that the guinea pig's outer segments, though short, are considerably broader than those seen in the other three species (Fig. 4.9). In keeping with this coarse packing the number of nuclei in the ONL is very much less in the guinea pig. The number of nuclei per linear 100μm in the outer nuclear layer is 62 ± 10 for the guinea pig, 144 ± 19 for the possum, 171 ± 9 for the quoll and 206 ± 10 for the rat (mean ± sd).

Table 4.I: Intralaminar retinal dimensions in two vascular and two avascular retinae. Retinal laminar thicknesses in μm (mean ± sd).

Layer	Rat	Quoll	Possum	Guinea Pig
GCL/NFL	31.7 ± 9.2	35.3 ± 3.5	24.8 ± 2.5	23.2 ± 0.7
IPL	59.9 ± 1.3	48.6 ± 3.5	30.1 ± 2.1	26.7 ± 1.5
INL	22.5 ± 2.2	25.1 ± 1.7	17.6 ± 0.5	16.7 ± 1.7
OPL	14.1 ± 1.7	16.9 ± 2.8	11.3 ± 1.6	10.0 ± 1.7
ONL	35.4 ± 7.6	48.4 ± 4.2	41.5 ± 2.4	21.4 ± 3.1
RSL	48.9 ± 7.6	44.5 ± 2.8	32.7 ± 1.4	38.3 ± 5.4
Totals	212.5	218.8	158.0	136.3

4.3.3.d Size of the eye

The eye size of the larger animals under investigation is presented in Table 4.II. The largest eye is seen in the cat (vascular retina), the smallest in the guinea pig (avascular retina). The possum (avascular retina) has a larger eye than the companion native cat (vascular retina).

Table 4.II: Average eye length as measured from the corneal vertex to the insertion of the optic nerve. Results presented in increasing order of axial length and based on the average of 4 animals in each group.

Animal	Weight gm ± sd	Eye length mm ± sd
Guinea pig	1 070 ± 110	9.3 ± 0.35
Quoll	1 000 ± 250	10.8 ± 0.52
Possum	3 450 ± 520	13.1 ± 0.68
Cat	3 000 ± 530	19.4 ± 0.95

Figure 4.8: Retinal organisation

Glycol methacrylate embedded retinae sectioned at 1μm and stained with 1% toluidine blue in 1% borax. (A) rat, (B) quoll, (C) possum, and (D) guinea pig. All animals show similar arrangement of laminae but with differing proportions in each layer. Most noticeable is the greater inner plexiform thickness seen in the vascular species. Scale bar = 20μm. RSL = receptor segment, ONL = outer nuclear layer, OPL = outer plexiform layer, INL = inner nuclear layer, IPL = inner plexiform layer, GCL/NFL = ganglion cell and nerve fibre layer.

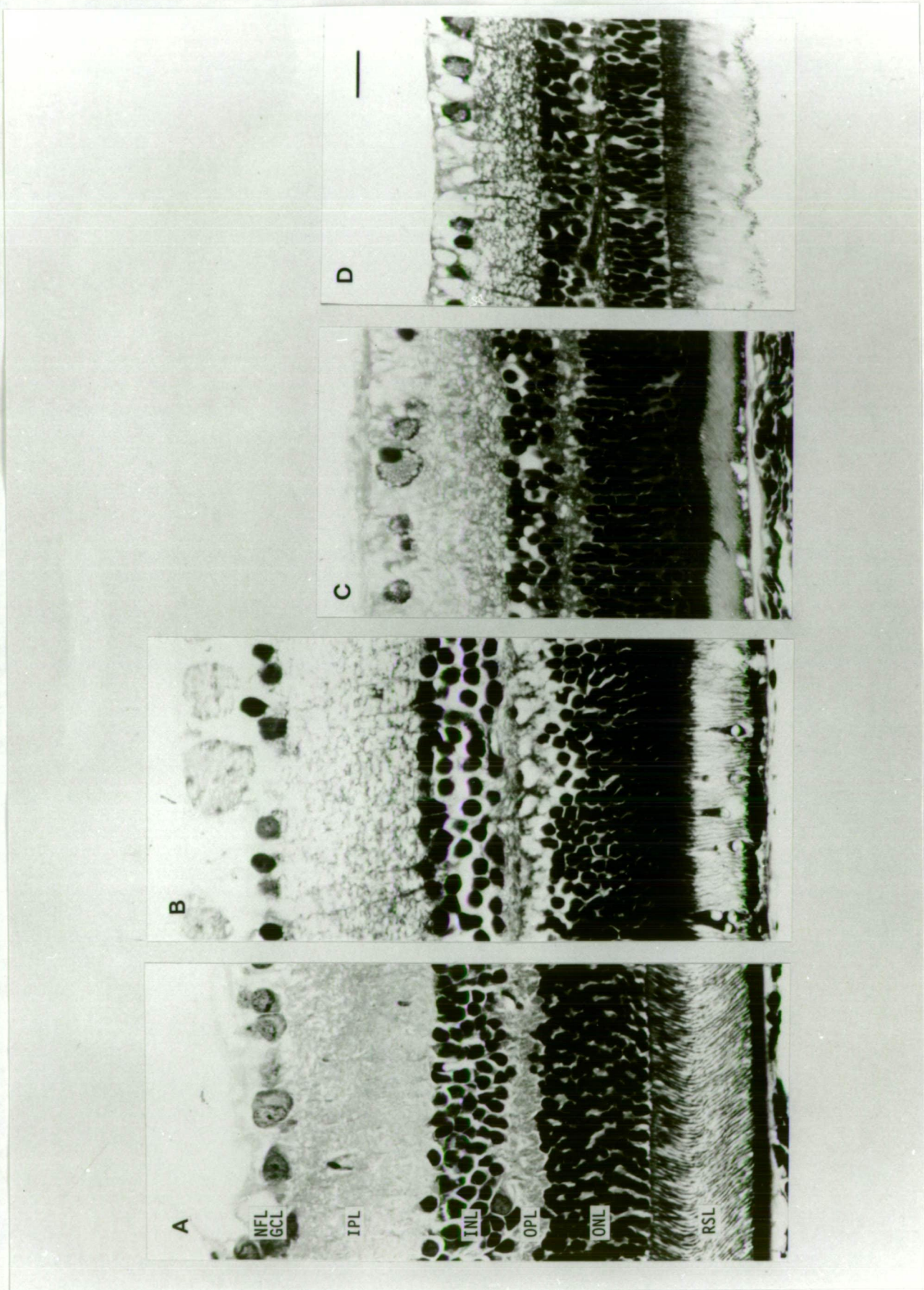
A
NFL
GCL
IPL
INL
OPL
ONL
RSL
B
C
D

Figure 4.9: Photoreceptor proportions

Higher power view of the outer (sclerad) retinal layers. (A) rat, (B) quoll, (C) possum, and (D) guinea pig. Note that the two avascular species, (A) and (B), are dissimilar in the sizes and density of photoreceptor cells. The guinea pig, (A), has photoreceptor outer segments which are stouter and far fewer in number than the possum, (B). The two marsupial species, (B) and (C), are not too disimilar in organisation. The number of nuclei per linear 100μm in the outer nuclear layer is 62 $\pm$ 10 for the guinea pig, 144 $\pm$ 19 for the possum, 171 $\pm$ 9 for the quoll and 206 $\pm$ 10 for the rat (mean $\pm$ sd). Scale bar = 20μm.

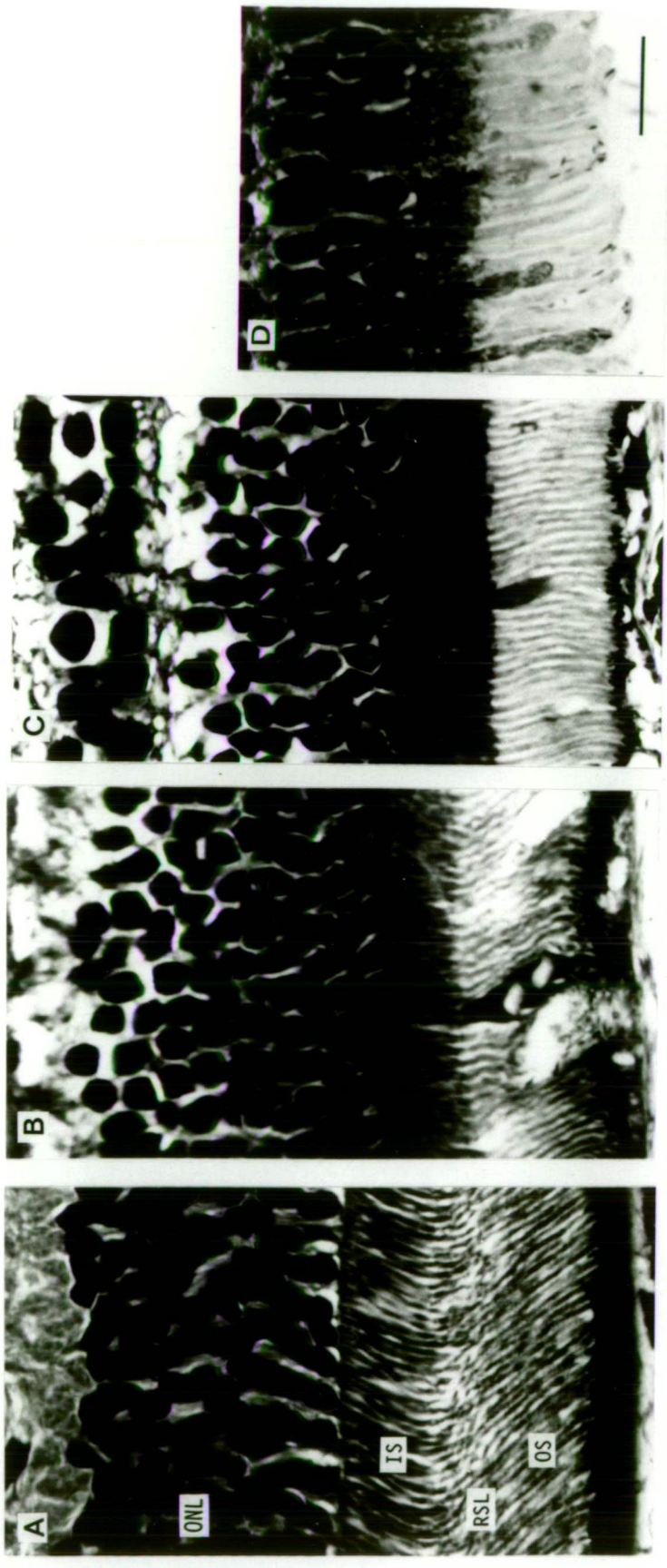
D
C
B
A
ONL
IS
RSL
OS

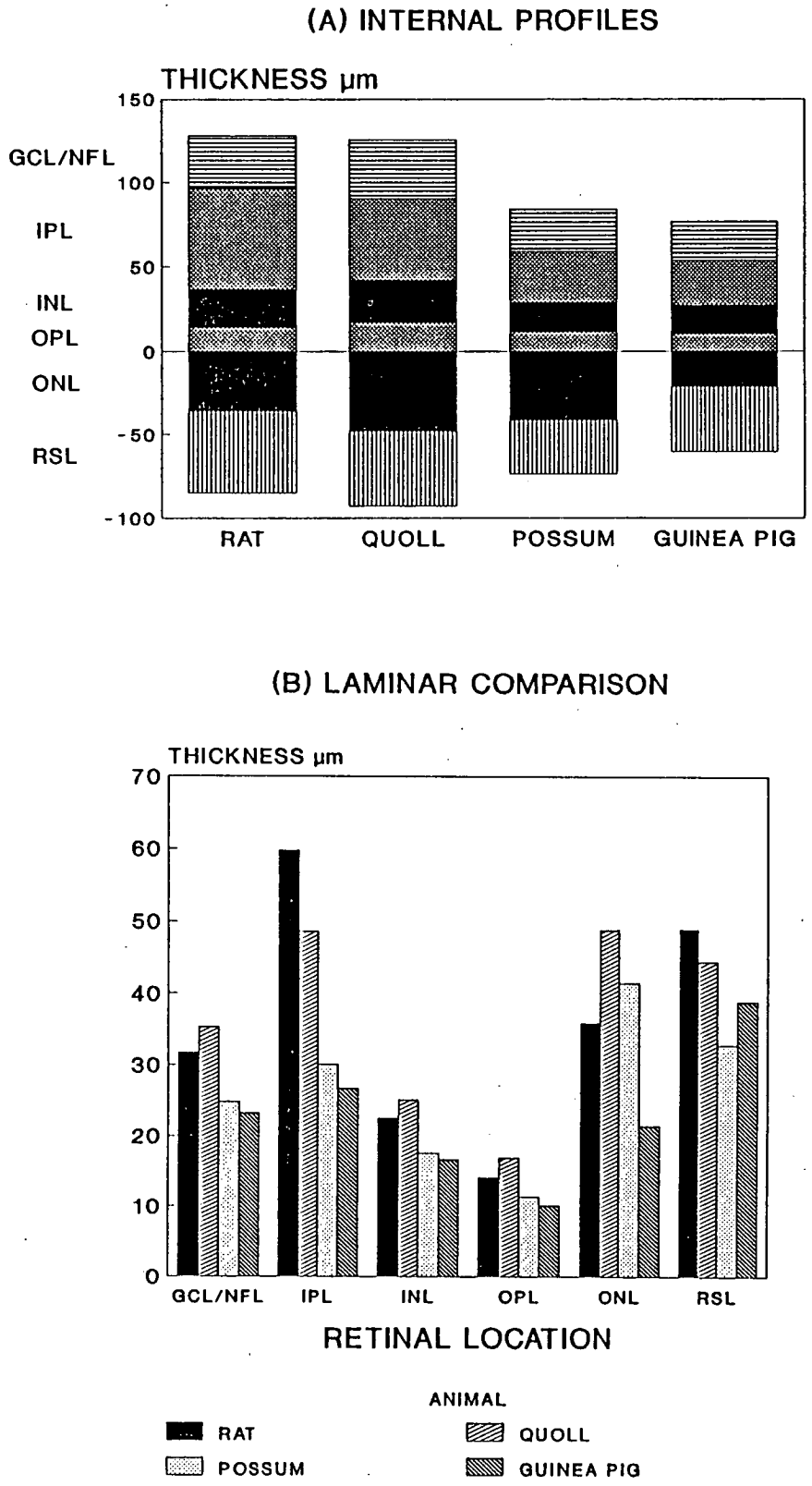

Figure 4.10: Absolute intraretinal proportions

(A) Internal profiles quantify the cytoarchitectural impression gained from the histological sections shown in Figures 8 and 9. Avascular species have thinner laminae but particularly the inner plexiform layer and, to a lesser extent, the photoreceptor layer. The figure is aligned along the ONL/OPL border in order to accentuate these differences. The OPL, INL and GCL/NFL show less marked differences. (B) Laminar comparison highlighting that the major difference in thickness between vascular and avascular retinae lies within the IPL

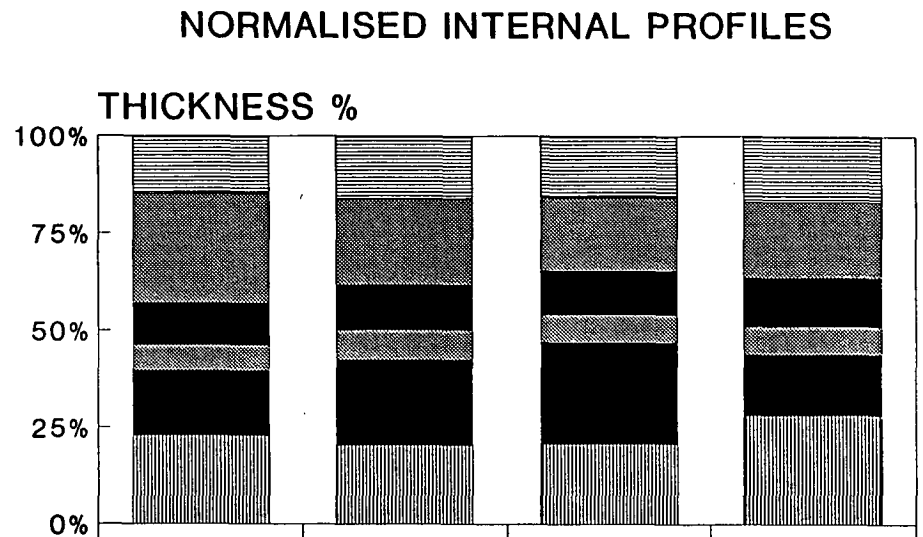

	RAT	QUOLL	POSSUM	GUINEA PIG
GCL/NFL	14.9	16.1	15.7	16.9
IPL	28.2	22.2	19.1	19.6
INL	10.6	11.5	11.1	12.3
OPL	6.8	7.7	7.2	7.3
ONL	16.7	22.1	26.3	15.7
RSL	22.9	20.3	20.7	28.1

Figure 4.11: Relative intraretinal proportions

When laminar thickness is normalised relative to overall retinal thickness, the differences become less pronounced suggesting that the relative retinal proportions are a more constant design feature. All show a similar proportionate contribution from the photoreceptor/outer nuclear layer, similar proportions for outer plexiform, inner nuclear layer and ganglion cell/nerve fibre layers. However, the contribution from the inner plexiform layer differs markedly, particularly when comparing the rat and guinea pig retinae.

4.4 DISCUSSION

4.4.1 Retinal thickness

4.4.1.a Retinal thickness: the normal range

Glickstein and Millodot (1970), in a consideration of retinal thickness relative to eye size and retinoscopy error, have suggested that mammalian retinal thickness is comparatively constant at around 135μm. For their purpose this is an adequate assumption, but, closer inspection of published data reveals at least a three fold range in thickness. See Table 4.III. Chase (1982) has summarised data from many different species and concludes that retinal thickness varies from 100 to 300μm. However, in this review article, the techniques used to gather the data were not discussed, casting some doubt on the reliability of the figures presented. Assuming that these data are accurate, it seems that avascular retinae are generally thinner than 143μm. Where there are clear adaptations, as for example in the avascular avian retina (pecten) or the megachiropteran bat retina (invasive choroidal papillae), then retinal thickness may approximate to that of vascular species.

In general, retinal thickness *per se* has attracted scant attention, often only being considered as a sidelight to other investigation. A search of the available literature has produced the following facts.

(1) Primates

Not surprisingly, the human retina is thought to be similar in thickness to the phylogenetically related rhesus monkey (Detwiler 1943). The adult human perifoveolar thickness is 230μm, the equatorial thickness around 120μm (Straatsma et al. 1969, Van Buren 1963), tapering to 100μm at the ora serrata (Hogan et al. 1971). The concentration of nerve fibres around the optic disc leads to increased thickness of up to 560μm in this area (Hogan et al. 1971).

Interestingly, in light of the suggested limits to thickness of avascular retinae, a primate exception is suggested by the work of Brown et al. (1965) for the foveal region. A scaled micrograph of the cynomologus monkey indicates a thickness of at least 160μm in the centre of the avascular fovea.

Table 4.III: Summary of retinal thickness of selected mammalian species

Species	Location	Retinal thickness (μm)	References
Human	perifovea:	230	
	equator:	120	1-3
	ora serrata:	100	
	optic disc:	500	
Cynomologous monkey	fovea:	160	4
Cat	nasal retina:	165-178	5-7[a,b]
	peripheral retina:	195	8[a]
	area centralis:	249	9[a]
	area centralis:	150-220	10-12[b]
Mouse	central retina:	130-237	13-16
Rat	central retina:	95-217	14,17-19[c]
Guinea pig	central retina:	130-140	14

References: 1 = Hogan et al., 1971; 2 = Straatsma et al., 1969; = Van Buren, 1963; 4 = Brown et al., 1965; 5 = Brown and Weisel 1959; 6 = Brown and Weisel, 1961a; 7 = Brown and Weisel, 1961b; 8 = Brown, 1968; 9 = Linsenmeier, 1986; 10 = Landers, 1978; 11 = Prince et al., 1960; 12 = Vogel, 1978; 13 = Balkema, 1988; 14 = Chase, 1982; 15 = Remtulla and Hallett, 1985; 16 = Sanyal et al., 1980; 17 = Chaudhuri et al., 1983; 18 = Hughes, 1979; 19 = O'Steen et al., 1987.

a measurement made during intraretinal electrophysiological recording.
b histologically measured thickness.
c The low figure of 95μm is most likely a result of the Bouin's fixative used in the study of O'Steen.

As one component of retinal morphology, nerve fibre layer thickness has been investigated in the primate (Ogden 1978, 1983, Radius 1980). Ogden (1983), undertook a painstaking histological analysis of cynomologos monkey retinae and prepared detailed maps of nerve fibre layer topography. Allowance was not made for shrinkage and assumed to be 10-15%. Variation in measurement was found to be up to 25-30% particularly in the peripheral retina, highlighting the variability and technical difficulty in obtaining accurate retinal maps.

(2) Cats

As one of the most commonly used experimental animals in vision research, quantitative data are available. Using histological techniques, the vascular cat retina has variously been measured between 145 and 260μm (Detwiler 1943, Landers 1978, Prince et al. 1960, Vogel, 1978, Wen et al. 1985). All these figures are liable to shrinkage factors introduced during processing.

Perhaps one of the more elegant approaches has been a by product of electrophysiological recordings within the retina. It is worth dwelling on these reports because they are more likely representative of true *in vivo* thickness providing useful validation of the technique employed in this study. Electrical characteristics of evoked potentials vary with depth of the recording electrode within the retina (Brown and Wiesel 1959). Not only can intraretinal location be recognised, but also the extremes of the retinal penetration. From such studies, Brown and Wiesel (1961a, b) have calculated the cat's retina to be a minimum of 165μm (range 165-250μm pending angle of penetration) at an unspecified distance along the nasal border of the tapetum. These studies, and a histological companion study (Brown and Tasaki 1961), report the thickness of paraffin embedded material to be 168-178μm at the same location whilst near the disc, thickness is around 240μm.

They claim (Brown and Wiesel 1959) that as the minimal penetration distance matched the histologically measured distance, tissue shrinkage did not occur during histological preparation and further imply that this value is representative of retinal thickness in all animals. This assumption about shrinkage is dubious, as is the implication. A more probable conclusion is that the minimal penetration distance represented cats with thinner retinae or distances further from the optic disc and is not representative of thickness throughout most of the retina. The absence of apparent shrinkage in histological processing would be very unusual, and could be explained by sampling from a thicker more central site or, alternatively, the section of the eye used for measurement may have been obliquely cut producing artificially enlarged results. Furthermore, these studies give little indication of regional variation. Representative retinal thickness therefore, is most likely greater than the claimed

minimal value of ca. 170μm and within the range of penetration measurements of 165-250μm. Indeed, followup studies (Brown 1968) show examples in which thickness in the peripheral retina is 195μm. Nonetheless, these studies provide useful information bearing in mind that their primary aim was not to measure retinal thickness.

Of recent times Linsenmeier (1986) has performed micromanipulator studies within the cat retina, but added to the sophistication of the technique by measuring both electrical activity and oxygen tension within retinal layers. As part of that study he was able to measure the length of full thickness retinal penetration using electrical endpoints and correcting for the angle of penetration. In this way, assuming that there has been minimal disturbance of retinal architecture, an *in vivo* estimate of thickness was achieved producing, in the region of area centralis of the cat, a value of 249μm; but still with a range in the raw data of up to $\pm$ 104μm. Even with great care there is still large variation in reported values of retinal thickness and substantial discrepancies in reports from various laboratories.

The conclusion from these electrophysiological studies is that the cat retina is around 250μm thick in the area centralis and between 165 to 250μm in the periphery, most probably averaging around 200μm. This is in agreement with my own data.

(3) Rodents

Using glycol methacrylate embedded material, the mouse retina was found by Sanyal et al. (1980) to be 170μm thick centrally and 100μm thick adjacent to the ora serrata. Balkema (1988) presented a figure of 130μm for plastic embedded mouse material. The data presented by Chase (1982) indicate that in the mouse retinal thickness is 180μm. By contrast, Remtulla and Hallett (1985) when calculating the schematic eye of the mouse, measured the thickness to be 237μm.

Hughes (1979a), using frozen sectioned material, calculated a value of 170μm for use in determination of the rat schematic eye. A similar calculation by Chaudhuri et al. (1983) produced a value of 217μm. Bouin's fixed, paraffin embedded rat material has been measured at less than 95μm (O'Steen et al. 1987). This low value is most likely a result of shrinkage due to the fixative employed (Deutsch and Hillman 1977). Chase (1982) rounds out the range with a figure of 190μm.

Hence, there is at least a two fold range of published figures for retinal thickness in the rat. The realistic thickness is most likely within the range 170 to 217μm, similar to my own results.

Another rodent, the ground squirrel (*Spermophilus beecheyi*), has a vascular retina at least 245μm thick though the peripheral retina is less than 100μm in thickness (Long and Fisher 1983). By contrast, the avascular guinea pig's retina is reported as being around 130-140μm in thickness (Chase 1982).

(4) Marsupials and monotremes

Little is known about retinal thickness in these animals. Stone's (1983) study of the avascular echidna's retina presents a micrograph of paraffin embedded material, and from this, thickness may be inferred to be at least 95μm. Amongst the marsupials, the American Virginia opossum's is known to be 210μm thick (Chase 1982).

Despite the Australian possum being a commonly observed marsupial (Sanderson 1984), little is known about overall retinal morphology in this, or any other, Australian marsupial. Since O'Day's (1938) report of the marsupial retina, attention has focused mainly upon retinal ganglion cell morphology and topography (Beazley and Dunlop 1983, Freeman and Tancred 1978, Hughes 1975, Tancred, 1981, Wong et al. 1986).

4.4.1.b Retinal thickness: changes with age

Developmental studies have addressed the question of differential growth and thickness within the rapidly changing retinal layers (For example, Robinson 1987, Tucker 1978). However, the emphasis has been on cellular division and death rather than upon the nutritional aspects. Spira (1975) has reported the guinea pig retina as having maximal thickness of 120μm during development.

With increasing age the adult retinal thickness diminishes (Gartner and Henkind 1981, Leopold and Calkins 1950, Shinowara et al. 1982, O'Steen et al. 1987, Weisse et al. 1974). These reports include rats and humans, and describe the major changes as occuring within the outer nuclear layer (ONL). The overall thickness changes in rats reported by O'Steen et al. (1987) are around 10μm, from 95 to 85μm in paraffin embedded sections. Five μm of this change is in the ONL. Furthermore, there is a difference in thickness between males and females with the "weaker sex" having thicker ONL, thicker retinae and being less susceptible to age related changes.

4.4.1.c Retinal thickness: pathological and interventional studies

(1) Retinal degeneration

In the pathological sphere, the effects of retinal degeneration in the mouse (Sanyal et al. 1980), vascular atrophy in the rat (Blanks and Johnson 1986) and stress (O'Steen et al. 1987) upon overall thickness, and development within laminae, have been investigated. These produce changes in thickness more marked in the outer (sclerad) retinal layers.

(2) Laser and light treatment

By contrast, photocoagulation of retinal blood vessels produces thinning of the inner (vitread) retinal layers. In keeping with a limit for choroidal oxygen diffusion, these retinae have been measured using paraffin embedded material at 135μm in the monkey (Brown et al. 1965) and less than 100μm for the cat (Stone 1969).

Retinal damage may occur from exposure to bright light (Noell et al. 1966). The retina becomes thinned and there is loss of the outer nuclear layer and photoreceptors (Bellhorn et al. 1980, Kuwabara and Gorn 1968, O'Steen and Donnelly 1982).

4.4.1.d Conclusions about published data

These results show a good deal of variation. In part this is due to normal biological variability, age related changes, location of retinal sample but I feel, most significantly, due to the way in which thickness has been measured.

4.4.1.e How best to measure thickness?

Whilst the length of a piece of string is dependent upon how it is measured so too is retinal thickness dependent upon measurement technique. Absolute measurement always suffers from the biological equivalent of the Heisenberg principle. In order to measure a physical (or biological) entity one must prod, touch, illuminate or interact in some way with the object under investigation (Beiser 1973). Uncertainty is introduced merely by the this act of measurement and, by implication, becomes greater when the object of regard becomes smaller relative to the probe being used.

So, too, the act of measuring a biological quantity depends upon interaction with, and modification of, the entity under investigation With the specific problem under investigation,

quantification of retinal thickness, a number of possible approaches may be used, most of which require manipulation, distortion and in the Heisenberg mold, uncertainty.

(1) Frozen sectioning

Using frozen sectioned material is not without problems. Hughes (1976) has calculated that the eye expands by 3% in circumference upon freezing, due in part to the volume change of the vitreous. Further error results when the retina lifts from the underlying choroid. The plane of section is no longer perpendicular to the retina producing large variations in thickness. Pilot studies using frozen sectioned rat eyes produced maximal thicknesses up to 390μm compared with actual values closer to 200μm. Furthermore identification of the exact location within the retinal transect was problematic.

(2) Tissue chopper and razor blade

Difficulty was encountered also in using the Sorvall tissue chopper, Oxford vibratome or a simple razor balde to produce cross sections of the retina. Sections were too thick, often very fragile, and orientation too easily lost. Water soluble embedding agents were really required for these approaches, but they themselves produce potential distortions. For example, 60°C agar is required to stabilise sections prior to cutting with the tissue chopper.

(3) Embedding and histological section

Paraffin embedded material may show considerable shrinkage (Humason 1972). This in part depends upon the fixative employed (Deutsch and Hillman 1977). Compare the 95μm thickness value obtained for the rat retina using paraffin embedded material (O'Steen et al. 1987) with the 170 to 217μm values for frozen sectioned material (Chaudhuri et al. 1983, Hughes 1979a). Clearly, interpretation of diffusional distances based on the paraffin material would be quite erroneous.

Other embedding procedures are prone to shrinkage. The acrylic embedded material used in this study showed shrinkage of up to 25% in thickness when compared with manipulator values. Similar percentage changes in volume have been reported for Epon embedded liver material (Nordestgaard and Rostgaard 1985). Even the process of cutting and flattening mounting may produce significant alteration in dimensions (Hanstede and Gerrits 1982).

(4) Electrophysiological sidelight

Electrophysiological recording within the retina, as already seen, may also yield information about thickness. Whilst being an *in vivo* procedure it is still susceptible to error. The distance measured on the inward retinal penetration is usually similar to that measured on the way out. However, this is referenced to a different zero point indicating a degree of distortion and tissue drag, which can be up to 80μm (Brown and Wiesel, 1959, 1961b). The standard deviation reported by Linsenmeier (1986) using this technique is quite large, being of the order of 100μm for a total overall thickness of 250μm. No doubt biological variation, distortion and assumptions concerning the angle of penetration taken by the recording electrode account for this variability.

(5) Optical and acoustic means

A recently reported clinical technique (Mori et al. 1988, Zeimer et al. 1989) shows promise in measurement of *in vivo* thickness, so important when gauging retinal pathological changes. They have used a coherent laser light source which is able to produce an oblique optical section of the retina. The width of intersection of the light beam is proportional to retinal thickness.

Another *in vivo* approach has been to use ultrasound "A" scanning (Emi et al. 1983, Decker et al. 1981, Tane et al. 1984). Even using computer aided enhancement of acoustic signals there still is large error in resolution with poor spatial localisation (Decker et al. 1981). Measurement have been estimated to show, at best, 20μm accuracy (Coleman and Lizzi 1979). This approach is more suited to pathological situations where acoustic separation occurs in tissue layers; eg. tumours and retinal detachment (Wu et al. 1989).

Clearly, all the above approaches have procedural and interpretive problems suggesting that the following, still not altogether fool proof, approach may be best.

4.4.1.f The micromanipulator technique

(1) Why go to these lengths?

Like a crime where the punishment should fit the deed, so too should the technique of measurement fit the need. For this application the need was for reasonably accurate results to address the question of diffusion distance within avascular retinae; the micromanipulator technique was employed to match the "deed". Accuracy was needed to distinguish reliably retinal thicknesses of 140μm from one of say 180 or even 200μm.

(2) Comparison with other techniques: the accuracy

The approach used in this study has produced results similar to those already published using other techniques. The cat's retinal thickness profile is very close to the theoretically accurate *in vivo* electrophysiological approach of Linsenmeier (1986) for the area centralis and the studies of Brown and Weisel (1959, 1961 a, b, 1968) for nasal retina, with the noted qualifications. Similarly the rat and guinea pig results are in accord with already published data; within 5-10μm for the guinea pig (Chase 1982) and 10-30μm for the rat (Chase 1982, Chaudhuri et al. 1983, Hughes 1979a).

Further verification that the approach is a valid and accurate representation of real distance comes from the internal controls. Biological material, liver, was found to be accurately measured by this technique and produced similar results to other measurement approaches.

(3) Effects of fixation

The use of chemical fixation carries with it potential problems and warrants separate discussion. Use of fresh retinal material as an alternative proved too difficult due to the fragile nature of the retinal sheet; hence fixation was employed literally to fix the soft and deformable retinal structure and to allow manageable handling. Empirically, avascular retinae were more difficult to fix, and together with their diminished thickness made them more prone to damage during processing.

Fixation is a poorly understood process. Dimensional changes during fixation may be summmarised as being a function of chemical binding of the fixing fluid with tissue components, osmotic effects of the fixative and vehicle and the alteration of the osmotic barriers by fixation itself (Gonzalez-Aguilar 1982). With perfusion fixation two further factors affect fluid exchange at the vascular level; oncotic and hydrostatic forces (Keele et al. 1984, Koenig et al. 1945). For simplicity, these latter effects may be neglected given the short time scale of the perfusion employed, a not altogether satisfactory assumption (Bohman and Maunsbach 1970).

The fixative employed, 4% formaldehyde (1.3 molar) in 0.9% sodium chloride, was chosen for the following theoretical reasons. Whilst the solution employed is hyperosmotic to an ideal semipermeable membrane, the fixing particles (formaldehyde) exert little or no effective osmotic pressure on biological material. This in part is due to the binding of the fixative itself to cell membranes diminishing osmotic sensitivity by a factor of around 10 (Gonzalez-Aguilar 1982). Until this effect becomes fully equilibrated, which could be many hours (Fox et al. 1985), the cell volume changes are primarily influenced by the osmotic pressure of the

vehicle, which in this case is the same as for the cell itself. The theoretical and observed result is little volume change (Fox et al. 1985, Small and Peterson 1982).

Furthermore, the fixative itself is able to produce shrinkage effects which, for formaldehyde over a wide concentration range in liver tissue, have been shown to be small (Fox et al. 1985).

The conclusion, supported by the control fixation study, is that the fixation process itself will produce minimal volume changes and, if anything, should diminish the overall cellular dimensions of the retina, yielding an underestimate of the true retinal thickness. Any dimensional changes occuring at this stage are likely to be far less than those resulting from later histological processing (Fox et al. 1985). The micromanipulator measurements of recently fixed material is clearly preferable to measurements of embedded and histologically processed material.

(4) Intraspecies variation: explanations

In the horizontal profile ananlysis, a standard deviation of typically 10μm was found for most retinal locations. In part this is accounted for by slight variations in preparation. Uncontrolled differences in fixation conditions, distortion during removal, and degree of flattening would account for a proportion of that variance. However, as with any biological measurement the population itself need not be uniform. Differences attributed to age, health, stress, sex, and genetic makeup, particularly when using wild populations, will readily account for further scatter of results.

The retina itself need not be flat nor uniform. Variation due to cellular impressions, nerve bundles and vessels also will add to dispersion of results. Never the less, the scatter is very small, 10μm being less than the dimensions of an average cell body.

4.4.1.g Biological considerations

Having discussed in considerable detail the accuracy, assumptions and limitations of the technique employed, the more important consideration is the biological significance of the retinal thickness measurements.

(1) How thick is an avascular retina?

As hypothesised, retinae dependant wholly upon choroidal nourishment are thinner than their vascular counterparts. However, not all mammalian avascular retinae are the same. The

guinea pig's retina conforms to the 143μm limit previously proposed (Chase 1982), but the possum's is up to 20 to 30μm thicker. A number of explanations for this difference are possible.

Could the technique employed have produced artefactually inflated results in the possum? This is unlikely as the internal controls and comparisons with published results present reassuring confirmation of the accuracy of the method. Furthermore, the technique employed for both avascular species was the same, adding further weight to the significance of any differences. A possible criticism relates to the perfusion pressure during fixation relative to normal arterial pressure in the two species. This may have altered fluid exchange at the capillary level, favouring expanded extracellular space in the possum. However, with normal arterial pressure in the guinea pig around 70 mmHg (Koenig et al. 1945) whilst that of the possum most likely is similar to the cat at 120 mmHg, any artefactual extravasation of perfusion fluid would have favoured increased extracellular space in the guinea pig and not the possum. The finding therefore most likely reflects a real difference.

Most other reported truly avascular retinae are indeed less than this 143μm distance. However, as already mentioned the avascular foveal region of the cynomologous monkey can be inferred at 160μm from the work of Brown et al. (1965) suggesting that there may be exceptions to the rule or that the rule is incorrect. This is not altogether surprising given the theoretical objections to the oxygen diffusion model of Dollery et al. (1969) and the interpretation of its findings by Chase (1982) to derive the figure of 143μm. If anything, based on the calculations of Dollery et al. (1969), if choroidal oxygen supply is the limiting factor in determining retinal thickness, then avascular retinae ought to be thinner than *60*μm. It will be shown that oxygen dependent metabolism is low within the inner retina of avascular species (Chapter 5) suggeting that while oxygen may be low, it is not the ultimate determinant of retinal thickness in the absence of intraretinal vasculature.

Perhaps the vascular system of the possum's choroid (and retina) may have some anatomical or physiological specialisaton allowing enhanced oxygen extraction. The rainbow trout (*Salmo gairdneri*) as known to possess an choroidal *rete mirable* which is able to concentrate oxygen to levels far in excess of those found in arterial blood (Desrochers et al. 1985, Fairbanks et al. 1969, 1974, Wittenberg 1962). As shown in Chapter 3, no similar adaption of the choroidal is present either in possums or guinea pigs. Though it could be hypothesised that the possum posseses a supplemental nourishment source, for example, through the vitreous from the ciliary body, this is unlikely based upon the conventional angiographic findings in this animal (Chapter 2) and upon the morphological appearances of the ciliary body (Chapter 3).

Finally, the possum may utilise energy in a different manner to other avascular species. The reliance upon oxygen dependent metabolism may be very much less in the inner retinal layers. Again a fertile source for further investigation is raised from this suggestion, highlighting the need to investigate the metabolic arrangements within avascular retina and between different species. See Chapter 5 for presentation of the results of oxidative histochemistry of avascular retinae and preliminary discussion about mitochondrial form and function.

(2) Regional variation

The thickness maps show far less variation in thickness than maps of intraretinal cellular counts, for example ganglion cells (Hughes 1977a). Rather than the many-fold variation in cellular distribution, thickness varies only at most by one third of maximal thickness between central and peripheral locations. Modest variation in thickness also underlies local organisational differences in cellular arrangement. The symmmetric arrangement of the rat's horizontal profile (Fig. 4.3) corresponds with the similarly symmmetrical ganglion cell distribution (Fukuda 1977, Lashley 1932). The small regional increase seen in the cat's temporal retina (Fig. 4.2A), corresponds to the area centralis (Stone 1965, Hughes 1975). By extrapolation, the native cat's profile (Fig. 4.4A) would suggest a similar increase in ganglion cell distribution temporally.

The avascular species appear to capitalise on already limited retinal thickness throughout most of the retina; there is little variation, with proportions approaching maximal thickness except in the peripheral retina. A local increase is seen though in the immediate vicinity of the optic disc of the possum, most likely related to the vascular leash shown to protrude from the disc into the vitreous (Fig. 2.11, angiography), possibly providing enhanced local nourishment.

The apparent symmetrical and minor regional difference in thickness need not however underly a corresponding organisational simplicity. Similar variation in ganglion cell allocation to that seen in the vascular retinae is found in the avascular possum retina (Freeman and Tancred 1978, Tancred 1981). When compared with vascular species, regional specialisation in function is still consistent with avascularity.

(3) Comparative aspects

Any rules that there may be with regard to vascularity and retinal thickness do not seem restricted to phylogenetic or lifestyle classes. Avascularity is found within both placental and

marsupial groups yet the representative of the more advanced placental group, the guinea pig, has a thinner retina and apparent simpler retinal organisation. The retinae of rats, cats and native cats are of similar dimensions yet come from differing behavioural backgrounds. Laboratory rats and guinea pigs whilst having similar nocturnal habits, and belonging to the same taxonomic order, have differing retinal thicknesses. Thickness *per se* is not correlated with functional needs nor visual performance.

4.4.2 Comparative intraretinal organisation

The retina as a laminated orderly outpost of the nervous system lends itself to quantification of its component parts and conclusions about retinal processing based upon the relative proportions of each layer; function correlated with structure (Kaneko 1979). Before considering the functional correlates, the limitations and assumptions of the technique must first be addressed.

4.4.2.a Validity of intraretinal measurements

Calculation of the intraretinal dimensions has been performed on processed embedded material. Assumed in the calculation is that the shrinkage has been uniform in all layers. Deutsch and Hillman (1977) have shown however that in formaldehyde fixed material greater shrinkage occurs in cytoplasm than in nuclei. The figures presented may not therefore represent true *in vivo* dimensions. However, given this caveat, useful information may be still be gleaned about retinal organisation. Unlike the thickness measurements of the whole retina, where comparison was being made with an absolute distance, the intraretinal semi-quantitative data is being interpreted in the light of known function within layers and being used to compare one species to another.

4.4.2.b Outer retinal organisation

Photoreceptors in the guinea pig retina are stouter in diameter, similar in overall length but markedly fewer in linear density than those of the possum. The absolute limits in spatial resolving power of the visual system are in part determined by this photoreceptor grating. In particular, the mosaic of receptors per angular distance, as measured from the nodal point of the eye, will set physical limits on the discrimination of separate visual objects (Westheimer 1987). The difference in angular distribution of photoreceptors is even more marked than shown by the linear photomicrograph representation (Fig. 4.8. 4.9). The eye of the guinea pig is smaller than that of the possum (Table 4.II), and therefore will subtend a larger angular

extent for the same retinal distance. As a consequence, the guinea pig eye would require *a finer* mosaic for the same resolution. As it is, based upon cell counts in the outer nuclear layer (Figs. 4.8, 4.9) the guinea pig has less than half the number of nuclei per linear distance than does the possum. The photoreceptor mosaic is similar in the two marsupials, with the number of nuclei per linear distance marginally less in the avascular possum than in the quoll (144 versus 160 per linear 100μm). When corrected for the physiologically more important subtended angular distance, the larger possum's eye becomes even closer in theoretical photoreceptor resolving power to that of the native cat.

However, photoreceptor density does not tell the whole anatomical story. The degree of convergence of photoreceptor information onto the ganglion cell population will further influence spatial resolution. No matter how fine the initial photoreceptor mosaic, if many photoreceptors feed onto a single ganglion cell, then the spatial area of this pooled signal will determine the ultimate resolution (Westheimer 1987). A typical example of this is the well known convergence seen in the human retinal periphery, where spatial resolution is sacrificed for enhanced sensitivity of night vision. Lower spatial acuity may not be a functional problem however if the need of the animal is for good illumination detection. A mosaic of coarse photoreceptors would enhance the sensitivity for detection of threshold levels of illumination. With a wider area gathering quantal information, a lower flux of light is required for visual stimulation.

In the absence of information about retinal wiring diagrams in these two avascular species, the circumstantial evidence is that the guinea pig eye should have lower spatial resolution based on its coarse photoreceptor mosaic. However, before making an estimate of anatomical acuity, other factors such as eye size, posterior nodal distance and ganglion cell numbers need consideration. See Chapter 6 (Spatial acuity and retinal vascularity, section 6.3) for a discussion of anatomical resolving power of the eye.

One final explanation for the difference in photoreceptor sizes could reside in degenerative and age related changes. As already seen, age, stress and even sex differences can influence structure. In the present case this seems unlikely as the animals were all healthy juveniles and had been reared under similar lighting conditions. The length of the photoreceptors argues against degenerative changes.

Given that avascular retinae need to be conservative with structural thickness, one suggestion has been that photoreceptors will be shorter in length (Chase 1982). This appears only to be loosely followed. In both avascular species the photoreceptor lengths are similar and not greatly different from those of the vascular native cat. Interestingly, the retinal proportions of

layers close to the choroidal nutrional source are similar in all species suggesting a common organisational pattern in this region.

4.4.2.c Inner retinal organisation

The synaptic layers have a multitude of functional roles in shaping the temporal, spatial and wavelength properties of retinal receptive fields (Cohen 1987, Kaneko 1979). An obvious, but simplistic, hypothesis is that the inner plexiform thickness might afford an approximation to the intricacy of the visual information being conducted centrally. This is a complex question which, in the absence of functional visual information, requires data about ganglion cell distribution, synaptic organisation of the inner retina, eye size and central visual organisation. Any conclusions are therefore very simplistic. Some of these aspects will be considered more fully in Chapter 6.

The vascular retinae have choroidal supply nourishing the outer retina and intraretinal networks of capillaries stretching from the the OPL to the GCL/NFL. The spacing of these inner retinal vessels might be expected to be similar to those found elsewhere in the CNS. Within gray matter the capillary bed is very dense with the half-intercapillary spacing being 12-22μm (Crone and Levitt 1984, Gannon et al. 1989). The absence of any capillaries whatsoever in the inner layers of avascular retinae provides a stark contrast to the vascular species. Should avascular retinae rely wholly upon choroidal supply (Chapter 3), without any other modifications or adaptations, then thickness ought to be limited to *less* than the equivalent photoreceptor to OPL distance of vascular species, around 80-90μm. Clearly, avascular retinae are thicker than this, with the outer retinal photoreceptor to OPL distance being at least 70μm. This would suggest that either the inner retinal layers are going to be restricted and/or there is some alternative coping strategy being employed within the inner retina of avascular species to compensate for the absence of a 12-22μm spaced capillary bed.

Inner retinal laminae of the avascular retinae are indeed thinner than those of the avascular species. Any differences however are small. Both avascular species show thinner IPLs compared with the vascular species (Figs. 4.8, 4.9, 4.10). The greatest difference in inner retinal organisation is seen within the placental order Rodentia and *not* between vascular and avascular species. Guinea pigs and rats display a marked difference, in both absolute and relative terms, in inner synaptic thickness. The two marsupial retinae however, proportionately appear to be more closely related. The possum's IPL is, on average, some 18μm thinner than the quoll's (30 versus 48μm) but differing by only 3% in relative proportions (cf guinea pig and rat which differ by 8.6% in IPL proportions).

Further away from the choroid there may be sacrifice of inner synaptic volume in the face of dwindling nourishment (Fig. 4.10). Perhaps a more appropriate conclusion regarding thickness limitations imposed by vascular lack is that the inner layers are scant, rather than restrictions being enforced upon photoreceptor length, as suggested by Chase (1982).

The inner synaptic layer is known to be involved in shaping the temporal qualities of the visual signal while the outer synaptic region is thought more important in coding spatial information (Cohen 1987). Such theoretical limitation in movement and orientation detection imposed by thinner IPL might not be a functional problem. It could be offset by more complex central visual processing. Limitation of IPL thickness within avascular retinae may not necessarily influence spatial actuity.

Little can be concluded from any differences in the cross sectional ganglion cell/nerve fibre layer thickness. More meaningful is a comparison of ganglion cell numbers as an estimate of spatial acuity (See Chapter 6). These figures are not readily derived form the cross sectional analysis. Known ganglion cell distributions would suggest that indeed spatial actuity need not suffer in avascular species (See Table 6.I). Anatomical estimates suggest that the possum has spatial acuity of 4.8 cycles/degree (c/d) and the guinea pig 2.7 c/d, marginally better than the rat at 1.2 c/d and quoll with acuity of 2.6 c/d.

4.4.2.d Intraretinal organisation: overall conclusions

All retinae, vascular or avascular, conform to a similar laminar organisation. In the avascular species examined, all retinal layers bear some restriction of thickness. The major limitation in retinal thickness lies within the IPL, the synaptic layer furthest from the choroidal blood supply. The greatest difference in intraretinal laminar proportions is seen amongst the two rodents. The two marsupials appear to be organised along similar proportional lines. The diprotodont possum's retina seems to be a miniature version of its polyprotodont counterpart (Figs. 4.8, 4.10, 4.11), diverging mainly in absolute, and less so in relative, thickness of the inner plexiform layer. Meaningful in deriving an anatomical estimate of spatial acuity is the ganglion cell distribution and the angular subtense of the retina in visual space. Spatial acuity need not suffer in avascular retinae. For a discussion of this see Chapter 6. The comparison between vascular groups would suggest that retinal thickness is greater than might be expected, if there were reliance upon choroidal blood supply alone, without other modifications. This suggests some adaptation within avascular retinae to adequately nourish the inner retina. If it is not vascular (Chapter 3), perhaps it is metabolic?

4.4.3 Eye size

4.4.3.a What determines axial length?

Finally, are the differences in ocular size sufficient to account for any enhancement of retinal volume overcoming limitation in retinal thickness?

Eye size *per se* is known to be allometrically correlated with body mass (Hughes 1977a). Hughes (1977) and Walls (1942) report an almost 100 fold difference in axial length between the smallest and largest mammalian eyes (1-100mm). In general within the animal kingdom, the major determinant of eye size is the mass of the animal. A double log plot of axial length and weight produces a linear relationship between the two variables. However for a particular body size there is still a three to four fold range of eye length, accounted for, in part, by the large ocular dimensions seen amongst birds.

4.4.3.b Size of avascular eyes

Given the variation in eye size, is there a consistent increase in those species with avascular retinae and, if so, is there sufficient increase to account for significant retinal volume enhancement and by implication enhanced function? This is based on the simplistic premise that quantity not necessarily quality of tissue is important. It also takes no account of any difference that there may be in the representation of angular space at the retinal surface, and hence the size of receptive fields per linear retinal distance.

The results (Table 4.II) do not support an unfailing relationship. The guinea pig's eye is smaller than the other species, the possum's larger and the cat's the largest eye of the series. The comparison worthiest of further consideration is that between the two marsupial members. Is the difference in axial length of possum and native cat eyes able to confer a retinal volume benefit upon the marginally thinner possum retina?

Consider the general case of two retinae, one of thickness t_1 (say 100μm) form an eye of radius R and another of thickness t_2 (say 200μm) from a smaller eye of radius r. What size is necessary for the larger eye if the two are to have the same retinal volume? Assume that the eye is a perfect sphere with radius half the axial length. Furthermore assume that thickness of the sclera and choroid is negligible and that the ocular radius represents the radius of the retinal shell. Consider the case were the radius of the smaller eye is 5mm, close to that of the native cat. For the volume of retinal tissue to be equal the following must apply:

$$^4/_3 \pi [(R+t_1)^3 - R^3] = {}^4/_3 \pi [(r+t_2)^3 - r^3]$$

(based on the volume formula for a sphere)

$$\text{or } [(R+t_1)^3 - R^3] = [(r+t_2)^3 - r^3]$$

But if $t_1 = 0.1\text{mm} = \frac{1}{2} t_2$

and $r = 5\text{mm}$ then

$$(5 + 0.2)^3 - 5^3 = (r + 0.1)^3 - r^3$$

Rearranging gives

$$15.6 = 0.3r^2 + 0.03r + 0.001$$

$$\text{or } 0.3r^2 + 0.03r - 15.607 = 0$$

Solving this quadratic equation for r gives a value between 7.1 and 7.2mm. Hence a retina of half the thickness would need an eye of 4mm larger diameter to have the same volume of neural tissue. The possum eye with axial length of 13.11mm or radius 6.5mm approaches this requirement. Furthermore, the necessary increase would not need to be that great as the thickness differs by only 30 to 50μm, less than the 100μm figure used in the calculation. Using a figure of 5.4mm for ocular radius and 200μm for retinal thickness in the quoll, and 150μm thickness for the possum retina, then the possum eye would need a radius greater than 6.25mm for the same retinal volume. It is very close to this at 6.5mm.

It seems unlikely that the increase in size is a deliberate attempt to enhance retinal processing capacity. If this were the case the marsupial eye might be expected to be larger than say the eye of a cat, a hypothesis not borne out in practice. This strategy though could well play a part within the avian realm as the visually acute bird's eye is known to be extraordinarily large (Hughes 1977a, Wood 1917), perhaps offering further volume advantages to an already thick retina and also producing greater representation of visual space per linear retinal distance.

This whole argument neglects the allometric scaling factors of animal and eye size. The small increase in the axial length of the possum eye most likely is a reflection of the fact that eye size in general is greater with larger animals; the possum being larger than the native cat. However either by design or accident the avascular possum retina could overcome limitation in retinal processing through the slightly larger ocular size, making it even more comparable in proportions to that of its polyprotodont cousin, the native cat. By contrast the anatomically simpler retina of the guinea pig has no such advantage coming from a small volume eye. It is unlikely that retinal avascularity is countered by a thin retina in a large eye.

4.5 CONCLUSIONS

1. In mammals, true avascular retinae are thinner than those in which there is an intraretinal blood supply.

2. Not all avascular retinae are equal to or less than the previously proposed figure of 143μm. The marsupial possum's retina is up to 170μm in thickness whilst that of the placental the guinea pig, is less at around 140μm.

3. The vascular retinae investigated in rats, cats and native cats, are around 200 to 250μm in thickness and display more marked centroperipheral gradients as well as minor regional variations in thickness.

4. Intraretinal organisation conforms to the same basic pattern in all species investigated.

5. Avascular species have similar photoreceptor lengths but the guinea pig has a much coarser photoreceptor mosaic suggesting an anatomical limitation to spatial acuity. The inner plexiform layer of the possum is a little thicker than that of the guinea pig.

6. The retinae of the two marsupials, one vascular, the other avascular are constituted along similar lines. Proportionately, the major difference is seen mainly in the contribution of the inner plexiform layer, which is thinner in the possum. The photoreceptor mosaic presents a similar grain in both species suggesting at this level little potential limitation in visual acuity in the avascular possum.

7. All species appear, as a first approximation, to have similar relative proportions in cross sectional profile throughout the retina. The major differences are found in the inner plexiform layer which is particularly thin in the guinea pig, though less so in the possum. This would suggest that within avascular retinae the necessary limitations placed upon thickness are borne by all layers but more so by the synaptic layers furthest from the vascular supply.

8. Eye size in the avascular possum is marginally larger than that of the native cat. While this could potentially offset limitation in thickness by increasing retinal volume, the increase is more likely related to the known increase in axial length with body size; the possum being larger than the native cat.

9. Not all avascular retinae are the same. The perception that avascularity need mean inferior vision is not supported by structural evidence within all avascular retinae.

CHAPTER 5

RETINAL HISTOCHEMISTRY:

CYTOCHROME OXIDASE HISTOCHEMISTRY AND OXIDATIVE METABOLISM WITHIN VASCULAR AND AVASCULAR RETINAE.

CHAPTER 5: FIGURES

5.1 INTRODUCTION

5.1.1 Retinal function, vascularity and metabolism

In thinking of retinal function, the overwhelming consideration centres upon neurotransmission, that is, the function of the eye in coding visual information. Light is transduced into chemical messages and this information is shaped by the retina into complex signals that the brain is able to interpret and process (Cohen 1987). To support this complex role of light detection and signal processing, the retinal *internal milieu* has certain chemical, physical and structural requirements, some of which are peculiar to the eye, but many of which are similar to those of neural tissue elsewhere. Cell membranes need to be structurally maintained, intracellular organelles are replenished, enzymes are being recycled and neurofilaments and microtubules are active not only in providing a supporting framework, but also in guiding axoplasmic transport throughout the cytoplasm. There is a background level of biochemical activity and structural homeostasis. There is a microcosm of trophic activity besides neurotransmission.

Energy is required for both maintenance tasks and for the well recognised role of neural processing. This latter process requires active membrane ionic pumps, and it is this task, which consume most of the cellular energy (Wong-Riley 1989). This role is energy intensive and a complex array of biochemical pathways exist to provide metabolic fuel. When thinking about retinal function, the energetic and homeostatic roles are often eclipsed by consideration of the more obvious cellular connections and neurotransmission. To complement, and distinguish from, an understanding of chemical coding of light, an appreciation of the more mundane, housekeeping functions of the retina is desirable. The way in which energy is produced, as one of those housekeeping functions, is nowhere more relevant than within avascular retinae.

5.1.2 Aims and questions

Retinal thickness in the avascular species has been shown to be less than in vascular species. The difference however is not great. Secondly, the choroidal circulation shows no structural adaptation within avascular retinae to suggest that there are enhanced functional properties of

the vasculature. These two observations combined suggest that retinal thickness in avascular species is greater than what would be normally expected from a sole choroidal supply in vascular species. Does this imply that energy consumption is lower within the inner retina of avascular species compared with vascular species? This is unlikely. As one indicator of energy consumption, Na^+-K^+ ATPase levels are known to be high in the avascular inner retina of the guinea pig (Ueno et al. 1981, 1984). Is there some supplemental pathway aiding diffusion throughout the inner retina, is there a reliance upon anaerobic glycolysis to supply inner retinal energy and what is the aerobic energy production profile within avascular retinae?

This chapter addresses the question of oxidative capacity through histochemical means. As one measure of oxidative energy consumption, the activity of the mitochondrial enzyme cytochrome oxidase (CO) has been determined within the retina. This enzyme is the final enzyme in the electron transport chain and accounts for most cellular oxygen consumption. If oxygen supply is limited within the inner retina of avascular species, as a consequence of reliance upon choroidal circulation, then this enzyme may have low activity.

This approach measures only one nutrient, oxygen It says nothing about supply of other metabolites, nor of any restrictions that may be placed upon removal of wastes by reliance on choroidal blood supply. There is some experimental evidence that oxygen supply within vascular retinae may be the limiting factor in determining the territory of supply of the choroidal vasculature. With obstruction of the retinal vasculature in cats, normal ERG activity may be maintained by percolating endogenous oxygen through the vitreous (Ben-Nun et al. 1988). This suggests that within the retina, all other nutrients and wastes may be adequately dealt with by the choroidal circulation alone, irrespective of the pattern of retinal vascularisation. Treatment with supplemental oxygen alone is extremely disappointing in the analogous pathological situation of central retinal arterial occlusion. In this situation, increased oxygen delivery through the choroidal vasculature is insufficient to maintain retinal function. This suggests that other substances may also be limited within the inner retina (Dollery et al. 1969). Where the intraretinal circulation is occluded, there is contradictory animal experimental evidence about the adequacy of increased choroidal oxygen supply (Flower et al. 1984). Landers (1978) has shown that after retinal arterial occlusion, choroidal supply alone may maintain vitreal oxygen tension in cats and monkeys, if 100% oxygen at one atmosphere pressure is inspired. However, Flower and Patz (1971) were able to produce only partial recovery of ERG activity with hyperoxic inhalation. Hyperbaric oxygen inhalation, as a means of further enhancing oxygen supply, is not without some risk, as retinal detachment has been reported in rabbits breathing 100% oxygen at 4 atmospheres pressure (Criswick and Harris 1967) and fluid exudation within the retina is produced at lower pressures in dogs

(Margolis 1966). Nonetheless, if oxygen therapy is to have any benefit in retinal arterial occlusion, there are good grounds for maintaining *light* adaptation, which decreases photoreceptor oxygen consumption and enhances inner retinal supply (Linsenmeier and Yancey 198).

The actual potential for choroidal oxygen supply to maintain a pathologically avascular retina still remains unknown as does the broader question of which nutrient (or waste product) limits the effective territory of supply of the choroidal circulation. In the absence of any easy measure of other metabolites, whose supply may also be limited, the oxidative capacity of avascular retinae has been investigated and compared with their vascular counterparts. It will be shown that CO levels are indeed low within avascular inner retina.

Cross sectional profiles of the intensity of reaction product have been determined using densitometry to provide semiquantitative comparisons. The time course of the CO reaction was closely monitored in order to ensure that the differences between vascular and avascular species were real, and not a reflection of non-optimal incubation conditions.

Changes in light and dark levels affect oxygen consumption (Stefánsson et al. 1983). Many biochemical pathways show diurnal cycling within the retina (Besharse 1982, Wirz-Justice et al. 1984). If CO levels in the retina show substantial diurnal variation, absence of CO activity might be seen in retinae collected at certain times of the day. This becomes of importance if the animals used are nocturnal or crepuscular in their habits and thus may have reversed patterns of metabolic activity to diurnally active animals. A pilot study was performed to determine if there were any diurnal light-dark differences in the pattern of CO activity. Despite these concerns, this preliminary study indicated that the observed low levels of CO activity in avascular retinae were not accounted for by diurnal variations in enzyme activity.

CO is an integral part of the inner mitochondrial membrane. Energy production is a major, but not the only, metabolic function of mitochondria (Stryer 1981). The questions become: does lowered oxidative enzymatic activity correlate with reduced mitochondrial numbers, altered mitochondrial form or merely reduced or inhibited enzyme activity? Qualitative impressions of mitochondrial numbers at varous sites within the retina are presented as an initial step to answering these questions.

This chapter concludes that the absence of retinal vessels correlates with reduced CO activity within the inner retina. This is likely to have produced other adaptations in energy pathways in order to maintain an adequate level of total energy supply.

5.2 MATERIALS AND METHODS

Adult mammals with avascular and vascular retinae from both placental and marsupial lineages have been compared.

5.2.1 Cytochrome oxidase histochemistry

5.2.1.a Subjects

Species with avascular retinae were placental guinea pigs, *Cavia cobaya*, (1 female and 3 males, weight 750-1070gm) and marsupial brushtail possums, *Trichosurus vulpecula* (4 males and 2 females, weight 1.4-4.0kg). The vascular species were placental Wistar rats (5 males, weight 250-300gm) and marsupial quolls, *Dasyurus viverrinus* (2 males and 4 females, weight 400-1000gm). The experimental approach was developed and verified using an additional group of rats.

5.2.1.b Subject preparation

Where whole mount retinal incubations were performed, animals were anaesthetised (Appendix 1), perfused with an intracardiac saline flush, followed by aldehyde fixatives. Short fixation times (less than one hour) were necessary to preserve enzyme activity for the subsequent histochemical reaction. Where unfixed material was used for cryomicrotomy, the animal was anaesthetised, then either perfused with a percardiac flush of the cryoprotectant 10% glycerol, or enucleated without any other preparation. An orientation stitch was placed at 12 o'clock at the junction of the sclera and limbus. The eyes were then snap frozen in isopentane chilled in liquid nitrogen. Avascular retinae proved to be more prone to damage during processing.

5.2.1.c Cytochrome oxidase incubation

For a detailed protocol see Appendix 4. The approach was essentially that of Seligman et al. (1968) which has been adapted for neural tissue application by Wong-Riley (1976, 1979). Retinae were either incubated whole, or sectioned frozen and then incubated. When incubated whole, the retina was then processed through glycol methacrylate resin or through paraffin, and sectioned at between 1 and 10μm. Resin sections were air dried, mounted and coverslipped. Paraffin sections were mounted, air dried, defatted, dehydrated and

coverslipped. Where counterstaining was required, toluidine blue was used for resin sections and haematoxylin for paraffin sections. Frozen sectioned material was incubated on the slide, fixed for 15-30 minutes in buffered 4% formaldehyde, dehydrated, cleared and coverslipped. For control incubations, the retina was incubated in the same medium, but with the addition of 0.01M potassium cyanide (KCN).

5.2.1.d Diurnal cytochrome oxidase histochemistry

For investigation of diurnal variation in retinal metabolism, a comparison was first made using rats (3 male pairs, one eye from each animal) then possums (1 male and 1 female, one eye from each). One animal was anaesthetised in the afternoon at 5 o'clock and perfused with 10% glycerol. Its eyes were then removed, marked, snap frozen and stored overnight at -87°C. Another animal was left overnight in the dark and treated in the same way at 7 o'clock the following morning. The animals were not fasted. Previous investigations using frozen eyes had shown minimal deterioration in reaction product when stored in this way. An eye from each species pair was orientated in a similar manner and blocked together into a carboxymethylcellulose mould. They were then sectioned on a cryostat at 48μm, mounted on the same slide and incubated in the CO medium until a dark reaction product was evident (Appendix 4).

5.2.1.e Densitometry of cytochrome oxidase histochemistry

To gain a relative measure of the amount of reaction product, densitometry was performed on frozen sectioned material incubated histochemically for CO. Although this does not provide absolute measures of enzyme activity, it was helpful in determining optimal incubation times, for allowing comparison of different species and for determining the laminar distribution of enzyme level. Only cryostat sections cut at 48μm thickness, mounted and incubated on the same slides were used. When comparisons between diurnal exposure or between species were to be made, eyes were blocked together and mounted on the same slide. Some sections were fixed for short periods prior to incubation. Nickel was added to the incubation medium to generate a dense black reaction product which could be readily detected photometrically. After incubation all sections were fixed in formaldehyde, dehydrated, defatted and coverslipped.

Representative regions from the retina were then examined using a Leitz Orthoplan microscope to which a video camera was attached. The automatic gain control was disabled so that the camera sensitivity was the same irrespective of the overall brightness of each section. The gain and background sensitivity were adjusted so that sections incubated for

short periods were measureable (minimise camera saturation) yet still able to detect differences in activity in darker sections (before chemical saturation occured). The camera was calibrated with neutral denstity filters and found to have a linear response curve over the mid range in which most of the readings were performed. There was some fall off in camera output at the extremes of illumination. The image was digitised into an array of 640x480 pixels of 256 gray levels and, through image analysis software, a line density profile across the retina was calculated.

5.2.2 Mitochondrial ultrastructure

The location and distribution of mitochondria within the retina was determined by electron microscopy in a selection of animals. Species with avascular retinae were placental guinea pig, *Cavia cobaya*, (1 male, weight 940gm) and the marsupial brushtail possum, *Trichosurus vulpecula* (2 males, weight 2.3-3.0kg). The vascular species used was the marsupial quoll, *Dasyurus viverrinus* (2 females, weight 750gm).

Animals were anaesthetised and the retinae were perfusion fixed with mixed aldehydes and processed for transmission electron microscopy (Appendix 3). One quoll retina was also incubated in the CO medium and subsequently processed for electron microscopy.

5.2.3 Photography

Light microscopy photography was performed using a Leitz Orthoplan microscope using either Kodak Panatomic X film for black and white, or Kodacolor Gold 100 with, a CB12 correction filter, for colour photography.

5.3 RESULTS

5.3.1 Cytochrome oxidase histochemistry

5.3.1.a Species comparison

(1) Vascular species

In transverse cross section the retinae of the rat and quoll show lamination of the CO reaction product (Fig. 5.1, 5.2). The darkest deposit is seen within the photoreceptor ellipsoid region. The cones in the marsupials, being located more sclerad in the photoreceptor lineup, stand out in contrast against the unstained rod outer segments (Fig. 5.2). The synaptic layers, OPL and IPL show a heavy deposit of chromogen. Sublamination within the IPL is apparent in the rat. Individual punctate accumulations in the OPL correspond to the synaptic terminals of the rods and cones (Fig. 5.1). The ganglion cell and nerve fiber layer are also well stained with prominent, though variable, activity within ganglion cell neuropil. At the optic disc, CO activity diminishes within the optic nerve (Fig. 5.3).

(2) Avascular species

The avascular guinea pig and possum retinae show a markedly different pattern of staining (Figs. 5.4, 5.5). There is very little staining within the inner (vitread) retinal layers. Very long incubation times of between one and two hours were necessary to demonstrate the little amount of activity vitread to the OPL. Reaction product in the vascular species is apparent in a fraction of this time, circa 15 to 30 minutes. Indeed in the early incubation studies, where lightly fixed material was used, no reaction product was consistently seen in the inner retina of possums and guinea pigs suggesting no oxidative activity in these regions at all. It was not until later that a low activity level was discovered in these species using long incubations periods in unfixed material.

Companion incubations of rat and guinea pig retinae were performed to demonstrate more clearly this difference between vascular and avascular retinae (Figs. 5.6, 5.7). Retinal cryostat sections from both animals were cut together, mounted on the same slide and incubated tegether until the pattern of the vascular rat retina was well demarcated and near maximal intensity (Fig. 5.6A) Under the same conditions, activity in the guinea pig retina is seen only within the photoreceptor ellipsoid, the inner retinal layers are devoid of any enzyme activity

whatsoever (Fig. 5.6B). Graphical comparison of guinea pig and rat are shown in figure 5.7, further highlighting the similarity of ellipsoid activity and contrasting the marked difference in inner retinal CO potential. The relative differences are similar in the quoll-possum pair, with little activity within the inner retina of the possum under conditions which produce maximal activity in the quoll. Control incubations using KCN were consistently negative (Fig. 5.8) indicating that the inner retinal activity under long incubation conditions was real and not just nonspecific, non enzymatic deposit of chromogen.

Activity within the ellipsoid of the photoreceptors, as determined by densitometry measures, is similar in all species examined, vascular and avascular. Within the OPL of the avascular species, essentially no reaction product is seen despite very long incubation times (Figs. 5.4, 5.5, 5.7). Only a weak histochemical deposit is seen in the IPL, NFL and surrounding ganglion cell nuclei.

5.3.1.b Incubation conditions

To gain more than a qualitative impression of the differential activity within retinal laminae, densitometry was performed. The time course of reaction product development is shown in Figure 5.9 along with the densitometry readings in Figure 5.10. If incubation conditions are too long, then all layers approach maximal optical saturation and appear to possess similar enzymatic activity levels (Fig. 5.10, 28 minute incubation). Relative differences are lost. For example, long incubation times yield a false impression of the activity within the ellipsoid in comparison with the inner retina. In the early stages of the incubation, the peak activity in the photoreceptors reaches its optical maximum whilst the other layers are just visible, indicating more accurately the *relative* differences of the CO activity in each laminae.

5.3.1.c Regional and diurnal variation

Regional variation in activity was sought but not found. Thus the pattern of staining can be considered representative no matter where in the retina the sample was taken. Comparison of typical nasal and temporal cross sections are shown in figure 5.11. There is little difference in transverse profiles.

The pilot study investigating diurnal pattern of activity revealed no significant differences at the two times examined, and was not pursued beyond the initial results in one vascular and another avascular species. The vascular rat retina showed little difference in reaction product profile whether the eye was taken at the beginning or end of the light-dark cycle (Fig. 5.12). The possum too, showed no diurnal difference in intensity or distribution of the reaction product between late afternoon and early morning samples. While this does not exclude subtle daytime differences in CO activity, it does suggest that any differences in activity between vascular and avascular species are not accounted for by sampling error.

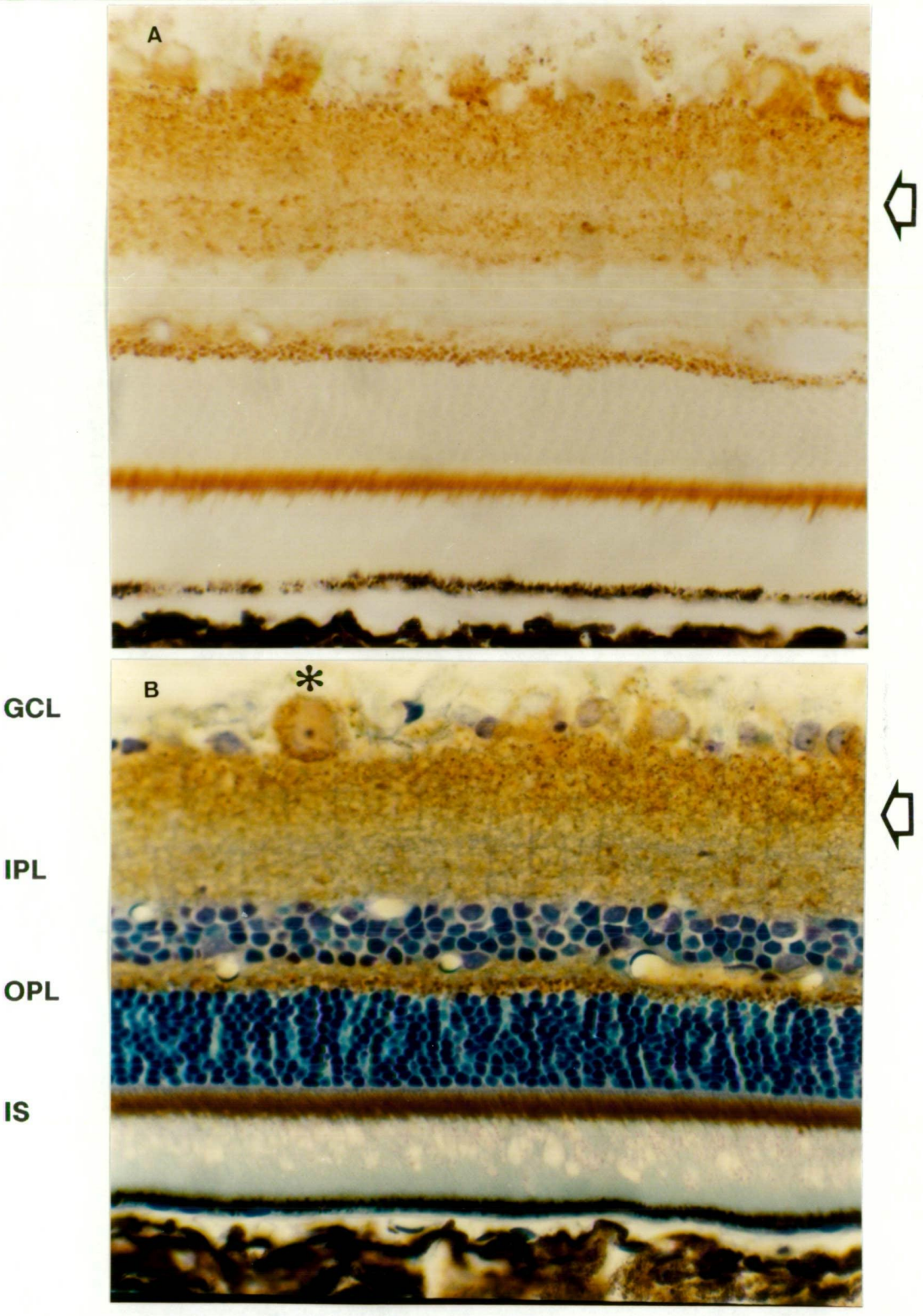

Figure 5.1: Rat retinal cytochrome oxidase **40μm**

Plastic embedded 10μm transverse section of rat retina incubated for cytochrome oxidase. Incubation performed on whole retina followed by embedding and sectioning. (A) no counterstain, (B) counterstained with toluidine blue. The most intense reaction product is seen in the photoreceptor inner segment (IS) followed by the plexiform layers (IPL, OPL) and ganglion cell layer (GCL). Large reactive ganglion cells are seen in the GCL (*). Note the line of low intensity in the IPL dividing the sclerad third from the more reactive vitread two thirds (arrow). Dot like reaction product may be seen outlining individual rod and cone terminals in the OPL.

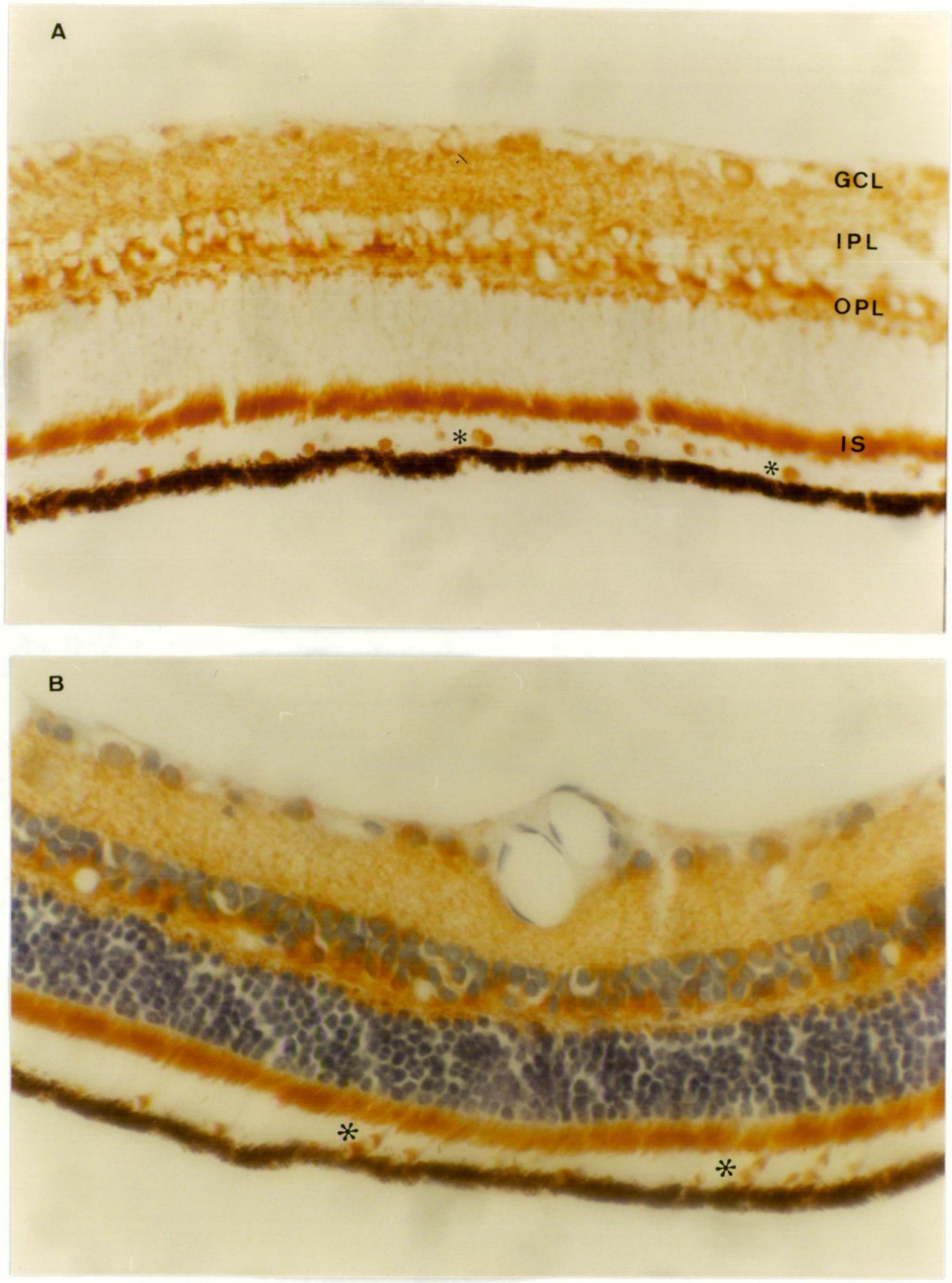

Figure 5.2: Quoll retinal cytochrome oxidase

Paraffin embedded 10μm section of quoll retina incubated for cytochrome oxidase. Incubation performed on whole retina followed by embedding and sectioning. (A) no counterstain, (B) counterstained with haematoxylin. The most intense reaction product is seen in the photoreceptor inner segment (IS) followed by the plexiform layers (IPL, OPL) and ganglion cell layer (GCL). The IPL staining is more uniform than the rat. Nuclear layers and outer segments are unstained. Note the CO staining of the cones (*). Scale bar = 40μm.

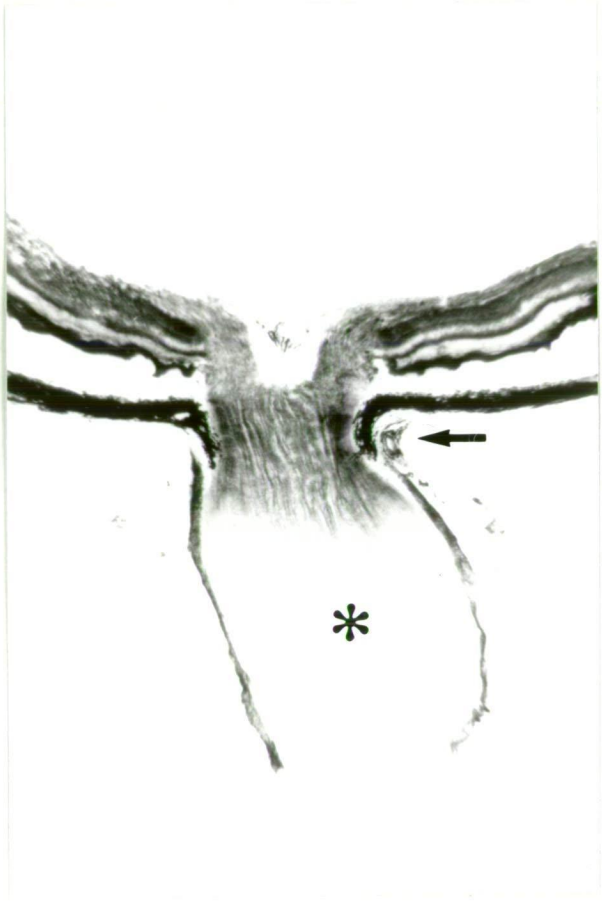

Figure 5.3: Rat cytochrome oxidase: optic disc

48μm cryostat section of rat retina and optic disc incubated for cytochrome oxidase with nickel intensification. No counterstain. At the level of the lamina cribrosa (arrow) CO activity changes. The reaction product is minimal within the myelinated optic nerve (*). Scale bar = 200μm.

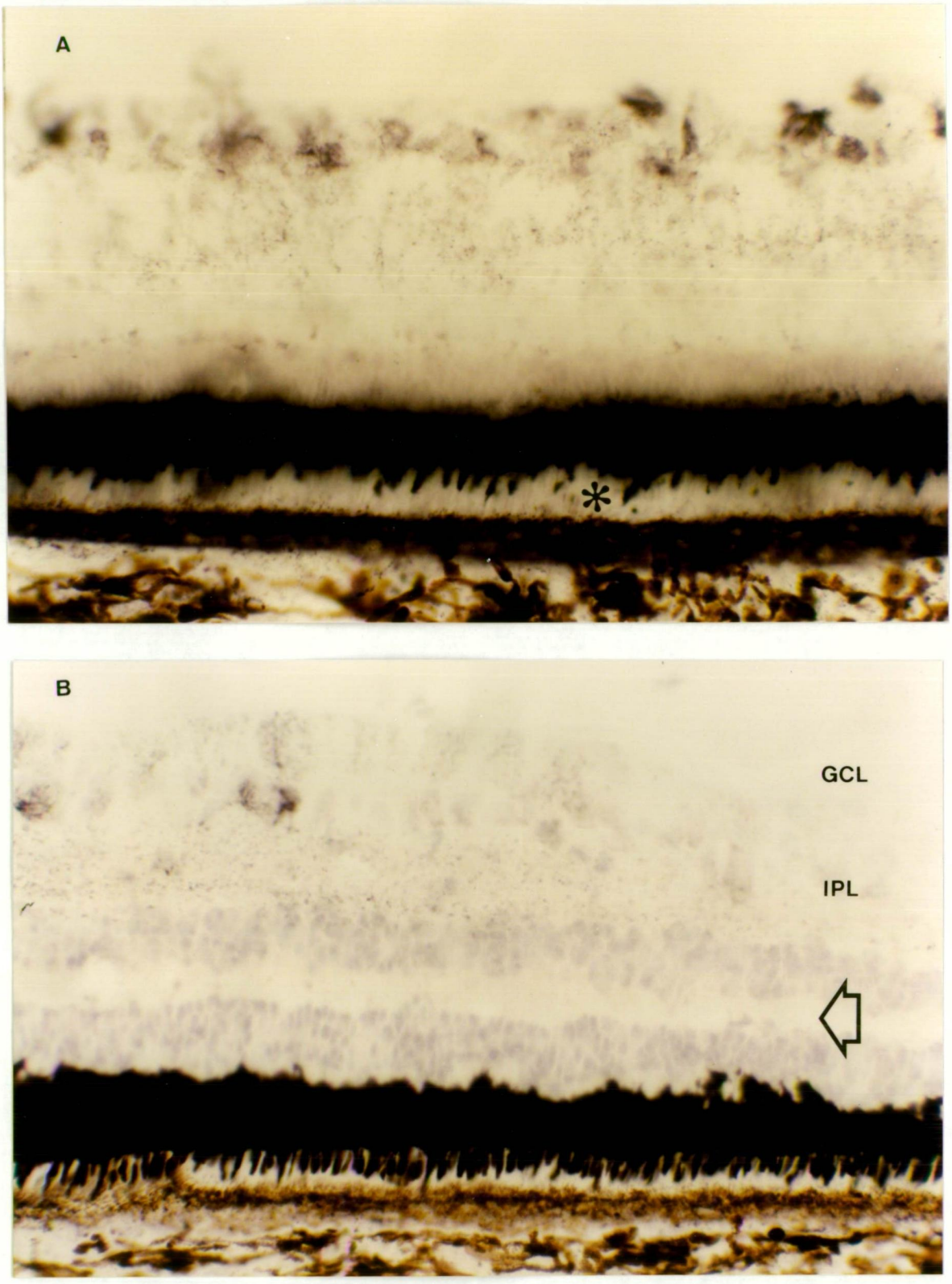

Figure 5.4: Guinea pig retinal cytochrome oxidase

(A) no counterstain, (B) counterstained 48μm unfixed transverse retinal cryostat sections. Incubated for cytochrome oxidase with nickel intensification. The reaction product is very dense within photoreceptor inner segments, the section having been overincubated for outer retina in order to demonstrate the low level of CO activity located within the inner retina. Note the sclerad projecting cone ellipsoids outlined by the unstained rod outer segments (*). There is no true staining of the outer segments. Little activity is seen in the OPL (arrow) with scattered label only in the GCL and NFL. Scale bar = 20μm.

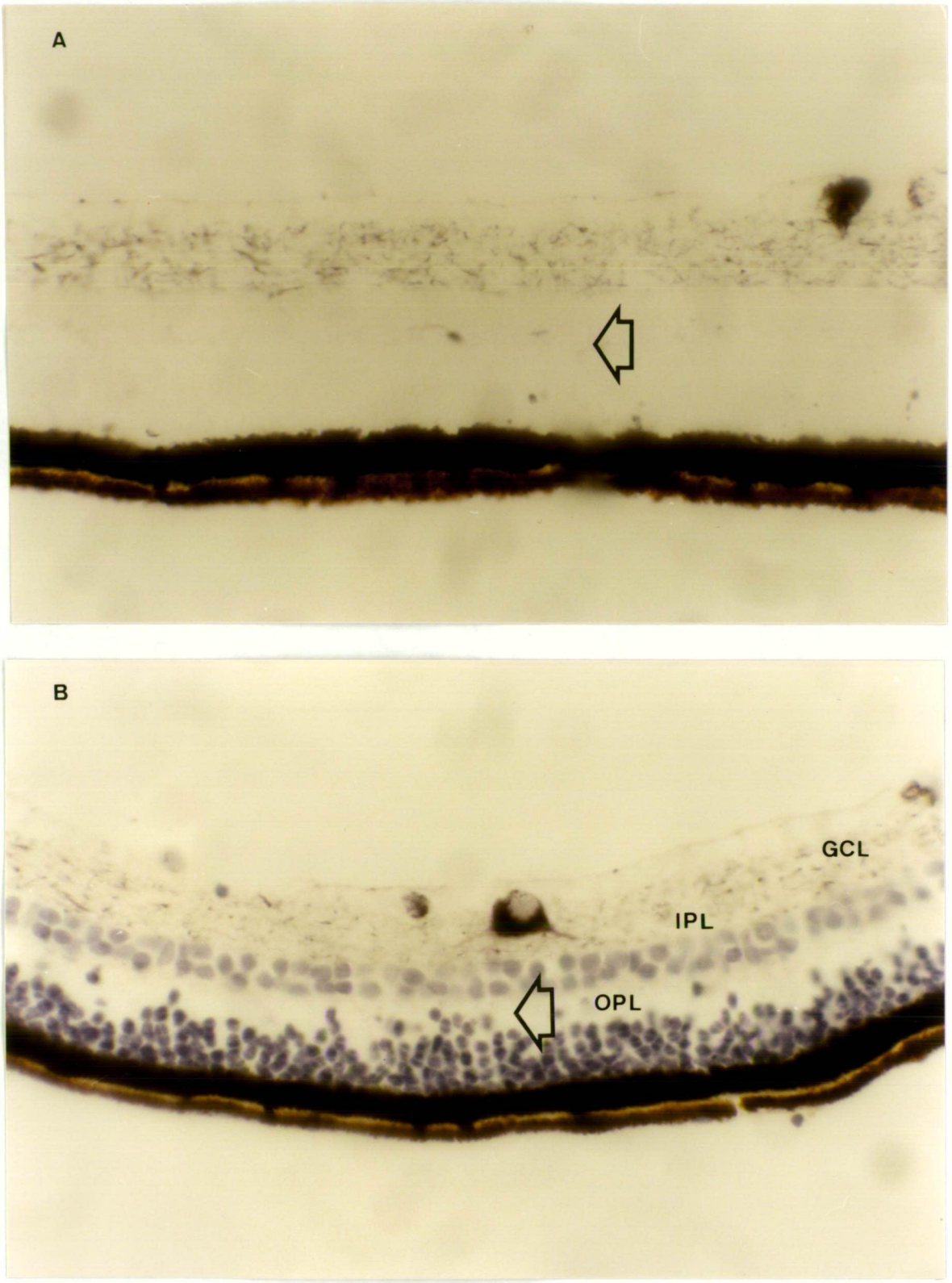

Figure 5.5: Possum retinal cytochrome oxidase

(A) Unstained, (B) counterstained 48μm unfixed transverse retinal cryostat sections. Incubated for cytochrome oxidase with nickel intensification. The reaction product is very dense within photoreceptor inner segments, the section having been overincubated for outer retina in order to demonstrate the low level of CO activity located within the inner retina. There is no true staining of the outer segments. Little activity is seen in the OPL (arrow) with scattered label only, in the GCL and NFL. Note the intensely staining, presumed ganglion cell (*). Scale bar = 40μm.

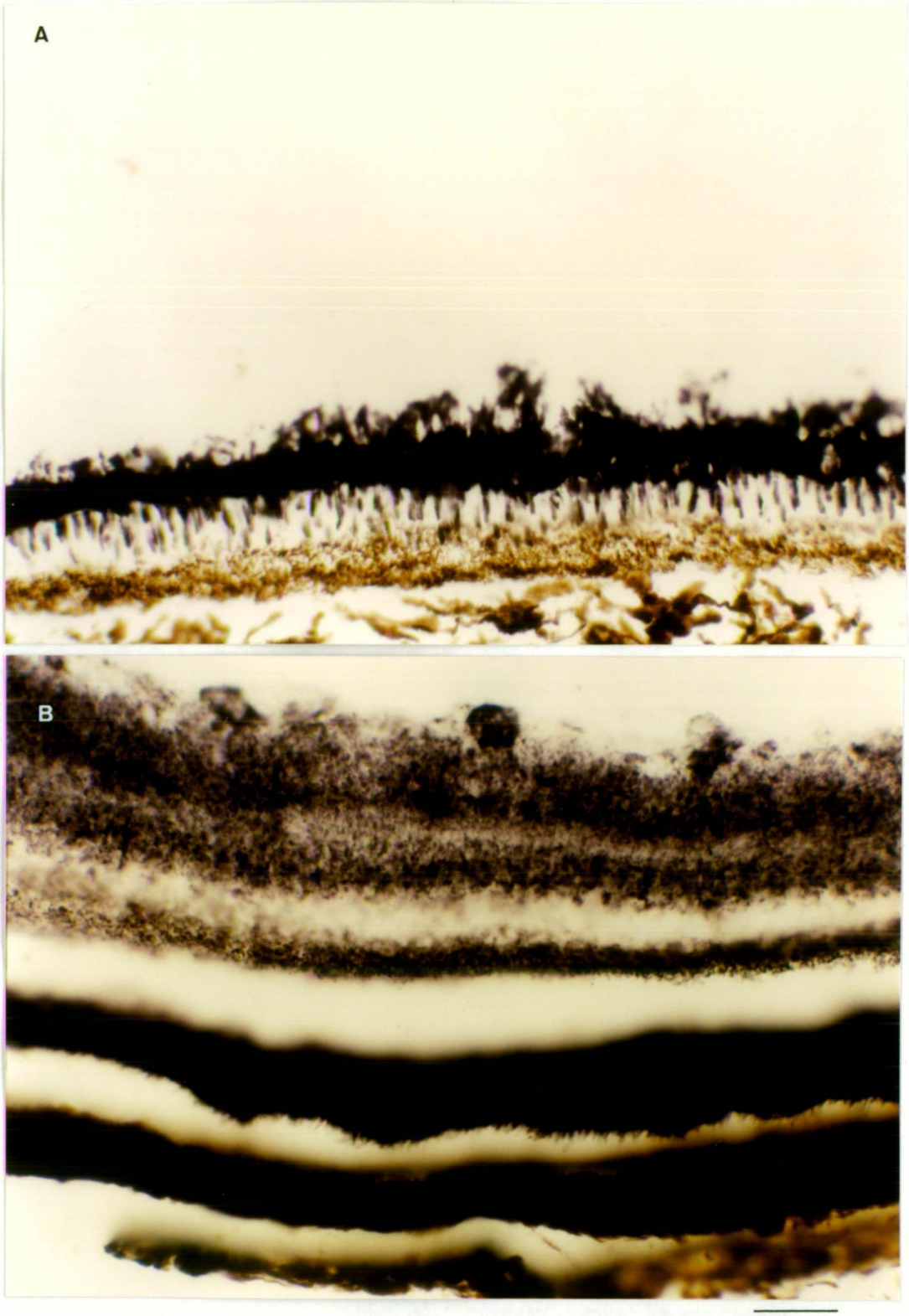

Figure 5.6: Comparison of rat and guinea pig retinal cytochrome oxidase

(A) avascular guinea pig, (B) vascular rat 48μm transverse retinal cryostat sections. Fixed for 10 minutes then incubated in nickel intensified cytochrome oxidase medium until normal rat pattern was evident. Treatment identical for both specimens. The reaction product is very dense and similar within photoreceptor inner segments of both animals. Whilst the CO reaction product is well differentiated in the rat, no reaction product is seen in the avascular guinea pig inner retina. Scale bar = 40μm.

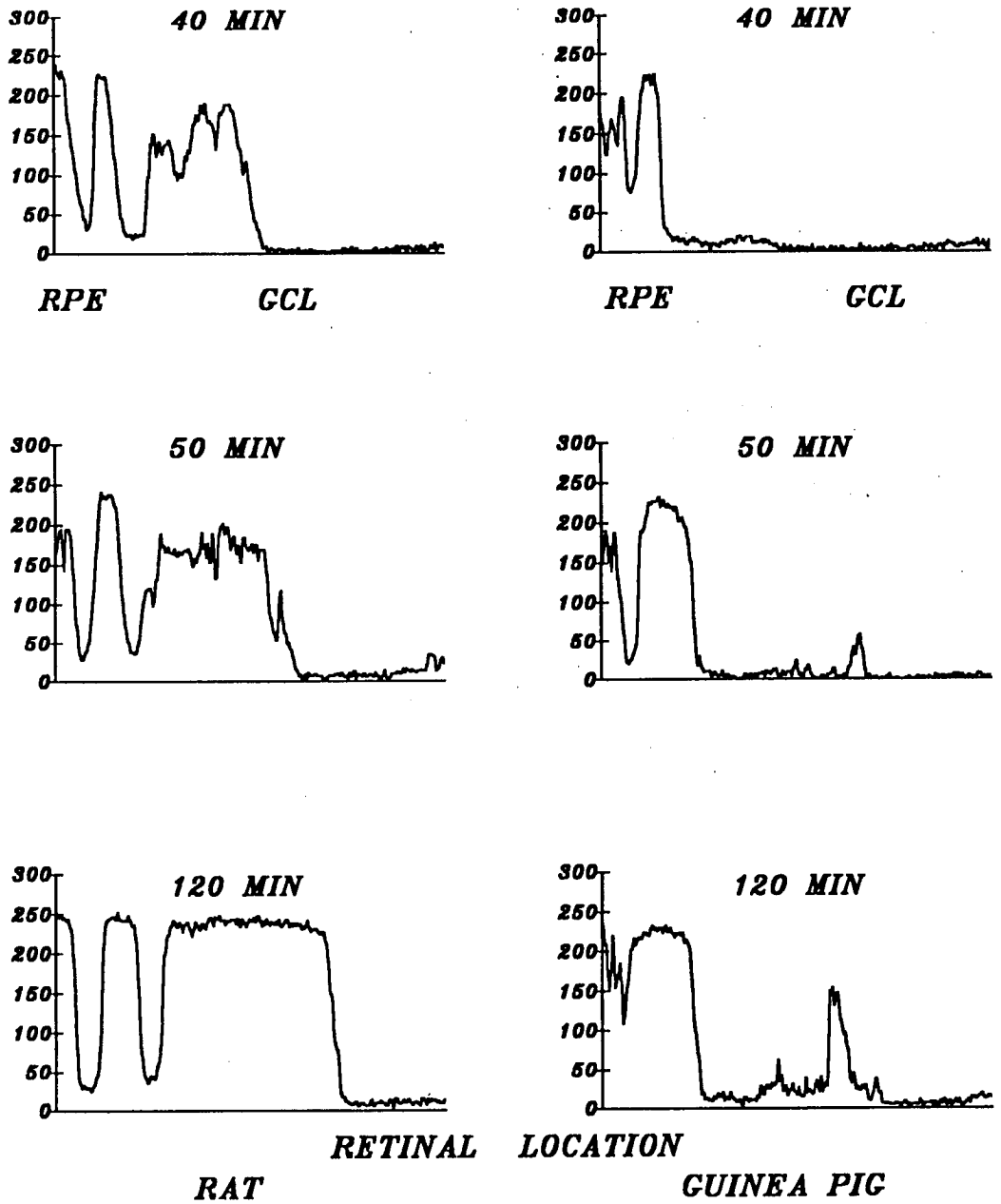

Figure 5.7: Densitometry of rat-guinea pig comparison

Densitometric measurements in guinea pig and rat transverse retinal sections. Cryostat sections fixed for 10 minutes then incubated in cytochrome oxidase medium. Same series as Fig. 5.6. Profiles taken at 40, 50 and 120 minutes incubation. Rat on the right and guinea pig on the left. Each graph represents a density scan across the retina. The first peak represents the RPE, followed by the photoreceptor CO deposit. The third peak is more variable representing the CO stain in OPL, IPL and GCL. This graphically demonstrates the low levels of CO activity in the avascular inner retina and the long incubations required for its demonstration. Y axis = gray value (0-256), 0 = no stain, 256 = heaviest stain.

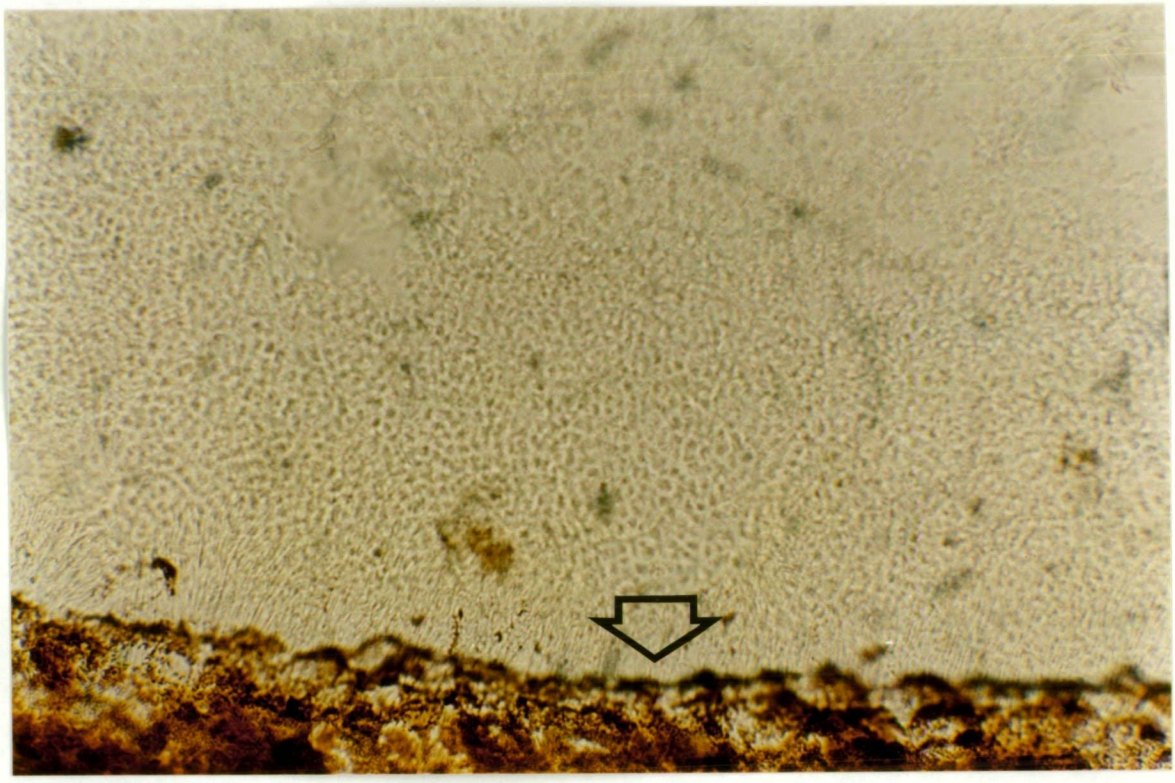

Figure 5.8: KCN control

Cryostat section of possum retina incubated in CO medium but with the addition of 0.01M KCN. No reaction product is seen. Only pigment within the retinal epithelium is visible (arrow).

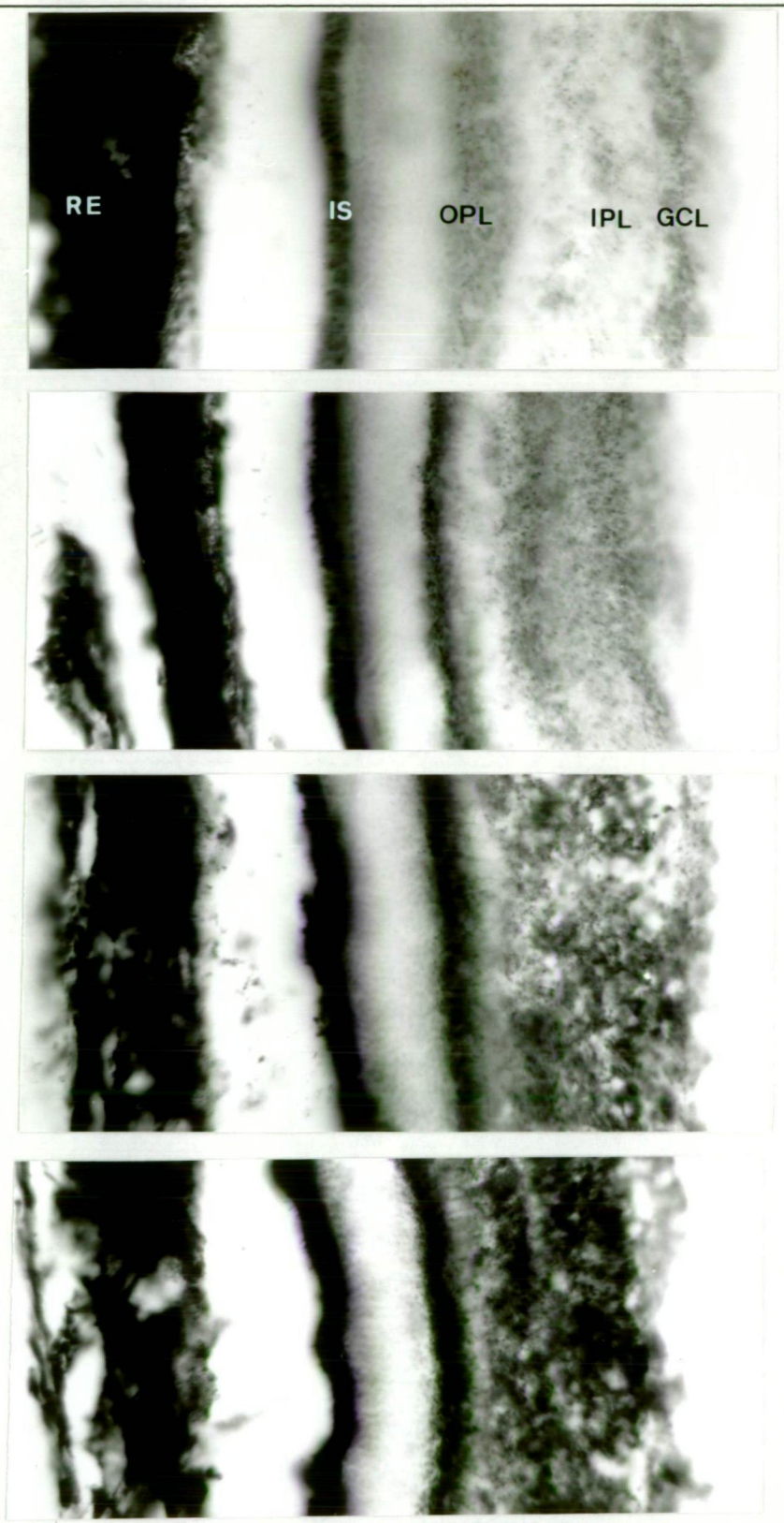

Figure 5.9: Time course of rat cytochrome oxidase incubation

Sequential specimens at 16, 20, 24 and 28 minutes incubation are shown. Cryostat sections were incubated in nickel intensified medium. The relative distribution of laminar deposit changes with time. Optical saturation of the inner segments is seen beyond 20 minutes. With longer incubations the activity of the inner layers approaches that of the photoreceptors. See also Fig. 5.10. Scale bar = 50μm.

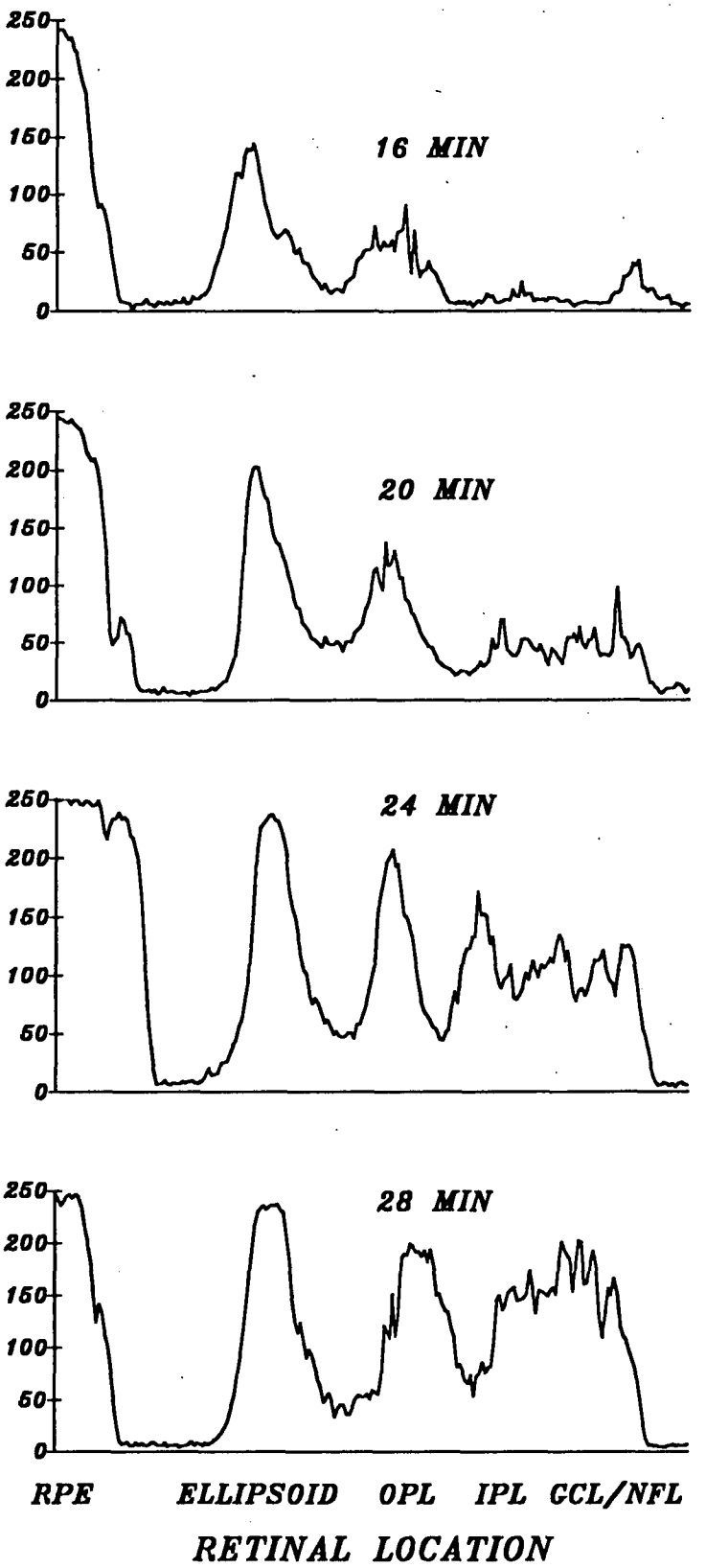

Figure 5.10: Densitometry of rat cytochrome oxidase incubation

The time course of the CO reaction has been measured. Cryostat sections were incubated in nickel intensified medium. The relative distribution of laminar deposit changes if incubation is too long. Optical saturation of the photoreceptor outer segment occured beyond 20 minutes. With longer incubation time the activity of the inner layers approached that of the photoreceptors. Y axis = gray value (0-256), 0 = no stain, 256 = heaviest stain.

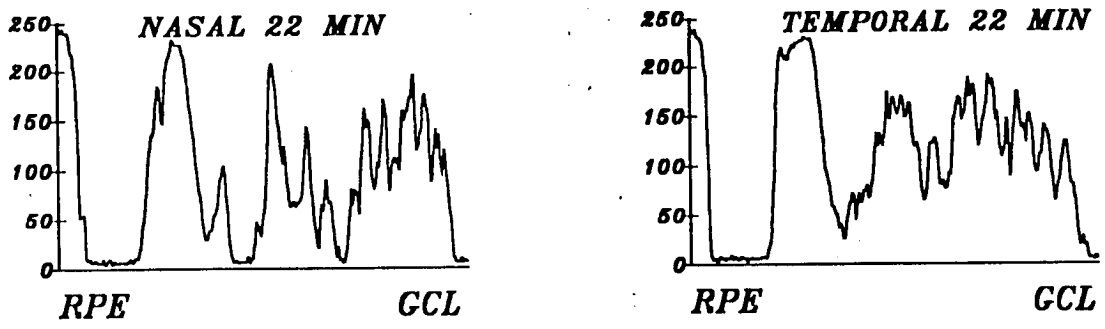

A B

Figure 5.11: Nasal and temporal comparison of rat cytochrome oxidase

Cryostat sections incubated for CO with nickel intensification. There is little differences in activity between nasal (A) and temporal (B) locations.

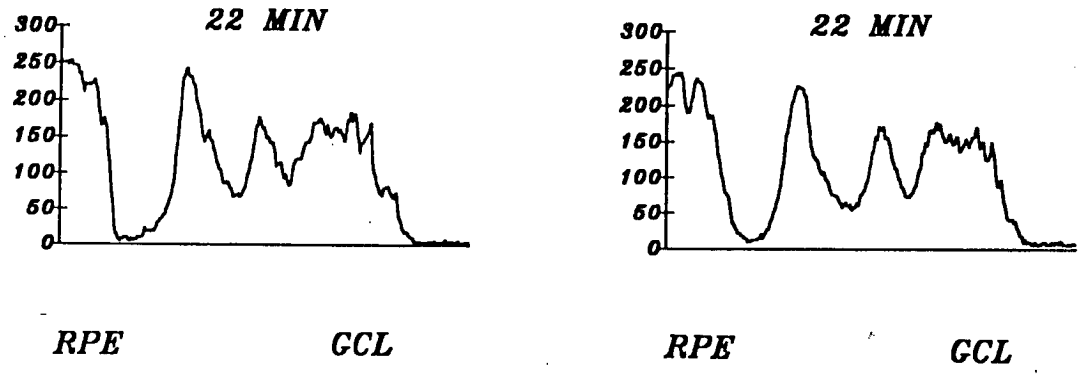

A (5 pm) B (7 am)

Figure 5.12: Diurnal variation of rat cytochrome oxidase

Rat cryostat sections incubated for CO with nickel intensification. Samples of transverse CO profiles from the same incubation run. (A) eye removed in the afternoon. (B) eye removed in the morning. Y axis = gray value (0-256), 0 = no stain, 256 = heaviest stain.

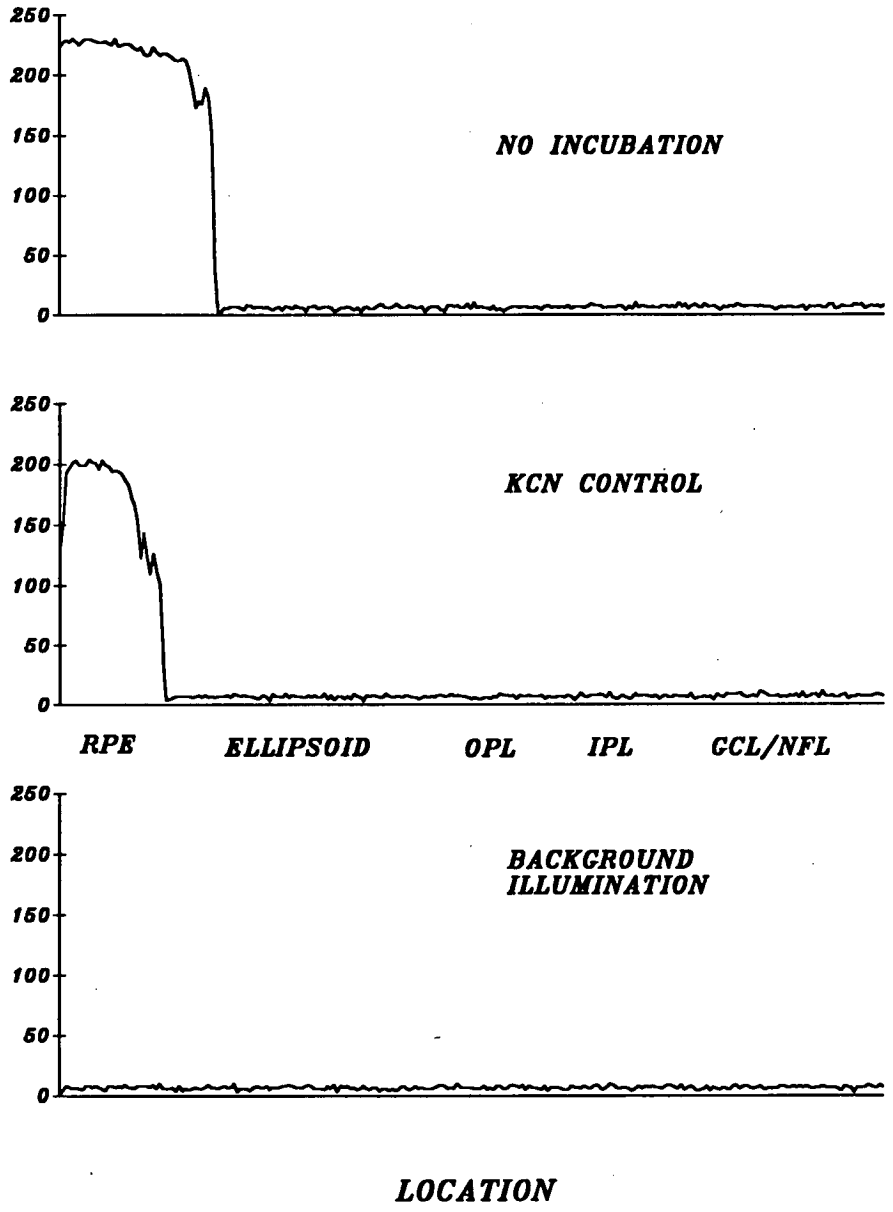

Figure 5.13: Control densitometry readings

Control cryostat sections. Only the RPE reading is visible for KCN controls and sections which were not incubated at all. No section produced minimal background level.

5.3.2 Mitochondrial distribution and structure

Qualitative impressions of retinal ultrastructure are presented with emphasis on the distribution and form of mitochondria.

5.3.2.a Quoll

In the quoll, mitochondria are distributed in accord with the CO staining pattern. The photoreceptor ellipsoid appears to be the same in all species and is densely packed with mitochondria (Fig. 5.14). The OPL has mitochondria distributed both in the terminal synaptic areas of the photoreceptors and scattered through the neuropil (Fig. 5.15). Synaptic ribbons, a common feature of photoreceptor terminals, are present. Examples of variable CO mitochondrial staining are also presented in figure 5.15. Not all mitochondria need show CO activity, and when present, it may differ in intensity from one mitochondrion to another **(See 5.4.3.c.7)**. Mitochondria are distributed within the IPL, among cells of the GCL and in the fibers of the NFL. They often have well defined inner mitochondrial membranes (Figs. 5.16, 5.17).

5.3.2.b Possum

The photoreceptor ellipsoid region in the possum is packed with mitochondria. The OPL however, shows *no* mitochondrial profiles within the spherules and pedicles of the photoreceptors (Fig. 5.18). Synaptic ribbons are present. Some mitochondria are seen surrounding the nuclei of the outermost cells of the INL. The IPL demonstrates many mitochondrial profiles, some of which have well defined cristae (Fig. 5.19). Within the innermost retina, a prominent feature is the finding of large, washed out areas of Müller cell cytoplasm (Fig. 5.20). Mitochondria are also present within the cellular and axonal profiles of the ganglion cells and nerve fibers.

5.3.2.c Guinea pig

The photoreceptor inner segment is densely populated with mitochondria. The OPL like that of the the avascular possum is devoid of mitochondrial profiles (Fig. 5.21). Mitochondrial profiles which often have poorly defined cristal structure are seen within the IPL. Prominent with the IPL are the widespread, insinuating processes of the Müller cells (Fig. 5.22). In the GCL, mitochondria are present within both the cytoplasm and in axonal profiles (Fig. 5.23).

Figure 5.14: Quoll ellipsoid

EM section of CO incubated retina. Note the concentration of mitochondria wihin the ellipsoid of the photoreceptor (Arrow). Most mitochondria show a positive CO reaction. This region is similar in the possum and guinea pig.

Figure 5.15: Quoll outer plexiform layer

Ultrastructural appearance of cytochrome oxidase incubated quoll OPL. Note the variable intensity of the mitochondrial CO reaction product. Some mitochondria within the photoreceptor synaptic region are heavily stained (closed arrow) and others have no stain at all (open arrow). Synaptic ribbons are present (*).

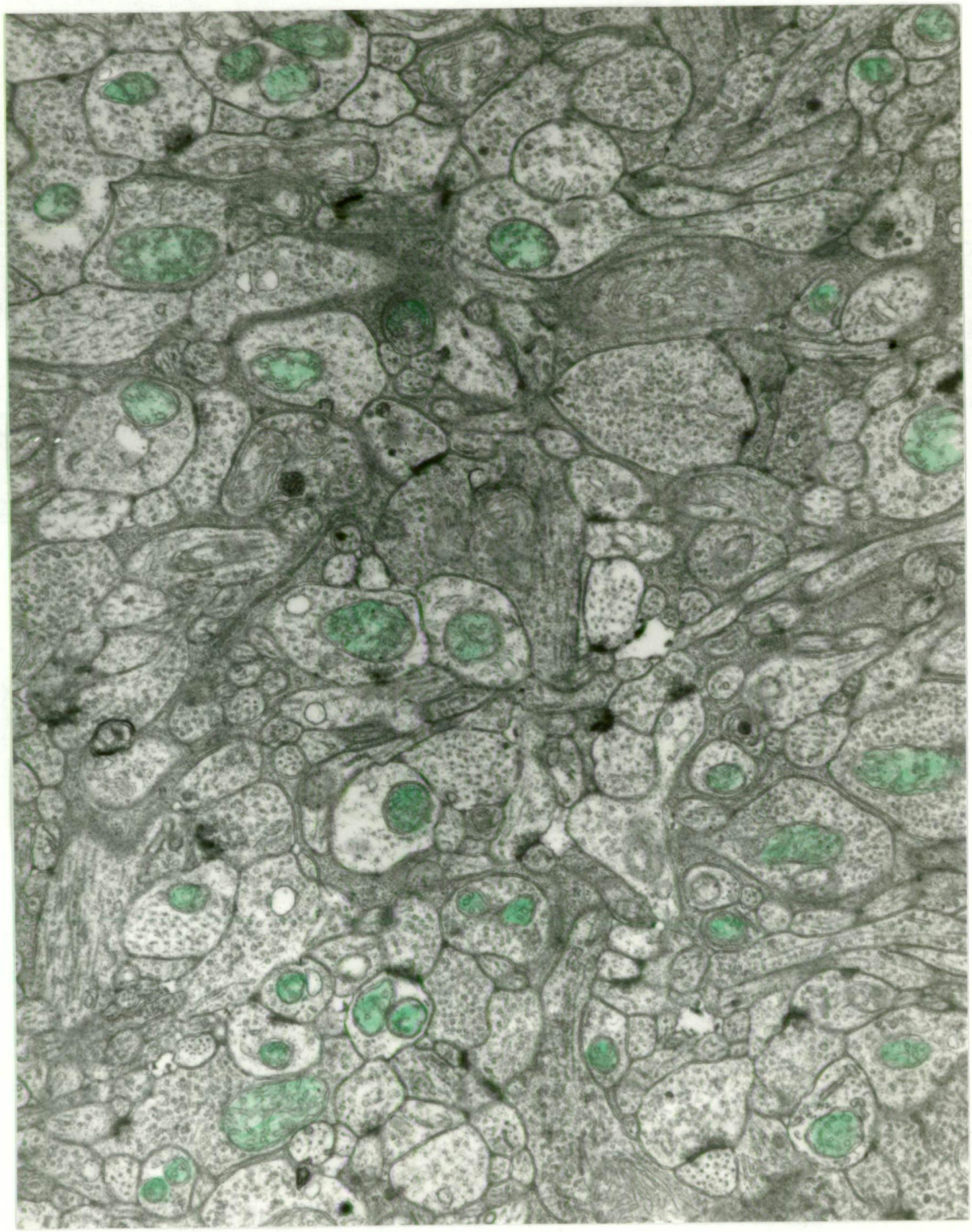

1μm

Figure 5.16: Quoll inner plexiform layer

Ultrastructural appearance of the quoll IPL. (No CO incubation). Numerous mitochondria are scattered throughout the neuropil (coloured).

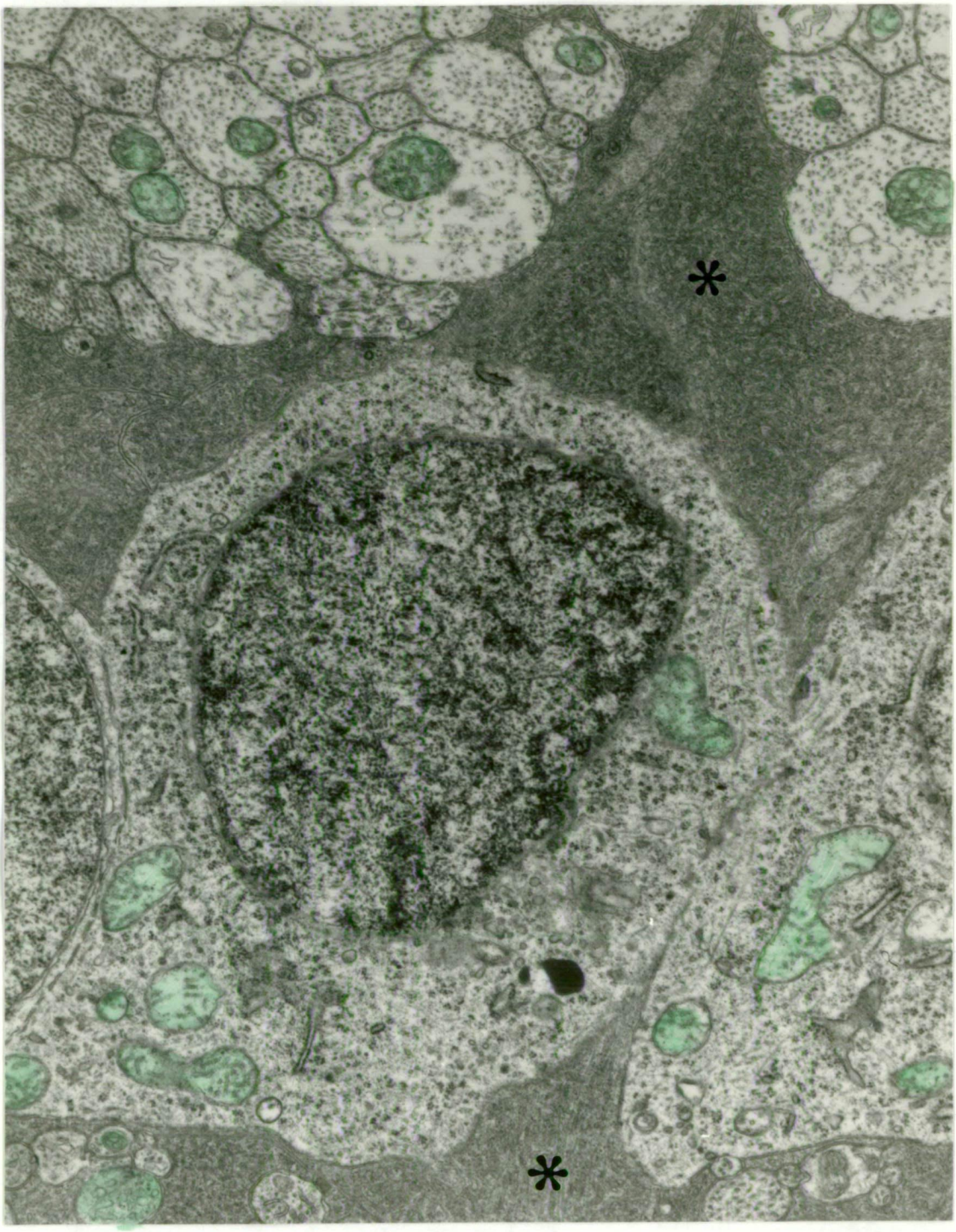

Figure 5.17: Quoll ganglion cell and nerve fiber layer

Ultrastructural appearance of the GCL and NFL. Numerous mitochondria are present throughout both layers. Note the Müller cell processes extending between cells and nerve fibers (*). (No CO incubation).

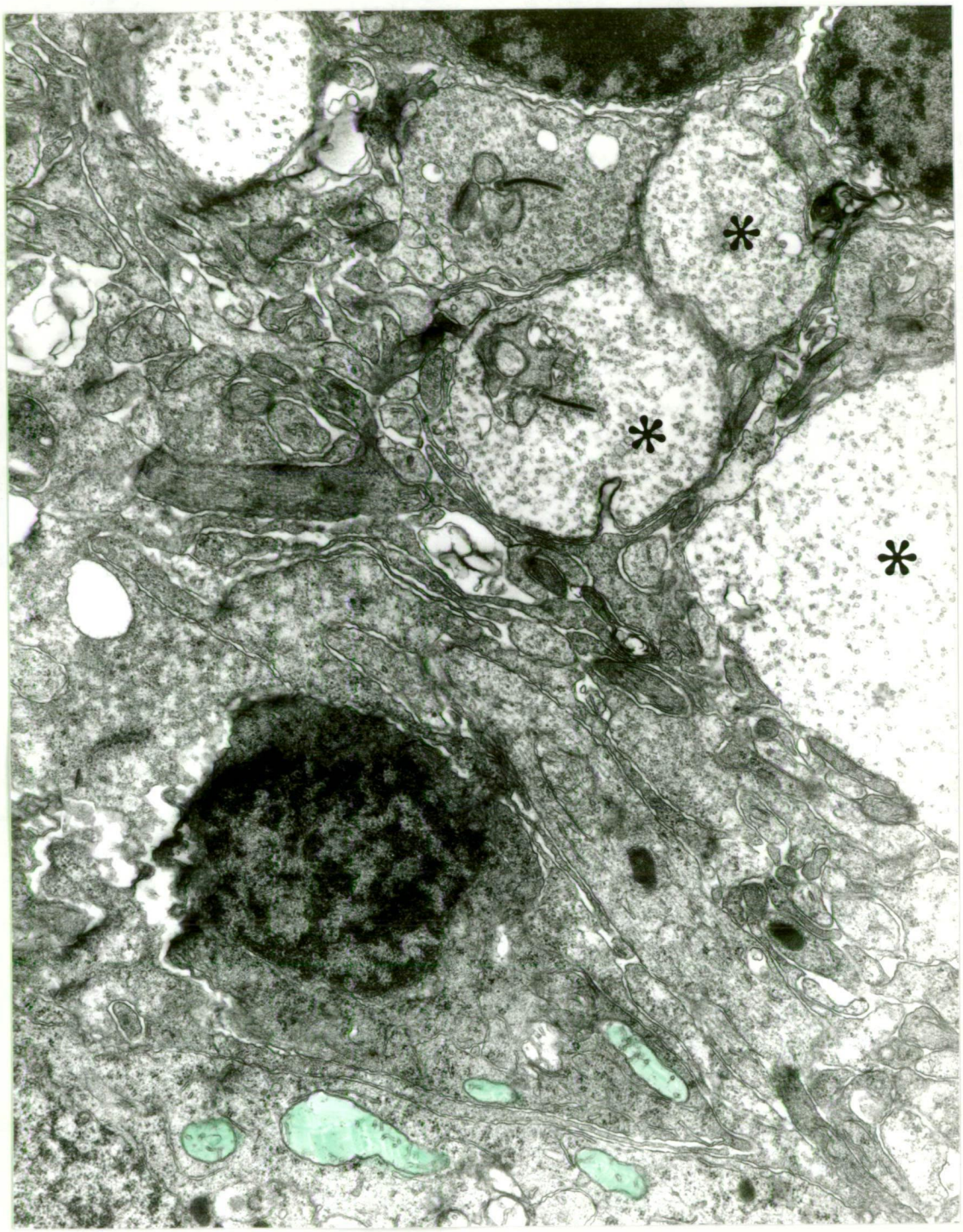

Figure 5.18: Possum outer plexiform layer

Ultrastructural appearance of the OPL. Note the absence of mitochondria from the synaptic regions of the photoreceptors (*). Occasional mitochondria may be seen surrounding the nuclei of cells in the innner nuclear layer (coloured). (No CO incubation).

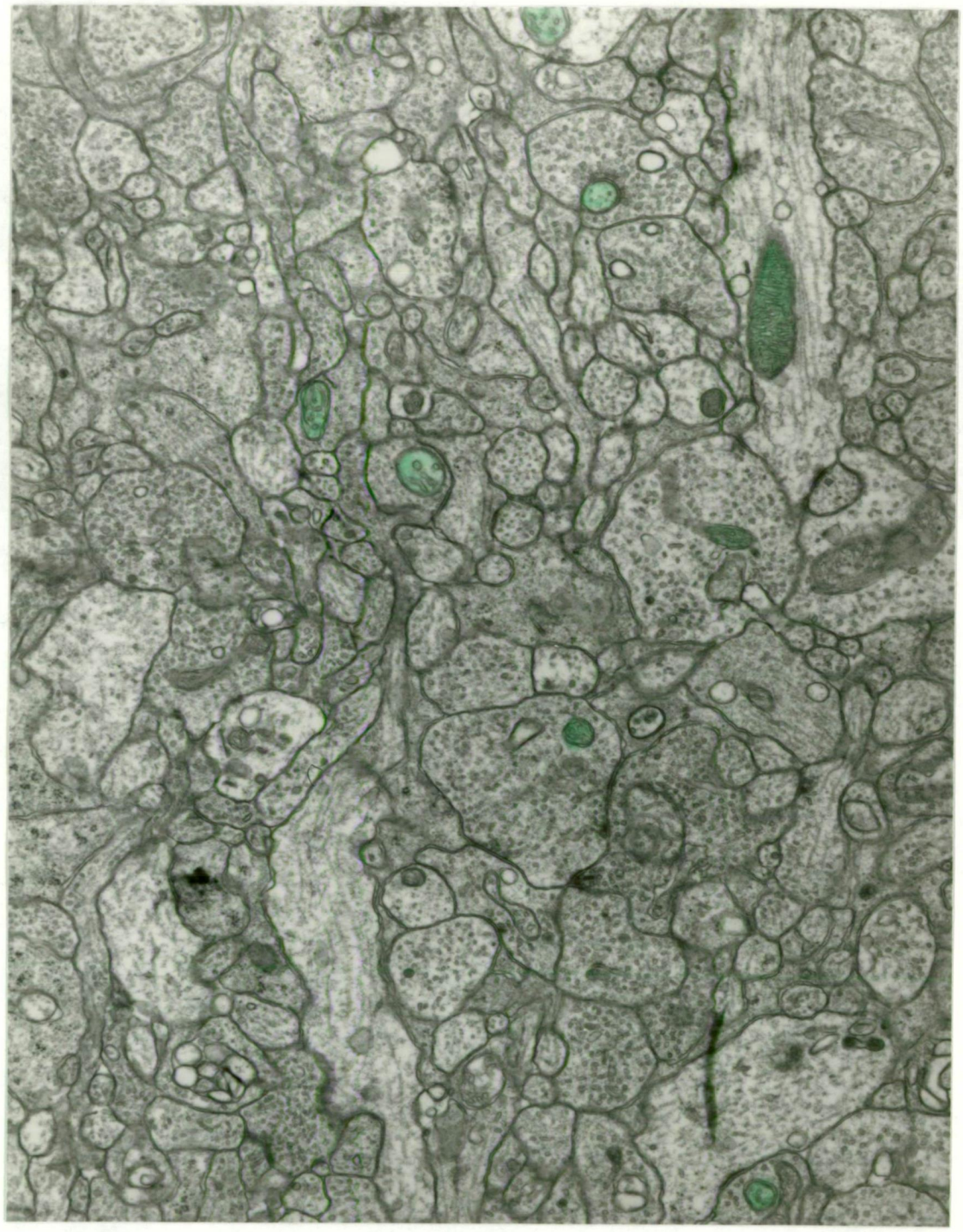

Figure 5.19: Possum inner plexiform layer

Ultrastructural appearance of the possum IPL. Mitochondria are scattered throughout the neuropil (coloured). The qualitative impression is that mitochondrial numbers are less than those in the quoll (Fig. 5.16). (No CO incubation).

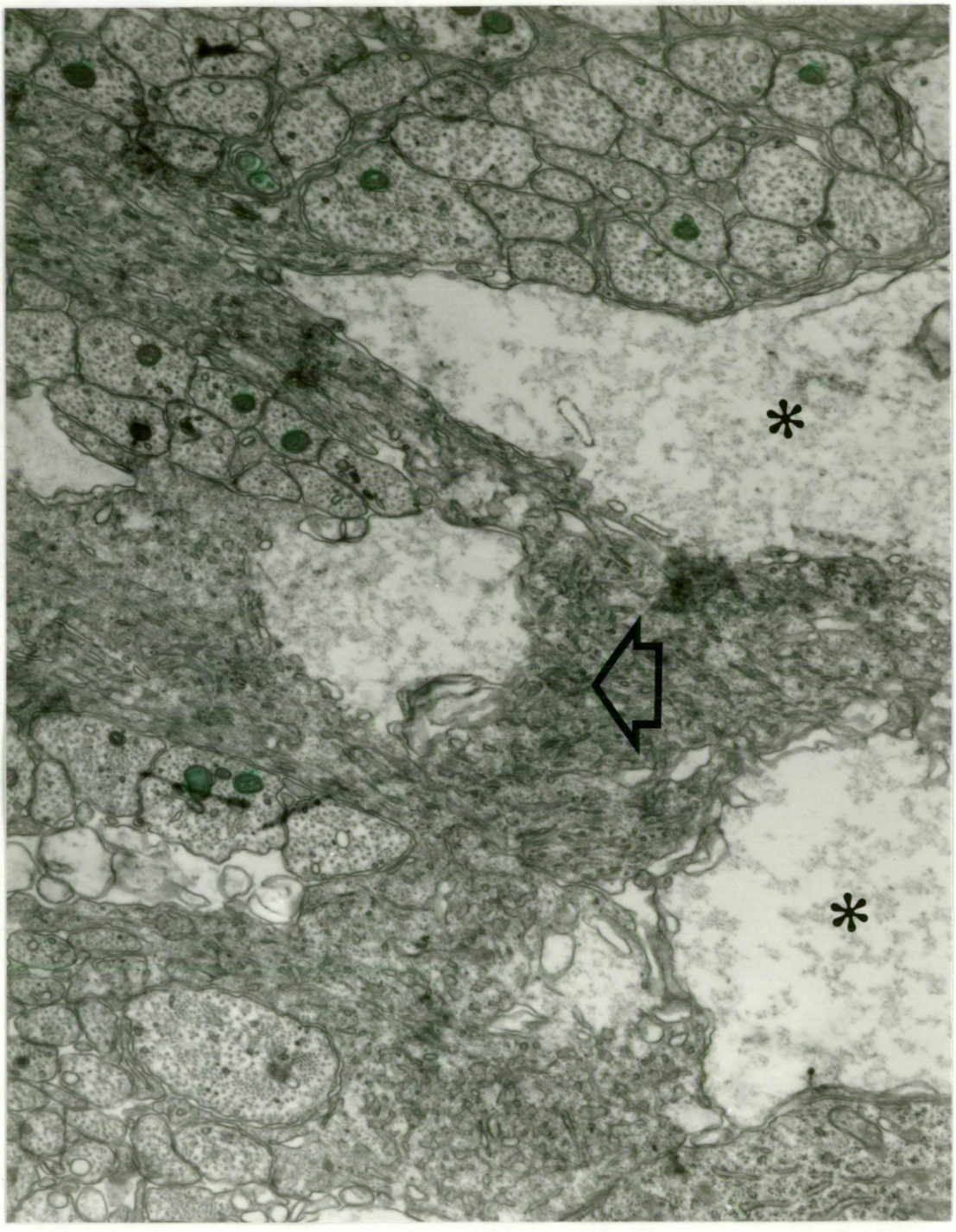

Figure 5.20: Possum ganglion cell and nerve fiber layer

Ultrastructural appearance of the possum GCL and NFL. Not the prominent Müller cell cytoplasm (arrow) with large void areas (*). There are small mitochondria present within the nerve fiber profiles (Coloured). These are not as numerous as seen in the quoll (Fig. 5.17). (No CO incubation).

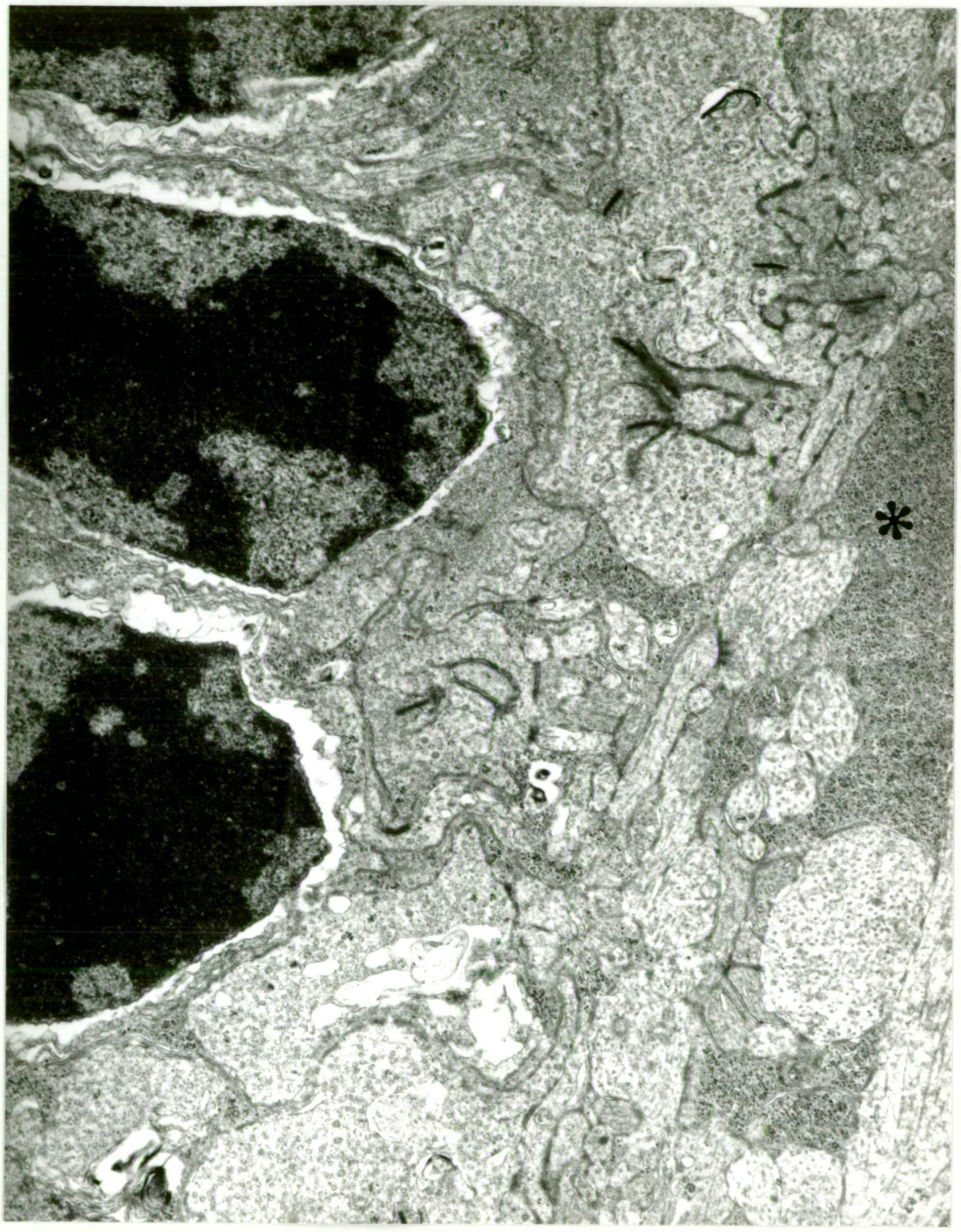

Figure 5.21: Guinea pig outer plexiform layer

Ultrastructural appearance of the guinea pig OPL. There is an absence of mitochondrial profiles within this layer. There is however, prominence of Müller cell cytoplasm (*). (No CO incubation).

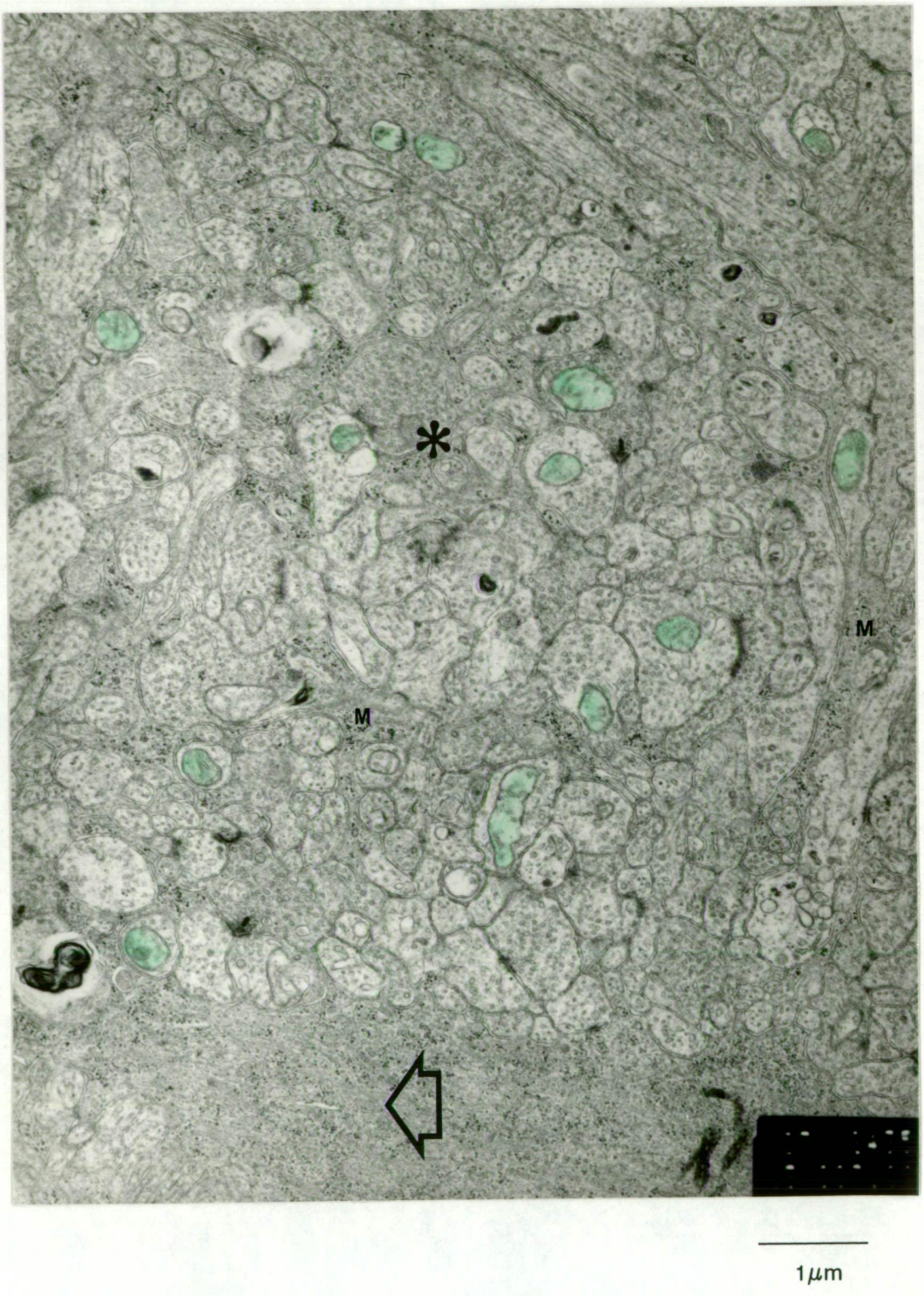

Figure 5.22: Guinea pig inner plexiform layer

Ultrastructural appearance of the guinea pig INL. There are mitochondria scattered through the synaptic regions. This sections shows prominent Müller cell profiles (M) between the neuropil (*) as well as the central cell body (arrow). (No CO incubation).

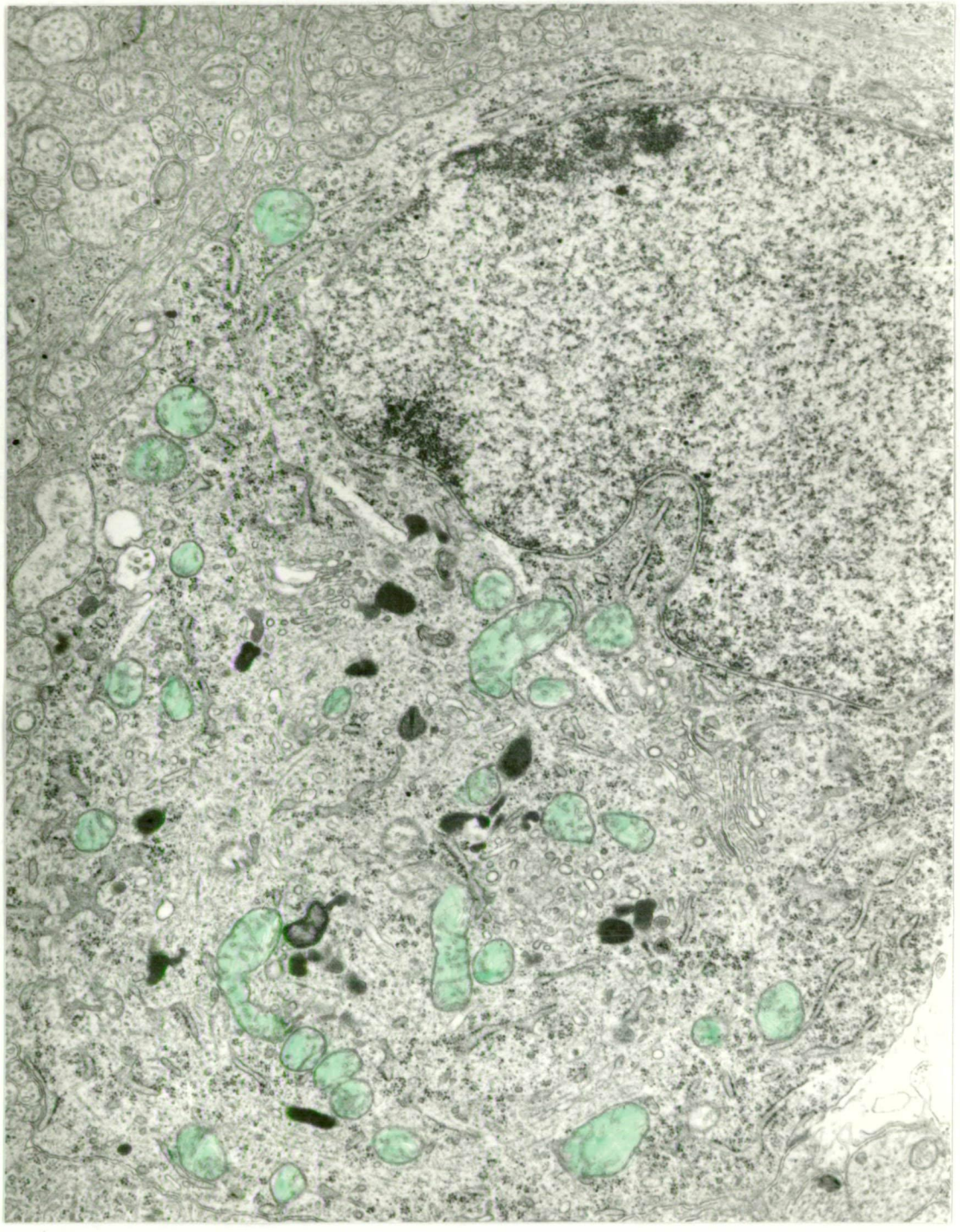

Figure 5.23: Guinea pig ganglion cell layer

Ultrastructural appearance of the GCL of the guinea pig. There are numerous mitochondria surrounding the cell body of the ganglion cell (coloured). (No CO incubation).

5.4 DISCUSSION

5.4.1 Histochemistry

Histochemical demonstration of enzyme activity is a useful approach to delination of the *in situ* location, and often the relative activity, of biochemical pathways and substrates (Barka 1988). Histochemistry is chemical anatomy, the combination of structural location with chemical function. As it lies at the boundry of many disciplines, it is not surprising that histochemistry has borrowed facets of immunology, physical sciences, analytical chemistry, biochemistry and morphology for its widespread application. In keeping with this service role the histochemical literature is weighted in favour of application and less so in favour of technique.

Nonetheless, there are well defined guidelines for the correct application of histochemical techniques and interpretation of the results. For quantitative use there should be adequate qualitative evidence for believing that the reaction is precise and specific. That is, the final reaction product should be deposited at the true site of activity (precision) and that it should reveal only that enzyme (specificity). In repeated trials the results should be reproducible and the amount of reaction product related to the activity or concentration of the enzyme (validity). For a thorough discussion of validation in quantitative histochemistry see Stoward (1980).

5.4.2. Approach to retinal metabolism: General comments

Retinal metabolism has been approached through a myriad of histochemical techniques. Microdissection (Dick 1984, Lowry et al. 1956, 1961, Ross and Godfrey 1985), *in vitro* incubation (Hansson 1971a, b), chemical histochemistry (Berkow and Patz 1961a, b, Cogan and Kuwabara 1959, Kuwabara and Cogan 1959, 1960b) and immunohistochemistry (for example, Akagi et al. 1984, Kumpulainen et al., 1983, Simurda and Wilson 1980, Wilkin and Wilson 1977) have all been used for delineation of metabolic intermediates and pathways. Of particular appeal when applying histochemical techniques to the retina is the laminar and orderly organisation which readily lends itself to comparative probing both one layer to another, and one species to another, in addition to the investigation of more intricate sublaminar organisation. Morphologic and metabolic compartmentation within the retina correlates well with its functional heterogeneity.

Many further studies have investigated retinal metabolites from the perspective of neurotransmitter location rather than the energetics of metabolism. The two perspectives overlap as many of the intermediates of energy metabolism are also neurotransmitters. For example, glutamate and aspartate are neurotransmitters, but also intermediates in the mitochondrial tricarboxylic acid cycle, and contribute energised substrate to the electron transport chain (see Bolz et al. 1985, Ross and Godfrey 1985).

The ease with which the retina is removed and a stable preparation made, have led some to approach metabolism, substrate utilisation and neurotransmission through more physiological *in vitro* methods (for example Ames and Nesbett 1981, Winkler 1975, 1981).

For this study, the simple histochemical approach of Seligman et al. (1968) has been employed to locate retinal CO activity. The emphasis in interpretation of results is from a general energetic viewpoint rather than the more usual application in determining functional neuronal classes.

5.4.3 Cytochrome oxidase histochemical technique

Cytochrome oxidase (cytochrome c oxidase: ferrocytochrome c: oxygen oxidoreductase, EC 1.9.3.1) is a complex of enzymes located in the inner mitochondrial membrane which catalyses the transfer of electrons from cytochrome c to oxygen. As the terminal event in the electron transport chain, this reaction consumes 90% of total oxygen uptake in most cells (Alberts et al. 1983). It might therefore be expected to be a good marker of oxidative metabolism.

Burstone (1959, 1960, 1962) popularised the histochemical location of CO using Nadi (**Na**phthol-**di**amine) reagents. The formation of a coloured indolamine from endogenous alpha-naphthol and a phenylenediamine is catalysed in the presence of oxygen and cytochrome oxidase (Kiernan 1981). The Nadi technique suffers from problems with diffusion of pigment, rapid fading, lipophilia and lack of specificity in some tissue (Bedetti 1985, Seligman et al. 1968). It is not suitable for electron microscopy (Seligman et al. 1968).

More accurate and precise is the histochemical method developed by Seligman et al. (1968), which produces a non-droplet reaction product, localised to the mitochondrial inner membrane. In the presence of exogenous, or sufficient residual endogenous cytochrome c, a bis-phenylene-diamine analog, 3,3'-diaminobenzidine (DAB), is polymerised to produce a reaction product which is visible at both light and electron microscopic levels.

The technique is well supported by information regarding fixation effects (Angermüller and Fahimi 1981), incubation conditions (Hoshino and Shannon 1979, Kugler et al. 1988), ultrastructural localisation of the reaction product (Nir and Pease 1974, Reith and Schüler 1972) and quantitative aspects (Frasch et al. 1978, Hiraoka et al. 1985, 1986, Kugler et al. 1988, Perotti et al. 1983).

An immunocytochemical approach has been described by Bedetti (1985), making this a useful technique where endogenous enzyme activity has previously been destroyed by prolonged fixation. Ultrastructural examination of the reaction product shows that is located at the inner mitochondrial membrane. Within the CNS, a comparative study of immunocytochemical and histochemical techniques has been performed, with good correlation of results (Hevner and Wong-Riley 1989).

5.4.4 CNS cytochrome oxidase histochemistry

Consideration of retinal structure and function can not be divorced from at least a cursory account of that within the central nervous system. Whilst the emphasis is weighted in favour of the retina in the following sections, the more general situtation within the CNS is also considered. Some of the observations have implications for the use of this technique in such broader applications.

5.4.4.a Cytochrome oxidase and chemoarchitecture

Cytochrome oxidase is one marker of electron transport chain activity and of aerobic energy production. Interest in this mitochondrial enzyme as a marker of metabolism within neural tissue, and hence as a means of identifying neuronal heterogeneity, has blossomed with the work of Wong-Riley (1976). This approach has been applied widely throughout the central nervous system in order to identify different subclasses of neurones, both at the light and electron microscopic level: for example, caudate nucleus (Difiglia et al. 1987), hippocampus (Kageyama and Wong-Riley 1982, Ribak 1981) and sensory cortex (Land and Simons 1985, Wong-Riley and Welt 1980).

However, most of the reports using CO histochemistry within the CNS relate to the visual system: for example, lateral geniculate nucleus (Kageyama and Wong-Riley 1985, 1986a, Kennedy et al. 1985, Lachica et al. 1987), optic tectum (Kageyama and Meyer 1988, Wiener, 1986), striate cortex (Carroll and Wong-Riley 1984, Horton and Hubel 1981, Kageyama and Wong-Riley 1986a, b, Kennedy et al. 1985 and others) and peristriate cortex (Rockland 1985,

Wong-Riley and Carroll 1984a). The popularity of the visual system is in part due to its ready accessibility, the already large body of background information which is already known about this orderly system and also due to the ease with which visual input may be experimentally manipulated. For examples of experimental manipulation and CO histochemistry see (Kageyama and Wong-Riley 1986c, Jen et al. 1989a, b, Sukekawa 1987, Wong-Riley and Carroll 1984b).

Hidden organisation within the visual system has often been revealed through CO histochemistry making this a useful chemoarchitectural tool. For example, "cytochrome oxidase patches" are seen in the primary visual cortex of many species (Horton and Hubel 1981), boundaries of association visual cortex may be discerned (Price 1985) and classes of darkly reactive neurones may be distinguished within the retina (Kageyama and Wong-Riley 1984, Land 1987, Li et al. 1989, Liu et al. 1985). In general, this technique has provided useful functional insights into the CNS. However, some care needs to be exercised in its interpretation.

5.4.4.b Interpretation of CO histochemistry

CO activity in this context is not being used to determine energy consumption *per se* but more for the understanding coding mechanisms in the nervous system. That is, a darkly staining neuron is interpreted as having more electrical activity than a lightly or non staining cell (Wong-Riley 1976). Implicit in the use of CO histochemistry for these purposes is the assumption that the metabolic differences are characterising differing functional groups of neurons. For most purposes this is most likely correct. Simplistically, it is assumed that most of the oxidative energy is used for maintenance of cellular membrane potentials, effectively being needed to supply the Na^+-K^+ ATPase membrane pumps (See Kageyama and Meyer 1988, Kageyama and Wong-Riley 1984, 1986b for discussion).

However, reduced activity need not imply reduced function, it may simply mean diminished supply of precursor substrates, ie, oxygen. Membrane pumps may well be supplied by other non-oxidative sources of energy. The inner retinal layers of the possum and guinea pig are deplete of CO (Figs. 5.4, 5.5). The level of Na^+-K^+ ATPase within the corresponding retinal layers of the guinea pig is known to be extensive (Ueno et al. 1984). Clearly, CO histochemistry is useful in chemically providing another means of architectural division of the nervous system with useful physiological implications. Although it can not be assumed that CO need correlate with energy consumption at the cell membrane (Na^+-K^+ ATPase), the evidence however in many situations is strong. Evidence may be summoned from the following observations. The CO activity at the level of the optic disc diminishes dramatically

(Fig. 5.3 and Kageyama and Wong-Riley 1984, Fig. 2G), the region where optic nerve fibers gain a myelin sheath. This correlates with lower energetic requirements for maintaining membrane equilibrium within myelinated nerves, that is, lower Na^+-K^+ ATPase requirements. This correlates with the 2-DG studies, another metabolic indicator of functional activity, within the optic nerve and retina (Bill 1985). CO and 2-DG have also been well correlated within the visual cortex of the monkey (Horton and Hubel, 1980). Similarly, when a pathway is deafferented the CO activity is reduced (Wong-Riley et al. 1978), presumptive evidence of a CO and Na^+-K^+ ATPase association.

The significance of the regional differences in histochemical CO distribution has been addressed by others. Variation in CO activity could be due to differences in activity or differences in amount of enzyme. CO activity determined by two different techniques within the CNS, one histochemical and the other immunohistochemical, correlate well, suggesting that variation is due to enzyme amount. This adds further weight to the accuracy of the microscopic histochemical patterns of staining reflecting functional CO activity (Hevner and Wong-Riley 1989).

Despite this information suggesting that CO histochemical results are mostly signifying functional membrane activity, the definitive study correlating Na^+-K^+ ATPase and CO still needs to be performed, particularly in light of the results of this study. The avascular retinal CO situation may be unique.

5.4.4.c Some comments on ultrastructural CO location

Considerable effort has been employed in characterising, at the electron microscopic level, the patterns of CO reaction product density within axons, dendrites and neural cytoplasm (Kageyama and Wong-Riley 1982, 1984, 1985, 1986b, 1986c). Heterogenous staining of mitochondria is seen, with some showing no CO reaction product whatsoever (Fig. 5.15). Homogenous staining of histochemical CO has been reported in heart and pancreas (Anderson et al. 1975, Perotti et al. 1983) and with immunocytochemical techniques in other tissues (Bedetti 1985). In at least some respects CO heterogeneity may be technique related. For example, all mitochondria within some areas of the CNS do stain (to variable degrees) when using cryostat sections, acetone and preincubation, to enhance tissue penetration of reagents (Kugler et al. 1988). Similar variable staining of another mitochondrial enzyme, succinate dehydrogenase, is also seen when membrane premeability has been altered by cell damage (Acosta and Wenzel 1975).

However, variation in penetration of reagents as a limiting factor in demonstrating activity still may have physiological significance. Mitochondrial structure varies with energisation and cellular respiration, an often neglected observation. Both an active "condensed" form and the more often portrayed "orthodox" configuration can be demonstrated under differing levels of oxidative load and preparation conditions (Hackenbrock 1966, 1968a, b, Hackenbrock et al. 1971, Hayat 1981, Knoll and Brdiczka 1983, Smith and Ord, 1983). Some, however, have claimed that these conformational difference are an artefact of preparation (Candipan and Sjöstrand 1984). Nonetheless, with energisation, mitochondrial membrane properties and porosity do change (Kamo et al. 1976, Sambasivarao and Sitaramam 1985). Variable CO staining may be reflecting variable activity levels through differences in energisation. Permability to reagents may reflect at least some of these differences. Some caution needs to be exercised in interpreting ultrastructural CO appearances.

5.4.5 Retinal cytochrome oxidase histochemistry

5.4.5.a Literature review

Earlier studies using the Nadi type reagents are less reliable. Using this method the retinal CO pattern has been reported for rats, mice, frogs, rabbits and guinea pigs (Eränkö et al. 1961, Niemi and Merenmies 1961b). Somewhat at variance with other reports, these studies have shown maximal activity in the *outer* segments of the photoreceptors. Species with avascular retinae showed diminished (but present) reaction product in the vitread retinal layers. A related paper has reported the absence of activity of another mitochondrial enzyme, succinate dehydrogenase, in the inner layers of avascular retinae (Niemi and Merenmies 1961a). The report of Berkow and Patz (1961a) in dogs, rabbits, guinea pigs, rats and other species indicated that the CO reaction product is limited to the *inner* segments of the photoreceptors with little deposit elsewhere, irrespective of the species, a further confusing observation. These earlier studies, whilst providing information to suggest that the retina is variable in its oxidative capacity, both within differing retinal layers, and from one species to another, present some contradictory details. The discrepancies are most likely related to the technique employed.

Using the modified Seligman technique (Seligman et al. 1968), most vascular mammalian retinae have been shown to conform to a similar CO cross sectional staining pattern. The greatest activity is seen in the mitochondria dense photoreceptor ellipsoid followed by the syanaptic layers, nerve fiber layer and ganglion cell layer. Recently, the retinal pattern has been reported for rats (Land 1987), mice (Liu et al. 1984) cats (Bolz et al. 1985, Kageyama

and Wong-Riley 1984), ferrets (Kageyama and Wong-Riley 1984), squirrel monkeys (Kageyama and Wong-Riley 1984), golden hamsters (Liu et al. 1985) and tree shrews (Wong-Riley and Norton 1988). The CO activity of the neighbouring RPE has been reported in rats (Caldwell and Slapnick 1989). Amongst non-mammals, a similar cross sectional profile has been reported for goldfish (Kageyama and Meyer 1988). Many of these reports also indicate that in whole mount preparations subclasses of ganglion cells stain intensely making this a useful adjunct to delineation of retinal cell subclasses (Kageyama and Wong-Riley 1984, Land 1987, Li et al. 1989, Liu et al. 1985).

No recent report of CO activity in avascular retinal species is available. Similarly there are no reports of CO within marsupial retinae or CNS. Therefore a analysis of marsupial findings, and a reanalysis of earlier reports for avascular species, is timely.

5.4.5.b Incubation conditions and regional variation

Before meaningful conclusions may be drawn about the differences between the vascular and avascular species it is necessary to ensure that the results have not been artefactually influenced by the regional and diurnal sampling errors or incorrect incubation conditions.

One explanation for the dramatic difference in CO activity between vascular and avascular species may have been diurnal variations in enzyme activity. It is known that deafferentation through removal of sensory stimulus or blockade of neural transmission through the application of the Na^+ channel blocker tetrodotoxin (TTX), produces reduction in CO activity (Kageyama and Wong-Riley 1986c, Land 1987, Sukekawa 1987, Wong-Riley, *et al* 1978, Wong-Riley acnd Carroll 1984, Wong-Riley and Norton 1988, Wong-Riley and Riley 1983, Wong-Riley and Welt 1980). Subtle changes in activity may be seen in the lateral geniculate nucleus as early as 1 day following intravitreal injection of TTX (Wong-Riley and Carroll 1984). A physiological variant upon the theme of functional deafferentation is the normal diurnal alteration in light exposure and therefore in retinal neural activity. Could CO activity be cycling in keeping with diurnal neourotransmission?

The results of this pilot study do not suggest that the dramatic differences in activity between vascular and avascular species can be accounted for by diurnal or light-dark sampling difference. There is little variation in activity irrespective of sampling time in both the vascular rat and avascular possum (Figs. 5.12). The investigation was not pursued further as the results answered the question under scrutiny. The results do not however, preclude subtle cycling of enzyme activity throughout normal light dark exposure. Larger scale metabolic rhythmic activity is well known for photoreceptor outer segments, which are shed selectively

through the light dark cycle (Besharse 1982, Herman and Steinberg 1982). Smaller scale lysosomal diurnal variation in enzyme levels has been reported in both the retina and pineal body (Vaughan et al. 1987). It would not be surprising to see variation in retinal CO, either in absolute amounts or by redistribution of sublaminar activity, with light and dark exposure. More refined techniques, for example thin section histochemistry or ultrastructural analysis, would be necessary to show any such changes.

Regional variation in CO activity is known within the retina. There is a population of darkly staining ganglion cells in the temporal retina of rats (Land 1987), and the temporal retina of neonatal hamsters is known to show more intense CO staining in transverse cross section than the nasal side (Wikler et al. 1985). How great are those differences and could a sampling artefact account for the low activity seen in the avascular species? Any regional differences seen are subtle (Fig. 5.11). The only area where CO activity diminished markedly was in the region of the optic disc.

The time course of the CO reaction became important when the differences between vascular and avascular species were discovered. In making quantitative or qualitative comparisons of CO activity, there is a need to optimise the incubation time. If too long, then some areas will saturate (Figs. 5.9, 5.10). Less active areas will continue to increase in density approaching the more active areas thus producing false impressions of the relative metabolic importance. If too short, then some areas will not have developed reaction product and false assumptions about inactivity will be made (Figs. 5.4, 5.5). These comments apply to the use of CO throughout the CNS, where comparisons about relative activity are often being made.

Having determined that the correct incubation time has been employed, it may be seen that the activity of the photoreceptor inner segment of the vascular species is around twice that of the inner retina in vascular species. Compare this result with the darkly stained Figure 7 of Land (1987), where all synaptic layers show similar levels of CO activity. The comparison of vascular and avascular species under the same conditions (optimal for the vascular rat retina, Figs. 5.9, 5.10) shows a real difference in activity which is not artefactually influenced by inappropriate incubation times (Figs. 5.6, 5.7).

5.4.5.c Cross sectional profiles

Vascular mammalian retinae investigated have laminated CO distribution and, when compared with avascular species, display greater activity of enzyme within the vitread layers. In vascular retinae, the location of deposit mirrors the known qualitative pattern of

mitochondrial distribution within the retina (Hogan et al. 1971). Nuclear layers display less CO activity than do synaptic and fiber layers.

Where quantitative data is reported (tree shrews, Wong-Riley and Norton 1988), the retinal cross sectional pattern resembles that seen in rats (Fig. 5.10). The pattern is also similar to that reported for other aerobic enzymes in vascular retinae; rat malate dehydrogenase (MDH) and aspartate aminotransferase (Ross and Godfrey 1985) and monkey MDH (Lowry et al. 1956).

Contrary to previous reports (Niemi and Merenmies 1961b), the outer segment shows no CO staining but rather the reaction product is restricted to the inner photoreceptor segment. The ellipsoid of the photoreceptor inner segment is rich in mitochondria in keeping with known high oxygen and energy usage required for maintenance of cell membrane potential in the area (Alberts et al. 1983, Alder et al. 1983, Linsenmeier 1986, Saari 1987). The high CO activity mirrors the clustering of other oxidative enzymes in this region, irrespective of retinal vascularity (Dick 1984, Lowry et al. 1956, Ross and Godfrey 1985). This suggest a common metabolic strategy in this retinal region.

Teleologically, mitochondrial clustering in the ellipsoid explains the large choroidal blood flow. High blood flow is able to achieve high choroidal tissue oxygenation providing the necessary oxygen diffusion gradient for the large mitochondrial oxygen sink. Mitochondrial aggregation is known to increase the oxygen concentration required for respiration dramatically (Jones 1984). Ultimately, the vascular arrangements and mitochondrial clustering are contingent upon the high metabolic needs of the area. Why these needs should be so high is obscure. Perhaps high metabolic demand and or mitochondrial clustering may offer some functional advantage for the detection of light or simply be an ontogenetic remnant, reflecting the cilia like origin of photoreceptors.

CO activity in the IPL in rats has been reported to be greater in the external sublamina a, the "off" center receptive field region known in other animals (Land 1987). Surprisingly, the results reported here do not necessarily support that finding. The rat IPL shown, if anything, has greater activity in the inner sublamina b (Fig. 5.1), whilst the quoll IPL is more uniformly stained (Fig. 5.2). A careful reappraisal of the IPL sublamination with particular regard to light and dark exposure prior to fixation would be desirable.

The metabolic energy production strategy varies within the inner retina. The histochemical results presented here support the hypothesis that there is low oxidative energy metabolism within the inner avascular retinal layers of guinea pigs and possums. Further evidence in

support of low oxygen levels within the inner retina may be summoned from elsewhere. Linsenmeier (1986) has calculated that during light adaption around one half, and during dark exposure, one quarter of the cat's 200-250μm thick (vascular) retina can be supplied by the choroidal oxygen alone. Assuming similarity of choroidal supply and oxygen diffusion properties in vascular and avascular species, this result gives some measure of the retinal territory that choroidal oxygen might be expected to reach. That is, less than 100μm, and more likely, closer to 60μm, of the outer retina would be expected distances for oxygen to travel from the choroid. Given that retinal dimensions in avascular species are thicker than this at 140-170μm (Chapter 4), then it is likely that oxygen levels are low within the avascular vitread layers, beyond the 30-40μm distance of the ellipsoid mitochondrial cluster from the choroid. The histochemical results suggest that there is still some CO activity though, implying oxygen availability, at this remove form the choroid in avascular species. This may be a true reflection of metabolic activity, in the presence of extremely low oxygen levels, or an artefact of *in vitro* incubation, indicating only the *potential* of the tissue for respiration. Perhaps there may be some supplemental oxygen supply, for example through the vitreous or through a retinal "tissue carrier" (Longmuir and Sun 1970). One final possibility for the NFL CO staining is that it could be staining mitochondria which are not contributing to energy production within the retina, but are in axoplasmic transit along the ganglion cell axons destined for more distal sites. The ultimate answer to the question of oxidative capacity within avascular retinae is reliant upon an *in vivo* study of the oxygen profile.

5.4.5.d CO histochemistry in context of overall energy pathways

The ultimate currency of energy transfer and usage is ATP. It may be produced through glycolysis in small amounts, or in larger quantities through the oxidation of energy intermediates, NADH and FADH, in the electron transport chain (Stryer 1981). The simple hypothesis within avascular retine is that, (1), glycolytic (anaerobic) production of energy and lactate predominates. This is a consequence of, (2), limited oxygen supply, an essential ingredient for oxidative phosphorylation of ATP (electron transport chain). A further assumption, (3), is that the total amount of energy required for homeostasis and neurotransmission is similar within both retinal types. What evidence is there to support this simple schema?

(1) Anaerobic metabolism

Where oxidative metabolism is low then anaerobic metabolism ought to be high for the same end level of energy consumption. This is a reasonable assumption. Histochemical studies report high levels of anaerobic metabolism within inner layers of the avascular rabbit,

mudpuppy and guinea pig retinae (Cogan and Kuwabara 1959, Dick 1984, Eränkö et al. 1961, Lowry et al. 1956).

Rabbit *in vitro* results indicate that glucose is consumed in the inner retina (Ames and Nesbett 1981). This animal has a merangiotic retina with vasculature only along the horizontal medullated nerve fiber layer. Most of the retina is avascular and the results may be applicable to anangiotic retinae. Oxygen consumption changes with light or dark exposure in keeping with known large photoreceptor requirements, whilst the 2-deoxyglucose (2-DG) consumption remains constant under these conditions. Conversely, when synaptic transmission is blocked (inner retinal layer activity), then 2-DG consumption falls suggesting glycolytic predominance within the rabbit inner retina. However, this does not show conclusively that non-oxidative metabolism is lacking, but rather that glucose consumption is high.

Electrophysiological studies in the rabbit further suggest that there is a degree of independence from oxygen within the inner retina. Anoxia produces changes within the receptor driven a-wave of the electroretinogram (ERG) prior to any changes in the inner retinal b-wave potential. This is the reverse of the pattern seen in the vascular retinae of the cat, man, rat and monkey under anoxic conditions, where the a-wave potential is more resistant to anoxia and the post receptor b-wave is lost early (Noell 1959, Wilkus et al. 1972).

One of the hallmarks of retinal metabolism is the need for glucose irrespective of retinal vascularity (Winkler 1981), and active anaerobic pathways are also found in vascular retinae. One enzymatic marker for anaerobic metabolism is lactate dehydrogenase, LDH. Lactate production and LDH activity are high, even in the presence of oxygen, the so called Warburg effect (Graymore, 1969, Warburg, 1929, Winkler, 1989). Normally, high oxygen inhibits lactate production, the Pasteur effect, but not so in the retina, whether vascular or avascular (Saari 1987). In keeping with this unusual functional role, the isoenzyme of LDH found in retinae is uncommon and bears a resemblance to that seen in embryonic tissue and tumours (Saavedra and Anderson 1983). Why should vascular retinae also need anaerobic energy supply? Areas which are anoxic most likely exist within vascular retina (Linsenmeier 1986, Winkler 1981). Thus, while avascular retinae have high anaerobic potential, so too do vascular retinae.

(2) CO and mitochondrial numbers, form and function

The results presented here support the contention that oxygen dependent metabolism is limited in the inner retinal layers. This is consistent with known patterns of other enzyme distribution in avascular species. The tricarboxylic acid enzymes, succinate dehydrogenase

and MDH, are involved in providing reduced intermediates for the electron transport chain. The level of these enzymes is low in avascular inner retinae (Eränkö et al. 1961, Lowry et al. 1956, Wislocki and Sidman, 1954).

Diminished CO could be due to either reduced mitochondrial numbers or reduced enzymatic activity or both. The initial impression regarding mitochondrial numbers is that they are marginally reduced (cf Figs. 5.16 and 5.19 with 5.22). Clearly, quantification is necessary. Reduction in retinal mitochondrial numbers is seen within the retina elsewhere. The pigeon retina, vitread to the ellipsoid, is devoid of mitochondria altogether (Hughes et al. 1972).

Not only absolute mitochondrial numbers but also mitochondrial structure serves as a guide to functonal regional metabolism. For example, the arrangement and density of cristae within mitochondria is usually correlated with the cell's energy requirements (James and Meek 1979). Differing mitochondrial phenotypes with differing metabolic activity are seen elsewhere within the CNS (Lai et al. 1977, 1985, Pysh and Khan 1972, Tolani and Talwar 1963). As yet, little is known about heterogeneity of retinal mitochondria.

Developmental changes occur in mitochondria and associated enzymes through oogenesis, spermatogenesis, embryogenesis and the neonatal period (Bawa and Werner 1988, Etingof and Shukolyukov 1965, Miki et al. 1988, Nogawa et al. 1988, Sellinger and Santiago 1972). Significant developmental change in metabolism and energy consumption has been reported in rabbit and rat retinae (Berkow and Patz 1964, Cohen and Noell 1960). Changes in retinal enzyme function may preceed morphologic differentiation. Within the developing chick retina, there is early broad distribution of mitochondria throughout the retina. Subsequently, oxidative metabolism diminishes, anaerobic activity predominates and mitochondria segregate and convert into pro-mitochondria (Buono and Sheffield 1989).

Alternatively, mitochondria need not be metabolically active. Cytochrome oxidase may just be switched off, as is known for sea urchin eggs prior to fertilisation (Maggio and Monroy 1959, Pollack and Sutton 1980). Polyanionic molecules are known to inhibit beef heart CO reversibly (Person and Fine 1960).

At the other end of the development scale, mitochondrial function is known to decrease with age, and mitochondrial DNA mutations have been postulated as a cause for aging and degenerative disease (Linnane et al. 1989, Trounce et al. 1989).

Mitochondria have functions other than energy production. Some mitochondria may have little or no interest in oxidative phosphorylation, but may be metabolising along other pathways. For example, a role as a store for intracellular ions, proteins and substrates, and hence as regulator of neurotransmission has been postulated for neural mitochondria (Abood 1969). The picture being painted for mitochondrial function is very much more complex than has been thought in the past (Yaffe and Schatz 1984).

What exactly the mitochondria within the the inner layers of avascular species are doing remains uncertain. They may represent metabolically inactive forms, organelles with little (but some) oxidative capacity or they may be present merely to provide the other non-oxidative mitochondrial functions.

(3) Overall energy consumption

The third aspect of the simple model is the overall energy usage. A reasonable assumption is that most of the energy required within the retina is used for membrane maintenance, predominantly through the activity of Na^+-K^+ ATPase (Wong-Riley 1989). Within the inner retinal layers of the guinea pig this enzyme is present in substantial amounts (Ueno et al. 1981, 1984). A laminar distribution has also been reported using immunohistochemical techniques in the rat (Stahl and Baskin, 1984). This is suggestive that, despite limited oxidative capacity within the inner layers of avascular retinae, the end product of energy consumption is the same as in vascular species.

This model also assumes an adequate supply of substrate for anaerobic metabolism. If oxygen is limited in the inner layers, so too may be glucose. The ready supply of glycogen in avascular retinae has been postulated as a means of overcoming this limitation (Chase 1982). Equally, metabolic wastes produced under this model must be adequately dealt with. High levels of lactate in the inner retina could provide a diffusion gradient for its removal through the choroid. This assumes that lactate does not produce metabolic substate inhibition of LDH. Despite the many unanswered aspects, this model provides a useful starting point for the consideration of metabolism within avascular retinae.

5.5 CONCLUSIONS

1. Retinal cytochrome oxidase activity is a useful marker of oxidative metabolism. Its level is very much reduced within the inner retinal layers of avascular retinae. Na^+-K^+ ATPase is known to be high in these regions, suggesting that anaerobic metabolism is prominent in energy production.

2. Photoreceptor CO levels are similar in all species examined. Its densitometric intensity in vascular species is around twice that seen in the synaptic layers.

3. The use of CO as a marker of neuronal activity requires careful interpretation. Low levels of activity need not mean low energy production and low membrane activity (Na^+-K^+ ATPase).

4. Mitochondria are present in avascular inner retinal layers though probably fewer in number than in vascular species. The OPL synaptic terminals are devoid of mitochondrial profiles altogether in the avascular retinae examined.

5. The differences in energy pathways amongst species highlights the care which must be taken in extrapolating metabolic results from one species to another.

CHAPTER 6

CONCLUSIONS AND FUTURE DIRECTIONS.

"This is not the end. It is not even the beginning of the end.
But it is, perhaps, the end of the beginning".
....Winston Churchill

This chapter links the previous experimental work into a more unified story, and offers explanation for the paradoxical arrangements in retinae without intrinsic blood vessels. Based upon available evidence, functional conclusions have been drawn about how well animals with avascular retinae are able to see. The findings of this study have merely laid the foundations for an appreciation of retinal avascularity. This appreciation is important as many clinical afflictions have their basis in vascular abnormalities with devastating effects upon vision. Many intriguing and unanswered aspects of retinal metabolism, vascularity and function still remain and are discusssed with an emphasis on proposed future directions of study. The problem of retinal avascularity still remains a conundrum. This study poses more questions than it is able to answer.

6.1 The requirements of ocular nutrition

There are opposing functional demands placed upon the structure of the eye. On one hand there is the need for optical clarity for the detection of light, whilst on the other, there are large energy requirements for the complex metabolic machinery needed to detect and code light with high degree of resolution. This latter aspect necessitates an adequate nutritional supply, either directly from the blood supply or in some modified, less direct, form. The presence of opaque vessels along the optical axis would degrade the quality of the optical image, so nature has provided a number of ingenious solutions to keep the visual axis clear. Whilst many of the solutions are a constant comparative feature, many are peculiar indicating that a number of different solutions have been used to solve the same problem. Constant amongst higher order animals is the presence of optically clear refracting surfaces with low metabolic demands (lens and cornea). These are nourished by a clear percolating blood filtrate, the aqueous. This, together with the vitreous, serves to distend the eye and maintain constant intraocular pressure.

Prominent in the variability with which the problem of detection of light has been approached is the location and nature of blood supply to the retina. An external choroidal blood supply is

constant, but intraretinal supply is variable both in its presence or absence, and when present, in its organisation. The absence of intrinsic retinal vasculature altogether is yet another added pressure placed upon already demanding nutritional arrangements within the eye.

6.2 The questions ... and some answers

At the centre of this dissertation is the question of how retinae without an intrinsic retinal supply are able to function. Pathological loss of retinal vessels in normally vascular species leads to infarction of the inner retina (Yanoff and Fine 1988), yet physiological avascularity is most likely compatible with adequate visual function. Are the retinae of avascular species structurally different? Are avascular retinae limited in thickness? Is the choroidal supply adapted to provide all the nutritional needs of the retina, or are there supplemental nourishment pathways? If, because of distance from the carrier supply, oxygen is limited within the retina, is there a reliance upon alternative non-oxidative energy pathways?

6.2.1 Retinal and choroidal organisation

I have been able to document some of the variability in retinal nutritional arrangements, particularly among the marsupials which, as do placental mammals, provide a convenient dichotomy in retinal vascularisation. Supporting earlier reports (Johnson 1901, 1968) the possum and sugar glider, representatives of the diprotodont marsupial line, possess avascular retinae, and the quoll, Tasmanian devil and Viginia opossum, which derive from the polyprotodont lineage, have vascular retinae. These retinae have been compared with those of the placental guinea pig (avascular retina) and vascular laboratory rat (vascular retina). The aspects investigated in this study would suggest common coping strategies in both placental and marsupial avascular retinae. This offers some support for extrapolation of complementary data from other avascular species in order to piece together the jigsaw of function within avascular retinae.

6.2.1.a Retinal organisation

Apart from lacking intraretinal vessels and some limitation in thickness of all intraretinal layers, the avascular retinae investigated are structurally similar to their vascular counterparts. While most differences are small, the greatest difference in intralaminar thickness is seen in the inner plexiform layer, the synaptic region furthest form the choroidal blood supply. Vascular retinae may be thicker than 200μm but true avascular retinae are usually less than 170μm in transverse dimension, a figure somewhat greater than the 143μm limit previously proposed

(Chase 1982). The pattern of intraretinal lamination is similar in both groups of retinae. Where differences do exist, the avascular retinae of the guinea pig and possum differ more from each other than does that of the possum from either of the two vascular species. The guinea pig retina has fewer nuclei in the outer nuclear layer and a coarser photoreceptor grain than that of the possum. While these observations have clear implications for visual performance, differences must be sought to explain the nutritive coping mechanisms of avascular retinae.

6.2.1.b Choroidal organisation

On purely morphological grounds, the vascular structure of the choroid appears not to offer any added nutritional benefit in avascular species. The avascular retinae of possums and guinea pigs is most likely one in which the intraretinal vessels are simply absent, and the entire retinal nutritional supply derives from an unmodified choroid. The choroidal supply is similarly arranged in both groups, with an outer layer of large draining and feeding vessels supplying short branches to the sinusoid-like choroidal lake, the choriocapillaris. Minor structural differences are seen in the way in which the arterial supply arises from the long and short posterior ciliary vessels and the accomodation of a reflecting choroidal tapetum between the outer and inner choroidal vascular layers. A tapetum located either within the retinal epithelium or choroid may be found, although by no means universally, in vascular species (Virginia opossum and quoll) but not in the Tasmania devil. The possum's retina, which relies wholly upon the choroid for its nourishment, has only pigment variation within the retinal epithelium but has no tapetum. A true tapetum within the choroid would intervene between the supplying vessels and choriocapillaris and presumably limit perfusion gradients, and hence diffusion capacity into the retina. There is no structural evidence of choroidal projections into the retina as seen in bats (Pedlar and Tilley 1969), nor oxygen concentrating specialisations within the choroidal circulation as seen in some fish (Copeland 1974, 1976, Desrochers et al. 1985).

Indirect suggestion of the reliance of avascular species upon the choroid may be gained from manipulative studies in the (mostly avascular) rabbit retina. Occlusion of the posterior ciliary vessels leads to rapid loss of glycogen from the whole retina. Posterior ciliary vascular occlusion in the monkey retina leads only to loss of glycogen from the retina sclerad to the outer limiting membrane (Mizuno and Sato 1975). Unfortunately this procedure is unable to localise exactly the source of nourishment as not only is the choroid implicated, but also anterior uveal structures supplied by the ciliary vessels (ciliary body and iris). It therefore does not preclude a trans-vitreal supply. This method indirectly localises the nutritional route of the rabbit and monkey retinae not so much by the detection of nutrients but rather by the loss of an intraretinal metabolite.

6.2.2 Other nourishment pathways?

Inner retinal nourishment via the vitreous is seen in birds (Meyer 1977) and some reptiles (Cole 1974). To facilitate the dispersion of nutrients by this route, the vitreous in many birds is structurally adapted with a fluid consistency throughout much of the cavity (Cole 1974). The frequent saccadic movements of the eye most likely further aids the dissemination of nutrients through the vitreous (Pettigrew et al. 1990). Production of a more fluid vitreous in cats following surgical vitrectomy increases the previtreal oxygen tension, perhaps through greater supply oxygen supply from the ciliary body (Stefánsson et al. 1990). The possum does possess a small "avian like" optic disc projection but this is small and, unlike the avian pecten, is fluorescein impermeable. In preparing wholemounts the vitreous of the avascular species was found to be viscid throughout the entire posterior segment of the eye, and no different from vascular species. This disc projection in marsupials is unlikey to be a major contributor to retinal nourishment, except possibly in the immediate vicinity of the optic disc.

Trans-vitreal flow from the ciliary body is also unlikely as the ciliary body vasculature shows no special morphologic arrangement in avascular species. The static measurement of the constituents of vitreous show no consistent difference between vascular and avascular species, apart from lower levels of in intravitreal oxygen levels in avascular species (see Cole 1974 for table). These figures do not exclude dynamic differences in vitreal composition, but nonetheless would suggest that this route is unlikely to be significant in inner retinal nutritional supply. This further supports the hypothesis that the avascular species are dependent wholly upon the choroid for nutrition, the choroid being structurally similar in both types of retinae.

6.2.3 Oxygen supply and metabolic strategy

There appear, however, to be major differences in energy metabolism within avascular retinae. To a common distance from the choroid in both vascular and avascular retinae, oxidative energy metabolism (as measured by cytochrome oxidase activity) is similar, but beyond this, the level of this enzyme is very much less in avascular species.

6.2.3.a Outer retinal metabolism

Up to 30-40μm from the choroidal blood supply (photoreceptor ellipsoid) the oxidative capacity as measured by cytochrome oxidase histochemistry, is the same in all retinae examined. This is close to the half intercapillary distance found in brain white matter, 26μm, and greater than the 12μm distance reported in cerebral cortex (Crone and Levitt, 1984), tissues which might be expected to have similar metabolic arrangements and diffusion properties. This distance most likely represents the typical oxygen diffusion distance for

neurological tissue, a figure which may be similar in retina. Further factors warrant consideration in determining oxygen delivery within the retina, especially to the outer retina. Firstly, the choroidal flow is not representative of CNS blood flow, being very much higher, and hence allowing greater oxygen extraction and provision for larger diffusion distances (Linsenmeier 1986). This is offset by the massive oxygen sink which is produced by the dense packing of mitochondria in the photoreceptor ellipsoid (Steinberg 1987). This region contains an estimated 90% of the total retinal mitochondrial population (Flower et al. 1984). As a direct consequence of this clustering, an increase in oxygen concentration is required for adequate mitochondrial respiration (Jones 1984). This would likely offset any potential gain for inner retinal oxygenation from high choroidal blood flow and oxygen extraction. The mitochondrial clustering and high choroidal flow are most likely matched to the energy demands of the photoreceptors, irrespective of retinal vascularity. Estimates based on frog *in vitro* preparations suggest that two thirds of total retinal oxygen utilization is accounted for by the RPE-photoreceptror complex (Weiter and Zuckerman 1980, Zuckerman and Weiter 1980). Oxygen utilisation is in keeping with the known high energy requirements of this region for maintenance of membrane potential (Saari 1987). The photoreceptor region thus acts as a gate to diffusion of oxygen to the inner retina masking the availability of choroidal oxygen (Flower et al. 1984). This gate may be opened by limiting photoreceptor oxygen consumption, for example, by retinal photocoagulation (Weiter and Zuckerman 1980). Partial opening of this gate occurs physiologically during light adaptation when photoreceptor energy requirements diminish by around 50% (Linsenmeier 1986, Zuckerman and Weiter 1980). This however would be insufficient to supply high oxygen levels throughout all the retina from the choroid alone. In the vascular cat retina it has been estimated that under the limiting circumstance of dark adaptation (gate closed) only the outer 30% of retina may be supplied by choroidal oxygen (Linsenmeier 1986).

6.2.3.b Inner retinal metabolism and oxygen levels

A plausible hypothesis is that oxygen levels are low beyond 30-40μm from the choroid in avascular species. Experimental evidence may be summoned to support this proposal. In the absence of information about oxygen delivery in avascular species qualified extrapolation of oxygen profiles from vascular species will be used and interpreted in light of the cytochrome oxidase results presented in Chapter 5. This interpretation relies upon the assumptions (that may not be correct) that in both vascular and avascular retinae there is similarity of choroidal blood supply, that metabolism within the outer retina is the same and that oxygen diffusing properties are identical. Simplistically, if the contribution of retinal circulation to oxygen supply were to be removed from a vascular retina, then the oxygen

profile would represent only choroidal oxygen delivery, and resemble that of an avascular retina. Intraretinal oxygen profiles in *vascular* retinae suggest a balance point in the region of the inner nuclear layer at which point the partial pressure of oxygen is at its lowest, (around 12 mmHg or less) and represents the interface of choroidal and retinal oxygen supply (Alder et al. 1983, Linsenmeier 1986). If the diffusion capacity of oxygen is the same in both vascular and avascular species, then beyond this point from the choroid in *avascular* retinae, oxygen tensions of 12 mmHg or less would be expected. This would contrast with the 20-30 mmHg and higher figures recorded in the vascular cat inner retina (Alder et al. 1983, Alder and Cringle 1989, Linsenmeier 1986). While no direct measurements of intraetinal oxygen profiles in avascular species are available, preretinal vitreal oxygen levels give an approximation to what might be expected for intraretinal oxygen levels. Preretinal tensions are less than 10 mmHg in the rabbit, a species with a largely avascular retina (Tillis et al. 1988). This compares with figures of 25 mmHg or more for preretinal oxygen in the cat, a species with intraretinal vessels (Alder and Cringle 1985). These extrapolations, together with the histochemical evidence that oxygen dependent metabolism is limited, suggests oxygen levels are low within the inner retina of avascular species.

Retinal oxygen diffusion has been considered by Dollery et al. (1969), who, using theoretical arguments, demonstrated how choroidal oxygen supply might be enhanced during pure oxygen breathing. These matters are still of some clinical concern in cases where the intrinsic retinal circulation is blocked but the choroidal flow remains unimpaired. Their calculations indicated that oxygen could diffuse up to 143μm through the retina when pure oxygen was breathed at one atmosphere. Diffusion distances of 250μm, or the entire thickness of a typical vascular retina, could be expected at 2.36 atmospheres (pure oxygen), whereas with air breathing at normal pressure the oxygen diffusion distance from the choroid would only be 60μm. These arguments, whilst providing a useful framework for oxygen transport, have not met with universal acceptance. For example, Popel et al. (1989) recently presented a general oxygen model based upon haemodynamically perfused tissue rather than upon the static, non-perfused models used previously. This model suggests that the actual oxygen permeability through tissue might be as much as an order of magnitude higher than that obtained using the static model employed by Dollery et al. (1969). Limitations to oxygen transport may reside mainly in the capillary wall and blood and not be uniformly distributed throughout all tissue layers (Federspiel and Popel 1986, Hellums 1977). If so, this would cast doubt upon the figures derived form Dollery's model. Furthermore, biological mechanisms may exist which could allow oxygen to reach much larger distances than previously thought. Oxygen diffusion has been shown to vary in similar tissue. For example, the diffusion coefficient for oxygen in oxidative skeletal muscle is higher than for glycolytic muscle (Ellsworth and Pittman 1984). Oxygen diffusion within tissue may be enhanced in the

presence of oxygen carriers as postulated by Longmuir and Sun (1970). Such proposed carriers could reside within the endoplasmic reticulum (Buerk and Saidel 1978), a structure prominent in retinal Müller cells (Magalhães and Coimbra 1972).

Nonetheless it would appear that both vascular and avascular retinae show similar metabolism up to 30-40μm from the choroid but beyond this distance I would postulate that the level of oxygen in avascular retinae would drop off dramatically. Cytochrome oxidase is located within mitochondria, and the presence of even small numbers of these organelles within the inner retinal layers does suggest that some oxygen is able to diffuse (or be carried) to this distance from the choroid, albeit in small quantities. Only very low levels of *intramitochondrial* oxygen are necessary to maintain oxidative metabolism, with an oxygen tension of only 1 mmHg producing 50% activity of CO within isolated liver mitochondria (Jones et al. 1985). Oxygen may not be present in sufficient quantities to support the more usual preponderance of aerobic dependent metabolism, but may nonetheless still be metabolically active.

6.2.3.c Inner retinal anaerobic metabolism and glycogen

Beyond the photoreceptor ellipsoid region, energy production strategies diverge in the two retinal groups. Non oxygen-dependent sources of energy are most likely being used within the inner retina of avascular species. Evidence may be summoned from other reports that the energy usage in avascular species is still high despite low oxidative capacity. The levels of Na^+-K^+ ATPase are known to be high within the inner retina of the avascular guinea pig retina (Ueno et al. 1980, 1981, 1984) as they are in the vascular rat retina (Stahl and Baskin 1984). Most likely ATP is produced by anaerobic glycolytic phosphorylation of ADP. However for each glucose molecule, only 2 molecules of ATP are generated from glycolytic production of lactate, but another 34 molecules of ATP could be generated from the citric acid cycle and oxidative phosphorylation (Stryer 1981). This implies that if oxygen dependent means of producing ATP are bypassed, an avascular inner retina requires larger amounts of precursor glucose for the same total energy production. To achieve this end, larger stores of glycogen have been proposed as means of providing glucose. As a general rule, the glycogen content of the retina has been claimed to be inversely proportional to intrinsic vasculature (Kuwabara and Cogan 1961, 1963b). This claim has not always been confirmed, as the glycogen content of the vascular monkey retina is as abundant as that of the mostly avascular rabbit (Mizuno and Sato 1975). Loss of glycogen during histological processing may explain differences between studies. Nonetheless, glycogen levels of avascular species are considerable, and in the (mostly avascular) rabbit retina, turnover is known to be greater within the inner retina

than outer retina (Magalhães and Coimbra 1970), consistent with the glycolytic dependence of energy production in this region.

The presence of glycogen elsewhere within the body implies a periodic need for a readily available energy substrate which, for short intense periods, cannot be met by the vascular supply (Stryer 1981). Such a role is less certain within the retina. Unlike liver glycogen, retinal glycogen shows no variation with food intake (Kuwabara and Cogan 1961). Its level is reported to show no difference with light or dark adaptation in the guinea pig (Kuwabara and Cogan 1961) although redistribution of glycogen with light and dark has been reported in the retina of the frog (Schabadasch and Schabadasch 1972a, b). Perhaps glycogen is stored in the inner retina during low metabolic periods (dark) and expended in times of demand (light). There most likely is insufficient build up of glycogen during periods of dark exposure to supply energy during periods of light adaptation, unless the reserve is continually replenished. Experimental ischaemia of the partially vascular rabbit retina, produces total glycogen depletion after 10-60 minutes, hardly sufficient to supply an extended period of constant metabolic demand (Kaskel et al. 1973, Mizuno and Sato 1975, Vassileva and Dabov 1976). One hypothesis has been that glycogen is not playing a cyclic role, but is serving to lower free glucose levels, enhancing the concentration gradient for diffusion of glucose from choroid to the inner retina (Chase 1982). This arrangement may be able to supply the large amount of glucose necessary for production of ATP through the low yield glycolytic pathway, in the absence of oxidative phosphorylation. This would require the transfer of glucose, or an energy intermediate, from glia to neuron. There is no experimental support for this hypothesis and the stimulus for demobilisation of glycogen, and its exact role, still remains uncertain (Ripps and Witkovsky 1985).

6.2.3.d Inner retinal Müller cells

Müller cells contain the bulk of retinal glycogen and they may play a central role in nourishment as well as the recognised biophysical role in influencing the extracellular electrolyte environment (Gardner-Medwin 1984, Ripps and Witkovsky 1985). Avascular retinae have a predominance of these radially arranged cells and their distribution may match that of ganglion cells (Rasmussen 1974, Reichenbach and Wohlrab 1986, Robinson and Dreher 1989). Within avascular retinae true astrocytes are absent (Stone and Dreher 1987), all support functions being assumed by Müller cells. The widespread location, and intimate relationship of Müller cells to retinal neurons, would place these cells in a ideal position to aid in the diffusion not only of glucose, but of other nutrients and wastes, to and from the inner retina. Perhaps the Müller cells are acting as gliovascular pathways, the avascular retina's answer to nourishment. If so, it would be an ingenious solution to the problem, matching the

elegance of percolating aqueous, the avian pecten or the choroidal loops in bats in providing nourishment without optical degredation. In the absence of retinal vessels these cells may be acting as preferential channels in dispersing nutrients throughout the retina (Magalhães and Coimbra 1972, Rasmussen 1973, 1974).

6.2.3.e What are the alternatives?

These conclusions are presumptive and do not preclude a pandora's box of alternative hypotheses. Other energy production pathways are possible. Facultative anaerobes which have a profound resistance to hypoxia, are able to gain small metabolic benefits from more efficient fermentation pathways and recycling of end products (Hochachka 1986). Perhaps the physiological energy requirements of the inner retina may not be entirely reflected in the histochemical level of Na^+-K^+ ATPase. The level of this enzyme may be indicating the potential of the tissue for membrane activity and not be representative of the normal functional energy consumption. The inner retina may be in a state of chronic metabolic arrest with matching membrane stability and low energy consumption, another more general strategy used to counter hypoxia (Hochachka 1986). These alternative hypotheses, which I consider unlikely, propose that avascular retinae have markedly different functional and metabolic properties to the well recognised patterns elsewhere within the CNS. Rather, the coping strategy is more likely to emphasis the production of energy through already existing (anaerobic) pathways for similar end levels of energy usage.

Despite these observations and arguments we are still left wondering whether oxygen levels are different within the inner layers of avascular retinae, or the same as vascular species, what the diffusion properties of oxygen are and what influence other metabolites and waste products play in metabolism. Clearly, there is a need for supportive *in vivo* physiological studies to elucidate the metabolic organisation of avascular retinae.

6.3 Spatial acuity and retinal vascularity

"Yes I have a pair of eyes," replied Sam, "and that's just it.
If they wos a pair o' patent double million magnifyin' gas microscopes of hextra power p'raps I might be able to see through a flight o' stairs and a lead door; but bein only eyes you see, my wision's limited."
.... Charles Dickens, Pickwick Papers.

The foregoing considerations assume nothing of the functional capabilities of avascular retinae as detectors and encoders of light. The emphasis in discussion has been upon retinal nutritional function with little attention given to the neurosensory and neurotransmission role

of the eye. How well is an *eye* with an avascular retina able to see? Not only must the retina come under close scrutiny, but also the capacity of the visual system as a whole must fall under the functional magnifying glass; how well does the *animal* see?

What does an avascular retina imply for vision? Before ruminating on this question, a little background is necessary on the subject of which parameters can be used to compare visual function and how these parameters can be measured.

6.3.1 Measurement and comparison of vision

Vision becomes limited at the extremes of illumination, is confined to a portion of the electromagnetic spectrum, is limited in terms of temporal discrimination, may be limited by the optical image produced by the refracting surfaces of the eye and importantly has shortcomings in resolution in the spatial domain. Vision is constrained within limits and it is these limits or thresholds which characterise the functional properties of the system. These thresholds determine the absolute best at which the complete system functions.

One measure of the spatial limit, visual acuity, is the threshold at which two nearby, high contrast objects may be just discerned as separate and distinct entities. This is the single most important measure of the integrity of the visual system (Westheimer 1987). However it does not completely characterise the functional properties of the visual system. Supposedly good spatial acuity may be present yet there be inadequate overall visual function if, for example, illumination is insufficient, field of view is limited, binocularity is not present or the need for colour vision is not met. Visual acuity as a measure of visual function must be interpreted in light of the behavioural requirements of the animal. Poor spatial acuity may be tolerated if other visual criteria are more important.

Lower spatial acuity *per se* is not in all situations a disadvantage; it may be that the most sensitive portion of the acuity spectrum is attuned to spatial objects in the animals environment (Campbell et al. 1973). For example, cats have lower spatial acuity than do humans, and would find it difficult to "read" the top line of the Snellen chart from 6 meters. The cat's visual system is, however, more attuned to detecting objects on a different scale. A cat would be able to detect a faint large shadow whilst that same shadow would escape the attention of the human visual system (Blake, 1988). Despite these caveats, visual acuity is the most commonly used single measure for comparing visual function.

6.3.2 Spatial visual acuity

6.3.2.a Units of measurement

Acuity is usually measured in terms of the subtended visual angle. A simple example is that of two parallel lines. When close together they appear as one, but, as they are moved apart a point is reached where two distinct objects are seen. This threshold at which detail becomes apparent determines the minimum angle of resolution, and is independent of the distance from the eye.

Alternatively, spatial acuity may be probed with a "grating" test object. Here a series sinusoidal fringes varying in intensity and spatial frequency are viewed, or projected into the eye; the point at which the pattern fuses into a continuous arrangement determining the threshold. Acuity is then measured in terms of the frequency of the sinusoidal pattern. This approach offers the advantage of being able to vary contrast independently which, of itself, can influence spatial acuity. Contrast merely relates the ratio of maximal to minimal illumination of the grating pattern. From this, the spatial contrast sensitivity function (CSF) of the visual system may be determined. Acuity measure in this way varies with the contrast of the test object. Spatial acuity of 1 cycle per degree (c/d) of visual angle is equal to a resolving power of 30 minutes of arc; this being the visual angle subtended between a maximum and minimum of the contrast cycle.

In general, minimum angle of resolution and grating acuity are related by the following formula:

$$\frac{60}{\text{cycles/degree} \times 2} = \text{minutes of arc}$$

To place some perspective on the various units, an acuity of 6 minutes of arc, or 5 c/d, would be equivalent to reading 6/60 on a Snellen chart; that is, being able to read the top line from 6 meters.

6.3.2.b Techniques of acuity measurement in animal studies

A number of methods are available to measure spatial acuity within the visual system.

(1) Psychophysical approach

The ultimate test of threshold acuity within the visual system is that based on behavioural assessment. This relies upon the integrity of the complete visual system. Such functional studies of visual acuity in their simplest form require a visual message and a response as to whether or not that message has been perceived. In clinical practice, this amounts to a verbal response as to whether or not the Snellen chart letters or contrast gratings are discernible. Psychophysical tests of animal acuity are understandably few in number, no doubt in part due to the logistic problems involved in behavioural studies. Reymond (1985) in such a study poignantly emphasises this in the one line paragraph: "It took over a year to test the eagle".

Clearly, in behavioural animal studies the question becomes more difficult to communicate and behavioural responses become more difficult to ellicit. Despite these communication problems, the same principle of making an either/or response to a visual message has been used in animal studies; an example being the two choice approach developed by Berkley (1970) and modified by Mitchell et al. (1977). The question as to which of two objects is more clearly visible becomes subtly disguised in test sessions requiring a visually based choice between two objects, and rewarding the correct choice, whilst the response becomes the physical, non-verbal choice between those two objects.

In the performance of such studies vigilance is necessary. Any approach to the determination of maximal visual acuity, as a measure of the best possible function of the visual system, presupposes that spatial threshold is the only factor under investigation. The test conditions must be such that illumination is adequate, spectral properties of the test object are matched to the sensitivity of the eye, and that the subject comprehends and cooperates, or has had adequate training to perform the behavioural test. This is highlighted in Reymond's (1981) psychophysical study of the eagle. Acuity was found to be inferior to man under the test conditions of 20 cd/m^2 illumination and green target grating. A subsequent study (Reymond 1985) under a larger range of illumunation conditions (up to 2000 cd/m^2 luminance), using black and white targets, revealed the acuity threshold to be at least three times that of man. In retrospect, both the illumination and spectral properties of the target in the earlier study were the limiting factors in visual acuity, rather than the maximal spatial resolution of the visual system *per se*. This is not to say however, that such a threshold for spatial acuity under limiting illumination conditions is not a valid entity, for, indeed it has true physiological meaning. Rather, the point at issue is that any determination of the maximal visual acuity must be performed under conditions wherby all other factors are optimal.

(2) Electrophysiological approach

An alternative approach has been to pursue the question of acuity through electrophysiological means. Following observations that the amplitude of evoked potentials are affected by the properties of the visual stimulus (for example see Harter and White 1968), Campbell and Maffei (1970) took this observation to the experimental extreme and determined the point at which the amplitude of the VER was extinguished; the spatial properties of the test object was taken to be the threshold acuity. This correlated with the psychophysical value known for man indicating that this indeed was an effective and valid alternative means of determining functional spatial acuity.

In principle the electrophysiological approach is similar to the psychophysical method, excepting that the need for an overt physical or verbal response from the test subject is replaced by the measurable electrical activity within the visual cortex; this answering the question as to whether or not the test object is visible. Given that the bottleneck to spatial resolution is most likely within the retina and determined by physical factors (Barlow 1986, Westheimer 1987), measurement of threshold electrical activity further down the processing line is merely going to reflect the limiting threshold of the retina and hence the system as a whole.

This approach has been further extended to gauge the functional refractive status of the eye (Berkley and Watkins 1973, Meyer and Salinsky 1977). The effect of correcting lenses upon the eyes optics is mirrored in changes in evoked electrical activity within the nervous system. The maximal response is taken to reflect the best optical correction.

Electrophysiology and refraction

This approach has proved valuable in the controversy regarding the presumed hypermetropia of small eyes. Enormous variation has been reported in the resting refractive state of the rat, covering a range of 30 dioptres (D); 17D hypermetropia to 13D of myopia (Hughes 1977b). Glickstein and Millodot (1970) have proposed that this may be due to artefactual reflections from the vitreous face in "objective" retinoscopic refraction producing an incorrect impression of farsightedness. The neurophysiological refraction undertaken by Hughes (1977b) and also by Meyer and Salinsky (1977), in addition to other evidence (Hughes 1977b, Hughes 1979), support the notion that these small eyes are indeed emmetropic and the large range of ametropia reported is artefactual in origin.

Clinical usefulness

In the preverbal infant evoked potential techniques have been used for assessment of visual acuity (Dobson and Teller 1978). This provides a useful adjunct to behavioural and clinical studies.

Intraretinal recording

A further elegant electrophysiological approach in determination of acuity has been to record the intraretinal properties of ganglion cells in response to contrast gratings. The cut off frequency is then used to determine spatial resolution (Cleland et al. 1979). As with the VER approach, the results correlate well with psychophysical acuity.

(3) Anatomical approach

Whilst visual acuity is dependent upon the interaction of the whole visual system from tear film to visual association cortex, the eye with its optical, anatomical and physiological constraints effectively determines acuity (Westheimer 1987). Based on the work of Young (1801), it is generally accepted that the optical qualities of the eye closely match the anatomical photoreceptor grating (Williams 1985, for review see Hughes 1986).

Like most rules there are exceptions; the cat for example is able optically to image spatial frequencies up to 20 c/d (Hughes 1981) yet functionally the best performance is 8 c/d resolution (Blake 1988). An exception is also claimed for the garter snake which is reported as having a optical resolving power at least twice that of the photoreceptor mosaic (Land and Snyder 1985). These variations from dogma suggest the situation to be a little more complex than first thought. Snyder et al. (1985) indeed argue on theoretical grounds that the optical limits should be significantly better than the photoreceptor array. Perhaps the "rule" is incorrect.

However, for simplicity the anatomical constraints to image quality may be considered as representative of the limits to spatial acuity. It is not unreasonable as a first approximation to assume that the anatomical, optical and physiological factors are linked in sensitivity.

Receptor mosaic

The photoreceptor grain limits the threshold of spatial acuity by limiting the capacity to detect differences in illumination. The physiological detection of distinctness is essentially that of intensity discrimination (Westheimer 1987). For a stimulus of intensity I, a change in intensity ΔI is necessary for the detection of any difference; the ratio $\Delta I/I$ being a constant over a wide range of intensity levels, and is referred to as the Weber-Fechner relation (Hart 1987).

Transposed into anatomical terms: For two objects to be seen as distinct and separate, there must be a difference delta I in the intensity of light falling upon adjacent photoreceptors. The physical separation of the photoreceptor elements may limit resolution. In particular, their distribution per linear degree of visual angle, determines this threshold. In general, there is high correlation between acuity based on the physical dimensions of the most densely packed photoreceptor region and the actual spatial threshold (Westheimer 1987). Unfortunately, this need not always be so. For example, the cat's cone mosaic exceeds its spatial resolution.

Ganglion cells

A common arrangement in the region of the retina designated for acute vision, is that the photoreceptors feed information on a one to one basis to the ganglion cells. Hence the ganglion cell distribution can also reflect spatial limits of resolution. This applies only where non-convergent flow of neural information occurs from photoreceptors through to ganglion cells. Convergence of information from many photoreceptors to one ganglion cell will of course diminish spatial acuity but to the benefit of intensity detection. Maximal ganglion cell counts are often used to approximate anatomical spatial resolution (Hughes 1977a), and these show better correlation with behavioural acuity than does acuity calculated from photoreceptor density (Pettigrew et al. 1988). Implicit in the calculation are a number of assumptions (Pettigrew et al. 1988). First, it is assumed that all ganglion cells are corectly identified. This may be not be correct as displaced amacrine cells are known to reside within the ganglion cell layer and may inflate estimates of true ganglion cells (Wong and Hughes 1987). Second, not all ganglion cells may be contributing to spatial resolution. The third source of error may occur in projection of the ganlion cell distribution into visual space. The relationship of the posterior nodal distance, used in calculation of the scaling factor for retinal magnification, varies with eye size and small measurement variations could yield potential large sources of error (Hughes 1977a). Despite the propensity to overestimate functional resolution, ganglion cell counts often correlate highly with behavioural acuity (See Tables 6.I, 6.II and 6.III).

An estimate of acuity based on ganglion cell counts may be derived from the following formulae:

$$\text{Degrees/mm} = \frac{2\pi \times \text{Posterior Nodal Distance}}{360}$$

$$\text{Cells/d} = \frac{\sqrt{\text{Ganglion Cells/mm}^2}}{\text{Degrees/mm}}$$

$$VA_g = \frac{\text{Cells/d}}{2} \quad \text{(c/d)}$$

The posterior nodal distance is usually between 52%-71% of axial length in a wide range of animals, being smaller in nocturnal animals and larger in diurnal species (Pettigrew et al. 1988). Where a calculation for PND is made based on axial length, a figure of 60% is often used (Hughes 1977a).

6.3.3 Animal studies: Psychophysical physiological and anatomical

A brief summary of known and calculated acuity for many animals follows. As the simplest single measure of visual function, spatial acuity has been compared to determine whether avascular and vascular retinal systems differ. Given comparability in other respects, does retinal avascularity imply inferior visual resolution? While birds are neither mammalian, nor possess a truly avascular retina, avian values have been include as a measure of what might be expected for maximal spatial resolution in an avascular, but nutritionally supplemented, retina. The data are summarised in Tables 6.I, 6.II and 6.III. Note that there is often good correlation between the many different approaches employed to measure acuity. This offers some reassurance that the simpler anatomical measures may approximate the more accurate, but difficult to obtain, behavioural measures.

6.3.3.a Rat

Lashley (1932, 1938) using behavioural studies estimated spatial acuity to be 26 minutes of arc (1.5 c/d) whilst Wiesenfeld and Branchek (1976) calculated acuity to be one degree of visual angle (0.5 c/d). Dean (1978) compared acuity before and after cortical and collicular lesions and found that the prelesion rats obtained acuity approaching 0.9 c/d (33 min of arc). Birch and Jacobs (1979) in a three choice performance test determined pigmented rat acuity to be 1.2 c/d (25 min of arc), whilst the albino rat had lower acuity at 0.34 to 0.43 c/d (70-88 min of arc). The consensus of these behavioural studies indicates that spatial acuity is at least 25 min of arc (1.2 c/d).

Combining optical data (Hughes 1979a) and anatomical data (Fukada 1977), the maximum distribution of ganglion cells per linear degree is around 4.7 cells/d; this corresponds to an acuity of 2.4 c/d or 13 min of arc. Similarly, the best optical resolving power of the rat has been estimated at 12 minutes of visual angle (Hughes and Wassle, 1979), about twice the value obtained with behavioural measures.

6.3.3.b Cat

Better correlation of behavioural estimates, ganglion cell counts and electrophysiological data is seen in the cat, which perhaps is the most widely used animal in visual research (Blake

1988). Functional assessments of acuity are consistantly around 6-8 min of arc (Bloom and Berkely 1977, Bisti and Maffei 1974, Jacobson et al. 1976 and for review see Blake 1988).

Evoked potential studies report similar acuity of around 6-8 c/d (Berkley and Watkins 1973, Campbell et al. 1973). Cleland et al. (1979) recording from ganglion cells were able to find cells with cut off grating frequency of 9.5 c/d in the area centralis.

From anatomical data, the ganglion cell dendritic spread is around 18μm corresponding to a visual angle resolution of 4.8 minutes of arc or 6 c/d (Leicester and Stone 1967). The ganglion cell distribution in the area centralis, using Stone's (1965) data, is 17.5 cells/d or a calculated acuity of 9 c/d. Using the figure of 10 000 ganglion cells per mm^2 (Hughes 1987), or 21 cells/d, the estimated acuity is only marginally better at 10 c/d resolution.

Within the area centralis the cone spacing is 35 cones per degree (Steinberg 1973). A grating of half this frequency, 17.5 c/d, could theoretically be resolved if only one photoreceptor were linked to one ganglion cell and the optical resolution matched the quality of the cone mosaic.

6.3.3.c Birds

Acuity in the avian realm is of great interest due to the combination of an avascular retina and the almost folklore-like reputation for very acute vision. Behavioural studies indeed show excellent vision. The eagle, *Aquila audax*, has an acuity of 132-143 c/d resolution when measured functionally under bright illumination conditions (Reymond 1985). The average cone-cone spacing in the deep fovea is 1.5μm whilst in the shallow fovea the spacing is 2.7μm. Knowing the angular magnification factor of the eagle's eye Reymond (1987) calculated the photoreceptor resolving power to be 140 c/d, very close to the measured behavioural data (see Table 6.III).

Such acuity is not available without some expense. An increased amount of neural tissue must be devoted to capturing and coding in such fine detail the visual image of the world. Not only is the retina abundantly thick, but also large in areal dimensions The eye itself is large, being 35mm in length; huge in comparison with the body weight. Consequently, retinal illumination, according to the inverse square law, is low necessitating the bird to operate under very bright luminance levels for maximal acuity; spatial acuity is hightened at the expense of light detection.

However, not all raptorial birds have such fine acuity. Owls are nocturnal predators with functional acuity less than that of man (Fite 1973, Martin and Gordon 1974). The retina is rod dominated with a 3 to 1 convergence of photoreceptors to ganglion cells within the foveal region (Fite 1973). Acuity is around 4-5 minutes of arc or 6 c/d, comparable with other nocturnal animals, for example owl monkey, or the pathological human rod monochromat at around 6 minutes of arc.

With owls, in direct contrast to the eagle, spatial acuity is sacrificed at the expense of illumination detection. This highlights the potential problems associated with extrapolation of

visual acuity from anatomical data. Both the photoreceptor and ganglion cell relationships must be used in drawing conclusions regarding acuity. A visual system with a fine, potentially acute, photoreceptor grating may not produce superior overall spatial resolution if a number of photoreceptors converge upon the one ganglion cell in the interests of hightened illumination detection.

6.3.3.d Marsupials

Little is known about the functional visual properties of the marsupials. The visual acuity of opossum's (American and South American) calculated from the ganglion cell distribution is around 2.5 c/d (Hokoç and Oswaldo-Cruz 1979, Oswaldo-Cruz et al. 1979, and Rapaport et al. 1981). An electrophysiological study undertaken by Silveira et al. (1982) indicates that visual acuity as measured by this technique is 1.25 c/d; very similar to that found in the rat and considerably less than that of the cat or indeed, man. However, the experimental technique involved dilating the pupil, and, anyone who has had diagnostic pupillary dilation will attest to a decrement in visual acuity which results from this optically unphysiological state. Hence visual acuity would be at least this value, if not greater. In keeping with the nocturnal behavioural pattern of this marsupial, there was no increase in threshold acuity with increase in luminance above 2.4 cd/m^2 into photopic levels.

There is some behavioural information about the Australian brush-tailed possum's visual system. The possum does possess a reasonable degree of eye-hand coordination (Megirian et al. 1977, Rees and Hore, 1970). Robinson (1982) has demonstrated that while the possum lacks a corpus callosum, there is considerable inter-ocular transfer of visual information from one hemisphere to the other. An anatomical estimate of acuity has been made for this avascular retina. The Australian possum, with a peak ganglion cell count of 5 000 cells per mm^2, has an estimated spatial acuity of 4.8 c/d (Freeman and Tancred 1978).

The vascular polyprotodont counterpart, the northern native cat, based on both behavioural and anatomical data has an acuity around 2.3 c/d (Harman et al. 1986, Robb et al. 1982), roughly half that of the possum's.

Ganglion cell counts are available for other marsaupials: pademelon, *Thylogale billarderii*; tammar wallaby, *Macropus eugenii*; Tasmanian devil, *Sarcophilus harrisii*; brown nosed bandicoot, *Isoodon obesulus*; the quokka, *Sertonix brachyurus* and a hairy nosed wombat, *Lasiorhinus latifrons*. If anything these reports indicate that the diprotodont kangaroos and possums (avascular retinae) generally have higher counts than do their more generalised polyprotodont kin (Beazley and Dunlop 1983, Freeman and Tancred 1977, Kolb and Wang 1985, Rapaport et al. 1981, Tancred 1981, Wong et al. 1986). Any differences are more in keeping with the functional visual requirements and life style than with retinal vascularity. Retinal avascularity need not limit ganglion cell numbers. The final extrapolation to anatomical acuity however, requires an estimate of the posterior nodal distance to determine the distribution of cells in visual space.

ANIMAL	AXIAL LENGTH (MM)	POSTERIOR NODAL DISTANCE (MM)	RETINAL MAGNIFICATION FACTOR	PHOTORECEPTOR GRATING	GANGLION CELL DENSITY	VISUAL ACUITY (CYCLES/DEGREE)	COMMENTS	REFERENCES
MAN	24.4	17.1	0.29 mm/d	Foveal cones 2-3μm spacing 100 000-324 000/mm^2	160 000 cells/mm^2 115 cells/d	VA_f = 40 VA_o = 60 VA_e = 35 VA_p = 60 VA_g = 55	Vascular retina, Acute vision	Curcio, 90 Polyak, 41 Snyder, 86 VanBuren, 63 Westheimer, 87
CAT	21.6	13.2 (Vakkar) 12.2 (Hughes)	0.227 mm/d 0.211 mm/d	Cone spacing 6μm Rod spacing 1-2μm 460 000 rods/mm^2	6000-10 000 cells/mm^2 21 cells/d	VA_f = 6-8 VA_o = 20 VA_e = 8 VA_p = 18 VA_g = 10.5	Vascular retina, Choroidal tapetum Rod dominated retina	Blake, 88 Cleland, 79 Hughes, 76 Leicester, 67 Stone, 65 Vakkar, 63 Steinberg, 73
RAT	6.304 (Chandhuri) 6.357 (Hughes)	3.33	0.059 mm/d		6500 cells/mm^2 4.7 cells/d	VA_f = 1.2 VA_o = 2.5 VA_e = ? VA_p = ? VA_g = 2.4	Vascular retina	Birch, 79 Chaudhuri, 83 Dean, 78 Fukuda, 77 Hughes, 79 Hughes/Wassle 79 Lashley, 32, 38 Sefton, 85
MOUSE	3.4 (power = 580 dioptres)	1.7	0.031 mm/d		8000 cells/mm^2 2.77 cells/d	VA_f = 0.5 VA_o = ? VA_e = ? VA_p = ? VA_g = 1.39	Vascular retina Very small eye Illumination 4X brighter than rat	Dräger, 81 Remtulla, 85 Sinex, 79
RABBIT	18.1	9.9	0.0172 mm/d		2500-4800 cells/mm^2	VA_f = 3.4 VA_o = ? VA_e = 3.4 VA_p = ? VA_g = 6.0	Horizontal streak Retina mostly avascular	Hughes, 72 Kulikowski,78 Provis, 79 Vaney, 80 Van Hof, 67

Table 6.I: Visual acuity in placental mammals

VA_f = visual acuity based on functional behavioural studies. VA_o = visual acuity based on measures of optical resolution of the eye. VA_e = visual acuity based on electrophysiological studies. VA_p = visual acuity calculated from photoreceptor grain. VA_g = visual acuity based on the ganglion cell distribution.

ANIMAL	AXIAL LENGTH (MM)	POSTERIOR NODAL DISTANCE (MM)	RETINAL MAGNIFICATION FACTOR	PHOTORECEPTOR GRATING	GANGLION CELL DENSITY	VISUAL ACUITY (CYCLES/DEGREE)	COMMENTS	REFERENCES
POSSUM	13	7.8	0.136 mm/d		5000 cells/mm^2 (9.6 cells/d)	VA_f = ? VA_o = ? VA_e = ? VA_p = ? VA_g = 4.8	Avascular retina	Freeman, 78
OPOSSUM	S. American 9.98	5.11	0.089 mm/d		2900 cells/mm^2 (4.7 cells/d)	VA_f = 1.25 VA_g = 2.3	S. American opossum larger Vascular retina Retinal tapetum	Hokoç, 79 Kolb, 85 Oswaldo-Cruz, 79 Rapaport, 81 Silveira, 82
	N. American			485 000 Rods/mm^2	2900 cells/mm^2 (5 cells/d)	VA_g = 2.5		
NATIVE CAT	10	6	0.11 mm/d		2600-3500 cells/mm^2	VA_f = 2.8 VA_o = ? VA_e = ? VA_p = ? VA_g = 2.6	Vascular retina Choroidal tapetum	Harman, 86 Robb, 82
ECHIDNA	9	5.4	0.099 mm/d		1800 cells/mm^2	VA_f = ? VA_o = ? VA_e = ? VA_p = ? VA_g = 2.1	Avascular retina	Stone, 83

Table 6.II: Visual acuity in marsupials and monotremes
VA_f= visual acuity based on functional behavioural studies. VA_o= visual acuity based on measures of optical resolution of the eye. VA_e= visual acuity based on electrophysiological studies. VA_p= visual acuity calculated from photoreceptor grain. VA_g= visual acuity based on the ganglion cell distribution.

ANIMAL	AXIAL LENGTH (MM)	POSTERIOR NODAL DISTANCE (MM)	RETINAL MAGNIFICATION FACTOR	PHOTORECEPTOR GRATING	GANGLION CELL DENSITY (CELLS/MM^2)	VISUAL ACUITY (CYCLES/DEGREE)	COMMENTS	REFERENCES
EAGLE	35	22.6	0.35 mm/d	Deep foveal cone 1.6μm spacing Shallow fovea 2.4μm spacing		VA_f = 135 VA_o = 160 VA_e = ? VA_p = 140 VA_g = ?	Avascular but supplemented retina	Reymond, 85
OWL				2-3μm spacing of cones at fovea	50 000 cells/mm^2	VA_f = 6.7 VA_o = ? VA_e = ? VA_p = ? VA_g = ?	Avascular but supplemented retina Good nocturnal vision	Fite, 73 Martin, 74
GARTER SNAKE	3.8	2.5		10μm cone spacing		VA_f = ? VA_o = 30 VA_e = ? VA_p = 2 VA_g = 2	Optical resolution superior to photoreceptor grain	Land, 85

Table 6.III: Visual acuity in birds and reptiles

VA_f = visual acuity based on functional behavioural studies. VA_o = visual acuity based on measures of optical resolution of the eye. VA_e = visual acuity based on electrophysiological studies. VA_p = visual acuity calculated from photoreceptor grain. VA_g = visual acuity based on the ganglion cell distribution.

6.3.4 Vascularity and acuity

The lack of retinal vasculature certainly need not infer limited resolution. It would appear that the possum could have greater acuity than the quoll. The estimate of 4.8 c/d published for the possum (Freeman and Tancred 1978), is around twice the 2.6 c/d figure for a closely related congenor of the quoll, *Dasyurus hallucatus* (Harman et al. 1986). This places the possum's acuity at the lower end of the 5-8 c/d reported for domestic cats (Blake, 1988), while the quoll's is at least twice that reported for the laboratory rat (Sefton and Dreher, 1985). Taking Hughes' (1977a) ganglion cell count of 3 000 cells/mm^2 for the guinea pig and using our axial measures of 9.3mm (unpublished data) to compute posterior nodal distance, an estimated acuity of approximately 2.7 c/d is calculated, a figure comparable to the quoll and in excess of that measured in rats. In our few examples, those species with avascular retinae demonstrate a greater potential for spatial acuity than do species with vascular retinae. The differences are not great though, particularly when compared with resolution of up to 60 c/d some in some vascular primate retinae (Westheimer, 1987 and up to 143 c/d seen in some avascular, but nutritionally supplemented, bird retinae (Reymond, 1985). Clearly an avascular retina may not be detrimental to visual acuity. Like other features of visual engineering, function is matched to need. Just as the optical quality of the eye is subservient to the requirements of the retina (Snyder et al. 1986), functional acuity is matched to biological needs of the animal, and not to a particular morphological feature such as the pattern of retinal vascularity. There is a need for supportive functional studies to elucidate more accurately acuity in both vascular and avascular species.

6.3.5 Central visual organisation

The anatomical evidence would suggest that while avascular retinae have the potential for the same degree of spatial resolution as those with intrinsic blood vessels, there may be a penalty in terms of potential for temporal resolution. Avascular retinae have thinner IPLs, the region considered important in temporal coding of the visual message (Cohen 1987, Dowling 1987). But, visual proecesing involves more than just the retina, relying also upon higher neuronal connections. What is the organisation of the more central visual pathways and could any retinal "deficiencies" be compensated for at higher levels within the CNS?

6.3.5.a Rats and guinea pigs

As with most mammals which fall into a non-diurnal habitus or in which visuomotor skills are not paramount to their lifestyle, the central organisation of the visual system, as reflected by neurological organisation within the dorsal lateral geniculate nucleus and other centres within the central nervous system is not particularly complex (Brauer et al. 1982, Shober et al. 1985, Reese 1988). It is thus somewhat perplexing why the retinae in these two rodent species with vaguely similar non-visual lifestyles should differ so markedly while available evidence suggests that centrally, their respective visual systems are organised along similar, rather simple morphological lines. There appears no compensatory complexity within the CNS in either species.

6.3.5.b Marsupials

Many diprotodont marsupials (avascular retinae) possess fairly complex visual systems when compared with their polyprotodont cousins and indeed in comparison with many placentals. Centrally, many diprotodont marsupials display specialisations paralleling those seen in highly visual placental mammals, specialisations which are either lacking or are not fully developed in dasyurids and didelphids (Haight and Sanderson 1990). In most diprotodonts retinal projections to the dorsal lateral geniculate (LGd), including the sugar glider and the brushtail possum, are fully segregated; that is, the two eyes have discrete, non-overlapping projection zones within the LGd (see Sanderson et al. 1984, Sanderson et al. 1987 - this paper also reports an exception to the rule). Total segregation is the rule in all known placentals (Kaas et al. 1972), but not in members of two polyprotodont families, the Didelphidae and Dasyuridae. In these there is substantial ocular overlap within the LGd, a feature normally only seen in fetal LGd's, whether placental or marsupial (Haight and Sanderson 1988, 1990, Sanderson et al. 1982, Shatz and Sretavan 1986, Wye-Dvorak 1984). Also, in diprotodonts the LGd often displays a degree of cytoarchitectural complexity which equals or exceeds that seen in primates which, among placentals, probably have the most complexly organised LGds known (Sanderson et al. 1984, Sanderson et al. 1987, Kaas et al. 1978). In contrast, laminar organisation in the polyprotodont LGd is generally much simpler (Haight and Sanderson 1988, 1990, Sanderson and Pearson 1977, Sanderson et al. 1979).

Visual cortex in the brushtail possum is large, displaying extensive inter and intrahemispheric connections with many other cortical regions (Haight et al. 1980, Heath and Jones 1971, Crewther et al. 1984). In the Virginia opossum, the only polyprotodont marsupial for which information about the organisation of visual cortex is available, it appears that visual cortex is proportionately much smaller and the thalamocortical relationships are not as complex as in the brushtail possum (Benevento and Ebner 1971a, 1971b). All of this suggests that many

members of the diprotodont lineage possess more complexly organised visual systems than do the more generalised polyprotodonts. In the absence of more comparative information about the functional properties of the marsupial visual system, it is unwise to claim that diprotodonts such as possums and gliders 'see better' than the polyprotodont quolls and devils, though this is strongly suggested by the available morphological evidence. One thing does seem certain. In diprotodont marsupials increasing organisational sophistication within the central visual system correlates well with retinal avascularity. The visual system of polyprotodonts, on the other hand, appears to be more simply organised. This could suggest that some retinal functional "deficiencies" may be transferred centrally in marsupial avascular retinae. A conclusion awaits further physiological examination of the visual CNS in marsupials.

The complex central organisation of the diprotodont visual system appears adequately served by a retina devoid of intrinsic vasculature.

6.4 Taxonomic considerations

The consideration so far has been of the biologcial problem of "what does it look like and how does it work?". Complementary to this consideration is the historical origin of biological adaptations: "how did it come into being?" (Bock 1988).

Behavioural factors need not be a factor in dictating whether the retina is vascularised or not. Consider the two placental species examined here, rats and guinea pigs. The former are nocturnal graminivores, tending towards omnivory while the latter are crepuscular and will eat most forms of vegetation (Walker et al. 1975). They both rely upon olfactory and tactile cues for much of their sensory input . Vision does not play a dominant role in the lifestyle of either of these two species. Despite the similarity of visual needs, behavioural function is not correlated with vascularity, as one is avascular (guinea pig), and the other vascular (rat). Even though rats and guinea pigs are related and both belong to the same taxonomic order, Rodentia, vascularity is more correlated with the family to which they belong than behavioural attributes.

Attempts to relate the trait of retinal vascularity to the broader evolutionary phylogenetic tree is less satisfactory. Consider the trees that have been developed using traits found within the CNS. Many features of brain morphology have been used to construct best fit evolutionary trees, using derived more advanced neourological features for classification (Johnson 1986). This overcomes the problems of parallelism, reversal and convergence, producing a tree

which is largely cladistic (Kirsch 1983, Kirsch and Johnson 1983, Kirsch et al. 1983). Applying the known pattern of retinal vascularisation to these evolutionary trees produces pockets of retinal avascularity both off and on the main stream of placental evolutionary development, with no consistent derived and primitive location.

The situation is clearer in the marsupials, an important group in evolutionary biology. With many millions of years of isolated and separate development, this group has adapted to fill a wide range of ecological niches. This places this group in an ideal position to draw comparative conclusion regarding form, behavioural function and evolution (Haight and Murray 1981, Meyer 1981).

Most marsupials are nocturnal and they occupy a wide range of different niches. The Eastern quoll used in this study is an active, ground dwelling predator while brushtail possums are semi-arborial browsers (Ride 1970, Strahan 1983). Brushtail possums and their relatives, the kangaroos, wallabies, wombats and a large variety of other possums, all possess avascular retinae (Johnson 1901, 1968, Walls 1942). These marsupials belong to the advanced marsupial order Diprotodonta which is thought to have evolved from a generalised line whose extant progeny include the quolls and their relatives plus virtually all of the American marsupials (Johnson 1986). Thus, for marsupials vascular retinae are likely to be a primitive feature and retinal avascularity is probably an advanced or derived taxonomic feature. Again, vascularity of the retina does not correlate with behavioural function, but more with taxonomic grouping.

6.5 Clinical considerations

Comparative anatomy has three broad aims - the three R's - rules, roots and relevance (Bullock 1984). The rules governing the function in avascular retinae have been considered as have the phylogenetic and evolutionary roots. What of the relevance of retinal avascularity to human pathological conditions.

The way in which the retina derives nourishment is just part of a complex and unique nutritional strategy which has been adopted throughout the eye. Whilst the approach that has been taken to solve the nutritional and optical dilemma of the eye has been solved in an ingenious manner, there are some disadvantages. The advantages are traded against the propensity of the eye to be afflicted by degenerative diseases (Bill 1975). Conditions affecting the vasculature of the retina are seen commonly in clinical practice. Occlusion of the retinal circulation is seen in diabetes mellitus, atherosclerosis, arteritis, hypertension, retinal vein

obstruction, retinopathy of prematurity and hyperviscosity syndromes (Kanski 1987). Loss of the retinal circulation produces devastating and irreversible loss of visual function. Can physiological avascularity replace pathological avascularity?

The answer currently is no, but the potential may be there for some improvement in function. The avascular retinal model suggests that choroidal circulation need have no specialisation to nourish an avascular retina. The existing choroidal circulation may be sufficient to nourish a pathologically affected retina. However, the area of supply is limited to the outer 170+μm of retinal thickness, unless there is supplemental nourishment by some other route. Therefore, this is insufficient to maintain function throughout the entire inner retina, particularly in the thickest region around the optic disc (around 500μm in thickness). Furthermore, even up to 170μm from the choroid in vascular species the metabolic machinery necessary to circumvent the limited oxygen supply may not be immediately available. Similarly, there is not the cellular accompaniment of avascularity, a preponderance of Müller cells.

Any chance of improved influence of the choroidal circulation requires modification of cellular structures and biochemical pathways. This is seen in pathological retinal obstruction, but in association with gliosis and loss of normal architecture. With time there is increase in glycogen content and Müller cell prominence of ischaemic retina (Hiscott et al. 1984). It may be possible to exploit humoral factors examples of which are known to be released under conditions of retinal hypoxia. These factors have been implicated in new vessel growth from the optic disc, iris and peripheral retina in diabetes mellitus, sickle cell disease and even in the subretinal neovascularisation of age related macular degeneration (Glaser 1986, Glaser et al. 1980). Vascular growth factors are just part of the broader control mechanism. The search for, characterisation and availability of growth and controlling factors throughout the CNS raises great hopes for being able to influence the populations of glia and neurones to circumvent pathological conditions (Rush 1989). Perhaps to aid the ischaemic retina, the Müller cell population may be artificially enhanced, and the metabolic machinery for anaerobic metabolism turned on, through the specific application of growth and controlling factors. Should this artificial transformation be possible, interim retinal support would be necesary. Intravitreal supply of oxygen through a catheter has been experimentally shown to maintain ERG activity in the presence of retinal arterial occlusion (Ben-Nun et al. 1988).

Full thickness support of a retina with an ailing circulation could conceptually be achieved by borrowing a leaf from the avian strategy book. A disc pecten in a modified and unsatisfactory form is seen with neovacularisation of the optic disc, for example in diabetic retinopathy. Often such a structure protrudes into the vitreous and is fluorescein permeable, just like the pecten. Unfortunately, pathologically derived new disc vessels are fragile and liable to

produce intravitreal hemorrhage. To turn pathological disc neovascularisation into physiologcial usefulness would require application of the same controlling mechanism as are applied to the avian pecten.

There are no immediate and readily achievable practical ways for enhanced nutrition in pathological retinal ischaemia, short of removing the underlying cause. There are clues though in the way in which nature has solved the problem of retinal nourishment in varied ways to suggest some hope for therapeutic manipulation.

6.6 Future directions

This study has addressed the broad aspects of retinal function and vascularity. Therefore, by necessity many questions have been only partly answered and many topics await further, more in depth, probing. This is particularly so where peripheral issues have been addressed outside the main theme of the coping mechanisms in retinae devoid of intrinsic vasculature. The second aspect of any future direction must be a reappraisal of the the original model in light of the experimental findings integtrated with a consideration of other physiological and anatomical information.

What are some of those peripheral, and equally important, issues and what questions have been raised as a direct consequence of results gained from this study?

6.6.1 Metabolism, Müller cells and mitochondria

The biggest difference between vascular and avascular retinae would seem to lie in the mode of energy production. The development of further hypotheses about the coping strategy within avascular retinae must therefore concentrate upon questions of metabolic function. Are the metabolic energy requirements the same in both types or retinae, are there alternative energy pathways, what are the oxygen levels throughout avascular inner retina, what are the glycogenolytic and glycogenic pathways and what are the levels of oxidised and reduced intermediates within avascular retinae? This is intimately related to a further understanding of the contribution of mitochondria to metabolic function; what are their numbers, structure, distribution, metabolic machinery and developmental history? This information is important in piecing together the picture of function based on the hypothesis that avascular retinal neurotransmission is the same as that in vascular retinae, and anaerobic metabolism predominates to provide these energy needs. Consideration of metabolism must have in the

background an appreciation of the neurotranmission function within the retina and the question asked " how well do avascular retinae see?"

The second aspect of energetic considerations is how are metabolites, wastes nutrients mobilised throughout the retina? The hypothesis that Müller cells are acting as gliovascular pathways places a further appreciation of these cells high on the list of priorities. Are they acting as pathways to and from the choroid and also producing energised intermediates for supply to surrounding neurones?

6.6.2 The ocular vasculature

Still far from certain is the contribution of non-choroidal structures to retinal nourishment. Further consideration is necessary of the role that ciliary body, iris and optic disc vasculature may make to inner retinal metabolism. The functional microdomain properties of the choriocapillaris may vary in the two retinal groups. What are the functional blood flow and oxygen extraction characteristeics of the choroid where the retina is avascular?

6.6.3 Embryology of the vascular system

The way in which avascular retinae develop embryologically, as well as how the unusual pattern of vascularisation of the marsupial polyprotodont retina is derived, are intriguing questions. How is the marsupial vascular system derived from the mesenchymal progenitor cells? Does the retinal circulation derive from a more general vascular network or do the paired arterial venous cords appear *de novo*? What happens to the early hyaloid system of vessels in the avascular retina? The ultimate determinant of the developmental choice in vascularisation of the retina is uncertain.

6.7 Finale

Whilst the coping strategies of avascular retinae still remain only partly answered some light has been shed on the alternative vascular patterns that have appeared during phylogenesis, most particularly within the marsupial lineage. Retinal avascularity is a satisfactory alternative in the many and varied ways in which nature has approached the problem of light detection and retinal nourishment. This is not the end *"but it is, perhaps, the end of the beginning"*.

.....

REFERENCES

Aaberg, T.M. (1980). Fluorescein angiography. Fluorescein angiography and acquired macular disease. In: Peyman, G.A., Sanders, D.R. and Goldberg, M.F. (Ed.) *Principles and Practice of Ophthalmology*. (pp. 905-954). W.B. Saunders Company, Philadelpelphia.

Abelsdorff, G. and Wessely, K. (1909). Vergleichendephysiologische Untersuchungen über den Flussigkeitwechsel des Auges in der Wirbeltierreihe: I Vogel. *Arch. Augenheilkd.* 64, 65-124.

Abood, L.G. (1969). Brain mitochondria. In: Lajtha, A. (Ed.) *Handbook of Neurochemistry*. (pp. 303-326). Plenum Press, New York.

Acosta, D. and Wenzel, D.G. (1975). A permeability test for the study of mitochondrial injury in *in vitro* cultured heart muscle and endothelial cells. *Histochem. J.* 7, 45-56.

Akagi, Y., Yajima, Y., Kador, P.F., Kuwabara, T. and Kinoshita, J.H. (1984). Localization of aldose reductase in the human eye. *Diabetes*. 33, 562-566.

Alberts, B., Bray, D., Lewis, J., Raff, M., Roberts, K. and Watson, J.D. (1983). *Molecular Biology of the Cell*. Garland Publishing Inc, New York.

Alder, V.A. and Cringle, S.J. (1985). The effect of the retinal circulation on vitreal oxygen tension. *Curr. Eye Res.* 4, 121-129.

Alder, V.A. and Cringle, S.J. (1989). Intraretinal and preretinal PO2 response to acutely raised intraocular pressure in cats. *Am. J. Physiol.* 256, H1627-H1634.

Alder, V.A., Cringle, S.J. and Constable, I.J. (1983). The retinal oxygen profile in cats. *Invest. Ophthal. Vis. Sci.* 24, 30-36.

Alm, A. and Bill, A. (1973). Ocular and optic nerve blood flow at normal and increased intraocular pressures in monkeys (*Macaca irus*): a study with radioactively labelled microspheres including flow determinations in brain and other tissues. *Exp. Eye Res.* 15, 15-29.

Alm, A. and Bill, A. (1987). Ocular circulation. In: Moses, R.A. and Hart, W.M. (Ed.) *Adler's Physiology of the Eye. Clinical Application*. (pp. 183-204). The C.V. Mosby Company, St Louis.

Ames III, A. and Nesbett, F.B. (1981). *In vitro* retina as an experimental model of the central nervous system. *J. Neurochem.* 37, 867-877.

Anderson, W.A., Bara, G. and Seligman, A.M. (1975). The ultrastructural localisation of cytochrome oxidase via cytochrome c. *J. Histochem. Cytochem.* 23, 13-20.

Angermüller, S. and Fahimi, H.D. (1981). Selective cytochemical localization of peroxidase, cytochrome oxidase and catalase in rat liver with 3,3'-diaminobenzidine. *Histochem.* 71, 33-44.

Ashton, N. (1963). Studies of the retinal capillaries in relation to diabetic and other retinopathies. *Brit. J. Ophthal.* 47, 521-538.

Ashton, N. (1968). Some aspects of the comparative pathology of oxygen toxicity in the retina. Donders Lecture. *Brit. J. Ophthal.* 52, 505.

Balkema, G.W. (1988). Elevated dark-adapted thresholds in albino rodents. *Invest. Ophthal. Vis. Sci.* 29, 544-549.

Barka, T. (1988). Reflections on histochemistry: The past fifty years. In: Pauly, J.E. (Ed.) *The American Association of Anatomists, 1888-1987. Essays on the History of Anatomy in America and a Report on the Membership - Past and Present.* (pp. 75-88). Williams and Wilkins, Baltimore.

Barlow, H.B. (1986). Why can't the eye see better?. In: Pettigrew, J.D., Sanderson, K.J. and Levick, W.R. (Ed.) *Visual Neuroscience.* (pp. 3-18). Cambridge University Press, Cambridge.

Barr, M.L. and Kiernan, J.A. (1983). *The Human Nervous System. An Anatomical Viewpoint.* Harper and Row, Publishers, Philadelphia.

Batson, O.V. (1955). Corrosion specimens prepared with a new material. *Anat. Rec.* 121, 425.

Bawa, S.R. and Werner, G. (1988). Mitochondrial changes in spermatogenesis of the pseudoscorpion, *Diplotemnus* sp. *J. Ultrastruct. Res.* 98, 281-293.

Beazley, L.D. and Dunlop, S.A. (1983). The evolution of an area centralis and visual streak in the marsupial *Sertonix brachyurus*. *J. Comp. Neurol.* 216, 211-231.

Bedetti, C.D. (1985). Immunocytological demonstration of cytochrome c oxidase with an immunoperoxidase method. *J. Histochem. Cytochem.* 33, 446-452.

Behrman, S. (1968). Richard Liebreich, 1830-1917. First iconographer of the fundus oculi. *Brit. J. Ophthal.* 52, 335-338.

Beiser, A. (1973). *Concepts of Modern Physics*. McGraw-Hill Kogakusha, Ltd, Tokyo.

Bell, K. and Wise, G.M. (1980). A modified technique of fluorescein angiography. *J. Ophthal. Photog.* 3, 32-34.

Bell, M.A. and Scarrow, W.G. (1984). Staining for microvascular alkaline phosphatase in thick celloidin sections of nervous tissue: Morphometric and pathological applications. *Microvasc. Res.* 27, 189-203.

Bellhorn, M.B., Bellhorn, R.W. and Poll, D.S. (1977). Permeability of fluorescein-labelled dextrans in fundus fluorescein angiography of rats and birds. *Exp. Eye Res.* 24, 595-605.

Bellhorn, R.W. (1980). Control of blood vessel development. *Trans. Ophthal. Soc. U.K.* 100, 328-331.

Bellhorn, R.W. and Bellhorn, M.S. (1975). The avian pecten. *Ophthal. Res.* 7, 1-7.

Bellhorn, R.W., Burns, M.S. and Benjamin, J.V. (1980). Retinal vessel abnormalities of phototoxic retinopathy in rats. *Invest. Ophthal. Vis. Sci.* 19, 584-595.

Ben-Nun, J., Alder, V.A., Cringle, S. J. and Constable, I.J. (1988). A new method for oxygen supply to acute ischaemic retina. *Invest. Ophthal. Vis. Sci.* 29, 298-304.

Ben-Sira, I. and Riva, C.E. (1973). Fluorescein angiography and ocular hemodynamics. *Invest. Ophthal. Vis. Sci.* 12, 896-903.

Benevento, L.A. and Ebner, F.F. (1971a). The areas and layers of cortical terminations in the visual cortex of the Virginia opossum. *J. Comp. Neurol.* 141, 157-190.

Benevento, L.A. and Ebner, F.F. (1971b). The contribution of the lateral geniculate nucleus to the total pattern of thalamic terminations in striate cortex of the Virginia opossum. *J. Comp. Neurol.* 141, 243-260.

Berkely, M.A. (1970). In: Stebbins, W. (Ed.) *In: Animal Psychophysics: the Design and Conduct of Sensory Experiments.* (pp. 231-247). Appleton, Century Crofts.

Berkley, M.A. and Watkins, D.W. (1973). Grating resolution and refraction in the cat estimated from evoked cerebral potentials. *Vision Res.* 13, 403-415.

Berkow, J.W. and Patz, A. (1961a). Histochemistry of the retina. I. Introduction and methods. *Arch. Ophthal.* 65, 820-827.

Berkow, J.W. and Patz, A. (1961b). Histochemistry of the retina. II. Use of phenazine methosulfate to demonstrate the succinoxidase system. *Arch. Ophthal.* 65, 828-831.

Berkow, J.W. and Patz, A. (1964). Developmental histochemistry of the rat eye. *Invest. Ophthal. Vis. Sci.* 3, 22-33.

Besharse, J.C. (1982). The daily light-dark cycle and rhythmic metabolism in the photoreceptor-pigment epithelial complex. In: Chader, G.J. (Ed.) *Progress in Retinal Research, Volume 4.* (pp. 81-124). Pergamon Press, Oxford.

Bill, A. (1968). A method to determine osmotically effective albumin and gammaglobulin concentrations in tissue fluids, its application to the uvea and a note on the effects of capillary 'leaks' on tissue fluid dynamics. *Acta. Physiol. Scand.*,

Bill, A. (1975). Blood circulation and fluid dynamics in the eye. *Physiol. Rev.* 55, 383-417.

Bill, A. (1984). Circulation in the eye. In: Renkin, E.M., Michel, C.C. and Geiger, S.R. (Ed.) *Handbook of Physiology, Section 2: The Cardiovascular System.* (pp. 1001-1034). American Physiological Society, Bethesda, Maryland.

Bill, A. (1985). Some aspects of the ocular circulation. The Friedenwald Lecture. *Invest. Ophthal. Vis. Sci.* 26, 410-424.

Bill, A., Sperber, G. and Ujiie, K. (1983). Physiology of the choroidal vascular bed. *Int. Ophthal.* 6, 101-107.

Bill, A., Tornquist, P. and Alm, A. (1980). Permeability of the intraocular blood vessels. *Trans. Ohthal. Soc. U.K.* 100, 332-336.

Birch, D. and Jacobs, G.H. (1979). Spatial contrast sensitivity in albino and pigmented rats. *Vision Res.* 19, 933-937.

Bischoff, P.M. and Flower, R.W. (1985). Ten years experience with choroidal angiography using indocyanine green dye: a new routine examination or an epilogue?. *Doc. Ophthal.* 60, 235-291.

Bisti, S. and Maffei, L. (1974). Behavioural contrast sensitivity of the cat in various visual meridians. *J. Physiol.* 241, 201-210.

Blacharski, P.A. (1985). Twenty-five years of fluorescein angiography. *Arch. Ophthal.* 103, 1301-1302.

Blake, R. (1988). Cat spatial vision. *Trends in Neuro. Sci.* 11, 78-83.

Blanks, J.C. and Johnson, L.V. (1986). Vascular atrophy in the retinal degenerative *rd* mouse. *J. Comp. Neurol.* 254, 543-553.

Bloom, M. and Berkley, M.A. (1977). Visual acuity and the near point of accommodation in cats. *Vision Res.* 17, 723-730.

Bock, W.J. (1988). The nature of explanations in morphology. *Amer. Zool.* 28, 205-215.

Bohlen, H.G. (1979). Arteriolar closure mediated by hyperresponsiveness to norepinephrine in hypertensive rats. *J. Appl. Physiol.* 236, H157-164.

Bohman, S-O, and Maunsbach, A.B. (1970). Effects on tissue fine structure of variations in colloid osmotic pressure of glutaraldehyde fixatives. *J. Ultrastruct. Res.* 30, 195-208.

Bolz, J., Thier, P. and Brecha, N. (1985). Localisation of aspartate aminotransferase and cytochrome oxidase in the cat retina. *Neurosci. Letts.* 53, 315-320.

Borwein, B. (1985). Scanning electron microscopy in retinal research. *Scanning Electron Micros.* II, 279-301.

Braekevelt, C.R. (1973). Fine structure of the retinal pigment epithelium and photoreceptor cells of an Australian marsupial *Setonix brachyurus*. *Can. J. Zool.* 51, 1093-1100.

Braekevelt, C.R. (1976). Fine structure of the retinal epithelium and tapetum lucidum of the opossum (*Didelphis virginiana*). *J. Morph.* 150, 213-226.

Braekevelt, C.R. (1986). Fine structure of the tapetum cellulosum of the grey seal (*Halichoerus grypus*). *Acta. Anat.* 127, 81-87.

Brauer, K., Winkelman, E., Nawka, S. and Strand, W. (1982). Vergleichende volumetrische Untersuchungen am Corpus geniculatum laterale von Säugetieren. *Z. Mikrosk.-Anat. Forsch.* 96, 400-406.

Broadwell, R.D., Charlton, H.M., Balin, B.J. and Salcman, M. (1987). Angioarchitecture of the CNS, pituitary gland and intracerebral grafts revealed with peroxidase cytochemistry. *J. Comp. Neurol.* 260, 47-62.

Brown, G.C and Tasman, W.S. (1983). *Congenital Anomalies of the Optic Disc.* (pp. 54-55). Grune & Stratton, New York.

Brown, K.T. (1968). The electroretinogram: its components and their origins. *Vision Res.* 8, 633-677.

Brown, K.T. and Tasaki, K. (1961). Localisation of electrical activity in the cat retina by an electrode marking method. *J. Physiol.* 158, 281-295.

Brown, K.T. and Wiesel, T.N. (1959). Intraretinal recording with micropipette electrodes in the intact cat eye. *J. Physiol.* 149, 537-562.

Brown, K.T. and Wiesel, T.N. (1961a). Analysis of the intraretinal electroretinogram in the intact cat eye. *J. Physiol.* 158, 229-256.

Brown, K.T. and Wiesel, T.N. (1961b). Localisation of origins of electroretinogram components by intraretinal recording in the intact cat eye. *J. Physiol.* 158, 257-280.

Brown, K.T., Watanabe, K. and Murakami, M. (1965). The early and late receptor potentials of monkey cones and rods. *Cold Spring Harb. Symp.* 30, 457-482.

Bruns, L. (1882). Studien über das Blutgefaszystem der Netzhaut. *Vergletch. Anat.* 77-100.

Bubis, J.J. and Luse, S.A. (1964). An electron microscopic study of the cerebral blood vessels of the opossum. *Cell Tissue Res.* 62, 16-25.

Buerk, D.G. and Saidel, G.M. (1978). Local kinetics of oxygen metabolism in brain and liver tissue. *Microvasc. Res.* 16, 391-405.

Buijs, R. and Dogterom, A.A. (1983). An improved method for embedding hard tissue in polymethyl methacrylate. *Stain Tech.* 58, 135-141.

Bullock, T.H. (1984). Comparative neuroscience holds promise for quiet revolutions. *Science.* 225, 473-478.

Buono, R.J. and Sheffield, J.B. (1989). Metabolism in the developing chick retina: mitochondrial segregation. *Invest. Ophthal. Vis. Sci.* 30, S226.

Burger, P.C., Chandler, D.B., Fryczkowski, A.W. and Klintworth, G.K. (1987). Scanning electron microscopy of microcorrosion casts: Applications in ophthalmic research. *Scan. Micros.* 1, 223-231.

Burstone, M.S. (1959). New histochemical techniques for the demonstration of tissue oxidase (cytochrome oxidase). *J. Histochem. Cytochem.* 7, 112-122.

Burstone, M.S. (1960). Histochemical demonstration of cytochrome oxidase with new amine reagents. *J. Histochem. Cytochem.* 8, 63-70.

Burstone, M.S. (1962). *Enzyme Histochemistry and its Application in the Study of Neoplasms.* (pp. 462-469). Academic Press.

Buttery, R.G., Haight, J.R. and Bell, K. (1990a). Vascular and avascular retinae in mammals: A fundoscopic and fluorescein angiographic study. *Brain Behav. Evol.* 35, 156-175.

Buttery, R.G., Hinrichsen, C.F.L., Weller, W.L. and Haight, J.R. (1990b). How thick should a retina be? A comparative study of mammalian species with and without intraretinal vasculature. *Vision Res.* In press.

Caldwell, R.B. and Slapnick, S.M. (1989). Increased cytochrome oxidase activity in the diabetic retinal pigment epithelium. *Invest. Ophthal. Vis. Sci.* 30, 591-599.

Campbell, F. and Maffei, L. (1970). Electrophysiological evidence for the existence of orientation and size detectors in the human visual system. *J. Physiol.* 207, 635-652.

Campbell, F.W., Maffei, L. and Piccolino, M. (1973). The contrast sensitivity of the cat. *J. Physiol.* 229, 719-731.

Candipan, R.C. and Sjöstrand, F.S. (1984). An analysis of the contribution of the preparatory technique to the appearance of condensed and orthodox conformations of liver mitochondria. *J. Ultrastruct. Res.* 89, 281-294.

Caprioli, J. (1987). The ciliary epithelia and aqueous humor. In: Moses, R.A. and Hart, W.M. (Ed.) *Adler's Physiology of the Eye. Clinical Application.* (pp. 204-222). The C.V. Mosby Company, St Louis.

Carati, C.J., White, G.H. and Gannon, B.J. (1989). The blood brain barrier: a marsupial alternative to the eutherian solution?. In: Baudinette, R.V.and Frappell, P.B. (Ed.) *Sixth Comparative Physiologists Meeting.* (pp. 5).

Carroll, E.W. and Wong-Riley, M.T.T. (1984). Quantitative light and electron microscopic analysis of cytochrome oxidase-rich zones in the striate cortex of the squirrel monkey. *J. Comp. Neurol.* 222, 1-17.

Charonis, A. and Wissig, S.L. (1983). Anionic sites in basement membranes. Differences in their electrostatic properties in continuous and fenestrated capillaries. *Microvasc. Res.* 25, 265-285.

Chase, J. (1982). The evolution of retinal vascularisation in mammals. A comparison of vascular and avascular retinae. *Ophthalmology.* 89, 1518-1525.

Chaudhuri, A., Hallett, P.E. and Parker, J.A. (1983). Aspheric curvatures, refactive indices and chromatic aberration for the rat. *Vision Res.* 23, 1351-1363.

Cleland, B.G., Harding, T.H. and Tulunay-Keesing, U. (1979). Visual resolution and receptive field size: examination of two kinds of cat retinal ganglion cell. *Science.* 205, 1015-1017.

Cogan, D.G. and Kuwabara, T. (1959). Tetrazolium studies on the retina: II. Substrate dependent patterns. *J. Histochem.* 7, 334-341.

Cogan, D.G. and Kuwabara, T. (1984). Comparison of retinal and cerebral vasculature in trypsin digest preparations. *Brit. J. Ophthal.* 68, 10-12.

Cohen, A.I. (1987). The retina. In: Moses, R.A. and Hart, W.M. (Ed.) *Adler's Physiology of the Eye. Clinical Application.* (pp. 458-491). The C.V. Mosby Company, St Louis.

Cohen, L.H. and Noell, W.K. (1960). Glucose catabolism of rabbit retina before and after development of visual function. *J. Neurochem.* 5, 253-276.

Cole, D.F. (1974). Comparative aspects of the intraocular fluids. In: Davson, H. (Ed.) *The Eye. Volume 5, Comparative Physiolgy.* (pp. 71-161). Academic Press, New York.

Cole, F.J. (1921). The history of anatomical injections. In: Singer, C. (Ed.) *Studies in the history and methods of science. Vol II.* (pp. 285-343). Clarendon Press, Oxford.

Coleman, D.J. and Lizzi, F.L. (1979). In vivo choroidal thickness measurement. *Am. J. Ophthal.* 88, 369-375.

Copeland, D.E. (1974). The anatomy and fine structure of the eye in teleost. II. The vascular connections of the lentiform body in *Fundulus grandis. Exp. Eye Res.* 19, 583-589.

Copeland, D.E. (1976). The anatomy and fine structure of the eye in teleost. IV. The choriocapillaris and the dual vascularisation of the area centralis in *Fundulus grandis. Exp. Eye Res.* 22, 169-179.

Copeland, D.E. and Brown, D.S. (1976). The anatomy and fine structure of the eye in teleosts. V. Vascular relations of choriocapillaris, lentiform body and falciform body in rainbow trout (*Salmo gardneri*). *Exp. Eye Res.* 23, 15-27.

Coyle, P. (1978). Special features of the rat hippocampal vascular system. *Exp. Neurol.* 58, 549-561.

Craigie, E.H. (1938a). The blood vessels in the central nervous system of the kangaroo. *Science.* 88, 359-360.

Craigie, E.H. (1938b). *The Comparative Anatomy and Embryology of the Capillary Bed of the Central Nervous System.* Williams and Wilkins Co., Baltimore.

Crewther, D.P., Crewther, S.G., and Sanderson, K.J. (1984). Primary visual cortex in the brushtailed possum: Receptive field properties and corticocortical connections. *Brain Behav. Evol.* 24, 184-197.

Criswick, V.G. and Harris, G.S. (1967). The effect of hyperbaric oxygen on adult rabbit retina. *Arch. Ophthal.* 78, 788-793.

Crone, C. and Levitt, D.G. (1984). Capillary permeability to small solutes. In: Renkin, E.M. and Michel, C.C. (Ed.) *Handbook of Sensory Physiology, Section 2: The Cardiovascular System.* (pp. 411-466). American Physiology Society, Bethesda Maryland

Curcio, C.A., Sloan, K.R., Kalina, R.E. and Hendrickson, A.E. (1990). Human photoreceptor topography. *J. Comp. Neurol.* 292, 497-523.

Cutright, D.E. and Bhaskar, S.N. (1967). A new method of demonstrating microvasculature. *Oral Surg. Oral Path. Conf.* 24, 422-426.

Dae, M.W., Heymann, A. and Jones, A.L. (1982). A new technique for perfusion fixation and contrast enhancement of foetal lamb myocardium for electron microscopy. *J. Microscopy.* 127, 301-305.

Davson, H. (1979). The little brain. The Bowman Lecture. *Trans. Ophthal. Soc. U.K.* 99, 21-36.

Davson, H. (1980). *Physiology of the Eye*. Churchill Livingstone, Edinburgh.

Dean, P. (1978). Visual acuity in hooded rats: effects of superior collicular or posterior neocortical lesions. *Brain Res.* 156, 17-31.

Decker, D., Faust, U. and Irion, K.M. (1981). Examination of thin tissue layers in the human eye. *Med. Progr. Technol.* 8, 83-91.

del Cerro M., Grover, D.A., Dematte, J. A., Williams, W.M. and Nobuo, I. (1985). Colloidal carbon as a combined ophthalmoscopic and microscopic probe of retinal and choroidal vascular integrity. *Ophthal. Res.* 17, 34-41.

Desrochers, P.E., Pratt, K.A., Fromm, P.O. and Hoffert, J.R. (1985). Oxygen diffusion in the trout retina. *Exp. Eye Res.* 41, 607-618.

Detwiler, S.R. (1943). *Vertebrate Photoreceptors*. Macmillan Company, New York.

Deutsch, K. and Hillman, H. (1977). The effects of six fixatives on areas of rabbit neurons and rabbit and rat cerebral cortex. *J. Microscopy.* 109, 303-309.

Dick, E. (1984). Enzymes of energy metabolism in the mudpuppy retina. *J. Neurochem.* 43, 1124-1131.

Dieterich, C.E., Dieterich, H.J. and Hildebrand, R. (1976). Comparative electron-microscopic studies on the conus papillaris and its relationship to the retina in night and day active geckos. *Albrecht v.Graefes Arch. klin. exp. Ophthal.* 200, 27

Difiglia, M., Graveland, G.A. and Schiff, L. (1987). Cytochrome oxidase activity in the rat caudate nucleus: Light and electron microscopic observation. *J. Comp. Neurol.* 255, 137-145.

Dobi, E.T., Puliafito, C.A. and Destro, M. (1989). A new model of experimental choroidal neovascularization in the rat. *Arch. Ophthal.* 107, 264-269.

Dobson, V. and Teller, D.Y. (1978). Visual acuity in human infants: a review and comparison of behavioural and electrophysiological studies. *Vision Res.* 18, 1469-1483.

Doft, B.H. (1983). Choroidoretinal vascular anastomosis. *Arch. Ophthal.* 101, 1053-1054.

Dollery, C.T. Bulpitt, C.J. and Kohner, E.M. (1969). Oxygen supply to the retina from the retinal and choroidal circulations at normal and increased oxygen tensions. *Invest. Ophthal. Vis. Sci.* 8, 588-594.

Dollinger, R.K. and Armstrong, P.B. (1974). Scanning electron microscopy of injection replicas of the chick embryo circulatory system. *J. Microscopy.* 102, 179-186.

Dom, R., Fisher, B.L. and Martin, G.F. (1970). The venous system of the head and neck of the opossum (*Didelphis virginiana*). *J. Morph.* 132, 487-496.

Dowling, J.E. (1987). *The Retina.* Harvard University Press, Cambridge MA.

Dräger, U.C. and Olsen, J.F. (1981). Ganglion cell distribution in the retina of the mouse. *Invest. Ophthal. Vis. Sci.* 20, 285-293.

Ducournau, D.H. (1982). A new technique for the anatomical study of the choroidal blood vessels. *Ophthalmologica.* 184, 190-197.

Dueker, D.K., Kier, E.L. and Rothman, S.L.G. (1974). Microangiography of the rabbit eye: a radiographic study. *Invest. Ophthal. Vis. Sci.* 13, 543-547.

Duke-Elder, S. (1963). *System of Ophthalmology. Vol III. Normal and Abnormal Development. Part I Embroyology.* H.K. Lewis, London.

Duke-Elder, S. and Wybar, K.C. (1961). *System of Ophthalmology, Volume II. The Anatomy of the Visual System.* The C.V. Mosby Company, St Louis.

Eccles, J.C., Ito, M. and Szentágothai, J. (1967). *The Cerebellum as a Neuronal Machine.* Springer-Verlag, New York.

Ellsworth, M.L. and Pittman, R.N. (1984). Heterogeneity of oxygen diffusion through hamster striated muscle. *Am. J. Physiol.* 246, H161-H167.

Emi, K., Kobayashi, Y., Chujo, S., Fujioka, C. and Yokayama, M. (1983). The biometry of each thickness of the human retina, choroid and sclera by using ultrasound and Fourier analysis-at the foveola. *Nippon Ganka Gakkai Zasshi.* 87, 74-78.

Eränkö, O., Niemi, M. and Merenmies, E. (1961). Histochemical observations on esterases and oxidative enzymes of the retina. In: Smelser, G.K. (Ed.) *The structure of the eye.* (pp. 159-171). Academic Press, New York.

Essner, E. Gordon, S.R. (1983). Observations on the permeability of the choriocapillaris of the eye. *Cell Tissue Res.* 231, 571-577.

Etingof, R.N. and Shukolyukov, S.A. (1965). Glycolysis of the retina and some properties of retinal mitochondria. *Fed. Proc. (Transl. Supp.).* 11, T758-T762.

Fairbanks, M.B, Hoffert, J.R. and Fromm, P.O. (1969). The dependence of the oxygen concentrating mechanism of the teleost eye (*Salmo gairdneri*) on the enzyme carbonic anhydrase. *J. Gen. Physiol.* 54, 203-211.

Fairbanks, M.B, Hoffert, J.R. and Fromm, P.O. (1974). Short circuiting the ocular oxygen-concentrating mechanism in the teleost *Salmo gairdneri* using carbonic anhydrase inhibitors. *J. Gen. Physiol.* 64, 263-273.

Favilla, I., Barry, W.R. and Turner, I.J. (1986). Video and digital fluorescein angiography. *Aust. and N.Z. J. Ophthal.* 14, 229-234.

Federspiel, W.J. and Popel, A.S. (1986). A theoretical analysis of the effect of the particulate nature of blood on oxygen release in capillaries. *Microvasc. Res.* 32, 164-189.

Fink, S. (1986). A new integrated concept for the improved preparation of sections of fresh frozen tissue for light microscope histochemistry. *Histochem.* 86, 43-52.

Fite, K.V. (1973). Anatomical and behavioural correlates of visual acuity in the great horned owl. *Vision Res.* 13, 219-230.

Flocks, M., Miller, J. and Chao, P. (1959). Retinal circulation time with the aid of fundus cinephotography. *Am. J. Ophthal.* 48, 3-6.

Flower, R.W. and Hochheimer, B.F. (1976). Indocyanine green dye fluorescence and infrared absorption choroidal angiography performed simultaneously with fluorescein angiography. *Johns Hopkins Med. J.* 138, 33-42.

Flower, R.W. and Hochheimer, B.F. (1977). Quantification of indicator dye concentration in ocular blood vessels. *Exp. Eye Res.* 25, 103-111.

Flower, R.W. and Patz, A. (1971). The effect of hyperbaric oxygenation on retinal ischaemia. *Invest. Ophthal. Vis. Sci.* 10, 605-616.

Flower, R.W., Hall, M.O. and Patz, A. (1984). Oxygen. In: Sears, M.L. (Ed.) *Pharmacology of the Eye*. (pp. 627-638). Springer-Verlag, Berlin.

Fox, C.H., Johnson, F.B., Whiting, J. and Roller, P.P. (1985). Formaldehyde fixation. *J. Histochem. Cytochem.* 33, 845-853.

François, J. and Neetens, A. (1974). Comparative anatomy of the vascular supply of the eye in vertebrates. In: Davson, H. and Graham, L.T. (Ed.) *The Eye. Volume 5. Comparative Physiology.* (pp. 1-70). Academic Press, New York.

Frasch, A.C.C., Itoiz, M.E. and Cabrini, R.L. (1978). Microspectrophotometric quantitation of the diaminobenzidine reaction for histochemical demonstration of cytochrome activity. *J. Histochem. Cytochem.* 26, 157-162.

Freeman, B. (1978). The retinal origins of the optic nerve conduction latency groups in the brush-tailed possum, *Trichosurus vulpecula*. *J. Comp. Neurol.* 179, 753-760.

Freeman, B. and Watson, C.R.R. (1978). The optic nerve of the brush-tailed possum, *Trichosurus vulpecula*: Fibre diameter and conduction latency groups. *J. Comp. Neurol.* 179, 739-752.

Freeman, B.and Tancred, E. (1978). The number and distribution of ganglion cells in the retina of of the brush-tailed possum, *Trichosurus vulpecula*. *J. Comp. Neurol.* 177, 557-568.

Friedenwald, J. (1949). A new approach to some problems of retinal vascular disease. *Am. J. Ophthal.* 32, 487.

Friedman, E., Smith, T.R. and Kuwabara, T. (1964). Retinal microcirculation in vivo. *Invest. Ophthal. Vis. Sci.* 3, 217-226.

Fryczkowski, A.W., Grimson, B.S. and Peiffer, R.L. (1984). Scanning electron microscopy of vascular casts of the human scleral lamina cribrosa. *Int. Ophthal.* 7, 95-100.

Fryczkowski, A.W. Grimson, B.S. and Peiffer, R.L. (1985b). Vascular casting and scanning electron microscopy of human ocular vascular abnormalities. *Arch. Ophthal.* 103, 118-120.

Fryczkowski, A.W., Hodes, B.L. and Walker, J. (1989). Diabetic choroidal and iris vasculature scanning electron microscopy findings. *Int. Ophthal.* 13, 269-279.

Fryczkowski, A.W., Peiffer, R.L., Merritt, J.C. Kraybill, E.N. and Eifrig, D (1985a). Scanning electron microscopy of the ocular vasculature in retinopathy of prematurity. *Arch. Ophthal.* 103, 224-228.

Fryzczkowski, A.W. (1987). Vascular casting and scanning electron microscopy in diabetes. *Scan. Micros.* 1, 811-816.

Fukuda, Y. (1977). A three-group classification of rat retinal ganglion cells: histological and physiological studies. *Brain Res.* 119, 327-344.

Funk, R. (1986). Studies on the functional morphology of rat ocular vessels with scanning electron microscopy. *Acta Anat.* 125, 252-257.

Funk, R. and Rohen, J.W. (1987). Intraocular microendoscopy of the ciliary-process vasculature in albino rabbits: Effects of vasoactive agents. *Exp. Eye Res.* 45, 597-606.

Gannon, B.J. (1978). Vascular casting. In: Hayat, M.A. (Ed.) *Principles and Techniques of Scanning Electron Microscopy. Biological Applications Volume 6.* (pp. 170-193). Van Nostrand Reinhold Company, New York.

Gannon, B.J. (1981). Preparation of microvascular corrosion casting media: procedure for partial polymerisation of methyl methacrylate using ultraviolet light. *Biomedical Res.* 2, 227-233.

Gannon, B.J. (1985). Vascular casting workshop. *Workshop, 10th N.Z. E.M. Congress.* 1-14.

Gannon, B.J., Baudinette, R.V., Runciman, S.I.C. and Frappell, P.B. (1989). Cardiorespiratory structure and function in macropodid marsupials. In: Grigg, G., Jarman, P. and Hume, I. (Ed.) *Kangaroos, Wallabies and Rat-Kangaroos.* (pp. 407-418). Surrey Beattie & Sons Pty Limited, Chipping Norton, NSW.

Garcia, O.S. and Essinger, L.A. (1985). Vascularisation of the retina and optic nerve of the opossum. *Rev. Bras. Biol.* 45, 13-20.

Gardner-Medwin, A.R. (1984). A foot in the vitreous fluid. *Nature.* 309, 113.

Gartner, S. and Henkind, P. (1981). Ageing and degeneration of the retina I. Outer nuclear layer and photoreceptors. *Brit. J. Ophthal.* 65, 173-179.

Ghinea, N. and Simionescu, N. (1985). Anionised and cationised hemeundecapeptides as probes for cell surface charge and permeability studies: Differentiated labeling of endothelial plasmalemmal vesicles. *J. Cell Biol.* 100, 606-612.

Gillilan, L.A. (1972). Blood supply to primitive mammalian brains. *J. Comp. Neurol.* 145, 209-221.

Glaser, B.M. (1986). Cell biology and biochemistry of endothelial cells and the phenomenon of intraocular neovascularisation. In: Adler, R. and Farber, D (Ed.) *The Retina, a Model for Cell Biology Studies, Part II.* (pp. 215-243). Academic Press, Orlando.

Glaser, B.M., D'Amore, P.A., Michels, R.G., Patz, A. and Fenselau, A. (1980). Demonstration of vasoproliferative activity from mammalian retina. *J. Cell Biol.* 84, 298-304.

Glauret, A.M. (1975). *Fixation, Dehydration and Embedding of Biological Specimens. Practical Methods in Electron microscopy.* North Holland, Amsterdam.

Glickstein, M. and Millodot, M. (1970). Retinoscopy and eye size. *Science.* 168, 605-606.

Gloor, B.P. (1987). The vitreous. In: Moses, R.A. and Hart, W.M. (Ed.) *Adler's Physiology of the Eye. Clinical Application.* (pp. 246-268). The C.V. Mosby Company, St Louis.

Goldstein, I., and Wexler, D. (1929). The preretinal artery. An anatomic study. *Arch. Ophthal.* 11, 324-334.

Gole, G.A., Gannon, B.J. and Goodger, A.M. (1982). Oxygen induced retinopathy: The kitten model re-examined. *Aust. NZ. J. Ophthal.* 10, 223-232.

Gonzalez-Aguilar, F. (1982). Cell volume preservation and the reflection coefficient in chemical fixation. *J. Ultrastruct. Res.* 80, 354-362.

Graymore, C.N. (1969). General aspects of the metabolism of the retina. In: Davson, H. (Ed.) *The Eye. Volume 1. Vegative Physiology and Biochemistry.* (pp. 601-645). Academic Press, New York.

Green, H.D., Schmid, U.E. and Rapela, C.S. (1964). Autoregulation in vascular beds - possible role of autoregulation in the increased resistance to flow in hypertension. *Hypertension.* XIII, 144-159.

Greene, E.C. (1955). Anatomy of the rat. *Trans. Amer. Phil. Soc.* 27, 177-337.

Grotte, D., Mattox, V. and Brubaker, R. (1985). Fluorescent, physiological and pharmacokinetic properties of fluorescein glucuronide. *Exp. Eye Res.* 40, 23-33.

Hackenbrock, C.R. (1966). Ultrastructural bases for the metabolically linked mechanical activity in mitochondria I. Reversible ultrastructural changes with change in metabolic steady state in isolated liver mitochondria. *J. Cell Biol.* 30, 269-29

Hackenbrock, C.R. (1968a). Ultrastructural bases for the metabolically linked mechanical activity in mitochondria II. Electron transport-linked ultrastructural transformations in mitochondria. *J. Cell Biol.* 37, 345-369.

Hackenbrock, C.R. (1968b). Chemical and physical fixation of isolated mitochondria in low-energy and high-energy states. *Biochem.* 61, 598-605.

Hackenbrock, C.R., Rehn, T.G., Weinbach, E.C. and Lemasters, J.J. (1971). Oxidative phosphorylation and ultrastructural transformation in mitochondria in the intact ascites tumor cell. *J. Cell Biol.* 51, 123-137.

Haight, J.H. and Sanderson, K.J. (1990). An autoradiographic analysis of the organisation and retinal projections to the dorsal lateral geniculate nucleus in two bandicoots, *Perameles gunnii* and *Isoodon obesulus*; do bandicoots see like polyprotodonts or diprotodonts. In: Seebeck, J.H. Brown, P.R., Wallis, R.L. and Kemper. R.L. (Eds.) *Bandicoots*. Surrey Beatty and Sons, Sydney.

Haight, J.R. and Murray, P.F. (1981). The cranial endocasts of the early Miocene marsupial, *Wynyardia bassiana*: An assessment of taxonomic relationships based upon comparisons with recent forms. *Brain Behav. Evol.* 19, 17-36.

Haight, J.R. and Sanderson, K.J. (1988). Retinal projections in two Australian polyprotodont marsupials: kowari, *Dasyuroides byrnei*, and fat-tailed dunnart, *Sminthopsis crassicaudata* (Dasyuridae). *Brain Behav. Evol.* 31, 96-110.

Haight, J.R., Sanderson, K.J., Neylon, L. and Patten, G.S. (1980). Relationships of the visual cortex in the marsupial brush-tailed possum, *Trichosurus vulpecula*, a horseradish peroxidase and autoradiographic study. *J.Anat.* 131, 387-412.

Hansson, H-A (1971a). A histochemical study on the distribution of oxidative enzymes in retinal cultures. *Exp. Eye Res.* 11, 89-97.

Hansson, H-A (1971b). The effect of phenazine methosulphate on the histochemical demonstration of oxidative enzymes in retinal cultures. *Exp. Eye Res.* 11, 89-97.

Hanstede, J.G. and Gerrits, P.O. (1982). The effects of embedding in water-soluble plastics on the final dimensions of liver sections. *J. Microscopy.* 131, 79-86.

Haraldsson, B., Ekholm, C. and Rippe, B. (1983). Importance of molecular charge for the passage of endogenous macromolecules across continuous capillary walls, studied by serum Lactate Dehydrogenase (LDH) isoenzyme. *Acta. Physiol. Scand.* 117, 123-130.

Harman, A.M., Nelson, J.E., Crewther, S.G. and Crewther, D.P. (1986). Visual acuity of the northern native cat (*Dasyurus hallucatus*)- behavioural and anatomical estimates. *Behav. Brain Res.* 22, 211-216.

Harper, R.N., Moore, M.A., Marr, M.C., Watts, L.E. and Hutchins, P.M. (1978). Arteriolar rarefaction in the conjunctiva of human essential hypertension. *Microvasc. Res.* 16, 369-372.

Hart, W.M. (1987). Visual adaptation. In: Moses, R.A. and Hart, W.M. (Ed.) *Adler's Physiology of the Eye. Clinical Application.* (pp. 389-415). The C.V. Mosby Company, St Louis.

Harter, M.R. and White, C.T. (1968). Effects of contour sharpness and check-size on visually evoked cortical potentials. *Vision Res.* 8, 701-711.

Hausler, H.R. and Siboy, T.M. (1959). A contribution to the injection technique for studying retinal blood vessels. *Am. J. Ophthal.* 48, 138.

Hayat, M.A. (1981). *Fixation for Electron Microscopy.* Academic Press, New York.

Hayreh, S.S. (1974). Recent advances in fluorescein angiography. *Brit. J. Ophthal.* 58, 391-412.

Hayreh, S.S. (1983). Macular lesions secondary to choroidal vascular lesions. *Int. Ophthal.* 6, 161-170.

Hayreh, S.S. (1983). Physiological anatomy of the choroidal vascular bed. *Int. Ophthal.* 6, 85-93.

Hayreh, S.S. and Scott, W.E. (1978). Fluorescein iris angiography. I. Normal pattern. *Arch. Ophthal.* 96, 1383-1389.

Hayreh. S.S. (1975). The segmental nature of the choroidal vasculature. *Brit. J. Ophthal.* 59, 631-648.

Hazlett, L.D. (1976). Fine structure of the opossum (*Didelphis virginiana*) retina. *Anat. Rec.* 184, 587.

Heath, C.J. and Jones, E.G. (1971). Interhemispheric pathways in the absence of a corpus callosum. An experimental study of commisural connexions in the marsupial phalanger. *J. Anat.* 109, 253-270.

Hellums, J.D. (1977). The resistance to oxygen transport in the capillaries relative to that in the surrounding tissue. *Microvasc. Res.* 13, 131-136.

Henkind, P. and De Oliveira, L.F. (1968). Retinal arteriolar annuli. *Invest. Ophthal. Vis. Sci.* 7, 584-591.

Henkind, P. and Wise, G.N. (1974). Retinal neovascularisation, collaterals and vascular shunts. *Brit. J. Ophthal.* 58, 413-422.

Herman, K.G. and Steinberg, R.H. (1982a). Phagosome movement and the diurnal pattern of phagocytosis in the tapetal retinal pigment epithelium of the opossum. *Invest. Ophthal. Vis. Sci.* 23, 277-290.

Herman, K.G. and Steinberg, R.H. (1982b). Phagosome degredation in the tapetal retinal epithelium of the opossum. *Invest. Ophthal. Vis. Sci.* 23, 291-304.

Hevner, R.F and Wong-Riley, M.T.T. (1989). Brain cytochrome oxidase: purification, antibody production, and immunohistochemical/histochemical correlations in the CNS. *J. Neurosci.* 9, 3884-3898.

Higuchi, S., Suga, M., Dannenberg, A.M. and Schofield, B.H. (1979). Histochemical demonstration of enzyme activities in plastic and paraffin embedded tissue sections. *Stain Tech.* 54, 5-12.

Hill, D.W. and Young, S. (1976). Arterial inflow studies of the cat retina using high-speed cine angiography. *Exp. Eye Res.* 23, 35-45.

Hiraoka, T., Hirai, K-I and Uyeda, T. (1985). A microspectrophotometric quantification of cytochrome oxidase activity by means of color-modified diaminobenzidine reaction. *Acta. Histochem. Cytochem.* 18, 283-292.

Hiraoka, T., Hirai, K-I and Uyeda, T. (1986). Cobalt acetylacetonate-diaminobenzidine reaction for microspectrophotometry of cytochrome oxidase. *Acta. Histochem. Cytochem.* 19, 429-436.

Hiscott, P.S., Grierson, I., Trombetta, C.J., Rahi, A.H.S., Marshall, J and (1984). McLeod, D. Retinal and epiretinal glia - an immunohistochemical study. *Brit. J. Ophthal.* 68, 698-707.

Hochachka, P.W. (1986). Defense strategies against hypoxia and hypothermia. *Science.* 231, 234-241.

Hochheimer, B.F. (1979). A dye for experimental choroidal angiography. *Exp. Eye Res.* 29, 141-143.

Hodde, K.C. and Nowell, J.A. (1980). SEM of micro-corrosion casts. *Scanning Electron Microscopy.* II, 89-106.

Hogan, M.J., Alvarado, J.A. and Weddell, J.E. (1971). *Histology of the Human Eye.* W.B. Saunders, Philadelphia.

Hokoç, J.N. and Oswaldo-Cruz, E. (1979). A regional specialisation in the opossum's retina: quantitative analysis of the ganglion cell layer. *J. Comp. Neurol.* 183, 385-396.

Horton, J.C. and Hubel, D.H. (1980). Correlation of cytochrome oxidase staining with 2-deoxyglucose uptake in the monkey visual cortex. *Arch. Biol. Med. Exp.* 13, 12.

Horton, J.C. and Hubel, D.H. (1981). Regular patchy distribution of cytochrome oxidase staining in primary visual cortex of macaque monkey. *Nature.* 292, 762-764.

Hossler, F.E. and Olson, K.R. (1984). Microvasculature of the avian eye: Studies on the eye of the duckling with microcorrosion casting, scanning electron microscopy, and stereology. *Amer. J. Anat.* 170, 205-221.

Hossler, F.E., Douglas, J.E. and Douglas, L.E. (1986). Anatomy and morphometry of myocardial capillaries studied with vascular corrosion casting and scanning electron microscopy: A method for the rat heart. *Scanning Electron Micros.* IV, 1469-147

Howell, W.L., Rapp, L.M. and Williams, T.P. (1982). Distribution of melanosomes across the retinal pigment epithelium of a hooded rat: implications for light damage. *Invest. Ophthal. Vis. Sci.* 22, 139-144.

Hughes, A. (1972). A schematic eye for the rabbit. *Vision Res.* 12, 123-138.

Hughes, A. (1975a). A quantitative analysis of the cat retinal ganglion cell topography. *J. Comp. Neurol.* 163, 107-128.

Hughes, A. (1975b). A comparison of retinal ganglion cell topography in the plains and tree kangaroo. *J. Physiol. (Lond.).* 244, 61-63.

Hughes, A. (1976). A supplement to the cat schematic eye. *Vision Res.* 16, 149-154.

Hughes, A. (1977a). The topography of vision in mammals of contrasting life style: comparative optics and retinal organisation. In: Crescitelli, F. (Ed.) *Handbook of sensory physiology. The visual system in vertebrates.* (pp. 615-756). Spriner Verlag, Berlin.

Hughes, A. (1977b). The refractive state of the rat eye. *Vision Res.* 17, 927-939.

Hughes, A. (1979a). A schematic eye for the rat. *Vision Res.* 19, 569-588.

Hughes, A. (1979b). The artefact of retinoscopy in the rat and rabbit eye has its origin at the retina/vitreous interface rather than in longitudinal chromatic aberration. *Vision Res.* 19, 1293-1294.

Hughes, A. (1981). One brush tailed possum can browse as much pasture as 0.06 sheep which may indicate why this arboreal animal has a visual streak: some comments on the terrain theory. *Vision Res.* 21, 957-958.

Hughes, A. (1986). The schematic eye comes of age. In: Pettigrew, J.D., Sanderson, K.J. and Levick, W.R. (Ed.) *Visual Neuroscience.* (pp. 60-89). Cambridge University Press, Cambridge.

Hughes, A. and Wassle, H. (1979). An estimate of the image quality in the rat eye. *Invest. Ophthal. Vis. Sci.* 18, 879-881.

Hughes, J.T., Jerrome, D. and Krebs, H.A. (1972). Ultrastructure of the avian retina. An anatomical study of the retina of the domestic pigeon (*Columba liva*) with particular reference to the distribution of mitochondria. *Exp. Eye Res.* 14, 189-195.

Humason. G.L. (1972). *Animal Tissue Technique.* W.H. Freeman, San Francisco.

Jacobson, S.G., Franklin, K.B.J. and McDonald, W.I. (1976). Visual acuity of the cat. *Vision Res.* 16, 1141-1143.

James, N.T. and Meek, G.A. (1979). Stereologial analyses of the structure of mitochondria in pigeon skeletal muscle. *Cell Tissue Res.* 202, 493-503.

Jampol, L.M. and Cunha-Vaz, J. (1984). Diagnostic agents in ophthalmology: sodium fluorescein and other dyes. In: Born, G.V.R. et al. (Ed.) *Handbook of experimental pharmacology. Pharmacology of the eye.* (pp. 699-714). Springer-Verlag, Berlin.

Jen, L.S., Chau, R.M.W.and Tsang, D. (1989b). Cytochrome oxidase activity in retinas transplanted to the brainstem in rats. *Neurosci. Letts.* 105, 275-280.

Jen, L.S., Zhao, L.P. and Chau, R.M.W. (1989a). Cytochrome oxidase activity in the rat retina following unilateral thalamic lesion. *Neurosci. Letts.* 103, 133-138.

Johnson, G.L. (1901). Contributions to the comparative anatomy of vertebrates, chiefly based on ophthalmoscopic examination. *Phil. Trans. Roy. Soc. London, B.* 194, 1-82.

Johnson, G.L. (1927). VII. Contributions to the comparative anatomy of the reptilian and the amphibian eye, chiefly based on ophthalmoscopic examination. *Phil. Trans. Roy. Soc. London, B.* 215, 315-352.

Johnson, G.L. (1968). Ophthalmoscopic studies on the eyes of mammals. *Phil. Trans. Roy. Soc. London, B.* 254, 207-220.

Johnson, J.I. (1977). Central nervous system of marsupials. In: Hunsaker, D. (Ed.) *The Biology of Marsupials*. (pp. 157-278). Academic Press, New York.

Johnson, J.I. (1986). Mammalian evolution as seen in visual and other neural systems. In: Pettigrew, J.D., Sanderson, K.J. and Levick, W.R. (Ed.) *Visual Neuroscience*. (pp. 196-207). Cambridge University Press, Cambridge.

Jones, D.P. (1984). Effect of mitochondrial clustering on oxygen supply in hepatocytes. *Am. J. Physiol.* 247, C83-C89.

Jones, D.P., Kennedy, F.G., Andersson, B.S., Aw, T.Y. and Wilson, E. (1985). When is a mammalian cell hypoxic? Insights from studies of cell versus mitochondria. *Mol. Physiol.* 8, 473.

Joris, I., DeGirolami, U., Wortham, K. and Majno, G. (1982). Vascular labelling with monastral blue b. *Stain Tech.* 57, 177-183.

Kaas, J.H., Guillery, R.W. and Allman, J.M. (1972). Some principles of organisation in the dorsal lateral geniculate nucleus. *Brain Behav. Evol.* 6, 253-299.

Kaas, J.H., Huerta, M.F., Weber, J.T. and Harting, J.K. (1978). Patterns of retinal terminations and laminar organization of the lateral geniculate nucleus of primates. *J. Comp. Neurol.* 182, 517-553.

Kageyama, G.H. and Meyer, R. (1988). Histochemical localisation of cytochrome oxidase in the retina and optic tectum of normal goldfish: A combined cytochrome oxidase-horseradish peroxidase study. *J. Comp. Neurol.* 270, 354-371.

Kageyama, G.H. and Wong-Riley, M.T.T. (1982). Histochemical localization of cytochrome oxidase in the hippocampus: correlation with specific neuronal types and afferent pathways. *Neuroscience*. 7, 2337-2361.

Kageyama, G.H. and Wong-Riley, M.T.T. (1984). The histochemical localization of cytochrome oxidase in the retina and lateral geniculate nucleus of the ferret, cat and monkey, with

particular reference to retinal mosaics and on/off-center visual channels. *Neuroscience.* 4, 2445-2459.

Kageyama, G.H. and Wong-Riley, M.T.T. (1985). An analysis of the cellular localisation of cytochrome oxidase in the lateral geniculate nucleus of the adult cat. *J. Comp. Neurol.* 242, 338-357.

Kageyama, G.H. and Wong-Riley, M.T.T. (1986a). The localization of cytochrome oxidase in LGN and the striate cortex of postnatal kittens. *J. Comp. Neurol.* 243, 182-194.

Kageyama, G.H. and Wong-Riley, M.T.T. (1986b). Laminar and cellular localization of cytochrome oxidase in the cat striate cortex. *J. Comp. Neurol.* 245, 137-159.

Kageyama, G.H. and Wong-Riley, M.T.T. (1986c). Differential effect of visual deprivation on cytochrome oxidase levels in major cell classes of the cat LGN. *J. Comp. Neurol.* 246, 212-237.

Kamo, N., Muratsugu, M., Kurihara, K. and Kobatake, Y. (1976). Change in surface charge density and membrane potential of intact mitochondria during energization. *FEBS Letters.* 72, 247-250.

Kaneko, A. (1979). Physiology of the retina. *Ann. Rev. Neurosci.* 2, 169-191.

Kanski, J.J. (1987). *Clinical Ophthalmology.* Butterworths, London.

Kaskel, D., Hockwin, O., Metzler, U. and Schedtler, C-M (1973). Glycogen content in the rabbit retina in relation to blood circulation. *Ophthal. Res.* 5, 177-185.

Keele, C.A., Neil, E. and Joels, N. (1984). *Samson Wright's Applied Physiology.* Oxford University Press, Oxford.

Kennedy, H., Bullier, J. and Dehay, C. (1985). Cytochrome oxidase activity in the striate cortex and lateral geniculate nucleus of the newborn macque monkey. *Exp. Brain Res.* 61, 204-209.

Kiernan, J.A. (1981). *Histological and Histochemical Methods: Theory and Practice.* Pergamon Press, Oxford.

Kikai, K. (1930). Uber die Vitalfarbung des hinteren Bulbusabschnittes. *Arch. Augenheilkd.* 103, 541-553.

Kirsch, J.A.W. (1977a). The classification of marsupials. In: Hunsaker, D. (Ed.) *The Biology of Marsupials.* (pp. 1-50). Academic Press, New York.

Kirsch, J.A.W. (1977b). The comparative serology of Marsupialia, and a classification of marsupials. *Aust. J. Zool. (Supp.).* 52, 1-152.

Kirsch, J.A.W. (1983). Phylogeny through brain traits: objectives and methods. *Brain Behav. Evol.* 22, 53-59.

Kirsch, J.A.W. and Johnson, J.I. (1983). Phylogeny through brain traits: trees generated by neural characters. *Brain Behav. Evol.* 22, 60-69.

Kirsch, J.A.W., Johnson, J.I. and Switzer, R.C. (1983). Phylogeny through brain traits: the mammalian family tree. *Brain Behav. Evol.* 22, 70-74.

Knight, G.E. (1966). Injection-digest method for studying retinal vessels. *Brit. J. Ophthal.* 50, 144-146.

Knoll, G. and Brdiczka, D. (1983). Changes in freeze-fractured mitochondrial membranes correlated to their membrane state. Dynamic interactions of the boundry membranes. *Biochim. Biophys. Acta.* 733, 102-110.

Koenig, H.M., Groat, R.A. and Windle, W.F. (1945). A physiological approach to perfusion-fixation of tissues with formalin. *Stain Tech.* 20, 13-24.

Kolb, H. and Wang, H.H. (1985). The distribution of photoreceptors, dopaminergic amacrine cells and ganglion cells in the retina of the North American opossum (*Didelphis virginiana*). *Vision Res.* 25, 1207-1221.

Kottow, M.H. (1980). Fluorescein angiography. Fluorescein angiography of the anterior segment. In: Peyman, G.A., Sanders, D.R. and Goldberg, M.F. (Ed.) *Principles and Practice of Ophthalmology.* (pp. 954-987). W.B. Saunders Company, Philadelphia.

Krebs, H.A. (1975). The August Krough principle: "For many problems there is an animal on which it can be most conviently studied". *J. Exp. Zool.* 194, 221-226.

Kugler, P., Vogel, S., Volk, H. and Schiebler, T.H. (1988). Cytochrome oxidase histochemistry in the rat hippocampus. A quantitative methodolgical study. *J. Histochem. Cytochem.* 89, 269-275.

Kulikowski, J.J. (1978). Pattern and movement detection in man and rabbit: separation and comparison of occipital potentials. *Vision Res.* 18, 183-189.

Kumpulainen, T., Dahl, D., Korhonen, L.K. and Nystrom, S.H.M. (1983). Immunolabeling of carbonic anhydrase isoenzyme C and glial fibrillary acidic protein in paraffin embedded tissue of human brain and retina. *J. Histochem. Cytochem.* 31, 879-886.

Kus, J. (1969). The history of injection methods in the morphological sciences. *Folia Morph.* 28, 134-146.

Kuwabara, T. and Cogan, D.G. (1959). Tetrazolium studies on the retina: I. Introduction and technique. *J. Histochem.* 7, 329-333.

Kuwabara, T. and Cogan, D.G. (1960a). Studies of retinal vascular patterns. Part I. Normal architecture. *Arch. Ophthal.* 64, 904-911.

Kuwabara, T. and Cogan, D.G. (1960b). Tetrazolium studies on the retina: III. Activity of metabolic intermediates and miscellaneous substrates. *J. Histochem.* 8, 214-224.

Kuwabara, T. and Cogan, D.G. (1961). Retinal glycogen. *Arch. Ophthal.* 66, 96-104.

Kuwabara, T. and Cogan, D.G. (1963a). Retinal vascular patterns: VI. Mural cells of retinal capillaries. *Arch. Ophthal.* 69, 492-502.

Kuwabara, T. and Cogan, D.G. (1963b). Glycogen in the retina. *Ann. Histochim.* 8, 223-228.

Kuwabara, T. and Gorn, R.A. (1968). Retinal damage by visible light. *Arch. Ophthal.* 79, 69-78.

Laatikainen, L.T. (1976). Regional blood flow in the cat retina. *Exp. Eye Res.* 23, 47-56.

Lachica, E.A., Condo, G.J. and Casagrande, V.A. (1985). Development of cytochrome oxidase staining in the retina and lateral geniculate nucleus: a possible correlate of ON- and OFF-centre channel maturation. *Exp. Brain Res.* 61, 204-209.

Lai, J.C.K., Sheu, K-F.R. and Carlson, K.C. (1985). Differences in some of the metabolic properties of mitochondria isolated from cerebral cortex and olfactory bulb of the rat. *Brain Res.* 343, 52-59.

Lai, J.C.K., Walsh, J.M., Dennis, S.C. and Clark, J.B. (1977). Synaptic and non-synaptic mitochondria from rat brain: isolation and characterization. *J. Neurochem.* 28, 625-631.

Lametschwandtner, A., Lametschwandtner, U. and Weiger, T. (1984). Scanning electron microscopy of vascular corrosion casts - technique and applications. *Scanning Electron Micros.* II, 663-695.

Land, M.F. and Snyder, A.W. (1985). Cone mosaic observed directly through natural pupil of live vertebrate. *Vision Res.* 25, 1519-1523.

Land, P.W. (1987). Dependence of cytochrome oxidase activity in the rat lateral geniculate nucleus on retinal innervation. *J. Comp. Neurol.* 262, 78-89.

Land, P.W. and Simons, D.J. (1985). Cytochrome oxidase staining in the rat SmI barrel cortex. *J. Comp. Neurol.* 238, 225-235.

Landers, M.B. (1978). Retinal oxygenation via the choroidal circulation. *Trans. Amer. Ophthal. Soc.* 76, 528-556.

Lashley, K.S. (1932). The mechanism of vision. V. The structure and image-forming power of the rat's eye. *J.Comp. Psychol.* 13, 173-200.

Lashley, K.S. (1938). The mechanism of vision XV. Preliminary studies of the rat's capacity for detail vision. *J. Gen. Psychol.* 18, 123-193.

Last, R.J. (1961). *Eugene Wolff's Anatomy of the Eye and Orbit.* H.K.Lewis, London.

Laux, U.R. (1976). Synchronous bilateral fluorescein angiography. *Archives Ophthal.* 94, 1403-1407.

Leber, T. (1903). Die Circulations und Ernahrungsverhaltnisse des Auges. In: Graefes, A. von and Saemisch, T. (Ed.) *Handbuch der Gesamten Augenheilkunde,* 2. Leipzig, Engelmann.

Lee, A.K. and Cockburn, A. (1985). *Evolutionary Ecology of Marsupials.* Cambridge University Press. Cambridge.

leFurgey, A., Ingram, P., Henry, S.C., Murphy, E. and Lieberman, M. (1983). Three dimensional configuration of the mitochondria in cultured heart cells. *Scan. Electron Microscopy*. 293-303.

Leicester, J. and Stone, J. (1967). Ganglion, amacrine and horizontal cells of the cat's retina. *Vision Res.* 7, 695-705.

Leopold, J.H. and Calkins, L. (1950). Age changes in the wistar rat eye. *Am. J. Ophthal.* 34, 1735-1741.

Leutweinm K. and Littman, H. (1985). The fundus camera. In: T.D. Duane Ed (Ed.) *Clinical Ophthalmology*. (pp. 61:1-8). Harper and Row, Philadelphia.

Li, Z.-K., Buttery, R.G. and Morgan, I.G. (1989). Cytochrome oxidase histochemistry reveals displaced ganglion cells in the chicken retina. *Neurosci. Letts.* 34, S108.

Linnane, A.W., Marzuki, S., Ozawa, T. an Tanaka, M. (1989). Mitochondrial DNA mutations as an important contributor to ageing and degenerative disease. *Lancet.* I, 642-645.

Linsenmeier, R.A. (1986). Effects of light and darkness on oxygen distribution and consumption in the cat retina. *J. Gen. Physiol.* 88, 521-542.

Linsenmeier, R.A. and Yancey, C.M. (1989). Effects of hyperoxia on the oxygen distribution in the intact cat retina. *Invest. Ophthal. Vis. Sci.* 30, 612-618.

Liu, H-C, Tsang, D.S.C., Chan, Y.W. and Yew, Y.W. (1984). A multiple approach to the study of high dose laser lesions on the retina. *Acta. Histochem. (Jena)*. 75, 9-25.

Liu, Z-H, Dai, Z-G. an Jen, L.S. (1985). Retinal ganglion cells with high cytochrome oxidase activity in the golden hamster. *Neurosci. Letts.* 20, S12.

Lockard, I., Barham, J.R., Forlidas N.G. and Meyers, R.B. (1959). Simultaneous histological demonstration of blood vessels, nerve cells and nerve fibers within the central nervous system. *J. Comp. Neurol.* 112, 169-183.

Long, K.O. and Fisher, S.K. (1983). The distribution of photoreceptors and ganglion cells in the Californian ground squirrel, *Spermophilus beecheyi*. *J. Comp. Neurol.* 221, 329-340.

Longmuir, I.S. and Sun, S. (1970). A hypothetical tissue oxygen carrier. *Microvasc. Res.* 2, 287-293.

Lowry, O.H., Roberts, N.R. and Lewis, C. (1956). The quantitative histochemistry of the retina. *J. Biol. Chem.* 220, 879-892.

Lowry, O.H., Roberts, N.R., Schulz, D.W., Clow, J.E., and Clark, J.R. (1961). Quantitative histochemistry of retina. II. Enzymes of glucose metabolism. *J. Biol. Chem.* 236, 2813-2820.

MacLean, A.L., and Maumenee, A.E. (1959). Haemangioma of the choroid. *Trans. Am. Ophthal. Soc.* 57, 171-194.

Magalhães, M.M. and Coimbra, A. (1970). Electron microscopic radiographic study of glycogen synthesis in the rabbit retina. *J. Cell Biol.* 47, 263-275.

Magalhães, M.M. and Coimbra, A. (1972). The rabbit retina Müller cell. A fine structural and cytochemical study. *J. Ultrastruct. Res.* 39, 310-326.

Maggio, R. and Monroy, A. (1959). An inhibitor of cytochrome oxidase activity in the sea urchin egg. *Nature*. 184, 68-69.

Mansour, A.M., Walsh, J.B. and Henkind, P. (1987). Arteriovenous anastomoses of the retina. *Ophthalmology*. 94, 35-40.

Mansour, A.M., Wells, C.G., Jampol, L.M. and Kalina, R.E. (1989). Ocular complications of arteriovenous communications of the retina. *Arch. Ophthal.* 107, 232-236.

Margolis, G. (1966). Hyperbaric oxygenation: the eye as a limiting factor. *Science*. 151, 466-468.

Mariani, A. P. (1987). Neuronal and synaptic organisation of the outer plexiform layer of the pigeon retina. *Amer. J. Anat.* 179, 25-39.

Martin, G.R. and Gordon, I.E. (1974). Visual acuity in the tawny owl (*Strix aluco*). *Vision Res.* 14, 1393-1397.

Masland, R.H. (1986). The functional architecture of the retina. *Sci. Amer.* 255, 90-99.

Megirian, D., Weller, L., Martin, G.F. and Watson, C.R.R. (1977). Aspects of laterality in the marsupial *Trichosurus vulpecula* (brush-tailed possum). *Annals New York Acad. Sci.* 299, 197-212.

Meyer, D.B. (1977). The avian eye and its adaptations. In: Crestcitelli, F. (Ed.) *Handbook of Sensory Physiology. Vol II/5. The Visual System in Vertebrates.* (pp. 550-611). Springer-Verlag, Berlin.

Meyer, G.E. and Salinsky, M.C. (1977). Refraction of the rat: estimation by pattern evoked visual cortical potentials. *Vision Res.* 17, 883-885.

Meyer, J. (1981). A quantitative comparison of the parts of the brains of two Australian marsupials and some eutherian mammals. *Brain Behav. Evol.* 18, 60-71.

Meyer, P.A.R. (1988). Patterns of blood flow in episcleral vessels studied by low-dose fluorescein angiography. *Eye*. 2, 533-546.

Michaelson, I.C. (1954). *Retinal Circulation in Man and Animals.* Thomas, Springfield, Ill.

Michaelson, I.C. and Campbell, A.C.P. (1940). The anatomy of the finer retinal vessels, and some observations on their significance in certain retinal diseases. *Trans. Ophthal. Soc. UK.* 60, 71-112.

Miki, A., Mizoguguchi, A. and Mizoguti, H. (1988). Histochemical studies of enzymes of energy metabolism in postimplantation embryos. *Histochem.* 88, 489-495.

Minamikawa, T., Miyake, T., Takamatsu, T. and Fujita, S. (1987). A new method of lectin histochemistry for the study of brain angiogenesis. Lectin angiography. *Histochem.* 87, 317-320.

Mitchell, D.E., Giffin, F. and Timney, B. (1977). A behavioural technique for rapid assessment of the visual capabilities of kittens. *Perception.* 6, 181-193.

Mizuno, K. and Sato, K. (1975). Reassessment of histochemistry of retinal glycogen. *Exp. Eye Res.* 21, 489-497.

Mori, M.T., Zeimer, R.C. and Goldberg. M. (1988). Noninvasive measurement of retinal thickness: a potential diagnostic tool for macular edema and atrophy. *Invest. Ophthal. Vis. Sci.* 29, 339.

Morrison, J.C. and Van Buskirk, E.M. (1984). Ciliary process microvasculature of the primate eye. *Amer. J. Ophthal.* 97, 372-383.

Morrison., J.C., DeFrank, M.P. and Van Buskirk, E.M. (1987a). Regional microvascular anatomy of the rabbit ciliary body. *Invest. Ophthal. Vis. Sci.* 28, 1314-1324.

Morrison., J.C., DeFrank, M.P. and Van Buskirk, E.M. (1987b). Comparative microvascular anatomy of mammalian ciliary processes. *Invest. Ophthal. Vis. SciQ.* 28, 1325-1340.

Murakami, T. (1971). Application of the scanning electron microscopy to the study of the fine distribution of the blood vessels. *Arch. Histol. Jpn.* 32, 445-454.

Murakami, T., Ohtani, O., Ohtsuka, A. and Kikuta, A. (1983). Injection replication and scanning electron microscopy of blood vessels. *Biomed. Res. Applications SEM.* 3, 1-30.

Nakaizumi, Y. (1964). The ultrastructure of Bruch's membrane I. Human, monkey, rabbit, guinea pig and rat eyes. *Arch. Ophthal.* 72, 380-387.

Naradzay, J.F.X. and Rosenstein, J.M. (1989). Vascular morphology and permeability in fetal CNS grafts to the renal capsule. *Exp. Neurol.* 104, 284-291.

Narat, J.K., Loef, J.A. and Narat, M. (1935). On the preparation of multi-coloured corrosion specimens. *Anat. Rec.* 64, 155-160.

Newsom, W.A., Leverett, S.D. and Kirkland, V.E. (1968). Retinal fluorescence angiography of the rhesus monkey. *Arch. Ophthal.* 79, 768-774.

Nielsen, N.V. (1982). The normal retinal fluorescein angiogram I. A study of the fluorescein angiograpic appearance of the retina in normal subjects without ophthalmoscopically obvious pathological changes. *Acta. Ophthal.* 60, 657-670.

Niemi, M. and Merenmies, E. (1961a). Cytochemical localization of the oxidative enzyme systems in the retina-I. *J. Neurochem.* 6, 200-205.

Niemi, M. and Merenmies, E. (1961b). Cytochemical localisation of the oxidative enzyme systems of the retina-II. *J. Neurochem.* 6, 206-209.

Nir, I. and Pease, D.C. (1974). The ultrastructural localisation of cytochrome c-oxidase complex in a lipid-retaining glutaraldehyde-urea embedment. *J. Histochem. Cytochem.* 22, 1019-1027.

Noell, W.K. (1959). The visual cell: electric and metabolic manifestations of its life processes. *Amer. J. Ophthal.* 48, 347-370.

Noell, W.K., Walker, V.S., Kang, B.S. and Berman, S. (1966). Retinal damage by light in rats. *Invest. Ophthal. Vis. Sci.* 5, 450-473.

Nogawa, T., Sung, W.K., Jagiello, G.M. and Bowne, W. (1988). A quantitative analysis of mitochondria during fetal mouse oogenesis. *J. Morph.* 195, 225-234.

Nopanitaya, W., Aghajanian, J.G. and Gray, L.D. (1979). An improved plastic mixture for corrosion casting of the gastrointestinal system. *Scanning Electron Micros.* II, 751-756.

Nordestgaard, B.G. and Rostgaard, J. (1985). Dimensional changes of isolated hepatocytes during processing for scanning and transmission electron microscopy. *Micron and Microscopy Acta*. 16, 65-75.

Nourse, A.E. (1972). In: Dubois, R., Margenau, H. and Snow, C.P. (Ed.) *The Body*. Time Life International (Nederland) N.V.

Novotny, H.R. and Alvis, D.L. (1961). A method of photographing fluorescence in circulating blood in the human retina. *Circulation*. 24, 82-86.

Nowak, J.Z. (1988). The isolated retina as a model of the CNS pharmacology. *Trends In Physiol. Sci.* 9, 80-91.

O'Day, K. (1938). The retina of the Australian mammal. *Med. J. Aust.* 326-328.

O'Steen, W.K. and Donnelly, J.E. (1982). Chronologic analysis of variations in retinal damage in two strains of rats after short term illumination. *Invest. Ophthal. Vis. Sci.* 22, 252-255.

O'Steen, W.K., Sweatt, A.J., Eldridge, J.C. and Brodish, A. (1987). Gender and chronic stress effects on the neural retina of young and mid-aged Fischer-344 rats. *Neurobiol. of Aging*. 8, 449-455.

Ogden, T.E. (1978). Nerve fibre layer astrocytes of the primate retina: morphology, distribution and density. *Invest. Ophthal. Vis. Sci.* 17, 499-510.

Ogden, T.E. (1983). Nerve fiber layer thickness of the primate retina: Thickness and glial content. *Vision Res.* 23, 581-587.

Ohkuma. H. and Ryan, S.J. (1983). Vascular casts of experimental subretinal neovascularisation in monkeys. *Invest. Ophthal. Vis. Sci*. 24, 481-490.

Olavarria, J., Anderson, P.A. and Van Sluyters, R.C. (1986). On the use of horseradish peroxidase to study cerebral angioarchitecture. *J. Neurosci. Methods*. 15, 349-351.

Olson, I.A. and Skuse, D.E. (1969). The use of liquid photographic emulsion for demonstrating blood vessels in histological sections. *J. Microscopy*. 89, 345-348.

Olver, J.M., and McCartney, A.C.E. (1989). Orbital and ocular micro-vascular corrosion casting in man. *Eye*. 3, 588-596.

Olver, J.M., Spalton, D.J. and McCartney, A.C.E. (1990). Microvascular study of the retrolaminar optic nerve in man: the possible significance in anterior ischaemic optic neuropathy. *Eye*. 4, 7-24.

Oswaldo-Cruz, E., Hokoç, J.N. and Sousa, A.P.B. (1979). A schematic eye for the opossum. *Vision Res.* 19, 263-278.

Pedlar, C. and Tilley, R. (1969). The retina of a fruit bat (*Pteropus giganteus*). *Vision Res.* 9, 909-922.

Peress, N.S. and Tompkins, D.C. (1982). Pericapillary permeability of the ciliary processes: role of molecular charge. *Invest. Ophthal. Vis. Sci.* 23, 168-175.

Perotti, M.E., Anderson, W.A. and Swift, H. (1983). Quantitative cytochemistry of the diaminobenzidine cytochrome oxidase reaction product in mitochondria of cardiac muscle and pancreas. *J. Histochem. Cytochem.* 31, 351-365.

Person, P. and Fine, A. (1960). Reversible inhibition of beef heart cytochrome c oxidase by polyanionic macromolecules. *Science*. 132, 43-44.

Peterson, R.A., Ringer, R. K., Tetzlaff, M. J. and Lucas, A.M. (1965). Ink perfusion for displaying capillaries in the chicken. *Stain Tech.* 40, 351-356.

Pettigrew, J.D., Dreher, B., Hopkins, C.S., McCall, M.J. and Brown, M. (1988). Peak density and density and distribution of ganglion cells in the retinae of microchiropteran bats: Implications for visual acuity. *Brain Behav. Evol.* 32, 39-56.

Pettigrew, J.D., Wallman, J. and Wildsoet, C.F. (1990). Saccadic oscillations facilitate ocular perfusion from the avian pecten. *Nature*. 343, 362-363.

Pino, R.M. (1985). Restriction to endogenous plasma proteins by a fenestrated capillary endothelium: An ultrastructural immunocytochemical study of the choriocapillary enothelium. *Amer. J. Anat.* 172, 279-289.

Pino, R.M. and Essner, E. (1981). Permeability of rat choriocapillaris to hemeproteins. *J. Histochem. Cytochem.* 29, 281-290.

Pino, R.M., Essner, E. and Pino, L.C. (1982). Permeability of the neonatal rat choriocapillaris to hemeproteins and ferritin. *Amer. J. Anat.* 164, 333-341.

Pino, R.M. and Essner, E. (1980). Structure and permeability to ferritin of the choriocapillary endothelium of the rat eye. *Cell Tissue Res.* 208, 21-27.

Pirie, A. (1961). Cholesterol in the tapetum lucidum of the opossum *Didelphis virginiana*. *Nature*. 191, 708-709.

Pirie. A. (1966). The chemistry and structure of the tapetum lucidum in animals. In: Graham-Jones, O. (Ed.) *Aspects of Comparative Ophthalmology*. Pergamon Press, Oxford.

Pollak, J.K. and Sutton, R. (1980). The differentiation of animal mitochondria during development. *Trends in Biochem. Sci.* 5, 23-27.

Polyak, S. (1957). *The Vertebrate Visual System.* University of Chicago Press.

Popel, A.S., Pittman, R.N. and Ellsworth, M.L. (1989). Rate of oxygen loss from arterioles is an order of magnitude higher than expected. *Am. J. Physiol.* 256, H921-H924.

Potter, R.F. and Groom, A.C. (1983). Capillary diameter and geometry in cardiac and skeletal muscle studied by means of corrosion casts. *Microvasc. Res.* 25, 68-84.

Price, D.J. (1985). Patterns of cytochrome oxidase activity in areas 17, 18, and 19 of the visual cortex of cats and kittens. *Exp. Brain Res.* 58, 125-133.

Prince, J.H. (1956). *Comparative Anatomy of the Eye*. Thomas, Springfield, Ill.

Prince, J.H., Diesem, C.D., Eglitis, I. and Ruskell, G.L. (1960). *Anatomy and Histology of the Eye and Orbit in Domestic Animals.* Charles C. Thomas, Springfield Il.

Provis, J.M. (1979). The distribution and size of ganglion cells in the retina of the pigmented rabbit: A quantitative study. *J. Comp. Neurol.* 185, 121-138.

Pysh, J.P. and Khan, T. (1972). Variations in mitochondrial structure and content of neurons and neuroglia in rat brain: an electron microscopic study. *Brain Res.* 36, 1-18.

Radius, R.L. (1980). Thickness of the retinal nerve fiber layer in primates. *Arch. Ophthal.* 98, 1625-1929.

Randall, H.W., Bogdanffy, M.S. and Morgan, K.T. (1987). Enzyme histochemistry of the rat nasal mucosa embedded in cold glycol methacrylate. *Amer. J. Anat.* 179, 10-17.

Rapaport, D.H., Wilson, P.D. and Rowe, M.H. (1981). The distribution of ganglion cells in the retina of the North American opossum *(Didelphis Virginina). J. Comp. Neurol.* 199, 465-480.

Rasmussen, K.E. (1973). A morphometric study of the Müller cells, their nuclei and mitochondria, in the rat. *J. Ultrastruct. Res.* 44, 96-112.

Rasmussen, K.E. (1974). The Müller cell: A comparative study of rod and cone retinas with and without retinal blood vessels. *Exp. Eye Res.* 19, 243-257.

Raviola, G. (1977). The structural basis of the blood-ocular barriers. *Exp. Eye Res.* 25 (Supp.), 27-63.

Raviola, G., Butler, J.M. (1984). Unidirectional transport mechanisms of horseradish peroxidase in the vessels of the iris. *Invest. Ophthal. Vis. Sci.* 25, 827-836.

Raviola, G., Butler, J.M. (1985). Asymmetric distribution of charged domains on the two fronts of the endothelium of iris vessels. *Invest. Ophthal. Vis. Sci.* 26, 597-608.

Rees, S. and Hore, J. (1970). The motor cortex of the brush-tailed possum (*Trichosurus vulpecula*): motor representation, motor function and the pyramidal tract. *Brain Res.* 20, 439-451.

Reese, B.E. (1988). Hidden lamination in the dorsal lateral geniculate nucleus: the functional organization of this thalamic region in the rat. *Brain Res. Rev.* 13, 119-137.

Reichenbach, A. and Wohlrab, F. (1986). Morphometric parameters of Müller (glial) cells dependent on their topographic localization in the nonmyelinated part of the rabbit retina. A consideration of functional aspects of radial glia. *J. Neurocytol.* 15, 119-137.

Reith, A. and Schüler, B. (1972). Demonstration of cytochrome oxidase activity with diaminobenzidine. A biochemical and electron microscopic study. *J. Histochem. Cytochem.* 20, 583-589.

Remtulla, S. and Hallett, P.E. (1985). A schematic eye for the mouse, and comparisons with the rat. *Vision Res.* 25, 21-31.

Reymond, L. (1985). Spatial visual acuity of the eagle *Aquila Audax*: a behavioural, optical and anatomical investigation. *Vision Res.* 25, 1477-1491.

Reymond, L. and Wolfe, J. (1981). Behavioural determination of the contrast sensitivity function of the eagle *Aquila audax*. *Vision Res.* 21, 263-271.

Rhodin, J.A.G. (1967). The ultrastructure of mammalian arterioles and precapillary sphincters. *J. Ultrastructure Res.* 18, 181-223.

Ribak, C.E. (1981). The histochemical localizsation of cytochrome oxidase in the dentate gyrus of the rat hippocampus. *Brain Res.* 212, 169-174.

Ride, W.D.L. (1970). *A Guide to the Native Mammals of Australia*. Oxford University Press, Melbourne.

Ringo, D.L., Brennan, E.F. and Cota-Robles, E.H. (1982). Epoxy resins are mutagenic: Implications for electron microscopists. *J. Ultrastruct. Res.* 80, 280-287.

Ringvöld, A. and Olsen, E.G. (1979). Choroidal fluorescein angiography in rabbit. *Acta. Ophthal.* 57, 513-521.

Ripps, H. and Witkovsky, P. (1985). Neuron-glia interaction in the brain and retina. In: Osborne, N.N. and Chader, G.J. (Ed.) *Progress in Retinal Research. Volume 4.* (pp. 181-219). Pergamon Press, Oxford.

Risco, J.M. and Nopanitaya, W. (1980). Ocular microcirculation. Scanning electron microscopic study. *Invest. Ophthal. Vis. Sci.* 19, 5-12.

Risco, J.M., Grimson, B.S. and Johnson, P.T. (1981). Angioarchitecture of the ciliary artery circulation of the posterior pole. *Arch. Ophthal.* 99, 864-868.

Robb, A.M., Crewther, D.P., Crewther, S.G. and Nelson, J.E. (1982). Visual acuity of the northern native cat, *Dasyurus Hallucatus*. *Proc. Aust. Physiol. Pharmacol. Soc.* 13, 197.

Robinson, S.R. (1982). Interocular transfer in a marsupial: the brush-tailed possum (*Trichosurus vulpecula*). *Brain Behav. Evol.* 21, 114-124.

Robinson, S.R. (1988). Ontogeny of the area centralis in the cat. *J. Comp. Neurol.* 255, 50-67.

Robinson, S.R. and Dreher, Z. (1989). The distribution and morphology of Müller cells in adult rabbit retinae: Functional implications. *Neurosci. Letts.* 34, S141.

Rockland, K.S. (1985). A reticular pattern of intrinsic connections in primate area V2 (area 18). *J. Comp. Neurol.* 235, 467-478.

Rodieck, R.W. (1973). *The Vertebrate Retina*. W.H. Freeman, San Francisco.

Ross, C.D and Godfrey, D.A. (1985). Distributions of aspartate aminotransferase and malate dehydrogenase activities in rat retinal layers. *J. Histochem. Cytochem.* 33, 624-630.

Rowe, M.H., Wilson, P.D. and Rapaport, D.H. (1981). Conduction velocity groups in the optic nerve of the North American opossum (*Didelphis virginiana*): retinal origins and central projections. *J. Comp. Neurol.* 199, 481-493.

Rush, R.A. (1989). Recent advances in the study of neuronal growth factors. *Neurosci. Letts.* 34, S35.

Saari, J.C. (1987). Metabolism and photochemistry in the retina. In: Moses, R.A. and Hart, W.M. (Ed.) *Adler's Physiology of the Eye. Clinical Appliaction.* (pp. 356-373). The C.V. Mosby Company, St Louis.

Saavedra, R.A. and Anderson, G.R. (1983). A cancer-associated lactate dehydrogenase is expressed in normal retina. *Science*. 221, 291-292.

Sambasivarao, D. and Sitaramam, V. (1985). Respiration induces variable porosity to polyols in the mitochodrial inner membrane. *Biochim. Biophys. Acta*. 806, 195-209.

Sanderson, K.J. (1984). Development of the visual system in the brushtailed possum. In: Stone, J., Dreher, B. and Rapaport, D.H. (Ed.) *Development of visual pathways in mammals.* (pp. 145-154). Alan R. Liss, New York.

Sanderson, K.J. and Pearson, L.J. (1977). Retinal projections in the native cat, *Dasyurus viverrinus*. *J. Comp. Neurol.* 174, 347-358.

Sanderson, K.J., Dixon, P.G. and Pearson, L.J. (1982). Postnatal development of retinal projections in the brushtailed possum, *Trichosurus vulpecula*. *Devel. Brain. Res.* 5, 161-180.

Sanderson, K.J., Haight, J.R. and Pettigrew, J.D. (1984). The dorsal lateral geniculate nucleus of macropidid marsupials: Cytoarchitecture and retinal projections. *J. Comp. Neurol.* 224, 85-106.

Sanderson, K.J., Nelson, J.E., Crewther, D.P., Crewther, S.G. and Hammond, V (1987). Retinogeniculate patterns in diprotodont marsupials. *Brain Behav. Evol.* 30, 22-42.

Sanderson, K.J., Pearson, L.J. and Haight, J.R. (1979). Retinal projections in the Tasmanian Devil, *Sarcophilus harrisii*. *J. Comp. Neurol.* 188, 335-346.

Sanyal, S., DeRuiter, A. and Hawkins, R.K. (1980). Development and degeneration of retina in rds mutant mice: light microscopy. *J. Comp. Neurol.* 194, 193-207.

Schabadasch, A.L. and Schabadasch, S.A. (1972a). Localisation and dynamic changes of glycogen in frog retina adapted to darkness or light-I. *Vision Res.* 12, 1595-1604.

Schabadasch, A.L. and Schabadasch, S.A. (1972b). Localisation and dynamic changes of glycogen in frog retina adapted to darkness or light-II. *Vision Res.* 12, 1605-1617.

Scharrer, E. (1939). The functional significance of the capillary bed in the brain of the opossum. *Anat. Rec.* 75, 319-340.

Scharrer, E. (1940a). Arteries and veins in the mammalian brain. *Anat. Rec.* 78, 173-196.

Scharrer, E. (1940b). Further experiments on the regeneration of end-arteries in the brain of the opossum. *J. Exp. Zool.* 85, 365-381.

Scharrer, E. (1950). A technique for the demonstration of the blood vessels in the developing central nervous system . *Anat. Rec.* 107, 319-327.

Schatz, H., Burton,T.C., Yannuzzi, L.A. and Rabb, M.F. (1978). *Interpretation of Fundus Fluorescein Angiography*. The C.V. Mosby Company, St Louis.

Schobl, J. (1878). Uber eine eigenthumliche Schleinfenbildung der Blutgefasse im Gehrin und Ruckenmark der Saurier. *Arch. mikr. Anat.* 15, 60-64.

Schobl, J. (1882). Uber die Blutgefasse des cerebrospinalen Nervensystems der Urodelen. *Arch. mikr. Anat.* 24, 87-92.

Schultz, R.L. and Case, N.M. (1970). A modified aldehyde perfusion technique for preventing certain artifacts in electron microscopy of the central nervous system. *J. Micros.* 92, 69-84.

Sears. M.L. (1981). The aqueous. In: Moses, R.A. (Ed.) *Adler's physiology of the eye. Clinical application*. (pp. 204-226). The C.V. Mosby Company, St Louis.

Sefton, A.J. and Dreher, B. (1985). Visual system. In: Paxinos, G. (Ed.) *The Rat Nervous System*. (pp. 169-221). Academic Press, Australia.

Seligman, A.M., Karnovsky, M.J., Wasserkrug, H.L. and Hanker, J.S. (1968). Nondroplet ultrastructural demonstration of cytochrome oxidase activity with a polymerising osmiophilic reagent, diaminobezidine (DAB). *J. Cell Biol.* 38, 1-14.

Sellinger, O.Z. and Santiago, J.C. (1972). Unequal development of two mitochondrial enzymes in neuronal cell bodies and glial cells of the rat cerebral cortex. *Neurobiol.* 2, 133-146.

Shah, S.K.H. and Nicol, S.C. (1989). Cephalic vasculature and distribution of blood flow through the cranial arterial circle of the Tasmanian devil, *Sarcophilus harrisii*. *J. Mamm.* 70, 123-131.

Shah, S.K.H., Nicol, S.C. and Swain, R. (1986). Functional morphology of the cranial vasculature in the Tasmanian devil, *Sacophilus harrisii* (Marsupialia: Dasyuridae): A marsupial carotid rete?. *Aust. J. Zool.* 34, 125-133.

Sharaki, K., Burns, M.S. and Bellhorn, R.W. (1983). Abnormal vessel patterns in phototoxic rat retinopathy studied by vascular replicas. *Curr. Eye. Res.* 2, 545-551.

Shatz, C.J. and Stretvan, D.W. (1986). Interactions between retinal ganglion cells during development of the mammalian visual system. *Ann. Rev. Neurosci.* 9, 171-207.

Shimuzu, K., Ujiie, K. and Henkind, P. (1978). *Structure of Ocular Vessels*. Igaku-Shoin, Tokyo.

Shinowara, N.L., London, E.D. and Rapoport, S.I. (1982). Changes in retinal morphology and glucose utilization in aging albino rats. *Exp. Eye Res.* 34, 517-530.

Shober, W., Werner, L. and Brauer, K. (1985). Das corpus geniculatum laterale des Meerschweinchens (*Cavia aperea f.domesticua*). Seine Gliederung unter Berüchsichtigung der retinalen Affertierung. *J. Hirnforsch.* 26, 73-84.

Silveira, L.C.L., Picanco-Diniz, C.W. and Oswaldo-Cruz, E. (1982). Contrast sensitivity function and visual acuity of the opossum. *Vision Res.* 22, 1371-1377.

Simionescu, M. and Simionescu, N. (1986). Functions of the endothelial cell surface. *Ann. Rev. Physiol.* 48, 279-293.

Simionescu, M., Simionescu, N. and Palade, G.E. (1982a). Differentiated microdomains on the luminal surface of capillary endothelium: Distribution of lectin receptors. *J. Cell Biol.* 94, 406-413.

Simionescu, M., Simionescu, N. and Palade, G.E. (1982b). Preferential distribution of anionic sites on the basement membrane and the abluminal aspect of the endothelium in fenestrated capillaries. *J. Cell Biol.* 95, 425-434.

Simionescu, N. (1979). Enzymatic tracers in the study of vascular permeability. *J. Histochem. Cytochem.* 27, 1120-1130.

Simionescu, N. (1983). Cellular aspects of transcapillary exchange. *Phyisol. Rev.* 63, 1536-1579.

Simionescu, N., Simionescu, M. and Palade, G.E. (1981). Differentiated microdomains on the luminal surface of the capillary endothelium. I. Preferential distribution of anbionic sites. *J. Cell Biol.* 90, 605-613.

Simpson, G.G. (1945). The principles of classification and a classification of mammals. *Bull. Amer. Mus. Nat. Hist.* 85, 1-350.

Simurda, M. and Wilson, J.E. (1980). Localization of hexokinase in neural tissue: Immunofluorescence studies on the developing cerebellum and retina of the rat. *J. Neurochem.* 35, 58-66.

Sinex, D.G., Burdette, L.J. and Pearlman, A.L. (1979). A psychophysical investigation of vision in the normal and reeler mutant mouse. *Vision Res.* 19, 853-857.

Small, C.S. and Peterson, D.I. (1982). The reliability of dimensions of formalin-fixed brains. *Neurology.* 32, 413-415.

Smith, P., Samuelson, D. and Brooks, D. (1988). Aqueous drainage paths in the equine eye: Scanning electron microscopy of corrosion casts. *J. Morph.* 198, 33-42.

Smith, R.A. and Ord, M.J. (1983). Mitochondrial form and function *in vivo*: Their potential in toxicology and pathology. *Int. Rev. Cytol.* 83, 63-134.

Smith, T.L., Osborne, S.W., and Hutchins, P.M. (1985). Long-term micro- and macrocirculatory measurements in conscious rats. *Microvasc. Res.* 29, 360-370.

Snyder, A.W. Bossomaier, T.R.J. and Hughes, A. (1986). Optical image quality and the cone mosaic. *Science.* 231, 499-501.

Snyder, G.K., Gannon, B. and Baudinette, R.V. (1989). Functional morphology of cerebral vasculature in a marsupial, the northern quoll (*Dasyurus hallucatus*). *J. Exp. Zool.* 251, 349-354.

So, K-F. and Aguayo, A.J. (1985). Lengthy regrowth of cut axons from ganglion cells after peripheral nerve transplantation into the retina of adult rats. *Br. Res.* 328, 349-354.

Sokolova, I.A., Manukhina, E.B., Blinkov, S.M., Koshelev. V.B. et al. (1985). Rarefaction of the arterioles and capillary network in the brain of rats with different forms of hypertension. *Microvasc. Res.* 30, 1-9.

Sollom, A.W. (1968). Conjugated fluorescein for fundus photography. *Brit. J. Ophthal.* 52, 691-694.

Spira, A.W. (1975). *In utero* development and maturation of the retina of a non-primate mammal: a light and electron microscopic study of the guinea pig. *Anat. Embryol.* 146, 279-300.

Spitznas, M. and Bornfeld, N. (1977). The architecture of the most peripheral retinal vessels. *Albrecht v. Graefes Arch. Klin. Exp. Ophthal.* 203, 217-229.

Stahl, W.L. and Baskin, D.G. (1984). Immunocytochemical localisation of Na+, K+ adenosine triphosphatase in the rat retina. *J. Histochem. Cytochem.* 32, 248-250.

Steen, J.B. (1963). The physiology of the swim bladder of the eel, *Anguilla vulgaris* III. The mechanism of gas secretion. *Acta. Physiol. Scand.* 59, 221-241.

Stefánsson, E., Wolbarsht, M.L. and Landers III, M.B. (1983). In vivo O_2 consumption in rhesus monkeys in light and dark. *Exp. Eye Res.* 37, 251-256.

Stefánsson, E. Novack, R.L. and Hatchell, D.L. (1990). Vitrectomy prevents retinal hypoxia in branch vein occlusion. *Invest. Ophthal. Vis. Sci.* 31, 284-289.

Steinberg, R.H. (1987). Monitoring communications between photoreceptors and pigment epithelial cells: effects of 'mild' systemic hypoxia. Friedenwald Lecture. *Invest. Ophthal. Vis. Sci.* 12, 1888-1904.

Steinberg, R.H., Reid, M. and Lacy, P.A. (1973). The distribution of rods and cones in the retina of the cat (*Felis domesticus*). *J. Comp. Neurol.* 148, 229-248.

Sterzi, G. (1904). Die Blutgefasse des Rückenmarks. Untersuchungen über ihre vergleichende Anatomie und Entwicklungsgeschichte. *Anat. H.* 24, 1-364.

Stewart, P.A. and Wiley, M.H. (1981). Developing nervous tissue induces formation of blood-brain barrier characteristics in invading endothelial cells: A study using quail-chick transplantation chimeras. *Dev. Biol.* 84, 183-192.

Stone, J. (1965). Quantitative analysis of the distribution of ganglion cells in the cat's retina. *J. Comp. Neurol.* 124, 337-352.

Stone, J. (1969). Structure of the cat's retina after occlusion of the retinal circulation. *Vision Res.* 9, 351-356.

Stone, J. (1981). *The Wholemount Handbook. A Guide to the Preparation and Analysis of Retinal Wholemounts*. Maitland Publications, Sydney.

Stone, J. (1983). Topographical organisation of the retina in a monotreme: Australian Spiny anteater *Tachyglossus aculeatus*. *Brain Behav. Evol.* 22, 175-184.

Stone, J. and Dreher, Z. (1987). Relationship between astrocytes, ganglion cells and vasculature of the retina. *J. Comp. Neurol.* 255, 35-49.

Stone, J. and Johnson, E. (1981). The topography of the primate retina: a study of the human, bushbaby, and New- and Old-world monkeys. *J. Comp. Neurol.* 196, 205-223.

Stoward, P.J. (1980). Criteria for the validation of quantitative histochemical enzyme techniques. *Ciba Foundation Symposium.* 73, 11-31.

Straatsma, B.R., Foos, R.Y. and Spencer, L.M. (1969). The retina - topography and clinical correlations. In: Cockerham, W.D. et al. (Ed.) *Symposium on Retina and Retinal Surgery.* (pp. 15-25). The C.V. Mosby Company, St Louis.

Strahan, R. (1983). *The Australian Museum Complete Book of Australian Mammals.* Angus and Robertson, London.

Streeter, G.L. (1918). The developmental alterations in the vascular system of the brain of the human embryo. *Contr. Embryol.* 8, 5-38.

Stryer, L. (1981). *Biochemistry*. W.H. Freeman and Company, New York.

Studer, R. and Potchen, J. (1971). The radioisotopic assessment of regional microvascular permeability to macromolecules. *Microvasc. Res.* 3, 35-48.

Sukekawa, K. (1987). Changes of cytochrome oxidase activity in the rat subcortical visual centers after unilateral eye enucleation. *Neurosci. Letts.* 75, 127-132.

Sunderland, S. (1941). The vascular pattern in the central nervous system of the monotremes and Australian marsupials. *J. Comp. Neurol.* 75, 123-129.

Tanaka, T. and Schimizu, K. (1987). Retinal arteriovenous shunts in Takayasu disease. *Ophthalmology.* 94, 1380-1388.

Tancred, E. (1981). The distribution and sizes of ganglion cells in the retinas of five Australian marsupials. *J. Comp. Neurol.* 196, 585-603.

Tane, S., Kohno, J., Horikoshi, J., et al. (1984). The study on the microscopic biometry of the thickness of the human retina, choroid and sclera. *Nippon Ganka Gakkai Zasshi.* 88, 1412-1417.

Tane, S., Kohno, J., Horikoshi, J., Kondo, K. Ohashi, K., Komatsu, A. and (1984). Kakeheshi, T. The study on the microscopic biometry of the thickness of the human retina, choroid and sclera by ultrasound. *Nippon Ganka Gakkai Zasshi.* 88, 1412-14

Tano, Y., Chandler, D.B. and Machemer, R. (1981). Vascular casts of experimental retinal neovascularisation. *Am. J. Ophthal.* 92, 110-120.

Tennent, R.J. (1974). The roles of platelets and macrophages in clearing particles from the blood. *M. Sc. Qual., University of Queensland.* (pp. 10).

Tillis, T.N., Murray, D.L., Schmidt, G.J. and Weiter, J.J. (1988). Preretinal oxygen changes in the rabbit under conditions of light and dark. *Invest. Ophthal. Vis. Sci.* 29, 988-991.

Tolani, A. and Talwar, G.P. (1963). Differential metabolism of various brain regions. Biochemical heterogeneity of mitochondria. *Biochem. J.* 88, 357-362.

Tompsett, D.H. (1970). *Anatomical techniques.* E. & S. Livingstone, London.

Toussaint, D., Kuwabara, T. and Cogan, D.G. (1961). Retinal vascular patterns. Part II. Human retinal vessels studied in three dimensions. *Arch. Ophthal.* 65, 137-143.

Trounce, I., Byrne, E. and Marzuki, S. (1989). Decline in skeletal muscle mitochondrial respiratory chain function: possible factor in ageing. *Lancet.* I, 637-639.

Tucker, G.S. (1978). Light microscopic analysis of the kitten retina: Postnatal development in the area centralis. *J. Comp. Neurol.* 180, 489-500.

Turner, I.J., Favilla, I. and Barry, W.R. (1981). Wide angle attachment for the fundus camera. *Aust. NZ. J. Ophthal.* 94, 315-319.

Ubels, J.L. and Hoffert, J.R. (1981). Ocular oxygen toxicity: The effect of hyperbaric oxygen on retinal Na-K ATPase. *Exp. Eye Res.* 32, 77-84.

Ubels, J.L. Edelhauser, H.F. and Antoine, M.E. (1984). Choroidal *rete mirabile* function and resistance to retinal oxygen toxicity in fish. *Exp. Eye Res.* 38, 353-362.

Ueno, S., Bambauer, H.J., Umar, H., Ueck, M. and Ogawa, K. (1984). Ultracytochemical study of Ca+ +-ATPase and K+-NPPase activities in retinal photoreceptors of the guinea pig. *Cell Tissue Res.* 237, 479-489.

Ueno, S., Mayahara, H., Tsukahara, I. and Ogawa, K. (1980). Ultracytochemical localization of ouabain-sensitive potassium-dependent p-nitro-phenylphosphatase activity in the guinea pig retina I. Photoreceptor cells. *Acta. Histochem. Cytochem.* 13

Ueno, S., Mayahara, H., Tsukahara, I. and Ogawa, K. (1981). Ultracytochemical localization of ouabain-sensitive potassium-dependent p-nitrophenylphosphatase activity in guinea pig retina II. Neurons and Müller cells. *Acta. Histochem. Cytochem.*,

Ujiie, K. and Hanyuda, T. (1977). Three-dimensional angioarchitecture of the peripheral choroid and ciliary body. *Acta. Soc. Ophthalmol. Jpn.* 81, 622-667.

Vakkur, G.J. and Bishop, P.O. (1963). The schematic eye of the cat. *Vision Res.* 3, 357-381.

Vakkur, G.J., Bishop, P.O. and Kozak, W. (1963). Visual optics in the cat, including posterior nodal distance and retinal landmarks. *Vision Res.* 3, 289-314.

Valtin, H. (1983). *Renal Function. Mechanisms Preserving Fluid and Solute Balance in Health*. Little, Brown and Company, Boston/Toronto.

Van Buren, J.M. (1963). *The Retinal Ganglion Cell Layer.* Thomas, Springfield. Ill.

Van Driel, D., Graydon, M. and Giorgi, P. (1985). The vasculature of the flying fox eye. *J. Anat.* 143, 237.

Van Hof, M.W. (1967). Visual acuity in the rabbit. *Vision Res.* 7, 749-751.

Van Reempts, J., Haseldonckx, M. and Borgers, M. (1983). A simple technique for the microscopic study of microvascular geometry and tissue perfusion, allowing simultaneous histopathological evaluation. *Microvasc. Res.* 25, 300-306.

Vaney, D.I. (1980). The grating acuity of the wild European rabbit. *Vision Res.* 20, 289-314.

Vassileva, P.I. and Dabov, S.B. (1976). Changes in the glycogen content and the electroretinogram in retinal ischaemia experimentally - induced in rabbits. In: Cant, J.S. (Ed.) *Vision and Circulation.* (pp. 66-78). The C.V. Mosby Company, Saint Loui

Vaughan, M.K., Chambers, J.P., Tsin, A.T.C., Vaughan, G.M. and Reiter, R.J. (1987). Pineal and retinal lysosomal rhythms. *Brain Res.* 417, 321-326.

Vaughan, T.A. (1986). *Mammalogy.* Saunders College Publishing, Philadelphia.

Venable, J.H. and Coggeshall, R. (1965). A simplified lead citrate stain for use in electron microscopy. *J. Cell Biol.* 25, 407-408.

Vogel, M. (1978). *Postnatal development of the cat retina*. Springer-Verlag, Berlin.

Voris, H.C. (1928). The arterial supply of the brain and spinal cord of the Virginian opossum (*Didelphis virginiana*). *J. Comp. Neurol.* 44, 403-423.

Walker, E.P., Warnick, F., Hamlet, S.E. *et al.* (1975). *Mammals of the World*. The Johns Hopkins University Press, Baltimore.

Walker, J. Vracko, R. and Brown, G.S. (1978). Flat mounts of the retinal vasculature. *Stain Tech.* 53, 360-362.

Walls, G.L. (1942). *The Vertebrate Eye and its Adaptive Radiation*. Hafner Publishing Company, New York.

Waltman, S.R. and Hart, W.M. (1987). The cornea. In: Moses, R.A. and Hart, W.M. (Ed.) *Adler's Physiology of the Eye. Clinical Application*. (pp. 36-59). The C.V. Mosby Company, St Louis.

Warburg, O. (1927). *Über den stoffwechsel der tumoren*. Springer, Berlin.

Weiger, T., Lametschwandtner, A. and Stockmayer, P. (1986). Technical parameters of plastics (Mercox CL-2B and various methacrylates)used in scanning electron microscopy of vascular corrosion casts. *Scanning Electron Microscopy*. I, 243-252.

Weisse, I., Stotzer, H. and Seitz, R. (1974). Age and light dependent changes in the rat eye. *Virchows Arch.* 362, 145-156.

Weiter, J.J. and Zuckerman, R. (1980). The influence of the photoreceptor-RPE complex on the inner retina. *Ophthalmol.* 87, 1133-1139.

Wen, G.Y., Sturman, J.A. and Shek, J.W. (1985). A comparative study of the tapetum, retina and skull of the ferret, dog and cat. *Lab. Animal Sci.* 35, 200-210.

Westheimer, G. (1983). Herman Helmholtz and origins of sensory physiology. *Trends in Neurosci.* 6, 5-9.

Westheimer, G. (1987). Visual Acuity. In: Moses, R.A. and Hart, W.M. (Ed.) *Adler's Physiology of the Eye. Clinical Application*. (pp. 415-429). The C.V. Mosby Company, St Louis.

Wiener, S.I. (1986). Laminar distribution and patchiness of cytochrome oxidase in mouse superior colliculus. *J. Comp. Neurol.* 244, 137-148.

Wiesenfeld, A. and Branchek, T. (1976). Refractive state and visual acuity in the hooded rat. *Vision Res.* 16, 823-827.

Wieslander, J.B., Mecklenburg, C.V., Dougan, P. and Stjernquist, U. (1986). Vascular and endothelial cell reactions caused by various perfusates. *Proc. XIth Int. Cong. Elect. Micros.* 2763-2764.

Wikler, K.C., Raabe, J.I. and Finlay, B.L. (1985). Temporal retina is preferentially represented in the early retinotectal projection in the hamster. *Develop. Brain Res.* 21, 152-155.

Wilkin, G.P. and Wilson, J.E. (1977). Localization of hexokinase in neural tissue: Light microscopic studies with immunofluorescence and histochemical procedures. *J. Neurochem.* 29, 1039-1051.

Wilkus, R.J., Chatrian, G.E. and Lettich, E. (1971). The electroretinogram during terminal anoxia in humans. *Electroenceph. Clin. Neurophysiol.* 31, 537-546.

Williams, D.R. (1985). Aliasing in human foveal vision. *Vision Res.* 25, 199-205.

Williams, T.W. (1948). The visualization of vertebrate capillary beds by intravascular precipitation of lead chromate. *Anat. Rec.* 100, 115-126.

Williamson, J.R., Tilton, R.G., Kilo, C. and Yu, S. (1980). Immunofluorescent imaging of capillaries and pericytes in human human skeletal muscle and retina. *Microvasc. Res.* 20, 233-241.

Wilson, D.J. and Green, R. (1987). Argon laser panretinal photocoagulation for diabetic retinopathy. Scanning electron microscopy of human choroidal vascular casts. *Arch. Ophthal.* 105, 239-242.

Winkler, B.S. (1975). Dependence of rat and rabbit photoreceptor potentials upon anaerobic and aerobic metabolism in vitro. *Exp. Eye Res.* 21, 545-548.

Winkler, B.S. (1981). Glycolytic and oxidative metabolism in relation to retinal function. *J. Gen. Physiol.* 77, 667-692.

Winkler, B.S. (1989). Editorial comments. Retinal aerobic glycolysis revisited. *Invest. Ophthal. Vis. Sci.* 30, 1023.

Wirz-Justice, A., Da Prada, M. Remé, C. (1984). Circadian rhythm in rat retinal dopamine. *Neurosci. Letts.* 45, 21-25.

Wise, G.N., Dollery, C.T. and Henkind, P. (1971). *The Retinal Circulation.* Harper and Row, Publishers, New York.

Wislocki, G.B. (1939). The unusual mode of development of the blood vessels of the opossum's brain. *Anat. Rec.* 74, 409-427.

Wislocki, G.B. (1940). Peculiarities of the cerebral blood vessels of the opossum: diencephalon, area postrema and retina. *Anat. Rec.* 78, 119-137.

Wislocki, G.B. and Campbell, A.C.B. (1937). The unusual manner of vascularization of the brain of the opossum (*Didelphys virginiana*). *Anat. Rec.* 67, 177-191.

Wislocki, G.B. and Sidman, R.L. (1954). The chemical morphology of the retina. *J. Comp. Neurol.* 101, 53-99.

Wittenberg, J.B. and Wittenberg, B.A. (1962). Active secretion of oxygen into the eye of fish. *Nature.* 194, 106-107.

Wong, R.O.L and Hughes, A. (1987). The morphology, number and distribution of confirmed displaced amacrine cells in the adult cat retina. *J. Comp. Neurol.* 255, 159-177.

Wong, R.O.L., Wye-Dvorak,J. and Henry, G.H. (1986). Morphology and distribution in the retinal ganglion cell layer of the adult tammar wallaby - *Macropus eugenii*. *J. Comp. Neurol.* 253, 1-12.

Wong-Riley, M.T.T. (1976). Endogenous peroxidase activity in brain stem neurons as demonstrated by their staining with diaminobenzidine in normal squirrel monkeys. *Brain Res.* 108, 257-277.

Wong-Riley, M.T.T. (1979). Changes in the visual system of monocularly sutured or enucleated cats demonstrable with cytochrome oxidase histochemistry. *Brain Res.* 171, 11-28.

Wong-Riley, M.T.T. (I989). Cytochrome oxidase: an endogenous metabolic marker for neuronal activity. *Trends In Neuro. Sci.* 12, 94-101.

Wong-Riley, M.T.T. and Carroll, E.W. (1984a). Quantitative light and electron microscopic analysis of cytochrome oxidase-rich zones in V II prestriate cortex of the squirrel monkey. *J. Comp. Neurol.* 222, 18-37.

Wong-Riley, M.T.T. and Carroll, E.W. (1984b). Effect of impulse blockade on cytochrome oxidase activity in monkey visual system. *Nature*. 307, 262-264.

Wong-Riley, M.T.T. and Norton, T.T. (1988). Histochemical localization of cytochrome oxidase activity in the visual system of the tree shrew: Normal patterns and the effect of retinal impulse blockade. *J. Comp. Neurol.* 272, 562-578.

Wong-Riley, M.T.T. and Riley, D.A. (1983). The effect of impulse blockage on cytochrome oxidase activity in the cat visual system. *Brain Res.* 261, 185-193.

Wong-Riley, M.T.T. and Welt, C. (1980). Histochemical changes in cytochrome oxidase of cortical barrels after vibrissal removal in neonatal and adult mice. *Proc. Nat. Acad. Sci. USA.* 77, 2333-2337.

Wong-Riley, M.T.T., Merzenich, M.M. and Leake, P.A. (1978). Changes in endogenous enzymatic reactivity to DAB induced by neuronal inactivity. *Brain Res.* 141, 185-192.

Wood, C.A. (1917). *The Fundus Oculi of Birds Espicially as Viewed by the Ophthalmoscope. A study in Comparative Anatomy and Physiology*. The Lakeside Press, Chicago.

Woodlief, N.F. (1980). Initial observations on the microcirculation in man. *Arch. Ophthal.* 98, 1268-1272.

Woodlief, N.F. and Eifrig, D.E. (1982). Initial observations on the microcirculation in man: The choriocapillaries. *Ann. Ophthal.* 14, 176-180.

Wu, G., Silverman, R.H., Coleman. D.J. and Lizzi, F.L. (1989). In vivo thickness of the human detached retina by ultrasound signal processing. *Graefes Arch. Clin. Exp. Ophthalmol.* 227, 21-25.

Wye-Dvorak, J. (1984). Postnatal development of primary visual projections in the tammar wallaby (*Macropus eugenii*). *J. Comp. Neurol.* 228, 491-508.

Yaffe, M. and Schatz, G. (1984). The future of mitochondrial research. *Trends in Biochem. Sci.* 9, 179-181.

Yanoff, M. and Fine, B.S. (1988). *Ocular Pathology. A Color Atlas*. J.B. Lippincott, Philadelphia.

Yoneya, S. and Tso, M.O.M. (1987). Angioarchitecture of the human choroid. *Arch. Ophthal.* 105, 681-687.

Yoneya, S. Tso, M.O.M. and Shimizu, K. (1983). Patterns of the choriocapillaris. A method to study the choroidal vasculature of the enucleated human eye. *Int. Ophthal.* 6, 95-99.

Yoshimoto, H., Murata, M., Yamagami, K. and Matsuyama, S. (1990). Studies in the angioarchitecture of the posterior choroid in the rat and role of posterior ciliary vein. *Invest. Ophthal. Vis. Sci.* 19, 1245-1250.

Young, T. (1801). On the mechanism of the eye. *Phil. Trans. Roy. Soc. B.* 92, 23-88.

Zeimer, R.C., Mori, M.T. and Khoobehi, B. (1989). Feasibility test of a new method to measure retinal thickness noninvasively. *Invest. Ophthal. Vis. Sci.* 30, 2099-2105.

Zuckerman, R. and Weiter, J.J. (1980). Oxygen transport in the bullfrog retina. *Exp. Eye Res.* 30, 117-127.

APPENDIX

APPENDIX 1: ANAESTHESIA

"When he wrote a letter, he would put that which was most material in the postscript, as if it had been a by matter" ..... Francis Bacon.

1.1 Small animal anaesthesia

(Rats, Guinea pigs and Sugar gliders)

1.1.1 Chloral Hydrate

Intraperitoneal (ip) dose is 0.3 ml/100 gm of body weight (9% solution).

For a 250-300gm rat, approximately 1ml is required. Where prolonged anaesthesia is needed or there is slow response to the initial loading dose, an additional 0.1 ml/100 gm may be given, titrated against the level of anaesthesia.

1.1.2 Nembutal (Sodium pentobarbitone)

The intraperitoneal dose is 0.1ml per 100gm body weight (60 mg/ml solution).

Nembutal may be infused for longer procedures at a rate of 8 mg/kg per hour intravenously (iv).

1.1.3 Ketamine

Intramuscular (im) dose is 2 mg/100 gm body weight (100 mg/ml solution).

This is ideal for short anaesthesia particularly where little operative intervention is required. Atropine (100 μgm/kg) may also be used to diminish respiratory secretions.

1.2 Larger animal anaesthesia

(Possums, Native cats, Tasmanian devils and Cats)

1.2.1 Halothane induction

Induce anaesthesia with inhalational halothane. For this the animal is held in an anaesthetic box. Once anaesthetised, continue halothane through a mask or endotracheal tube, or administer a systemic agent such as nembutal or chloralose.

1.2.2 Nembutal maintenance

IP dose is 1.0ml/1.5kg body weight

For iv use, administer a bolus loading dose of 0.5ml/1.5kg body weight. Follow this with subsequent 0.1ml doses, titrated against the level of anaesthesia, at 30-45 minute intervals (approx. 8 mg per kg per hour).

1.2.3 α-Chloralose maintenance

IV dose of 60 mg/kg. Made as a 50 mg/ml solution (5% in 5% sodium metaborate).

The solution is made by heating approximately 160ml of water to 40° and dissolving 10gm of sodium metaborate (Kodalk). Ten gm of chloralose is added slowly whilst stirring. Make up to 200ml, filter and store in a dark bottle.

1.3 Suppliers

Nembutal: Bomac Laboratories Pty. Ltd., 7 Kelray Place, Asquith, NSW, 2078.

Ketamine: Parke-Davis, 32 Cawarra Rd Caringbah, NSW, 2229.

Halothane: ICI Aust. Pharmaceutical Division Christina Rd, Villawood, 2163.

APPENDIX 2: GLYCOL METHACRYLATE PLASTIC EMBEDDING

2.1 Introduction

Glycol methacrylate (GMA) embedding kits consist of glycol methacrylate monomer, a plasticiser, such as polyethylene glycol 400 (PEG 400), an activator (benzoyl peroxide with 50% plasticizer) and hardener, a barbituric acid derivative.

Infiltration solution: 50ml monomer solution with 0.5gm of benzoyl peroxide. This may be stored for several weeks if refrigerated.

Embedding solution: 15ml of infiltration solution and 1.0ml of hardener. Polaron Glycol methacrylate kit also requires the addition of PEG 400 to this solution in proportion of 0.5-1.5ml per 15ml GMA. Optimal mixture was found to be 0.75ml PEG per 15ml GMA.

2.2 Embedding and sectioning procedure

1. Wash specimen in buffer prior to dehydration: 15 min x 2.

2. Dehydrate through graded alcohols: 30%, 50%, 75%, 90%, and 95% x 2. Fifteen minutes for each step is usually sufficient for retina. In general, 1 hour per step is necessary for tissue of up to 2mm minimum dimension.

3. Wash in 1:1 100% alcohol: glycol methacrylate infiltration media for up to 1 hour.

4. Immerse in infiltration solution (glycol methacrylate); 2 changes of each 1 hour.

5. Prepare embedding media by adding 1.0ml of hardener to 15ml of Historesin infiltration solution. For the Polaraon kit, add 1.0ml of hardener and 0.75ml of polyethylene glycol to 15.0ml of monomer solution. Mix thoroughly.

6. Immerse and orientate the specimen in the mould, cover with embedding media and then cover with the microtome chuck. Allow to polymerise for 2 hours at room temperature.

7. Remove section from the mould and section at 1-10μm with a triangular glass knife using a Sorvall JB-4 or similar microtome.

8. Gather sections with fine forceps and then float on distilled water at room temperature. Collect sections onto cleaned glass slides and allow to dry on a hot plate at 60-70°C.

2.3 Toluidine blue staining

1. Place slide with section on 60°C hot plate.

2. With a syringe and 0.2μm millipore filter, cover the section with 1% toluidine blue in 1% borax. Leave for 1 minute.

3. Wash with running tap water, air dry and coverslip in DPX or similar mountant. Enhanced differentiation of staining may be achieved by passing the section through 100% alcohol and then xylene prior to coverslipping.

2.4 Precautions

Resin solution and hardener may cause irritation and gloves should therefore be used. Benzoylperoxide is explosive and a strong oxidising agent.

2.5 Suppliers

Polaron GMA Kit for LM, Cat No. 2040: Bio-Rad Laboratories, 8/17 King Rd, PO Box 33, Hornsby NSW.

Historesin Embedding Kit, LKB 2218-500: Linbrook Int. Pty Ltd, 170 Forster Rd, Mt Waverly.

APPENDIX 3: ELECTRON MICROSCOPY

3.1 Perfusion and Fixation

Anaesthetise the animal (see Appendix 1).

A thoracolaparotomy is performed by first opening the abdomen with a midline incision, disinserting the diaphragm anteriorly and extending the incision bilaterally to open the thorax. The thoracic flap is then reflected toward the head to allow access to the heart and great vessels. To conserve fluid, the descending aorta is clamped. The pericardium is incised and reflected. An optional injection into the left ventricle of heparin (750 units/kg) may be performed at this stage. A small slit is made into the apex of the left ventricle and the already primed perfusion catheter is inserted through the ventricle, into the ascending aorta and clamped into position. To allow outflow of the perfusion fluid the right atrium is then incised and the flush solution may then be released. The flush, for example Hartmann's solution or normal saline, is best filtered before use. The flush is continued for around 2-3 minutes. Complete clearing of the vascular system is not necessary, merely sufficent flushing so that the fixative does not coagulate the remaining blood.

Once the flush is completed, the perfusing fluid is changed to the fixative solution. This is continued until 200-500ml has been perfused in the smaller animals, or 500-700ml in the larger animals. For best preservation of retinal tissue, especially in the avascular species, a pars plana injection of 1-2ml of fixative into the eye may be employed. When this is performed, a simultaneous scleral incision needs to be made for the outflow of excess fixative.

3.2 Perfusion solutions

3.2.1 Phosphate buffer: 0.2M

Part A: (alkaline)

Dissolve 28.36gm of anhydrous dibasic sodium phosphate (Na_2HPO_4) in 1 litre of distilled water. (35.61gm of dihydrate)

Part B: (acidic)

Dissolve 24.00gm of anhydrous monobasic sodium phosphate (NaH_2PO_4) in 1 litre of distilled water. (31.21gm of dihydrate)

Mix A and B until the correct pH is achieved. For ph 7.4, an excess of part A is required.

3.2.2 Fixative

4% paraformaldehyde

2% glutaraldehyde

4% sucrose

2.0mM $CaCl_2$

0.1M phosphate buffer, pH 7.4

1. To make 1 litre, dissolve 40gm of paraformaldehyde in approximately 300ml of alkaline distilled water by heating to 60° whilst stirring. Heating beyond 60° produces formic acid. Cool to 30°.

2. While stirring, add 40gm of sucrose and 2.2ml of 10% $CaCl_2$.

3. Add 80ml of EM grade glutaraldehyde.

4. In a 1 litre flask make this up to 500ml with distilled water, then add 500ml of 0.2M phosphate buffer for a final volume of 1000ml.

5. Filter and use within 24 hours. Perfuse using fluid at room temperature.

3.3 Electron microscopic processing

1. Select desired specimen and place in 10ml processing bottle. Cut into pieces so that it is no larger than 1mm in thickness. The specimen may be conveniently identified by placing in the bottle a small pencil labelled paper square.

2. Fix in 1% OsO_4 in 0.1M phosphate buffer for 30-60 minutes. Take care when using osmium as it is toxic. Perform in the fume hood.

3. Wash in 0.1M buffer, 2 x 5 minutes followed by a distilled water wash for 5 minutes.

For subsequent steps place specimen bottles in the rotator to aid penetration of reagents.

4. Dehydrate through graded alcohols, 25%, 50% and 70%, depending on the size of the specimen, but usually for retina, 5 minutes each.

5. *En bloc* staining with a 1% solution of uranyl acetate in 70% alcohol for 30 minutes may be employed at this stage. An alternative is to perform this step after osmication in 4% uranyl acetate in distilled water.

6. Further dehydrate through 70%, 95%, 100% and 100% alcohol x 5 minutes each.

7. Before resin infiltration, the specimen is passed through transition fluid, propylene oxide, for 5 minutes x 2. Be careful to avoid drying of specimen at this stage.

8. Mix last change of propylene oxide with an equal volume of embedding medium, for example Epon. Infiltrate with this 50/50 mixture, with agitation, for 2 hours.

9. Change into 100% Epon overnight followed by further change allowing 6-10 hours prior to blocking tissue.

10. Orientate specimen in mould with Epon media. Cure in the oven for 6-20 hours at 37°, 45° and 65° each.

11. Epon is mixed according to the manufacturers instructions based on the activity of the batch and desired hardness. This would be approximately:

25gm	LX122	11.75gm
	DDSA	5.25gm
	NMA	8.0gm

Keep covered and mix for 15 minutes using mechanical stirrer. Add accelerator:

	DMP-30	0.35gm

Mix for further 15 minutes. This resin should be used within 12 hours. Care needs to be taken when handling Epoxy resins because of their mutagenic potential (Ringo et al. 1982).

3.4 Cutting and staining

1. When specimen is cured, remove from the oven, allow to cool and roughly trim to size. Place specimen in an ultramicrotome chuck.

2. Section block using an ultramicrotome (eg. LKB Nova) at 0.5-1μm using as glass knife. Collect specimens onto glass slides and stain with 1% toluidine blue in 1% borax at 75° for 30-60 seconds (see Appendix 2.3).

3. Having selected the area of interest, the block may be further trimmed and then sectioned to produce silver-gold thin sections. These are floated onto water as they are cut, collected onto grids, or formvar coated slots, and dried.

3. Stain firstly using 4% uranyl acetate (UA) in distilled water for 15-45 minutes. This is conveniently performed by placing a drop of UA onto parafilm and floating the grid on this drop. Wash in distilled running distilled water and dry over hotplate at 50-60°.

4. This is followed by lead staining for 3-6 minutes. A drop of lead solution is placed on parafilm under cover with a few pellets of NaOH in the dish. Following staining, the grid is gently washed in running distilled water and dried.

To make lead stain, dissolve 0.4gm of NaOH in 100ml of freshly distilled water. Dissolve with agitation, 0.12gm of lead citrate in 10ml of NaOH solution (0.1N). Filter before use (Venable and Coggeshall 1965).

APPENDIX 4: CYTOCHROME OXIDASE HISTOCHEMISTRY

4.1 Fixation

Short fixation times are required, usually use less than one hour. For light microscopy, 0.1 M phosphate buffered formaldehyde (2-4%) is an adequate fixative. For electron microscopic visualisation of the reaction product, glutaraldehyde (0.5-1%) is required in addition to formaldehyde, but with longer incubation times being necessary in order to offset the added enzyme inhibition of glutaraldehyde.

4.2 Preincubation steps

4.2.1 Whole retinal incubations

After fixation time of around 1 hour, the retina is removed from the eyecup (Stone 1981). As much vitreous as possible is removed with scissors followed by the optional application of protamine sulphate 1% solution to collapse the remaining vitreous.

Wash in phosphate buffer, 3 x 10 minutes.

For enhanced histochemical reaction, sodium borohydride quenching of the aldehyde fixatives may be used. The retina is immersed in 1% $NaBH_4$ dissolved in 0.1M buffer for 15 minutes, followed by further buffer wash for 15 min (until retina stops fizzing) then a further 5 minute wash.

4.2.2 Frozen section material

The cryopretectant 10% glycerol, perfused trans cardially prior to enucleation, offers improved morphological preservation. For later orientation, the eyes are marked with a stitch at 12 o'clock and then frozen in liquid nitrogen cooled isopentane. A mould of 1% carboxymethyl cellulose (CMC) allows attachment of the eye to the cryostat chuck. The eye is placed in an embedding mould of liquid CMC and then frozen in liquid nitrogen cooled isopentane. This block is then attached to a precooled chuck with a layer of CMC. Cut sections at desired thickness, for example 48μm which produces 3 sections per revolution of the thickness gauge. The sections are attached to subbed slides and then allowed to air dry. Treatment

with fixatives and quenching agents may be employed prior to a buffer wash and subsequent incubation. For refinements in the frozen section technique see Fink (1986).

4.3 Incubation

Incubate at 37°C until macroscopic reaction product is evident. Normal endpoint is a dark brown colour, whilst if nickel enhancement is used, the reaction product is black. Usual time between 1 and 2 hours.

For fresh frozen sectioned material, incubation time is around 20 minutes.

4.4 Post incubation

Wash in buffer after incubation.

Post fixation steps may be added. For example, fix fresh frozen material in buffered 10% formalin for 30 minutes.

For cross sectional study of whole retinae dehydrate and embedd in paraffin or glycol methacrylate.

4.5 Solutions and reagents

Cytochrome C (Sigma C7752) This is best kept dried and frozen as moisture makes dissolution more difficult.

DAB (Sigma D5637)

Nickel Chloride $6H_2O$ (Univar)

0.2M phosphate buffer (or cacodylate) pH 7.4

Sodium Borohydride (BDH)

Mix 50mg DAB in 50ml of distilled water. This should dissolve readily. Add 30mg cytochrome C. For Nickel intensification add 50mg or less of NiCl to 50ml of 0.2M phosphate buffer and add to cyto C/DAB solution. Otherwise add 50ml of 0.2M phoshphate buffer.

For KCN control use 0.01M solution. ie, 32mg KCN per 50ml of solution.

APPENDIX 5: PUBLICATIONS

Abstracts

Buttery, R.G., Haight, J.R. and Bell, K. (1987). Fluorescein angiography in mammalian retinae. In: Perry, M.A. and Garlick, D.G. (Ed.) *Progress in Microcirculation Research. Proceedings of the Fourth Australian and New Zealand Symposium.* (pp 26). University of NSW Press, Sydney.

Buttery, R.G., Haight, J.R. and Bell, K. (1987). Fluorescein angiography of mammalian retinae. *J. Anat.* 255, 253.

Buttery, R.G., Weller, W.L. and Haight, J.R. (1988). Retinal cytochrome oxidase: A missing link in the electron transport chain? *Neurosci. Letters.* S30, 52.

Buttery, R.G., Hinrichsen, C.F.L. and Weller, W.L. (1989). How thick is the mammalian retina? *Neurosci. Letters.* S34, 66.

Papers to date

Buttery, R.G., Haight, J.R. and Bell, K. (1990). Vascular and avascular retinae in mammals: A fundoscopic and fluorescein angiographic study of marsupial and placental retinae. *Brain Behav. Evol.* 35, 156-175.

Buttery, R.G., Hinrichsen, C.F.L., Weller, W.L. and Haight, J.R. (1990). How thick should a retina be? A comparative study of mammalian species with and without intraretinal vasculature. *Vision Res.* In press.

Buttery, R.G. and Weller, W.L. (1990). Cytochrome oxidase histochemistry in vascular and avascular retinae. Submitted for publication.

Papers in preparation

Buttery, R.G. and Haight, J.R. Vasculature of the marsupial eye. A comparative corrosion cast study.

Buttery, R.G. and Haight, J.R. The retinal epithelium of two Australian marsupials; the polyprotodont quoll and the diprotodont brushtail possum.

Unrelated publications

Buttery, R.G., Wise, G.M., Nicholls, S.G. and Bell, K. (1987). The P300 peak of the visual evoked response. *Neurosci. Letters*. S27, 61.

Hinrichsen, C.F.L. and Buttery, R.G. (1988). The nature of posterior hypothalamic projections to the cardiorespiratory centers in the brainstem. *Experientia*. 44, 504-505.

Buttery, R.G. and Wise, G.M. (1988). Conal anaesthesia: a new approach to retrobulbar anaesthesia. *Aust. NZ. J. Ophthal*. 17, 63-69.

Mackey, D.A., Chen, J.D., Fuller, H., Wise, G.M., Serravalle, S., Olsson, J., Buttery, R.G. and Denton, M.J. (1989). Localization of the locus for X-linked megalocornea to Xq12-q26. *Cytogen. Cell Genetics*. 51, 1037.